PROJECT TUGBOAT: EXPLOSIVE EXCAVATION OF A HARBOR IN CORAL

Walter C. Day, et al

Army Engineer Waterways Experiment Station
Livermore, California

February 1972

AD_____

TECHNICAL REPORT E-72-23

PROJECT TUGBOAT
EXPLOSIVE EXCAVATION OF A HARBOR IN CORAL

Walter C. Day

February 1972

U. S. Army Engineer Waterways Experiment Station
Explosive Excavation Research Laboratory
Livermore California

Approved for Public Release; Distribution Unlimited

217

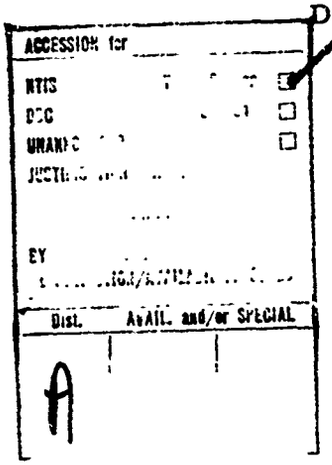

Destroy this report when no longer needed.
Do not return it to the originator.

The findings in this report are not to be construed as an official Department of the Army position unless so designated by other authorized documents.

Printed in USA. Available from Defense Documentation Center,
Cameron Station, Alexandria, Virginia 22314 or
National Technical Information Service,
US Department of Commerce,
Springfield, Virginia 22151

Unclassified

Security Classification

DOCUMENT CONTROL DATA - R & D

(Security classification of title, body of abstract and indexing annotation must be entered when the overall report is classified)

1 ORIGINATING ACTIVITY (Corporate author) US Army Engineer Waterways Experiment Station Explosive Excavation Research Laboratory	2a. REPORT SECURITY CLASSIFICATION Unclassified 2b. GROUP

3 REPORT TITLE

EERL Technical Report E-72-23 - Project TUGBOAT
Explosive Excavation of a Harbor in Coral

4. DESCRIPTIVE NOTES (Type of report and inclusive dates)

Final Report

5. AUTHOR(S) (First name, middle initial, last name) Principal Author & Editor - Walter C. Day
CPT Wade Wnuk, Colin C. McAneny, LT Kenneth Sakai, Dr. D. Lee Harris, Dennis Berg, Richard Kanayama, Paul Kawamoto, Robert F. Ballard, Jr., Luke Vortman, Joseph Nicoletti, James Keith, Bing Mah, R. E. Marks

6. REPORT DATE 1972	7a. TOTAL NO. OF PAGES 217	7b. NO. OF REFS 43
8a. CONTRACT OR GRANT NO. b. PROJECT NO. c. d.	9a. ORIGINATOR'S REPORT NUMBER(S) EERL-TR-E-72-23 9b. OTHER REPORT NO(S) (Any other numbers that may be assigned this report)	

10 DISTRIBUTION STATEMENT

Approved for public release; distribution unlimited.

11. SUPPLEMENTARY NOTES	12. SPONSORING MILITARY ACTIVITY

13 ABSTRACT

A portion of a planned small boat harbor was explosively excavated in a weak coral material using twelve 10-ton charges of an aluminized ammonium nitrate slurry explosive. This experiment-demonstration executed by the US Army Engineer Nuclear Cratering Group, now designated as the US Army Engineer Waterways Experiment Station Explosive Excavation Research Laboratory, was code-named Project TUGBOAT. The charges were emplaced approximately 36 feet deep in the coral reef which was overlain with about an average 6-foot depth of water. Charges were spaced 100 feet and 120 feet apart. A series of five calibration tests preceded the main harbor detonations. Apparently because of inadequate boostering, two of the main charges did not fully detonate and one charge deflagrated. An additional array of sixteen 1/2-ton charges were subsequently emplaced and detonated to clear that portion of the channel. The detonations resulted in a channel varying in width from about 150 feet to 260 feet at a minimum project water depth of 12 feet. The berthing basin is almost a square area 400 feet on a side at the 12-foot water depth contour. The explosive craters were broad and shallow with no lips and were actually better suited to harbor excavation than the less wide and deeper craters typical of dry land cratering detonations. The cratering mechanism appears to be one of densification of the coral through crushing and subsequent settling. The crater remains devoid of water for several seconds after detonation and then is filled by coral and water as the crater walls fail into the crater. The extent of crushing action of the detonations was crudely defined by acoustic profiling surveys.

(continued on reverse side)

DD FORM 1 NOV 65 1473

Unclassified

Security Classification

14 KEY WORDS	LINK A		LINK B		LINK C	
	ROLE	WT	ROLE	WT	ROLE	WT
Explosive Excavation						
Underwater Excavation						
Harbor Excavation in a Weak Coral						
Large Detonations in Coral						
Effects of Large Underwater Explosions on Marine Organisms						

ABSTRACT (continued)

Several technical programs were conducted including a wave measurement program, a study of the effect of the detonations on the marine environment, a ground motion measurement program, a structures response study, an airblast measurement program, and a measurement program to determine the peak pressure and the acceleration and velocity of the water directly over the charge positions. Results of all of these programs are included in this report.

TID-4500, UC-35

EERL TECHNICAL REPORT E-72-23

PROJECT TUGBOAT
EXPLOSIVE EXCAVATION OF A HARBOR IN CORAL

Principal Author and Editor

Walter C. Day

Contributing Authors

CPT Wade Wnuk Colin McAneny LT Kenneth Sakai	EERL, WES	Robert F. Ballard, Jr.	Soils Division WES
		R. E. Marks	LLL
Dr. D. Lee Harris Dennis Berg	CERC	Luke Vortman	Sandia Laboratories Albuquerque
Richard Kanayama Paul Kawamoto	State of Hawaii Fish & Game	Joseph Nicoletti James Keith Bing Mah	J. A. Blume & Associates Engineers

U.S. ARMY ENGINEER WATERWAYS EXPERIMENT STATION
EXPLOSIVE EXCAVATION RESEARCH OFFICE
Livermore, California

MS. Date: February 1972

Preface

This report is a summary report for Project Tugboat, the explosive excavation of a small boat harbor. It is the only formal report that will be published for the project and therefore includes results of all technical programs conducted under it.

The editor and contributing authors to this report wish to acknowledge the participation of persons in the many agencies who helped make this project a success.

The project marks the initial attempt of the Explosive Excavation Research Laboratory to apply to an actual civil works project the knowledge and expertise derived during its participation in the Plowshare program. Despite some detonation problems, the project was successfully excavated with explosives without any postdetonation reliance on conventional dredging to finish the job.

The U.S. Army Engineer Waterways Experiment Station (USAEWES) Explosive Excavation Research Laboratory (EERL) was the USAEWES Explosive Excavation Research Office (EERO) prior to 21 April 1972. Prior to 1 August 1971 the organization was known as the USAE Nuclear Cratering Group.

Directors of the Explosive Excavation Research Office (and NCG) during the 2-yr period over which this project was conceived and executed were LTC Bernard Hughes, COL William E. Vandenberg, and LTC Robert L. LaFrenz.

Abstract

A portion of a planned small-boat harbor was explosively excavated in a weak coral material using twelve 10-ton charges of an aluminized ammonium nitrate slurry explosive. This experiment-demonstration executed by the U.S. Army Engineer Nuclear Cratering Group, now designated as the U.S. Army Engineer Waterways Experiment Station Explosive Excavation Research Laboratory (EERL), was code-named Project Tugboat. The charges were emplaced approximately 36 ft deep in the coral reef which was overlain with a water layer averaging approximately 6 ft in depth. Charges were spaced 100 and 120 ft apart. A series of five calibration tests preceded the main harbor detonations. Apparently because of inadequate boostering, two of the main charges did not fully detonate and one charge deflagrated. An additional array of sixteen 1/2-ton charges was subsequently emplaced and detonated to clear that portion of the channel. The detonations resulted in a channel varying in width from about 150 to 260 ft at a minimum project water depth of 12 ft. The berthing basin is almost a square area 400 ft on a side at the 12-ft water depth contour. The explosive craters were broad and shallow with no lips and were actually better suited to harbor excavation than the less wide and deeper craters typical of dry land cratering detonations. The cratering mechanism appears to be one of densification of the coral through crushing and subsequent settling. The crater remains devoid of water for several seconds after detonation and then is filled by coral and water as the crater walls fail into the crater. The extent of the crushing action of the detonations was crudely defined by acoustic profiling surveys.

Several technical programs were conducted including a wave measurement program, a study of the effect of the detonations on the marine environment, a ground-motion measurement program, a structures response study, an airblast measurement program, and a measurement program to determine the peak pressure and the acceleration and velocity of the water directly over the charge positions. Results of all of these programs are included in this report.

Conversion Factors

Units of measurement used in this report can be converted to metric units as follows:

Multiply	By	To Obtain
inches	2.54	centimeters
feet	0.3048	meters
cubic feet	0.02832	cubic meters
cubic yards	0.764555	cubic meters
pounds	0.4535924	kilograms
pounds per square inch	0.00689476	meganewtons per square meter
pounds per cubic foot	16.02	kilograms per cubic meter
Fahrenheit degrees	5/9	Celsius or Kelvin degrees[a]
foot-pounds	0.138255	meter-kilograms

[a]To obtain Celsius (C) temperature readings from Fahrenheit (F) readings, use the following formula: C = (5/9) (F - 32); to obtain Kelvin (K) readings, use: K = (5/9) (F - 32) + 273.15.

Contents

PREFACE ii

ABSTRACT iii

CONVERSION FACTORS iv

SECTION 1. INTRODUCTION 1

Purpose of Report 1
Objectives of Project 1
Scope of Project Tugboat 2
Major Technical Programs Conducted 2
Summary of Results 5
Project Organization 8

SECTION 2. CONSTRUCTION, EXECUTION, AND POSTDETONATION INVESTIGATIONS 9

Location 9
Site Description 13
Project Design 24
Supporting Construction and Execution 28
Results 45
Subsurface Investigations 63
Discussion of Underwater Cratering in Coral 77
Summary and Conclusions 79

SECTION 3. WAVE MEASUREMENTS 82

Introduction 82
Experimental Procedure 85
Results 86
Analysis and Interpretation of Wave Data 95
Conclusions 101
Recommendations for Future Experiments 101

SECTION 4. FISH AND WILDLIFE STUDIES 102

Objectives 102
Materials and Methods 102
Results and Discussion 104
Summary and Conclusions 121

SECTION 5. SEISMIC- AND STRUCTURAL-MOTION MEASUREMENTS . . 123

Program Objectives 123
Experimental Procedures 123
Predictions 127
Results 130
Analysis and Interpretation 134
Summary and Conclusions 144

SECTION 6. STRUCTURAL-RESPONSE ANALYSIS 144

Objective 144
Structural Inventory 144
Pre-Phase I Recommendations 146
Post-Phase I Analysis 146
Post-Phase II Analysis 154
Conclusions 163

SECTION 7. AIR-OVERPRESSURE MEASUREMENTS 163

Objectives 163
Predictions 164
Instrumentation and Station Locations 166
Results 170

SECTION 7 (Continued)

Discussion of Results 177
Summary 191
Conclusions 191

SECTION 8. PRESSURE, ACCELERATION, AND VELOCITY MEASUREMENTS IN WATER SURFACE LAYER 192

Program Objectives 192
Experimental Procedures 192
Results 193
Conclusion 198

REFERENCES 199

FIGURES

1 Project Tugboat organization 9
2 Project Tugboat site located on vicinity map 10
3 Map of general site, Project Tugboat 11
4 Coastal area near harbor site (Kawaihae) 12
5 Aerial photo of Tugboat site showing zones of coral growth and sedimentation 14
6 Typical coral head in Project Tugboat area 16
7 Tugboat site hydrography, May 1969 (contours represent depths in feet below Mean Lower Low Water; map does not show all details of irregular coral heads) 17
8 Exploratory borings and seismic traverses, Project Tugboat site 19
9 Typical drill core recovery from exploratory borings . . . 20
10 Pressure-volume data for Tugboat coral (samples from Hole No. 45, 35- to 60-ft depth) 22
11 Stress-strain data for Tugboat coral (samples from Hole No. 45, 35- to 60-ft depth) 22
12 Bracing on steep wall of Puukohola heiau prior to detonations in Phase I of Project Tugboat 24
13 Cable and timber bracing used on corners of heiaus 24
14 Surface ground zero locations for Phase I calibration tests 26
15 Plan view of charge locations for Phase II 27
16 Conceptual drawing of completed small-boat harbor, Kawaihae Bay, Hawaii 28
17a Project Tugboat remedial design for area at channel entrance where Charge A1 was used to remove nose that protruded into channel 29
17b Project Tugboat remedial design for area over Charge Locations II-C and II-D 30
17c Project Tugboat remedial design for area over Charge Location II-G where two high spots existed in channel bottom 31
18 Truck-mounted fold-over derrick-type bucket auger used to drill Phase I emplacement holes 31
19 Removal of Phase I causeway by dragline 33
20 Drilling platform used during Phase II emplacement construction 33
21 Charge emplacement design for Phase II 34
22 Flange modification to charge emplacement design for Charges II-E, II-F, II-G, II-H, II-I, II-J, II-K, and II-L 34
23 Standard Phase I booster arrangement 36
24 Explosive emplacement operations during Phase I 37

FIGURES (Continued)

25	Booster design for Detonations II-ABCD and II-IJKL	38
26	Booster design for all charges in Detonation II-EFGH	38
27	Explosive emplacement operations during Phase II	39
28	Field-fabricated booster used to detonate Charges II-I, II-J, II-K, and II-L	41
29	Field-fabricated booster used to detonate Charge II-H	42
30	Remedial work drilling platform	43
31	Air lift used during emplacement of remedial work charge container	43
32	Remedial work drilling method	44
33	Thin-wall 6-in.-diameter air lift pump design and use	44
34	Loading of explosive used in remedial work	45
35	Booster design used in remedial excavation	45
36	Sequential photos of Phase I, 1e (Echo) 10-ton detonation	46
37	Project Tugboat Phase I: crater cross sections for 1a (Alpha) and 1b (Bravo) detonations	47
38	Project Tugboat Phase I: crater cross sections for 1c (Charlie) and 1d (Delta) detonations	47
39	Project Tugboat Phase I: crater cross sections for 1e (Echo) detonation	48
40	Comparison of 1e (Echo) crater profile with dry land crater profile having dimensions assumed in preliminary design	48
41	Sequential photos of Detonation II-IJKL that created berthing basin	49
42	Charge layout just prior to Detonation II-IJKL	50
43	A rial photo taken just after detonation	50
44	Detonation II-IJKL showing shock interaction and cavitation phenomena at water surface	50
45	Changes in shock interaction and cavitation phenomena	50
46	Breakwater construction activity following Phase II detonations	51
47	Final harbor area excavated to 12-ft depth contour compared with required dimension	51
48	Final harbor configuration	52
49	Sea-bottom topography, May 1970, following Phase II detonations	52
50	Sea-bottom topography, December 1970, following remedial blasting	53
51	Isopach map showing amounts of excavation (or fill) produced by Phase II detonations	54
52	Isopach map showing material moved by remedial detonations, December 1970	55
53	Isopach map showing amounts of excavation (or fill) accomplished by entire Project Tugboat program: Phase II and remedial	56
54	Longitudinal profiles of Project Tugboat channel	57
55	Locations of survey profiles shown in Figs. 56 through 64 (in addition longitudinal profile was run—see Fig. 54—from 250 ft seaward of Charge II-A to 170 ft west of Charge II-K)	58
56	Transverse profiles, Project Tugboat Channels 1, 2, and 3	59
57	Transverse profiles, Project Tugboat Channels 4, 5, and 6	59
58	Transverse profiles, Project Tugboat Channels 7, 8, and 9	60
59	Transverse profiles, Project Tugboat Channels 10, 11, and 12	60

FIGURES (Continued)

60	Transverse profiles, Project Tugboat Channels 13, 14, and 15	61
61	Transverse profiles, Project Tugboat Channels 16, 17, and 18	61
62	Transverse profiles, Project Tugboat Channels 19, 20, and 21	62
63	Transverse profiles, Project Tugboat Channels 22, 23, 24, and 25	62
64	Transverse profiles, Project Tugboat Channels 26, 27, and 28	63
65	Locations of acoustic profiling lines and postshot borings	64
66	Pulser records for Echo crater, December 1969	65
67	Pulser records, May 1970	66
68	Pulser records, May 1970	67
69	Pulser records, May 1970	68
70	Location of probings of Echo crater, December 1969	69
71	Profile of Echo crater inferred from probings, December 1969	70
72	Penetration and density data, Borings 55 and 56	72
73	Penetration and density data, Borings 57 and 58	72
74	Penetration and density data, Borings 59 and 60-60A	73
75	Penetration and density data, Boring 61	74
76	Penetration and density data, Borings 62 and 63	74
77	Standard penetration data from all preshot borings	75
78	Natural coral conditions persisting outside Project Tugboat channel in area between Borings 56 and 60	76
79	Broken coral adjacent to Project Tugboat channel in vicinity of Borings 56 and 57	77
80	Typical conditions in Project Tugboat channel in area between Charge Sites II-B and II-E	78
81	Whirlpool effect observed following Detonation II-EF	79
82	Photography of wave staffs, Detonation II-IJKL	80
83	Generation of water wave by explosion beneath seafloor	83
84	Aerial photograph of explosion-generated wave, Phase I, Detonation Alpha	84
85	Map showing location of wave gages, Phase I	85
86	Location of wave gages and wave poles, Phase II	86
87	Wave records for Detonations Alpha and Bravo, Phase I	87
88	Wave records for Detonation Charlie, Phase I	87
89	Wave records for Detonation Delta, Phase I	88
90	Wave records for Detonation Echo, Phase I	88
91	Wave records for Detonation II-ABCD	90
92	Wave records for Detonation II-EF	90
93	Wave records for Detonation II-IJKL	91
94	Breaking wave propagating past shoreward wave staff Camera Line B, Detonation II-IJKL	93
95	Breaking wave propagating past Camera Line C, Detonation II-IJKL	94
96	Complex surface motions and vortices over crater area, Detonation II-EF	96
97	Rush of water and fractured coral into dewatered crater area, Detonation II-IJKL	97
98	Propagation of waves outward from Surface Ground Zero, Detonation II-EF	98
99	Maximum wave height scaling relationship	100
100	Travel time for crest of maximum wave	100
101	Underwater fish counts to record densities and species composition of marine life at project site	102

FIGURES (Continued)

102	Approximate locations of 11 fish-counting stations in relation to Surface Ground Zeros of Phase I and Phase II detonations	103
103	Gil nets were fished in areas that were too murky for fish counting by divers (only limited information was obtained through this method)	104
104	Lantern basket containing live fishes being set out to determine distances to which fishes were affected by detonations	104
105	Spiny puffer, Diodon hystrix, being netted after Detonation 1c (Charlie)	105
106	Thick layer of brownish scum, resulting from detonations, hampered postdetonation fish collecting efforts	111
107	A 2-3/4-in. grouper of Genus Ypsigramma (Family Serranidae) killed by Detonation II-ABCD; this specimen was believed to be only the second of species collected from Hawaiian Islands	111
108	Sorting of fishes collected after Detonation II-IJKL (most of fishes showed no sign of external injuries)	115
109	Lacerated damselfish collected after Detonation II-ABCD (only a few of fishes collected after detonation were as severely lacerated)	115
110	Seismic station locations, Phase I	124
111	Seismic station locations, Phase II	125
112	Heiau ground-motion station, Phases I and II	127
113	Water tank ground-motion station, Phase I	128
114	Roth home instruments, Phases I and II	128
115	Sugar conveyor and terminal facility, Phases I and II	129
116	Ultramar warehouse, Phases I and II	129
117	Instruments installed at center and corner of roof of Ultramar warehouse, Phase II	130
118	Spencer Park pavilion instruments, Phases I and II	130
119	Close-up of model clay bonding used on lava at Spencer Park pavilion, Phases I and II	131
120	Promenade of Mauna Kea Beach Hotel (instruments installed behind middle column on right) Phases I and II	131
121	Second floor station at Mauna Kea Beach Hotel, Phases I and II	132
122	North roof station at Mauna Kea Beach Hotel, Phases I and II	132
123	South roof station at Mauna Kea Beach Hotel, Phases I and II	133
124	Project Tugboat ground-motion predictions	134
125	Vertical peak particle velocity, Phase I	139
126	Vertical peak particle velocity, Phase II	139
127	Radial peak particle velocity, Phase I	139
128	Radial peak particle velocity, Phase II	139
129	Transverse peak particle velocity, Phase I	140
130	Transverse peak particle velocity, Phase II	140
131	Maximum peak particle velocity, Phase I	140
132	Maximum peak particle velocity, Phase II	140
133	Maximum peak particle velocity, Phases I and II	141
134	Selected ground-motion data, Mauna Kea Beach Hotel	143
135	Plan showing location of structures of interest	145
136	Seismic motion for 50% chance of tipping a rock	147
137	Temporary bracing for heiaus	148
138	Typical cross section of sugar conveyor support structure	149

FIGURES (Continued)

139	Velocity records at sugar conveyor station for Detonations Echo, Delta, II-ABCD, and II-IJKL	150
140a	Plan, Ultramar Warehouse	151
140b	Elevations, Ultramar Warehouse	152
141a	Response spectra for Ultramar foundation, Phase I Echo (radial)	153
141b	Response spectra for Ultramar foundation, Phase I Echo (transverse)	154
142	Plan of seismic instrument locations for Phase II	155
143	Columns A-1 and B-1, Pre-Phase II Detonations; Column B-1 Post Phase II-IJKL Detonation	156
144a	Velocity records of Ultramar Stations, II-ABCD	158
144b	Velocity records of Ultramar Stations, II-IJKL	158
145a	Response spectra, Ultramar foundation, Phase II, II-IJKL (radial)	160
145b	Response spactra, Ultramar foundation, Phase II, II-IJKL (transverse)	161
146	Derived time histories of relative displacement for Ultramar foundation II-IJKL	162
147	Map showing locations of overpressure measurement stations	167
148	Air overpressure record at Station AM-4 for 1-ton Bravo detonation of Phase I (1 July 1970)	170
149	Air overpressure record at Station AM-4 for 10-ton Echo detonation of Phase I	170
150	Air overpressure record at Station AM-4 for Detonation II-ABCD of Phase II (18 August 1970)	177
151	Air overpressure record at Station AM-4 for Detonation II-EF of Phase II	177
152	Air overpressure record at Station AM-4 for Detonation II-IJKL of Phase II (11 August 1970)	177
153	Measured peak pressure vs distance for 1-ton Alpha detonation of Phase I	178
154	Measured peak pressure vs distance for 1-ton Bravo detonation of Phase I	178
155	Measured peak pressure vs distance for 1-ton Charlie detonation of Phase I	178
156	Measured peak pressure vs distance for 1-ton Delta detonation of Phase I	178
157	Measured peak pressure vs distance for 10-ton Echo detonation of Phase I	179
158	Phase I peak overpressures predicted and measured at scaled distance of 50 $ft/lb^{1/3}$	180
159	Comparison of airblast from underwater detonations and Phase I detonations of Project Tugboat at a scaled distance of 10 $ft/lb^{1/3}$	180
160	Peak pressure vs distance for Detonation II-ABCD	181
161	Peak pressure vs distance for Detonation II-EF	182
162	Peak pressure vs distance for Detonation II-IJKL	182
163	Impulse vs distance for 1-ton Alpha detonation	183
164	Impulse vs distance for 1-ton Bravo detonation	184
165	Impulse vs distance for 1-ton Charlie detonation	184
166	Impulse vs distance for 1-ton Delta detonation	184
167	Impulse vs distance for 10-ton Echo detonation	184
168	Positive impulse for Phase I events	185
169	Impulse vs distance for II-ABCD detonation	186
170	Impulse vs distance for II-EF detonation	186
171	Impulse vs distance for II-IJKL detonation	187
172	Station AM-2 record for Detonation II-ABCD, typical of stations to north of SGZ (14 August 1970)	187

FIGURES (Continued)

173	Station AM-3 record for Detonation II-ABCD showing slightly different wave form broadside to row (14 August 1970)	187
174	Station AM-2 record for Detonation II-EF showing two primary peaks in first positive pulse	188
175	Station AM-3 record for Detonation II-EF showing very complex first positive pulse	188
176	Station AM-9 record for Detonation II-IJKL showing two prominent peaks in first positive pulse as would be expected in direction perpendicular to one side of array (30 July 1970)	189
177	Station AM-2 record for Detonation II-IJKL (30 July 1970)	189
178	Station AM-10 record for Detonation II-IJKL (30 July 1970)	189
179	Plan view of instrumentation layout	193
180	Diagram of typical instrument canister installation	194
181	Instrumentation systems	195
182	Surface canister (WS-1) data from Charge II-D	195
183	Subsurface canister (UW-1) data from Charge II-D	196
184	Pressure and acceleration signals on Charges II-I and II-J	197
185	Pressure and acceleration signals on Charges II-K and II-L	197

TABLES

1	Tugboat charge designations and yields, and detonation dates	5
2	Surface temperature and rainfall summary for Kawaihae area	15
3	Stress-strain measurements	23
4	Actual charge depths and weights for Phase I	25
5	Actual charge depths and weights for Phase II	28
6	Actual charge loadings and depths for remedial detonations	32
7	Sequence of charge loading for Phase II	40
8	Drilling equipment used in remedial work	42
9	Summary of maximum wave heights, Phases I and II	89
10	Travel time of crest of maximum wave	101
11	Fishes inhabiting project site	106
12	Twelve most abundant fishes at project site as determined from fish counts at 11 stations in September 1969	108
13	Results of predetonation fish counts	109
14	Species and numbers of fishes collected after Phase I and Phase II detonations	112
15	Effects of detonations on caged fishes	117
16	Areas affected by Phase II detonations	119
17	Results of postdetonation fish counts	120
18	Summary of data for four underwater observations in pounds of fish per acre of reef area	122
19	Location of Phase I seismic stations	126
20	Location of Phase II seismic stations	126
21	Installation of sensors for Phase I	133
22	Installation of sensors for Phase II	135
23	Structure- and ground-motion maximum amplitude velocity predictions, Project Tugboat, Phase I	135
24	Structure- and ground-motion predictions, Project Tugboat Phase II (40-ton event)	136

TABLES (Continued)

25	Structure- and ground-motion measurements during Phase I	137
26	Structure- and ground-motion measurements during Phase II	138
27	Detonation summary and predicted overpressure for Phase I	165
28	Summary of Phase II detonations	165
29	Data for five-charge square array detonation, one charge in center, 64-lb TNT per charge, 6 ft burial depth	165
30	Tugboat Phase II range of expected overpressures	168
31	Window Census—Tugboat	168
32	Instrumentation for Phase I	169
33	Changes in instrumentation for Phase II	170
34a	Summary of results—Detonation Alpha	171
34b	Summary of results—Detonation Bravo	171
34c	Summary of results—Detonation Charlie	172
34d	Summary of results—Detonation Delta	172
34e	Summary of results—Detonation Echo	173
34f	Summary of results—Detonation II-ABCD	174
34g	Summary of results—Detonation II-EF	175
34h	Summary of results—Detonation II-IJKL	176
35	Comparison of predicted and measured peak overpressure—Phase I	179
36	Estimate of risk of damage from airblast for Detonation Echo	181
37	Estimate of risk of damage from airblast for Detonation II-IJKL	183
38	Summary of attenuation equations for airblast data	190
39	Comparison of airblast data from single- and multiple-charge detonations	190
40	Instrumentation results from Charge II-D detonation	195
41	Results of instrumentation on Charges II-I, II-J, II-K, and II-L	196

EERL TECHNICAL REPORT E-72-23
PROJECT TUGBOAT
EXPLOSIVE EXCAVATION OF A HARBOR IN CORAL

Section 1
Introduction

PURPOSE OF REPORT

This report presents the final results of Project Tugboat, the explosive excavation of a small boat harbor. The report includes details of site investigations, experimental programs and procedures, preliminary and final design, results and analysis of data, and a statement of conclusions for each technical program.

OBJECTIVES OF PROJECT

The U.S. Army Corps of Engineers (CE) and the U.S. Atomic Energy Commission (AEC) have been engaged in a joint research program since 1962 to develop the basic technology necessary to use nuclear explosives in conjunction with the construction of large-scale civil engineering projects. The Explosive Excavation Research Laboratory (EERL) of the Waterways Experiment Station (U.S. Army Engineer Nuclear Cratering Group at the time of the experiment) has been accomplishing the Corps' portion of this joint program. The major part of the program has been the execution of chemical explosive excavation experiments. In the past, these were preliminary to planned nuclear excavation experiments. The experience gained and the technology developed in accomplishing these experiments have led to an expansion of the EERL research mission. The mission has been expanded to include the development of chemical explosive excavation technology to enable the Corps to more economically accomplish Civil Works Construction projects of intermediate size. The Project Tugboat was planned to provide data that could be used in the development of both chemical and nuclear excavation technology. It was also the first experiment to be conducted at the specific site of an authorized Civil Works Construction project for the purpose of providing a useful portion of the planned project.

Therefore, the objectives of Project Tugboat can be generally stated as (1) to provide a useful portion of the authorized Civil Works lightdraft boat harbor planned for Kawaihae Bay, Island of Hawaii, State of Hawaii; (2) to test the applicability of the cratering technique for harbor construction in a coral medium at a reasonable scale with chemical explosives; and (3) to provide technical data which can be used in the design of other chemical or nuclear explosive harbor excavations.

SCOPE OF PROJECT TUGBOAT

Project Tugboat extended over about a 2-yr period from the initiation of planning to the completion of a postdetonation investigation program. A site investigation program was the first on-site work and was conducted during the summer of 1969. This was followed by a series of five site calibration detonations in November of 1969. Execution of these detonations was officially designated as Phase I of Project Tugboat. These tests were followed by a period of data evaluation and the subsequent reworking of the original conceptual design into the final explosive harbor design. Execution of this explosive excavation design occurred during late April and early May of 1970 and was officially designated as Phase II of Project Tugboat. During the summer of 1970, a breakwater was built to provide some protection to the excavated berthing basin. Because of a misfire and incomplete detonation of two of the charges during the execution of Phase II, a portion of the entrance channel did not meet the project criteria. A small remedial explosive excavation program was successfully executed during December of 1970 to clear the channel. This program was followed immediately by a postdetonation engineering properties technical program that extended in time through to early 1971. This report will cover all phases of the described work.

MAJOR TECHNICAL PROGRAMS CONDUCTED

Many programs of a technical nature were carried out during the 2-yr period. Some were one-time programs on one or two of the three detonation phases, while others were more or less continuous throughout the period of execution of the entire project. The programs conducted during each period of field operations are briefly described in the paragraphs that follow.

Site Investigations

A site investigation program was initiated during the summer of 1969 which included geophysical surveys of the project area, hydrographic and topographic mapping, geologic investigations, wave analysis for the proposed conceptual harbor design, collection of site meteorological data, archeological explorations and mapping, an initial documentation of the fish and other marine life in the blast area, and a preliminary structural engineering survey.

Crater Measurements

Engineering surveys were conducted following the Phase I, Phase II, and remedial explosive excavation detonations by the Honolulu Engineer District to determine the crater profiles and the resulting entrance channel and harbor basin dimensions.

Seismic Motion Measurements

A comprehensive seismic motion measurement program was undertaken during both Phases I and II. The objective of the Phase I program was to provide data as a function of yield, range, and depth of burst specific to the site that was subsequently used to determine the maximum safe yield for detonations in Phase II. During Phase II, measurements were made to verify safety predictions and to

provide seismic motion and structural response data as a function of range and firing conditions. The planned firing conditions were (1) four 10-ton charges in a row fired simultaneously, (2) four 10-ton charges in a row fired sequentially, and (3) four 10-ton charges in a square array fired simultaneously. As described in Section 2. problems occurred with the firing of items (1) and (2) which negated some of the objectives of the technical program.

The program was accomplished by personnel from the Waterways Experiment Station (WES) of the Corps of Engineers.

Structural Engineering Survey

John A. Blume & Associates, an engineering firm specializing in the effects of seismic motions on structures, was engaged to advise EERL in this vital area. The objective of the program was to assist in the determination of the maximum yield which could be safely fired during the Phase II harbor excavation detonations. The scope of the program was as follows:

1. To make an initial survey and examination of structures in the vicinity of the project site to ascertain present conditions (accomplished during site investigations).

2. To estimate the level of ground motion at which incipient architectural damage could be expected.

3. To make recommendations for changes in the planned ground motion and structural-response measurements to be made during Phase I to provide needed data.

4. To assess the results of initial survey and estimates based on the ground motion and building response recorded during Phase I, and to submit revised recommendations.

5. To resurvey structures following Phase II to determine whether any changes had occurred.

Intermediate Range Seismic Measurements

Seismic measurements were attempted by the University of Hawaii on other islands in the Hawaiian chain using instrument stations already established for a continuing earthquake study. Because of some operational difficulties, records suitable for a detailed analysis of the magnitude of motion were not obtained.

Close-in Air-Overpressure Measurements

A comprehensive program of ground level air-overpressure measurements was conducted during the execution of both Phases I and II by the Sandia Laboratory, Albuquerque, New Mexico. The objective of the Phase I program was to provide air-overpressure data as a function of yield, range, and depth of burst specific to the harbor site and the slurry explosive. These data were subsequently used in conjunction with other safety data to estimate the maximum safe yield for the detonations of Phase II. The objective of the program during Phase II was to verify the safety predictions and to provide data as a function of range and firing conditions. As described in Section 2, problems occurred with the firing of the first two detonations during Phase II which negated somewhat the comparison of air overpressure from a simultaneously fired row with that from a sequentially fired row of charges.

Fish and Wildlife Studies

A comprehensive program was performed by the State of Hawaii, Department of Land and Natural Resources, to determine the effects of the explosive cratering detonations on the marine environment in Kawaihae Bay. The program included:

1. A recording of the species, composition, and densities of marine life existing at the project site prior to the commencement of work by underwater transecting and photography by Scuba-equipped divers. This program was accomplished during the site investigations phase of the project.

2. A determination of the effects of the detonations in relation to the total number and/or poundage of fish and invertebrates killed or injured, the total area affected by the blast, and the distance from the blast center to which fish kills were effected.

3. A determination of the time required for and the nature of repopulation of the affected area.

Aerial Photography (Phases I and II) and Wave Measurements (Phase I)

ESSO Production Research, a division of Humble Oil Company, sponsored a program of motion picture aerial photography of the Phase I and II detonations and a wave measurement program during the Phase I detonations only. The purpose of the photography was to provide documentation of the late time crater formation process and to view the wave pattern produced by the detonations. The Phase I wave measurement program provided the first known wave data for underwater cratering detonations of significant yield.

Wave Measurements (Phase II)

The Coastal Engineering Research Center (CERC) of the Corps of Engineers conducted a wave measurement program during Phase II. The program was intended to be a follow-on to the program conducted during Phase I. Data from both programs are summarized in Section 3 of this summary report.

Pressure, Velocity, and Acceleration Measurements in Water Surface Layers

The Lawrence Livermore Laboratory (LLL) of the University of California conducted a program to test instrumentation designed to measure shock pressure, velocity, and acceleration in the surface water layer in an underwater cratering test such as Tugboat. The instruments were designed to make measurements extended in time in the very high pressure and acceleration environment encountered at the Surface Ground Zero (SGZ) location.

High-Speed Photography from Ground Stations

High-speed photography of all detonations was taken from ground stations by personnel of EERL. This photography was primarily for documentary purposes.

Postshot Engineering Properties Investigations

A program of drilling and sampling in the crater area was accomplished following the remedial explosive excavation detonations in the berthing basin area and in the channel area to try to determine the extent of fracturing of the coral. Results of this program are reported here except for final results of surveys taken after 1 yr and after a major storm to determine

long-term changes in the bottom conditions.

SUMMARY OF RESULTS

Project Tugboat detonations were executed in three phases. Detonation yields and dates of detonation are given in Table 1. These detonations successfully produced a harbor basin and entrance channel which exceeded the design requirements in both width and depth. The detonations resulted in a channel varying in width from about 150 to 260 ft at a minimum project water depth of 12 ft. The berthing basin is almost a square area 400 ft on a side at the 12-ft water depth contour. The minimum channel design width was 120 ft and the berthing basin design requirement was a square 240 ft on a side.

The site medium is a weak coral. Tests on cores recovered in preshot drilling show a compressive strength ranging between 760 and 1738 psi, a mean bulk dry density of 1.37 g/cm^3, a mean saturated bulk specific gravity of 1.76 g/cm^3, and a mean porosity of 49%. The reef mass possesses, by an indeterminate amount, a lower mean strength, a lower mean density, and a higher mean porosity than the tests indicate.

Drilling of the charge emplacement holes during Phase I was done from a causeway which was later removed by dragline. Phase II holes were drilled from a jack-up floating platform. The aluminized ammonium nitrate slurry

Table 1. Tugboat charge designations and yields, and detonation dates.

Charge designation	Charge yield (lb)	Date of detonation	Remarks
	A. Phase I		
1a (Alpha)	2,000	0901 6 Nov '69	—
1b (Bravo)	2,000	1101 6 Nov '69	—
1c (Charlie)	1,975	1001 4 Nov '69	—
1d (Delta)	1,950	0901 5 Nov '69	—
1e (Echo)	20,200	1101 7 Nov '69	—
	B. Phase II		
II-ABCD	52,000	0916 23 Apr '70	Charges C and D did not detonate full-yield
II-EF	40,000	0901 28 Apr '70	—
II-IJKL	80,000	0901 1 May '70	—
II-GH	20,000	0901 8 May '70	Charge G deflagrated
	C. Remedial Detonation		
G1, G2 C1 to C13 A1	14,800	8 Dec '70	—

blasting agent was pumped into the charge canisters after the canisters had been placed in the drilled hole and stemmed. The slurry was pumped with a truck-mounted pump through a rubber hose down a 4-in. fill line that extended from the top of the canister to the surface.

Calibration tests provided information that permitted a redesign of the harbor excavation using a little more than half the original drill holes and half of the quantity of blasting agent estimated to be required in the preliminary design. The craters were broad and shallow with no lips and were actually better suited to harbor excavation in this situation than the less wide and deeper craters typical of dry land cratering detonations. The cratering mechanism appears to be one of densification of the coral through crushing and subsequent settling. Aerial photography showed that the crater remains devoid of water for several seconds after detonation and then is filled by coral and water as the crater walls fail into the crater. Wave staffs that were placed in the coral near the craters moved toward the crater before being overrun by the outrunning water wave (further evidence of this failure process).

The 10-ton Echo crater had a radius to the 12-ft depth contour of about 60 ft. This parameter was used to design the harbor detonations. Spacing between charges was set at two times this number.

Low-order detonation of Charges II-C and II-D and the deflagration of Charge II-C apparently was due to inadequate boostering. These misfires made it necessary to do some small remedial detonations which were successful in clearing the channel.

The final channel surface is flat, level, and sandy, with scattered small coral blocks lying on it. Foundation conditions in the channel are similar to those in medium to dense sand. A short distance outside the channel, natural coral conditions exist. The material in the channel is more homogeneous than that of the natural coral reef. In the berthing basin area, a layer of soft mud from 2- to 9-ft thick lies at the surface. This layer is not present in the outer part of the channel.

Crater zones were not satisfactorily defined by the drilling program. They were crudely defined by the acoustic profiling surveys; the true crater by the limit of dipping beds within the crater, and the rupture zone by the limit of the basalt reflection. To define the true crater specifically by drilling would be very difficult.

A long-term settling effect in both the channel and the surrounding natural coral was detected by surveys taken during May and December 1970. On the average the surface was lowered during this 7-mo period by 1 or 2 ft. This effect supports results of the acoustic profiling, which indicate that the natural coral was shattered by the blasts to large distances out from and below the cratered channel.

The photography taken in the wave measurement programs aided in an understanding of the crater formation process and showed the wave patterns generated by the detonations to be very complex. The wave of maximum height was found usually to be the first wave of the explosively generated system, and it is characterized by a high crest followed by a long, shallow trough. The maximum wave

height generated was during the II-EF detonation and was about 11 ft in height at the closest point of measurement (230 ft). Scaling relationships were developed for predicting wave height and travel time.

The programs to determine the effect of the detonations on the marine environment were very comprehensive. The marine life at selected locations was observed and recorded during and following the major detonations. The distances from the detonations to which fish kills and injuries were effected were determined by the anchored fish cage technique. Also, the dead and stunned fish were picked up immediately following each detonation; then they were studied and recorded.

A total of 111 different species representing 34 families of marine fishes was found at the project site through underwater observations by divers and through collections of dead and injured fishes after the detonations. Of the 76 species that were recorded by the divers, 37 were not found during postdetonation collections, and conversely, 35 of the 74 species found during postdetonation collection activities were not observed during the underwater observations. These discrepancies were attributed to the limitations inherent in the observation and collection methods that were employed.

For the large detonations of Phase II, the distances to which all fish in fish cages were killed were 100 ft for detonation II-ABCD, 120 ft for detonation II-IJKL, and 210 ft for detonation II-EF. The maximum distance to which any fish were killed or injured probably did not exceed 300 ft on any of the three detonations.

As estimated from the collections made following the detonations, the families of fishes most affected within the area of dead and injured fish were squirrelfish, butterfly fish, damselfish, surgeonfish, cardinal fish, and the puffer. Not all fishes collected following the detonations were dead. Some were just stunned. As a test, a live but stunned fish that was picked up was kept in a tank for several weeks and appeared to be in good health at the end of that time. The observation data indicate that segments of the project site still containing coral (i.e., immediately adjacent to the blasted channel and berthing basin) are being rapidly repopulated from adjacent unaffected areas. These observations also show that the detonations altered the immediate areas of the channel and berthing basin from one of clear water and hard, coral bottoms to one containing a silt bottom and murky waters similar to those found at the Phase I detonation site prior to the blasts. It is suspected that the final species composition and density in these areas will reflect the changes that were incurred to the habitat.

Instrumented ground-motion seismic stations in the vicinity of Project Tugboat were observed to respond in a fairly uniform manner. Maximum peak particle velocities recorded during the 1-ton events ranged from about 1.5 cm/sec at a distance of about 1500 ft to about 0.1 cm/sec at a distance of 8200 ft. Data recorded during the 10-ton detonation ranged from about 4 cm/sec at a distance of 1800 ft to about 0.4 cm/sec at a distance of 8000 ft. Finally, 40-ton amplitudes diminished from about 6 cm/sec at a distance of 2600 ft to about 0.8 cm/sec

at a distance of 7600 ft. No reliable seismic amplitude dependence upon depth of burst could be established. Two yield scaling methods verified one another in defining a yield scaling factor of about $W^{0.52}$. The II-EF sequential detonation produced measurably lower ground motions than the expected motion for simultaneous detonation of the same charges.

Predictions of building response to the Tugboat detonations identified the Ultramar Warehouse to be the critical structure from an architectural damage standpoint. Detonations during Phase II were limited to 40 tons to minimize the possibility of any damage. No damage claims were filed as a result of any of the detonations.

Positive peak airblast overpressures and positive phase impulse from the Tugboat Phase I explosions were about five times those predicted on the basis of measurements made from cratering explosions in soil. Peak overpressures estimated by applying multiple-charge overpressure amplification factors to the Echo detonation results were small enough that the possibility of blast damage on the Phase II detonations was expected to be acceptable.

Peak overpressures for Detonation II-ABCD, II-EF, and II-IJKL multiple-charge Phase II detonations were approximately 1, 1.4, and 2.5 times that for a single-charge detonation having a yield equal to one of the charges in the multiple-charge array. Positive impulses were about 2, 2, and 4 times that for a comparable single charge. These data indicate that in Detonation II-ABCD, Charges II-C and II-D contributed very little to the positive phase impulse observed. The data pertaining to the reduction of overpressure from the delay of successive charge detonations in a row were not adequate to draw more definite conclusions.

No glass was broken and the estimates of probability of breakage based on maximum measured peak overpressures was never greater than 5 panes per thousand.

Charge II-D SGZ area was instrumented for pressure, velocity, and acceleration measurements in the water. Peak velocities of 66 and 61 ft/sec were measured by the subsurface and surface gages, respectively. Peak accelerations were 356 and 311 g, respectively. The subsurface pressure gage measured 414 psi. The II-IJKL detonation was also instrumented, but accelerations were nearly double the design limit of the gage canisters. These accelerations resulted in early destruction of the canisters and the loss of considerable data. Peak accelerations of 2780 g and pressures of 2513 psi were recorded. The experience was very useful in developing LLL's capability to instrument surface water environments. It was fortuitous for this program that Charge II-D did not go full-yield as much more information was obtained about the overall capabilities of the instrumentation.

PROJECT ORGANIZATION

The organization for the planning and the execution of Project Tugboat is shown in Fig. 1. Explosives Safety, arming and firing technical support was provided by the Lawrence Livermore Laboratory. Operational support was provided by the Honolulu Engineer District of the Corps of Engineers. This included Contract

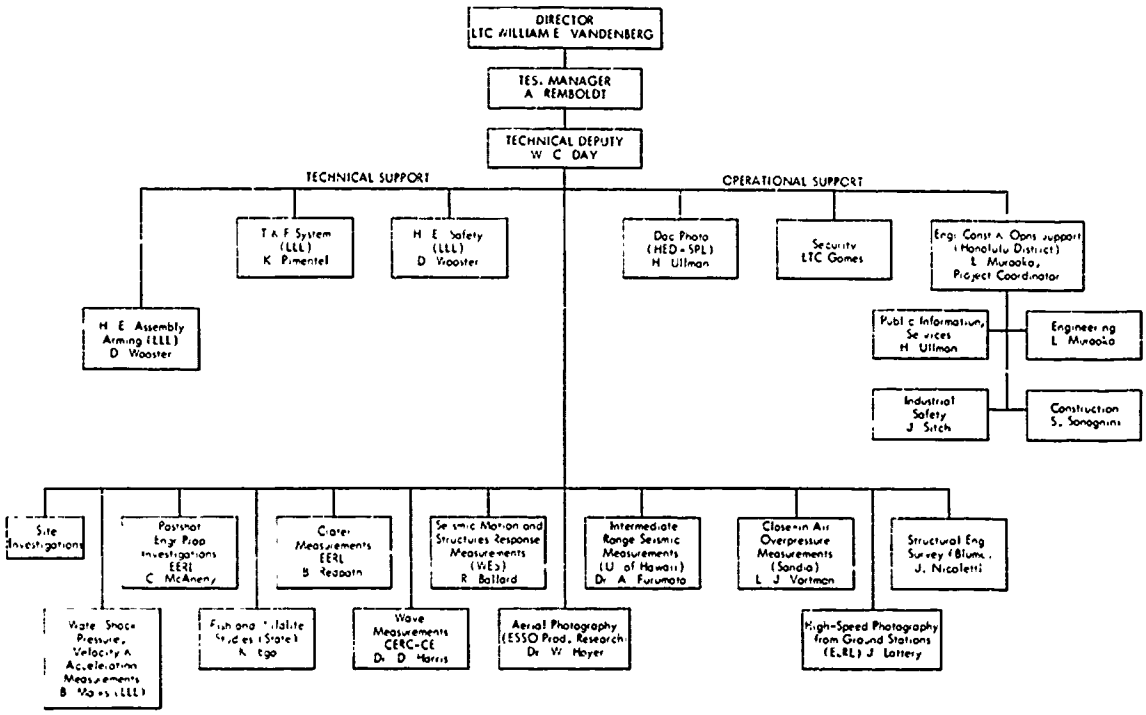

Fig. 1. Project Tugboat organization.

Administration and the associated Engineering Construction and Operations work, industrial safety, security, public information services, and documentary photography. A separate contract was negotiated with the Los Angeles District to provide documentary photography of construction and execution of the Project. The explosives contractor was the Dow Chemical Company, and the charge emplacement construction work and break water construction work was performed by the Mile High Drilling Company of Boulder, Colorado.

Section 2
Construction, Execution, and Postdetonation Investigations

LOCATION

Project Tugboat is located at the site of a planned small-boat harbor on the Island of Hawaii, State of Hawaii (see Fig. 2). The small-boat harbor is near the village of Kawaihae on the northwest coast of Hawaii and in Kawaihae Bay from which the village gets its name. The Kawaihae Small-Boat Harbor was authorized as a Federal Civil Works Project by the Congress of the United States in the Rivers and Harbors Act of 1965 and is planned as a jointly-funded Federal and State project in the statewide system of small-boat harbors.

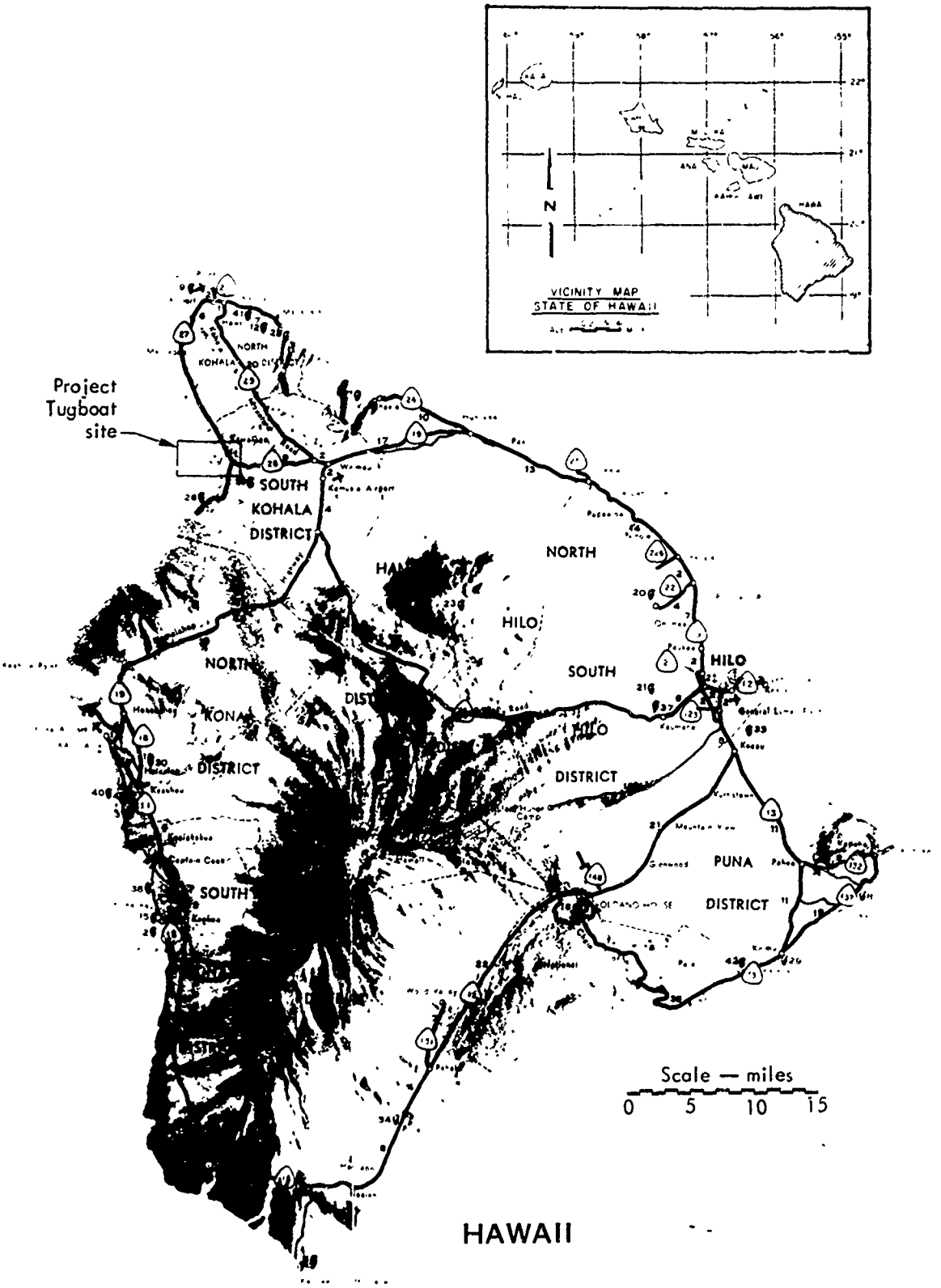

Fig. 2. Project Tugboat site located on vicinity map.

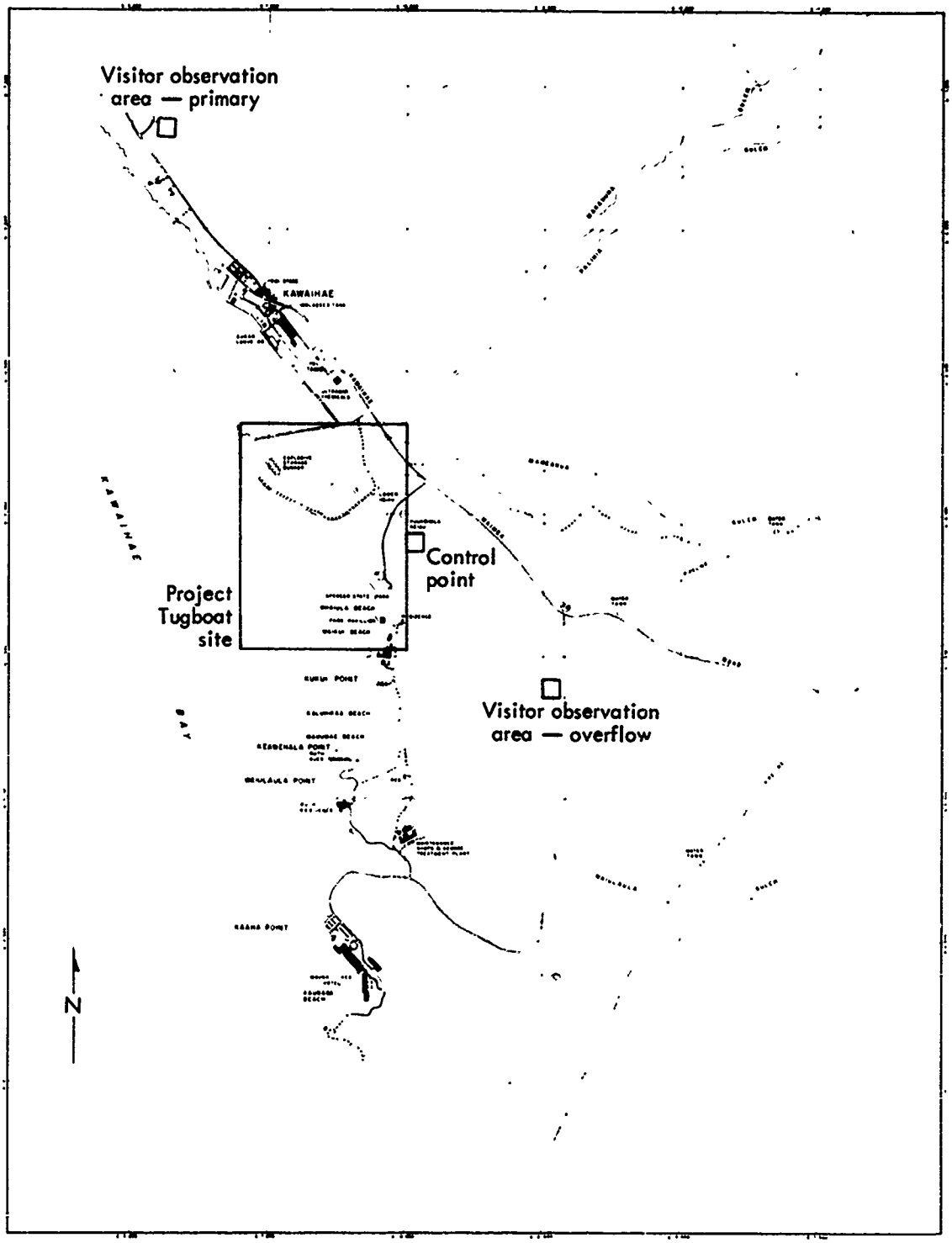

Fig. 3. Map of general site, Project Tugboat.

(a) South of harbor site.

(b) Adjacent to harbor site.

(c) North of harbor site.

Fig. 1. Coastal area near harbor site (Location).

A local site map is presented in Fig. 3. There is an existing deep-draft harbor at the town of Kawaihae (Fig. 3) with an adjacent coral fill area. The project site is to the south of this fill area in shallow water and in a region of inactive-to-active coral growth. The site is located about 10 road miles west of the town of Waimea on State Route No. 26 and 19 miles south of the town of Hawi on State Route No. 27. Aerial photos of the coastal area near the harbor site are shown in Fig. 4. The village of Kawaihae consists of wooden frame dwellings, two general stores, a gas station, and some other local businesses. In addition to the village, there is a wide variety of structures in the harbor facility, including storage tanks for oil and molasses, a bulk sugar warehouse and associated conveyor system for loading ships, a metal warehouse structure, a large service terminal, and a combination poured concrete and concrete block bulk chemical warehouse. Adjacent to the small boat harbor area is a county park with a swimming beach, stone and wood pavilion, and rest room and shower facilities. On down the coast there are several houses and a large resort hotel facility. All of these structures were in the zone of concern for airblast and ground-motion effects and had to be monitored during the large-yield detonations.

In addition to these structures there are archeological structures of historical interest adjacent to the harbor area for which special investigations were conducted. These "heiaus" are discussed later in this section.

SITE DESCRIPTION

General

The Island of Hawaii, like all the Hawaiian islands, was constructed by the geological process of volcanism, and is composed predominantly of basaltic rock. In places along Hawaiian coasts where conditions are favorable, coral reefs have grown. Such conditions exist in the Kawaihae area, so that the basic geologic situation at the Tugboat site is one of a coral reef founded at some depth upon basaltic rock, the latter being continuous with the basalt which forms the adjacent land mass.

The Kawaihae coral reef is not continuous up and down the coast of Kawaihae Bay, but is restricted to a stretch slightly less than 2 miles long extending from the vicinity of Kawaihae village southward to about Waiulaula Point (Fig. 3). The reef averages about 3000 ft in width from the shoreline to its outer edge. Before the construction of the Kawaihae deep-draft harbor, the shoreline lay slightly to the southwest of the Kawaihae-Waimea road between Kawaihae village and Makeahua stream (Fig. 3). The deep-draft harbor was constructed in 1957-1959 by excavating the coral reef with a cutter-type dredge to a depth of 39 ft. Material dredged from the harbor was used to make the land fill on which the present harbor terminal facilities, oil storage tanks, etc., are located. Excess dredged material was dumped to form the present coral stockpile area, the outer edge of which was revetted with large basalt stones. The Project Tugboat site was

located in the coral reef seaward at this revetment (Fig. 5).

Meteorology and Climate

The climate of the Hawaiian Islands is governed by the northeast trade winds, which blow nearly continuously from an east-northeasterly direction during most of the year. Marked differences therefore occur on all the islands between the windward (easterly and northerly) and the leeward (westerly and southerly) sides.

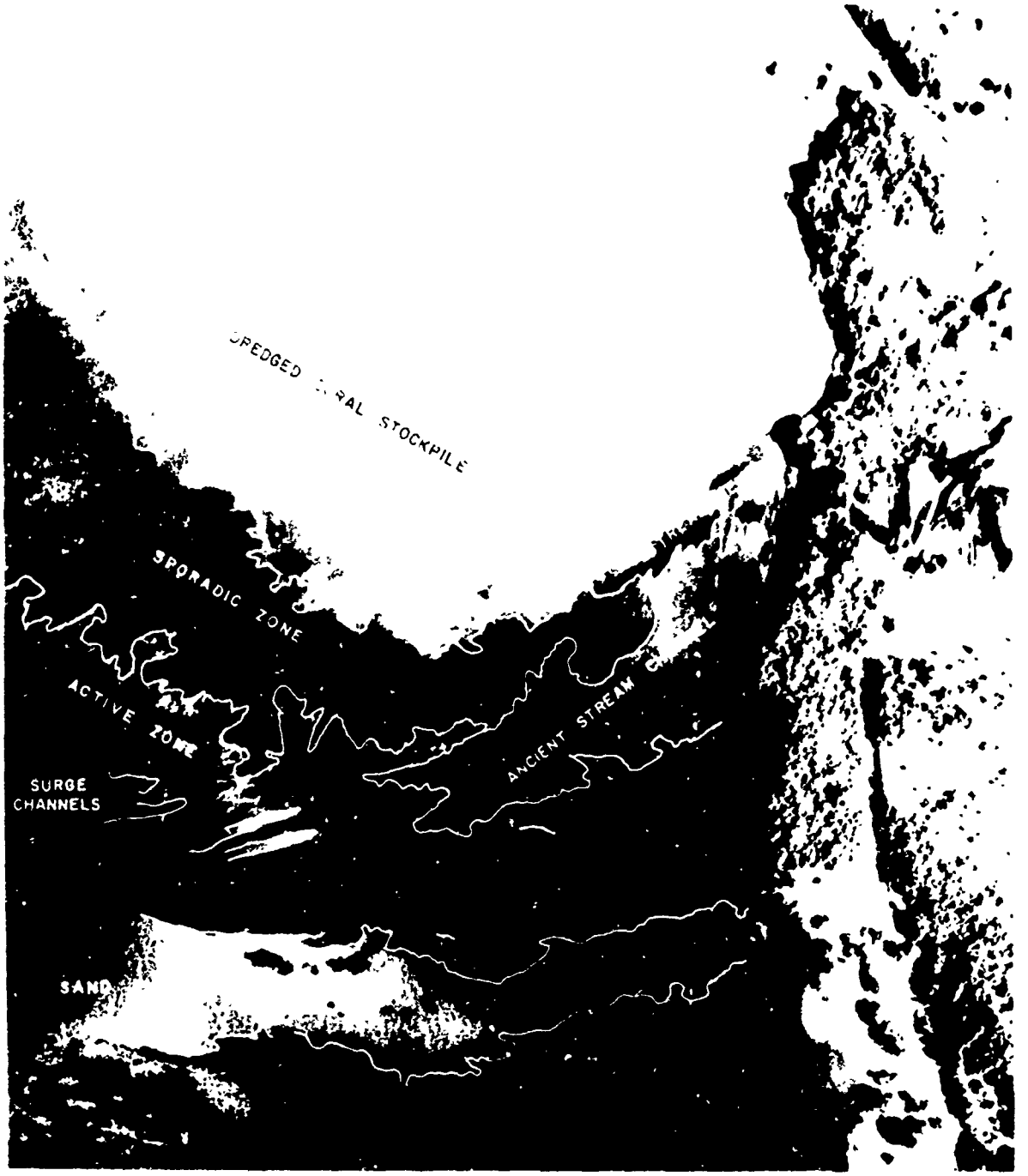

Fig. 5. Aerial photo of Tugboat site showing zones of coral growth and sedimentation.

Table 2. Surface temperature and rainfall summary for Kawaihae area.

Month	Average high temperature (°F)	Average low temperature (°F)	Average rainfall (in.)
January	80.8	63.4	3.14
February	80.4	63.0	2.54
March	80.4	63.9	2.22
April	81.4	65.3	1.44
May	83.4	67.1	0.69
June	85.4	68.9	0.18
July	86.4	70.1	0.43
August	87.0	71.0	0.35
September	86.7	70.0	0.25
October	85.5	69.1	0.87
November	82.9	67.0	1.52
December	80.6	64.8	2.70
Annual	83.4	67.0	16.33

The windward sides experience abundant rainfall and nearly continuous moderately rough seas; they therefore have thick soils with abundant vegetation steadily flowing streams with well-defined stream valleys, and bold, cliffed sea coasts. The climate of Kawaihae is typical of the leeward sides. During most of the year rainfall is sparse and winds are light and variable. The area is semidesert: sunshine is plentiful, soil is thin, vegetation is scanty and composed of hardy, drought-resistant plants. Temperatures vary from warm during the night to hot during the day. A summary of surface temperature and rainfall data for the Kawaihae area is given in Table 2. The daily cycle of warming and cooling of the land results in sea breezes during the day and land breezes at night. A typical day begins with westerly winds at 5 to 8 mph at 9 to 10:00 a.m. These winds blow continuously throughout the day until 7 to 10:00 p.m. during which time the winds usually shift to easterly at 7 to 10 mph and continue until 3 to 4 hr after sunrise. During wind shift times, the wind speed is rather light and the direction is quite variable. During the winter months, the steady pattern of the trade winds occasionally breaks down for periods of several days. During these periods "Kona" (leeward) storms may occur, bringing fresh to strong southwesterly winds and heavy rains.

Hydrography

The ocean bottom at the site was very irregular because of numerous coral heads, some of which caused variations of as much as 12 ft within a few feet horizontally. One such coral head is shown in Fig. 6. Numerous coral heads can be seen on careful examination of the aerial view in Fig. 5. Water depths over the coral at the Tugboat site ranged in general between 4 and 12 ft.

Fig. 6. Typical coral head in Project Tugboat area.

Hydrographic fathometer surveys were run in May 1969. The resulting bottom contour map is shown in Fig. 7. This map does not show the highly irregular surfaces of individual coral masses.

Tidal ranges in Kawaihae Bay are low, with a maximum of about 3 ft. Tides show diurnal inequality. Mean lower low water (MLLW) is taken as the datum for all ocean depths and land elevations in the area.

Geology

The geology of the Tugboat site is essentially that of the coral reef, since the underlying basalt foundation lies at depths greater than any of the explosive detonations and greater than any of the exploratory borings drilled either before or after the shots.

Coral is composed of the limy skeletal materials secreted by numerous species of marine invertebrate animals, and also by symbiotic lime-secreting algae. Collectively these animals and plants form colonies, and an assemblage of these colonies forms a reef. A coral reef is a complicated ecological system, and the limy material shows a complicated variety of structures, even though the structures are all made of the same material, calcium carbonate. Some colonies are massive and domelike, some are branching and shrublike, with a fragile skeleton that is easily shattered or broken. The substructure of a visible coral reef represents reef materials that grew in the past. Numerous animals besides the actual coral-formers live in and around the coral reef. On death, the calcareous remains of these organisms (shells, spines, etc.) combine with broken parts of the more fragile coral structures to form calcareous sand and silt, which filter into and partially fill voids in the coral framework. At some time in their geological evolution, reefs and their infilling sediment may, but do not necessarily, become cemented together by deposition of a calcareous cement, resulting in formation of a solid limestone rock.

Coral-forming organisms live and grow only in clear warm saline water. Fresh water and turbidity inhibit their growth or kill them. In a land-fringing reef such as at Kawaihae, fresh water and turbidity are introduced periodically by silty runoff after exceptional Kona storms. There is thus a cycle: growth, killing storm, death; period of stagnation; reinvasion by new living colonies; renewed growth. The result of such cycles in the past has been discontinuities in the reef substructure.

Longitudinal openings across the surface of a reef, normal to the shore, are a common feature. These "surge channels" occur at semiregular intervals, and

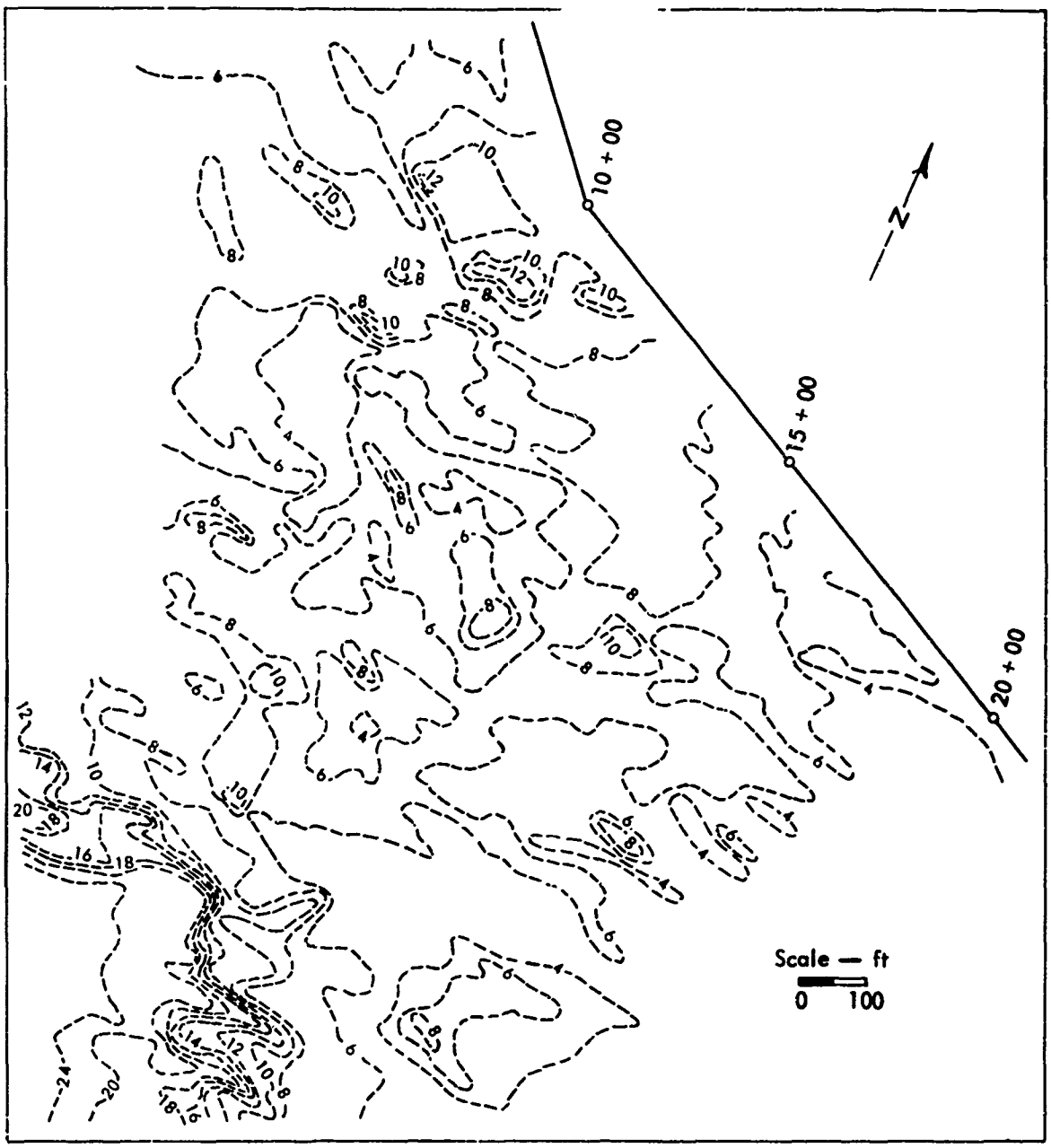

Fig. 7. Tugboat site hydrography, May 1969 (contours represent depths in feet below Mean Lower Low Water; map does not show all details of irregular coral heads).

have dimensions of a few feet. The floors of such channels are flat or slope gently seaward, and are covered with coral sand. Similar but larger channels occur opposite fresh-water springs or the mouths of fresh-water streams.

The Kawaihae coral reef is typical of the generalized reef described above. The construction of the Kawaihae deep-draft harbor in 1957 to 1959, however, altered part of the Kawaihae reef, including the portion in which Project Tugboat

was sited. The dumping of the coral stockpile covered the shoreward portion of the reef. Pumping of dredged fines to the area seaward of the stockpile produced a deposit of fine sediment which infiltrated the upper part of the reef structure, and resulted in the establishment of a series of concentric zones (Fig. 5), as described below.

Adjacent to the coral stockpile the sediment zone has blue-gray silty sand to depths of 2 to 8 ft. The water is continuously turbid, and there is no living coral.

Outward from the sediment zone, in the sporadic zone, the ocean floor is covered by a brown, slimy seaweed, and the water is turbid most of the time. Only hardy coral types grow, forming large, knobby heads.

Further to seaward the active zone was unaffected by the earlier deep-draft harbor construction. Active growth is occurring: some colonies are dome-shaped, some are branching and thick, others are branching and delicate. The reef is incised by surge channels.

In the period since deep-draft harbor construction, the winnowing action of the surf has washed the fine sediment out of the outer zones, but not out of the sediment zone.

The geological investigations prior to Project Tugboat, described below, showed the coral at the site to have undergone no secondary calcification or cementation, and to be characterized by loosely bound, interlocking, shrublike branches. The material was soft (for rock), easily scratched, and subject to crumbling under small loads. The reef was determined to be Recent in geologic age, possibly only a few hundred years old.

Geologic Investigations

A drilling program was carried out in June and July of 1969 to investigate subsurface conditions at the Project Tugboat site. Fifteen borings were drilled to depths as great as 76 ft below MLLW (Fig. 8). Ocean-floor conditions were studied by divers at each hole site to select the best position for the drilling scaffold, to photograph coral outcrops, and to sample ocean-floor materials. A combination of split-spoon drive sampling, 4-in.-diameter core drilling, and Denison sampling was used. Some intervals were washed and jetted.

All told, 687 ft (linear) of hole were drilled, of which 304 ft were core-drilled. All holes required casing to their full depth except for the final drill run or two. From the 304 ft in which coring was attempted, 123 ft of material was recovered (40% recovery). Only 7 ft of core was recovered in lengths of 6 in. or more, and the longest piece recovered was 1.6 ft. Typical core recovery is illustrated in Fig. 9.

The poor core recovery is attributable to the discontinuous nature of the reef structure, and is compatible with results experienced during construction of the Kawaihae deep-draft harbor, during which about 3 million yd^3 of material was excavated without the need for blasting except in a small area of the entrance channel. Nine-tenths of the excavated material was soft enough to cause little wear on the dredge cutterheads. Ten percent or less, principally in the seaward areas, was dense coral which caused substantial wear on the cutterheads.

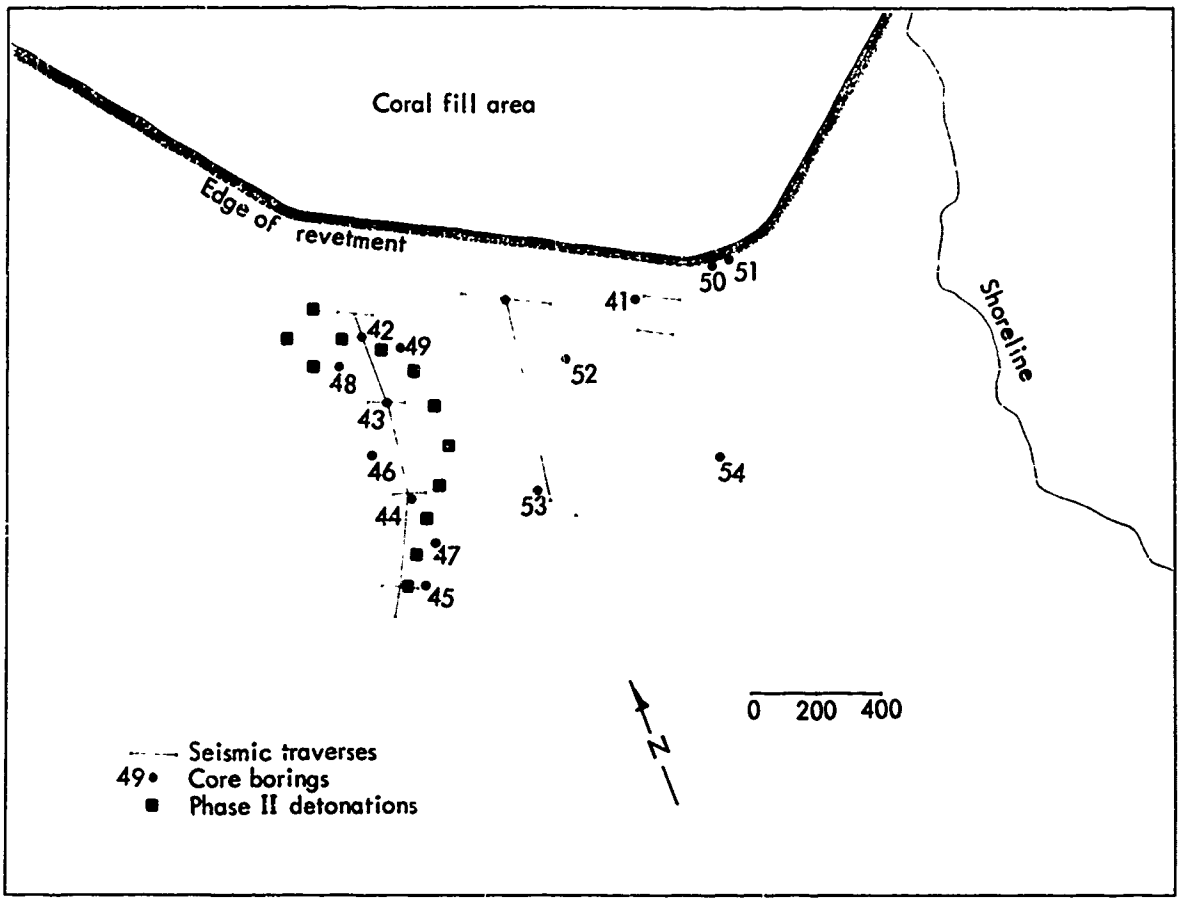

Fig. 8. Exploratory borings and seismic traverses, Project Tugboat site.

Physical Testing

A limited amount of testing of the physical properties of the coral material was carried out, with the following results.

Unconfined Compressive Strength

Samples: Rectangular blocks, average 1-1/2 × 1-1/2 × 2-1/2 in., cut from core from two of the borings

No. of tests: 10

Direction of application of stress: Some parallel, some normal to coral cellular structure

Mean strength: 1080 psi

Maximum strength: 1738 psi

Minimum strength: 760 psi

Mode of failure: Crumbling

Specific Gravity

Procedure: ASTM Standard, method C-127 (Specific Gravity and Absorption of Coarse Aggregate)

Source of samples: Coral samples collected from walls of surge channel (comparable to core samples)

No. of tests: 5

Results:

	Mean	Maximum	Minimum
Bulk specific gravity	1.37	1.54	1.27
Bulk specific gravity (saturated surface-dry basis)	1.76	1.89	1.65
Apparent specific gravity	2.24	2.46	1.98
Absorption, percent	28.3	38.4	22.5

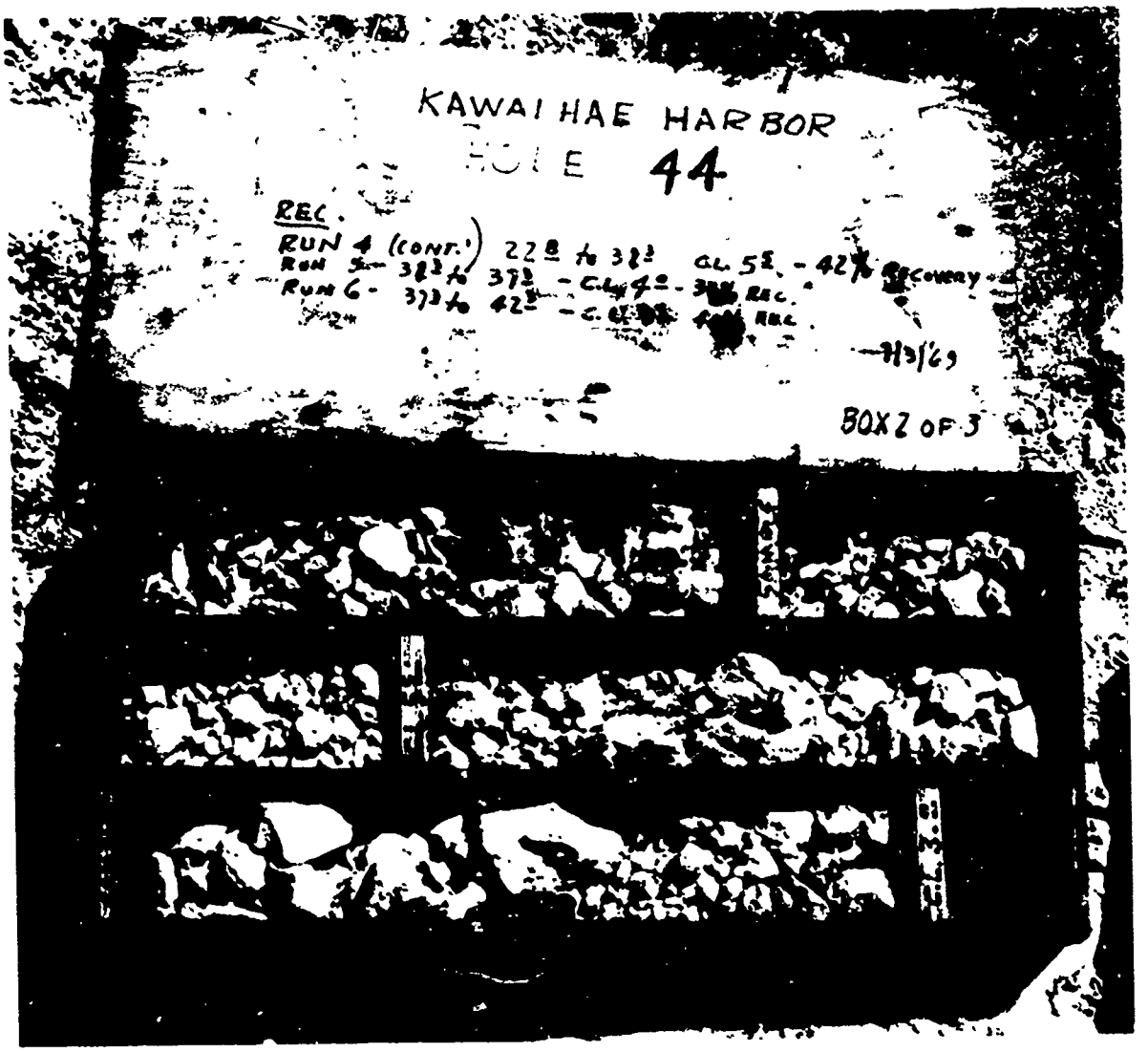

Fig. 9. Typical drill core recovery from exploratory borings.

Remarks: ASTM "bulk specific gravity" is essentially the same as bulk dry density, expressed in metric units. The mean bulk dry density of the samples was thus 1.37 g cm^3 or 85.5 lb/ft^3. The ASTM "apparent specific gravity" is the same as apparent specific gravity as defined in Engineer Manual EM 1110-2-1906 (Ref. 1) and reflects the presence of microscopic voids in the material. It would equal the specific gravity of the substance composing the coral (chiefly aragonite, orthombic calcium carbonate, spec. grav. 2.93, according to X-ray diffraction analysis of a core sample at LLL) if there were no voids.

Unit Weight (dry)

Procedure: EM 1110-2-1906 (Ref. 1)

Samples: Same as for unconfined compressive strength, above

No. of tests: 2

Results: 72.4 lb/ft^3, 66.8 lb/ft^3 (both oven-dry); mean 69.6 lb/ft^3.

Remarks: This test is essentially the same as the bulk specific gravity test above. The difference in mean values apparently represents variability of material.

Porosity

Procedure: EM 1110-2-1906 (Ref. 1)

Tested at Honolulu by Honolulu Engineer District (HED):

Samples: As for unit weight, above

No. of tests: 2

Results: 45%, 64%, mean 54.5%

Tested at Livermore by NCG (now EERL):

Samples: Core samples

No. of tests: 5

Results: Maximum 56%, minimum 37%, mean 49%.

Remarks: These results measure only the porosity of the laboratory samples due to small voids within the coral material. The porosity of the reef would be greater, since it would be due as well to the macroscopic voids between various coral branches, etc.

General Remarks: All test values are valid only for the laboratory samples, not for the reef mass as a whole, because of the open, branching structure of the latter. (In effect, the lab samples are not truly representative of the reef mass as a whole.) The reef mass possesses, by an indeterminate amount, a lower mean strength, lower mean density, and higher mean porosity than the test values indicate.

Pressure-Volume Measurements (Tested by LLL)[2]

Procedure: Piston-cylinder device where the advance of the piston into the cylinder is monitored as the pressure is varied (see Ref. 3 for details of the procedure).

Remarks: LLL was interested in knowing the high pressure mechanical properties of coral for possible future reference. The samples used in these tests were taken from drill hole No. 45, between 35 and 60-ft depth. They were received in an unsaturated condition and were completely saturated in seawater before tests were done. The samples tested had an initial density of 1.88 ± 0.03 g/cm^3, a bulk modulus of 50 kbar and a water content of 28.3% or 52% by volume; they contained no gas-filled porosity.

Results: The loading and unloading pressure-volume data are presented in Fig. 10.

Stress-Strain Measurements (Tested by LLL)[2]

Procedure: Both Brazil and triaxial tests were performed at confining pressures ranging up to 3.5 kbar using standard techniques (see Ref. 4).

Remarks: Test data are summarized in the Table 3 and plotted in Fig. 11.

Geophysical Investigations

A seismic refraction survey was made at the Tugboat site area in May 1969 (Fig. 8). Six 110-ft lines and one 275-ft line were run parallel to the revetment, one 650-ft line was run oblique to the revetment, and an 825-ft traverse made up of three 275-ft segments was run oblique to the revetment and along the then-proposed channel alinement.

All lines showed low-velocity material at shallow depths, with P-wave velocities

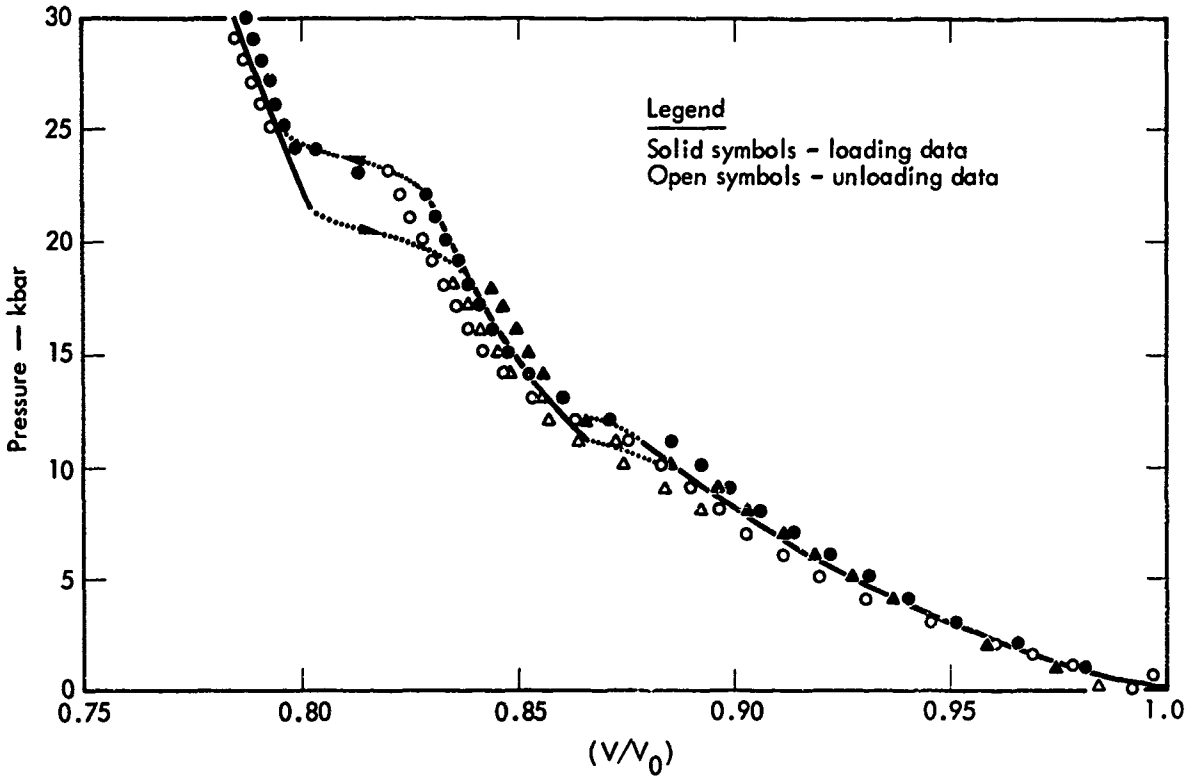

Fig. 10. Pressure-volume data for Tugboat coral (samples from Hole No. 45, 35- to 60-ft depth).

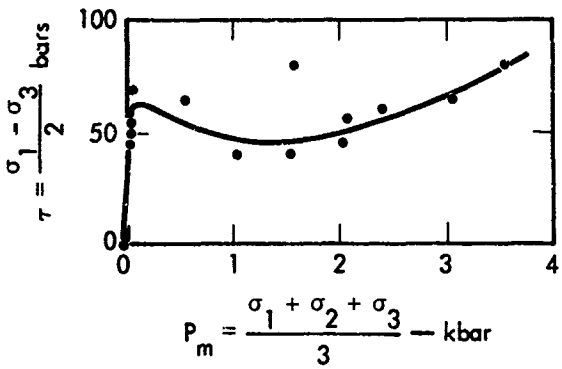

Fig. 11. Stress-strain data for Tugboat coral (samples from Hole No. 45, 35- to 60-ft depth).

in the range of 5100 to 6600 ft/sec (only slightly above the velocity of water, which is about 5000 ft/sec). This material represents the coral reef. Only the 650-ft line effectively explored material deeper than 100 ft below the ocean floor. This line detected the presence of higher-velocity material at about 70-ft depth, 150 ft from the revetment, sloping down to 110-ft depth 750 ft from the revetment. This material had an average velocity of 10,650 ft/sec and was presumed to be the basalt foundation on which the coral reef rests. This higher-velocity material was detected only on this one line.

The seismic data suggested considerable lateral variation within the coral. The highest velocity within the coral, 7240 ft/sec, was measured along the long axis of a single continuous coral reef.

Wave Analysis

Wave action in the Kawaihae Bay area was analyzed to provide criteria for the design of the explosively excavated harbor. The study findings were that the

Table 3. Stress-strain measurements.

Test type	Depth (ft)	σ_1 (kbar)	σ_2 (kbar)	σ_3 (kbar)	$\frac{\sigma_1 - \sigma_3}{2} = \tau$ (kbar)	$\frac{\sigma_1 + \sigma_2 + \sigma_3}{3} = P_m$ (kbar)
Brazil	35-40	0.08	0	-0.03	0.055	0.03
Brazil	35-40	0.07	0	-0.02	0.045	0.03
Triaxial	35-40	0.14	0	0	0.07	0.05
Triaxial	35-40	0.12	0	0	0.06	0.04
Triaxial	45-53	0.12	0	0	0.06	0.04
Triaxial	45-53	0.11	0	0	0.06	0.04
Triaxial	45-53	0.09	0	0	0.05	0.03
Triaxial	45-53	0.630	0.50	0.50	0.065	0.54
Triaxial	35-40	1.08	1.00	1.00	0.040	1.03
Triaxial	45-53	1.58	1.50	1.50	0.040	1.53
Triaxial	45-53	1.67	1.50	1.50	0.080	1.56
Triaxial	45-53	2.11	2.00	2.00	0.055	2.04
Triaxial	35-40	2.095	2.00	2.00	0.045	2.03
Triaxial	45-53	2.47	2.35	2.35	0.060	2.39
Triaxial	35-40	3.13	3.00	3.00	0.065	3.04
Triaxial	45-54	3.68	3.50	3.50	0.090	3.56

Remarks: The average failure envelope occurs at a very low but more or less constant shear stress of approximately 50 bars up to a mean pressure, P_m, of about 2.5 kbar. Beyond this pressure the shear stress seems to increase slightly. The possible slight decrease followed by an increase in shear strength with pressure is very uncommon with the exception of several high-porosity tuffs from the Nevada Test Site which were tested in both the saturated and dry condition. It is believed that initially this effect is due to the progressive collapse of the matrix framework into the existing pore volume with increasing dilational strain (1.5 kbar and later by the added distortional strain 1.5 kbar). Thus, at the higher confining pressure, the material has a higher initial density and work-hardens faster. It can be expected that, at some mean pressure greater than 4 kbar, this envelope must assume the more normal behavior and become asymptotic to some unknown higher value of shear stress. With the exception of the samples deformed by triaxial and Brazil tests at atmospheric pressure, the material behaved in a ductile fashion in all cases.

theoretical maximum waves anticipated to act on the breakwater are between 6 and 8.5 ft. The maximum wave height that can be expected at the mouth of the entrance channel is 18 ft (nonbreaking wave). The critical direction of waves are N67°30'W with a period of 8 sec for the breakwater, and N67°30'W with a period of 15 sec at the entrance to the channel.

Archeological Explorations and Mapping

Because there existed some major archeological structures of great importance to the Hawaiian culture in the vicinity of the project site, the Corps of Engineers requested that the Bernice P. Bishop Museum undertake a study to locate, map, and otherwise document the existence of those artifacts to serve as a control to reveal any damage caused by

the harbor detonations. A comprehensive study was conducted which is reported in Ref. 5. Major artifacts and two heiaus on the hill overlooking the site were studied (see Figs. 3 and 4b). The larger one is called Puukohola and the smaller one, Mailekini. Other artifacts located and studied include a third heiau that is underwater and partially covered with silt; a stone seat adjacent to the shoreline and the underwater heiau; and ruins of John Young's principal house near the Puukohola heiau.

There was some concern that the Puukohola and Mailekini heiaus would be damaged by seismic motion from the larger detonations; i.e., some of the stones would start to move and the heiau would collapse. Because of this concern, an extensive program was undertaken to mark the location of individual stones on the surface of the heiaus. This would permit some exactness in reconstruction work that might have to be done. In addition, the steeper slopes and corners of the structures were braced with timbers, cable, and plywood as shown in Figs. 12 and 13. However, the bracing was not needed because the motions were not sufficient to cause the structures to collapse (see Section 6).

The archeological report[5] contains a very interesting history by Russel A. Apple of these heiau structures; it is recommended to those interested in the history of the Hawaiian Islands. Some major historical events in the rise of King Kamehameha as the first ruler of the entire chain of islands occurred at the site of these heiaus.

Fig. 12. Bracing on steep wall of Puukohola heiau prior to detonations in Phase I of Project Tugboat.

Fig. 13. Cable and timber bracing used on corners of heiaus

PROJECT DESIGN

Preliminary Design

A preliminary design for Project Tugboat was made prior to the availability of site geology or geophysical data. The material was assumed to be coral over the depth in which the detonations would take place. Because of a lack of experience in cratering in a coral underwater, assumptions had to be made for the crater dimensions expected, and it was assumed

that the shape of such a crater would be similar to that experienced on land. The required project depth was 12 ft below MLLW. The following were the assumed crater dimensions:

DOB = Depth of burst = 140 ft/kt$^{1/3.4}$

R_a = Apparent crater radius = 200 ft/kt$^{1/3.4}$

D_a = Apparent crater depth = 90 ft/kt$^{1/3.4}$

H_{al} = Average crater lip height = 0.5 D_a

The preliminary design based on these scaled crater dimensions utilized ten each 10-ton charges to provide an entrance channel 600 ft long and 120 ft wide and ten each 10-ton charges in two rows of five each to provide a berthing basin 330 ft long and 180 ft wide. The actual depth of burst and crater dimensions used in this design were:

DOB = 36 ft

R_a = 52 ft

D_a = 23 ft

H_{al} = 12 ft

Phase I—Calibration Tests

The calibration tests were designated 1a, 1b, 1c, 1d, and 1e. Tests 1a through 1d were 1-ton detonations over a range of DOB's, and test 1e was a 10-ton detonation at what was predicted to be the optimum DOB. The locations of these detonations are shown in Fig. 14. The actual as-built yields and depths are given in Table 4.

Phase II—Entrance Channel and Berthing Basin

Following execution of Phase I, the Phase II design was radically changed. In the new design, twelve instead of twenty 10-ton charges were emplaced 42 ft below MLLW. The craters obtained in Phase I had been much larger and of a different shape than anticipated, permitting the reduction in the number of charges required (see Results). The design plan view is shown in Fig. 15. The emplacement hole locations are designated II-A through II-L. The design provides an entrance channel that starts in deep water at the edge of the reef and curves around the site of a future extension to a breakwater (built as part of the explosive excavation project) ending in a wider berthing area. For the outer four charges, spacing is 100 ft between

Table 4. Actual charge depths and weights for Phase I.

Charge designation	Date and time	Charge weight	Depth below coral surface (ft)	DOB (depth in ft below MLLW to charge center) (ft)	Charge cavity (cylindrical diameter × height) (ft)
1a (Alpha)	0901 6 Nov	2,000	11.0	16.33	2.4 × 5.2
1b (Bravo)	1101 6 Nov	2,000	14.3	16.66	2.4 × 5.2
1c (Charlie)	1001 4 Nov	1,975	17.6	20.12	2.4 × 5.2
1d (Delta)	0901 5 Nov	1,950	20.6	24.74	2.4 × 5.2
1e (Echo)	1101 7 Nov	20,200	35.7	41.1 - 41.6	5.1 × 11.3

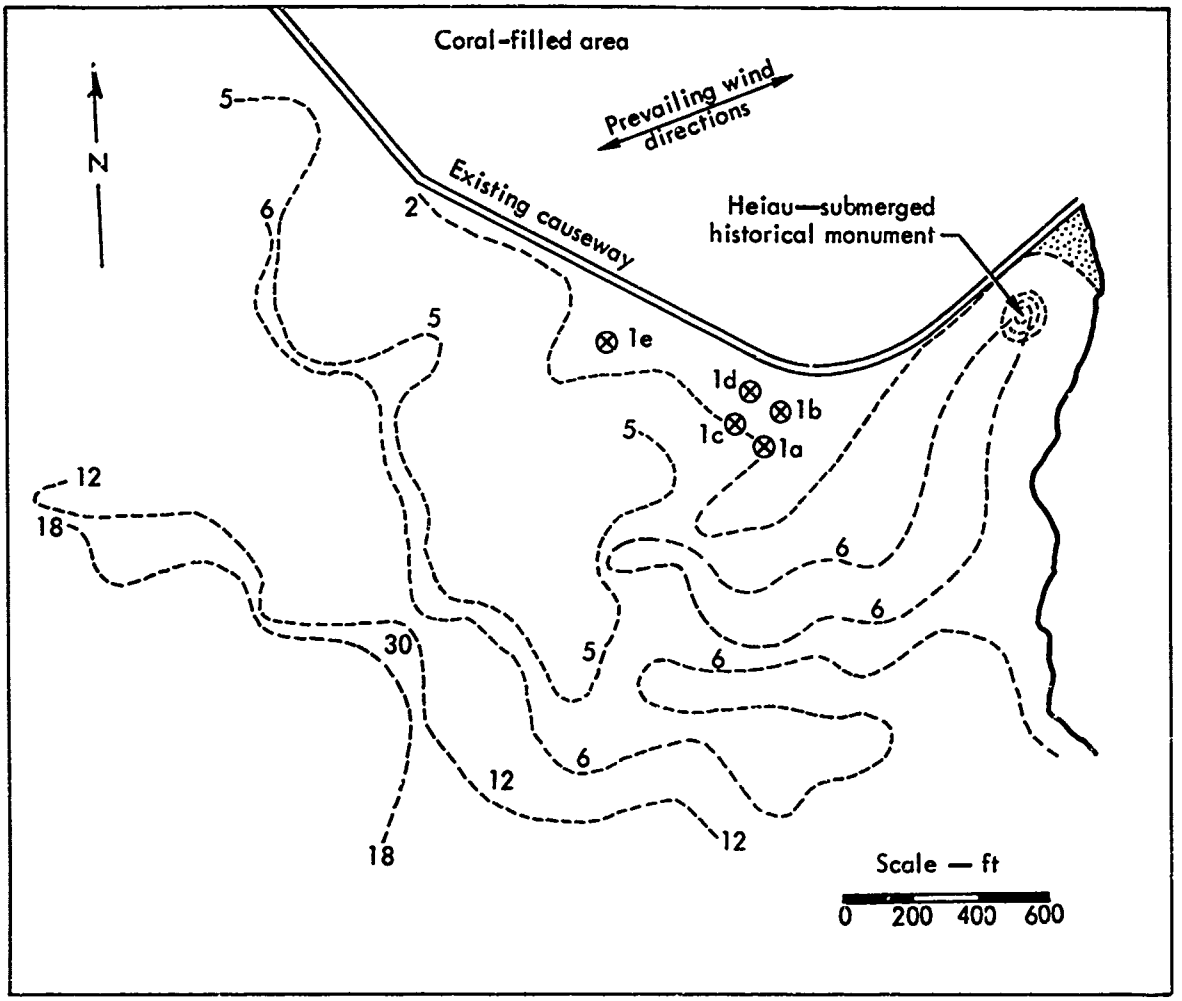

Fig. 14. Surface ground zero locations for Phase I calibration tests.

charges. For the remainder of the charges spacing is 120 ft. The closer spacing on the outer four charges was intended to provide movement of fine sand in the bottom of the channel out to sea.

The berthing basin design used four charges in a square array. The same relatively large spacing was used here also (120 ft). Because it was not necessary to throw out the cratered material but only to crush and compact it to get the apparent crater volume, the material in the center of the array was of little concern. It was to be subjected to four converging shock waves and receive more crushing action than the remainder of the material.

The breakwater was to be constructed adjacent to the berthing area following the detonations in Phase II. It was to be monitored by successive field surveys over a period of about one year.

Actual as-built charge yields and depths are given in Table 5.

This design was to provide a portion of a much larger final harbor development plan for this location by the Honolulu Engineer District (HED) and the State of Hawaii. A plan of this final harbor development is shown in Fig. 16.

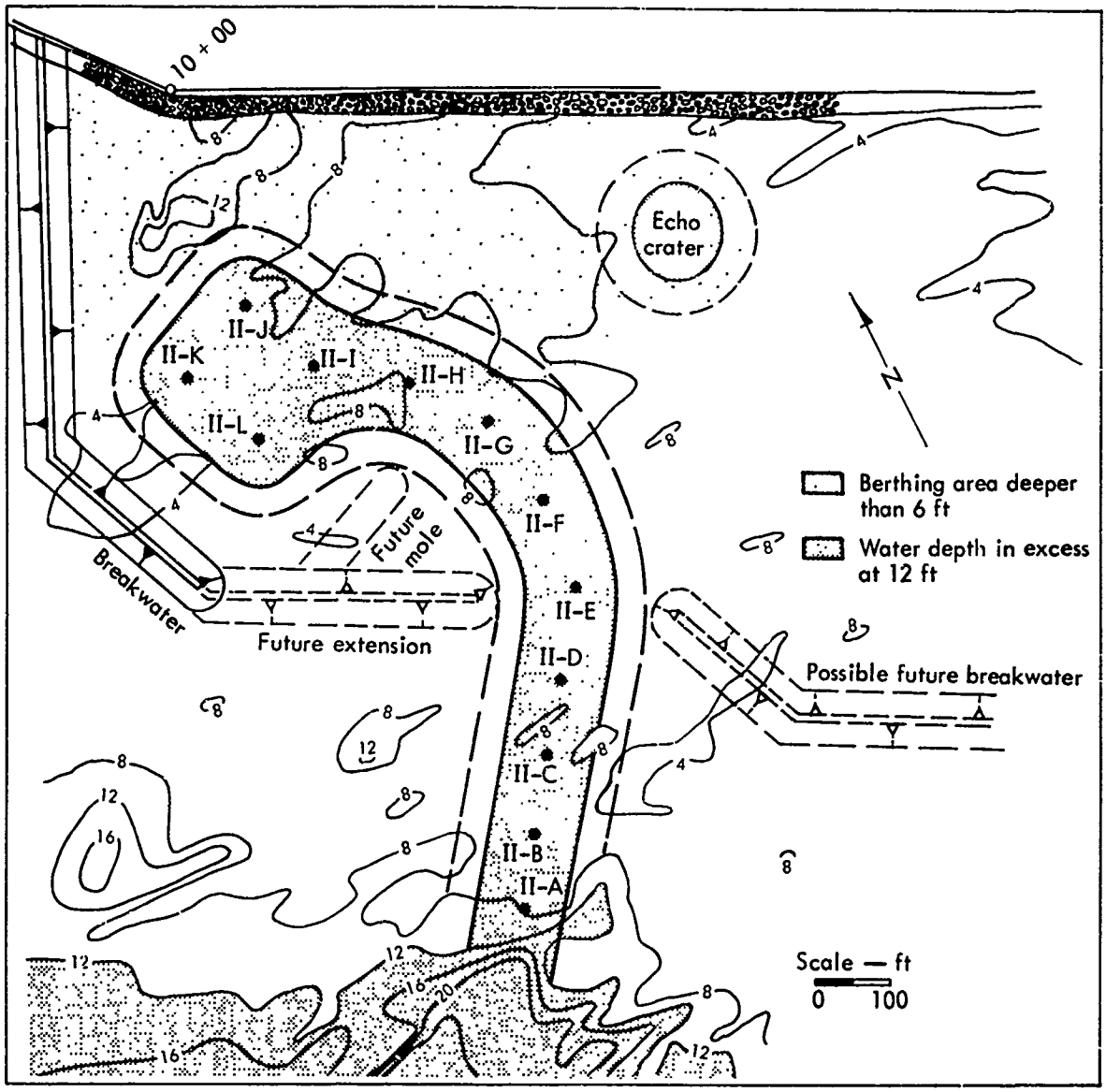

Fig. 15. Plan view of charge locations for Phase II.

As indicated in the table, Charges II-A, II-B, II-C, and II-D were to be fired simultaneously, Charges II-E, II-F, II-G, and II-H were to be fired with a 100-msec delay between each charge starting with Charge II-E, and Charges II-I, II-J, II-K, and II-L were to be fired simultaneously.

Remedial Explosive Excavation Design

As described in "Supporting Construction," several misfires occurred during the execution of Phase II. Because of these misfires, two portions of the channel did not meet the project depth requirement of a minimum 12-ft depth below

Table 5. Actual charge depths and weights for Phase II.

(Weight of each charge = 20,000 lb)

Charge designation		Depth of burial (depth in ft below MLLW to charge center) (ft)	Charge cavity (cylindrical diameter × height) (ft)
II-A	a	43.2	5.1 × 11.3
II-B		43.2	5.1 × 11.3
II-C		42.6	5.1 × 11.3
II-D		41.0	5.1 × 11.3
II-E	b	42.1	5.1 × 11.3
II-F		42.4	5.1 × 11.3
II-G		43.0	5.1 × 11.3
II-H		42.0	5.1 × 11.3
II-I	c	41.9	5.1 × 11.3
II-J		41.7	5.1 × 11.3
II-K		42.1	5.1 × 11.3
II-L		41.5	5.1 × 11.3

[a] Fired together.

[b] Fired with 100-msec delay between charges starting with Charge II-E. Although all four were fired, only II-E and II-F detonated. Charges II-G and II-H were fired again later, II-H detonating fully and II-G deflagrating.

[c] Fired together.

MLLW. A remedial explosive excavation design was prepared to clear the channel. Half-ton charges were emplaced in three areas as shown in Figs. 17a, 17b, and 17c. The actual as-built charge loadings and depths are given in Table 6.

SUPPORTING CONSTRUCTION AND EXECUTION

Two major contracts were used to execute Project Tugboat. The contract for construction included all operational support and construction of the project office, explosive storage and assembly and handling facilities, surface markers, camera bunker, temporary roads, and parking area. The major part of the contract was the construction of the 17 emplacement holes. Mile High Drilling Company, Inc. was awarded this contract. The second contract, awarded to the Dow Chemical

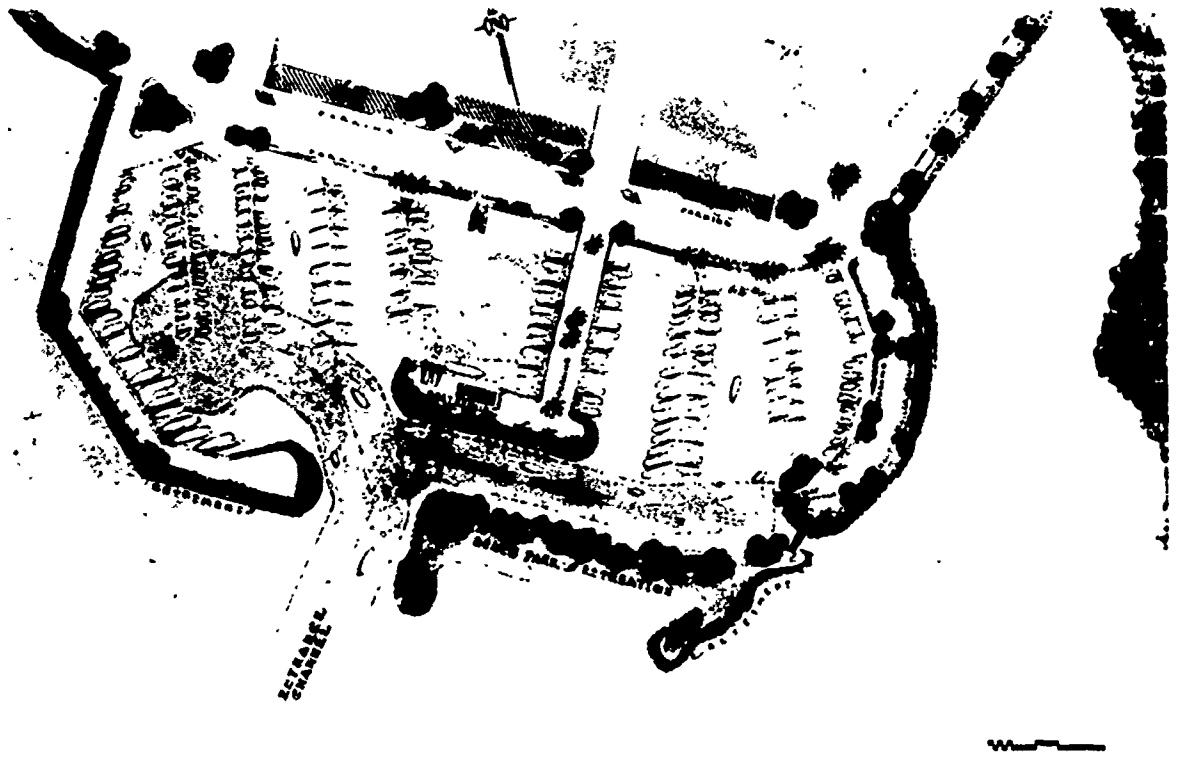

Fig. 16. Conceptual drawing of completed small-boat harbor, Kawaihae Bay, Hawaii.

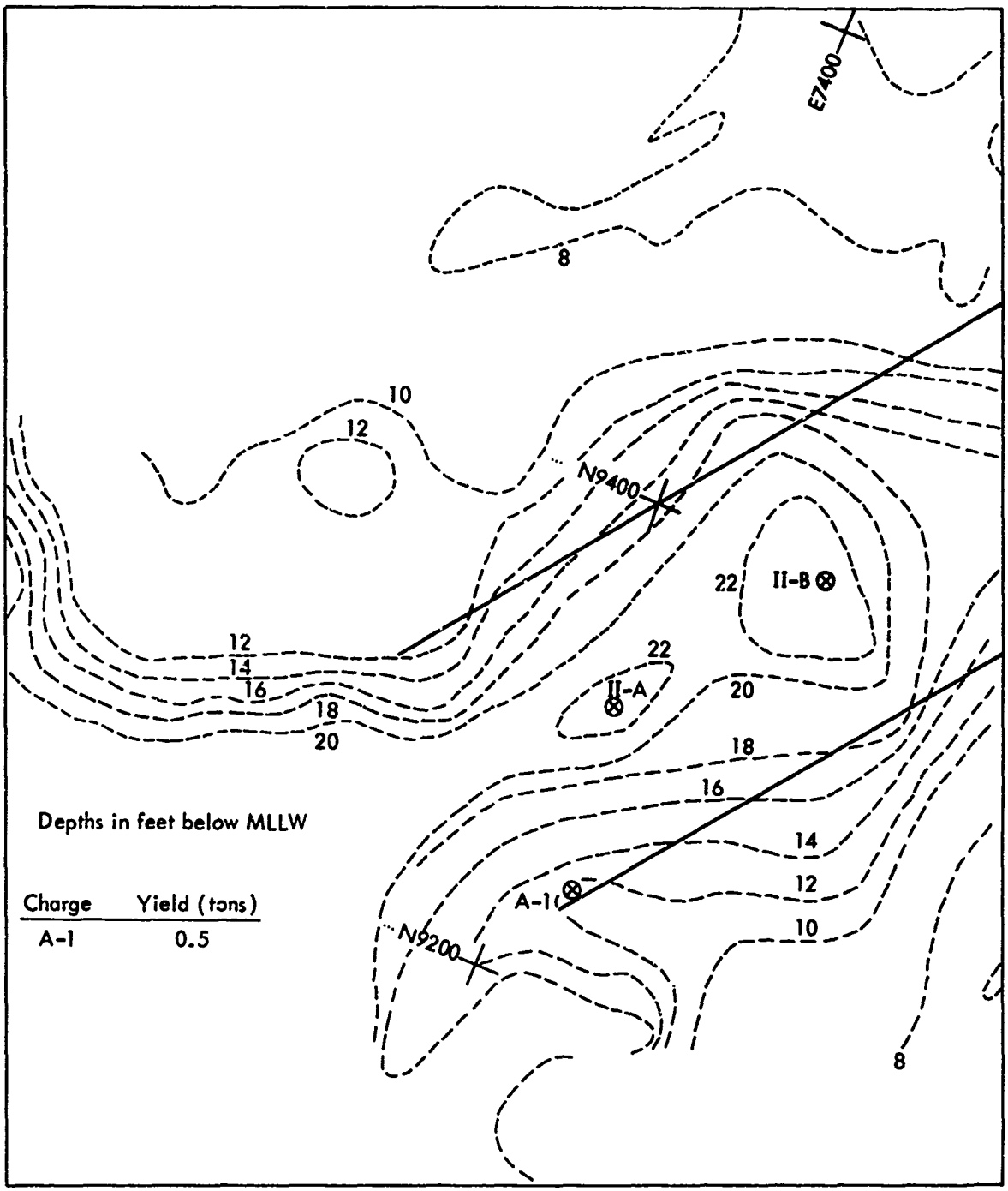

Fig. 17a. Project Tugboat remedial design for area at channel entrance where Charge A1 was used to remove nose that protruded into channel.

Company, was for the procurement and placement downhole of explosives for all Phase I and Phase II detonations. A small contract for emplacement of charge containers was let to Continental Drilling of Honolulu to accomplish the remedial explosive excavation work. The U.S. Army Engineer District, Honolu' ., Hawaii, provided construction and operational support in accomplishing the project, and

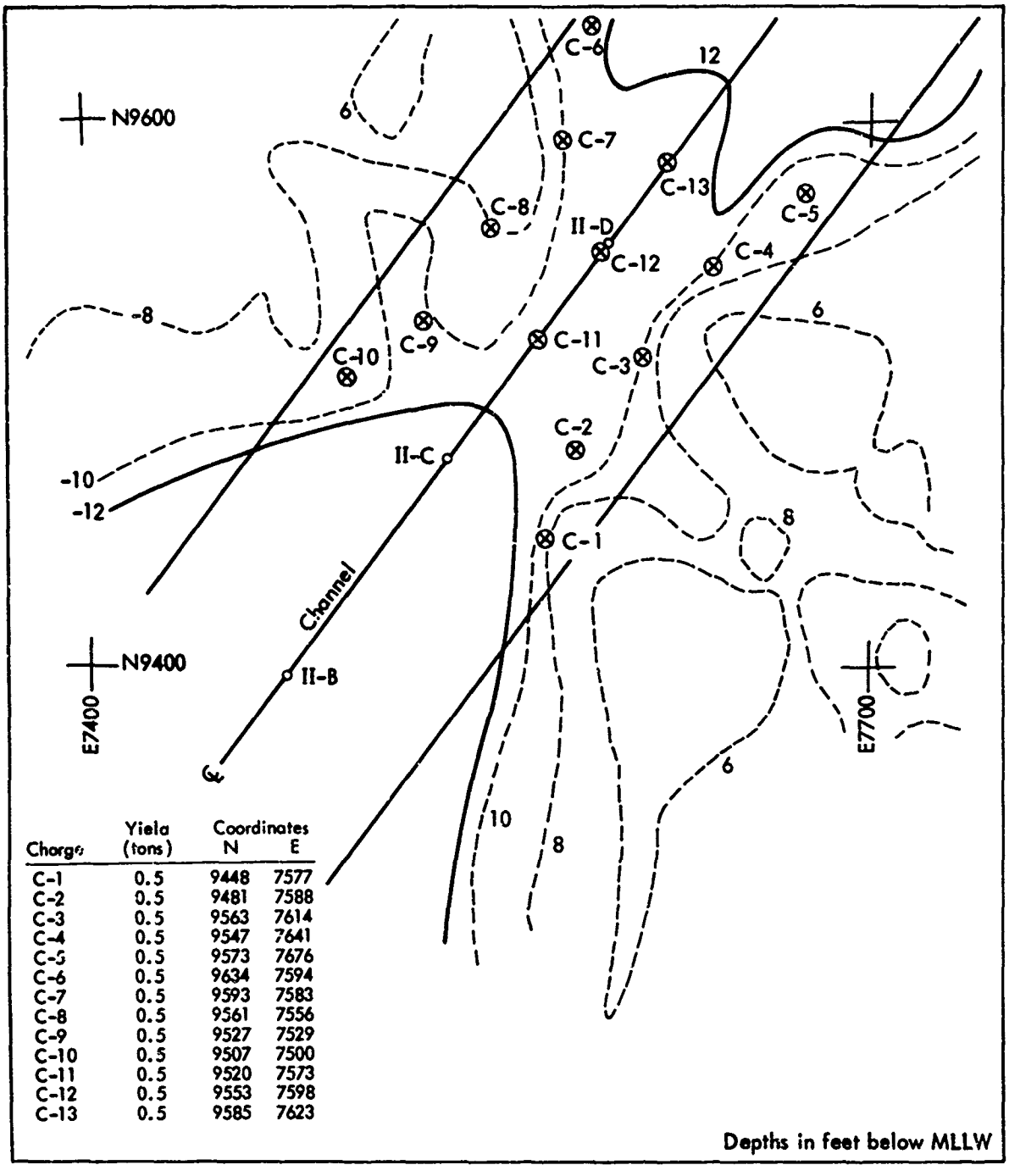

Charge	Yield (tons)	Coordinates N	E
C-1	0.5	9448	7577
C-2	0.5	9481	7588
C-3	0.5	9563	7614
C-4	0.5	9547	7641
C-5	0.5	9573	7676
C-6	0.5	9634	7594
C-7	0.5	9593	7583
C-8	0.5	9561	7556
C-9	0.5	9527	7529
C-10	0.5	9507	7500
C-11	0.5	9520	7573
C-12	0.5	9553	7598
C-13	0.5	9585	7623

Fig. 17b. Project Tugboat remedial design for area over Charge Locations II-C and II-D.

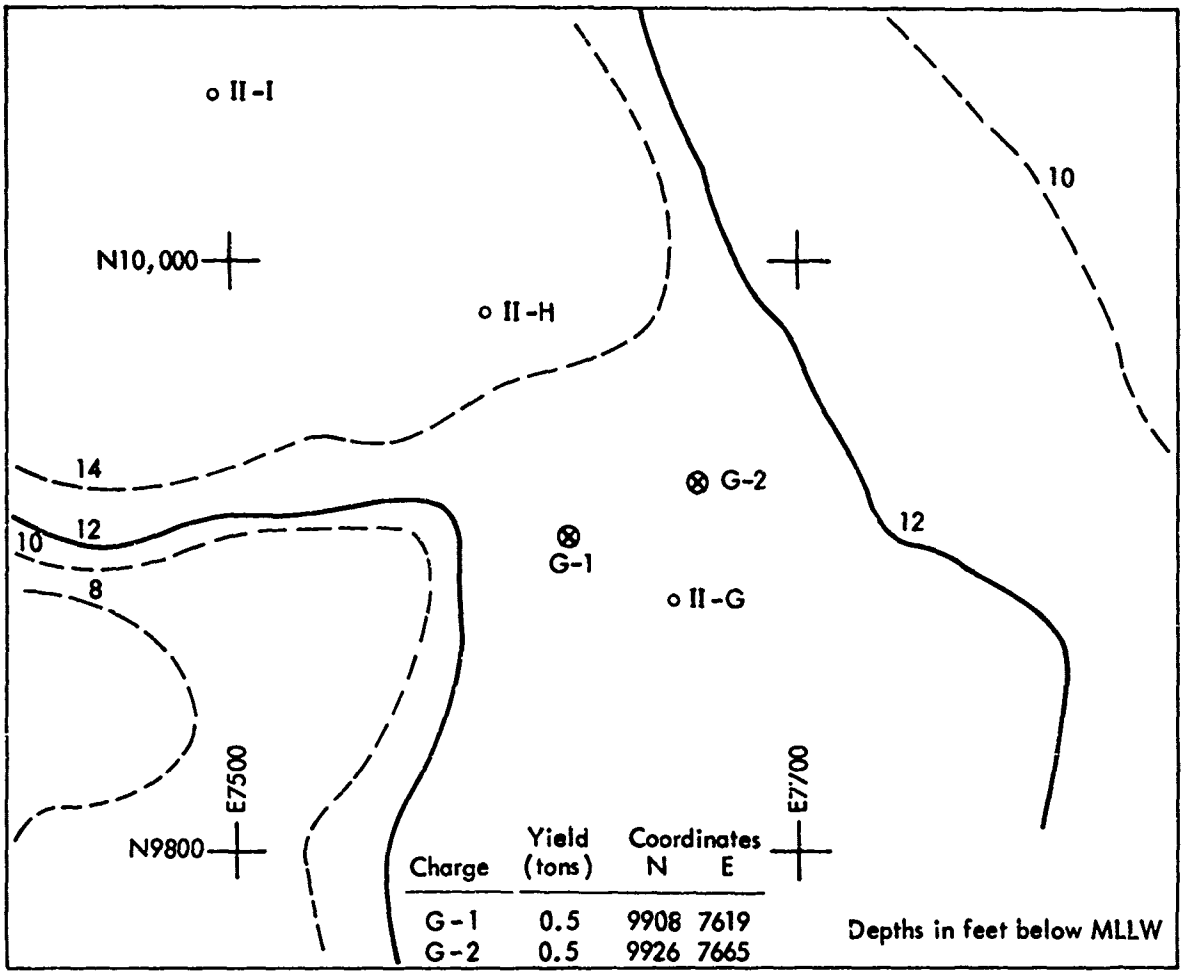

Fig. 17c. Project Tugboat remedial design for area over Charge Location II-G where two high spots existed in channel bottom.

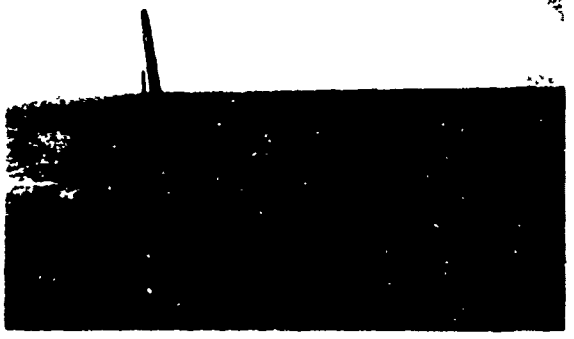

Fig. 18. Truck-mounted fold-over derrick-type bucket auger used to drill Phase I emplacement holes.

acted as contract administrator for these contracts.

Emplacement Hole Construction

Phase I

Because ground zeroes for Phase I were close to the coral fill area, the construction contractor built temporary causeways which extended over the charge emplacement locations. These causeways were used for drilling, placement of containers for the explosives, explosives

Table 6. Actual charge loadings and depths for remedial detonations.

Hole No.	Depth from MLLW to ocean floor (ft)	Depth of casing below ocean floor (ft)	Charge weights explosive (lb)
G1	13.0	11.5	720
G2	13.5	11.0	720
C1	11.0	11.0	1000
C2	12.0	11.0	1000
C3	9.5	11.0	1000
C4	10.0	11.5	1000
C5	11.8	12.0	1000
C6	12.5	11.5	960
C7	8.7	11.0	1000
C8	9.1	11.0	1000
C9	12.0	11.0	960
C10	13.6	11.0	900
C11	13.6	10.5	900
C12	12.6	11.5	960
C13	11.0	11.5	1000
A1	14.5	11.8	720

emplacement, and placement of the stemming material. Coral gravel from the existing stockpile in the vicinity was utilized to construct the 18-ft-wide causeways. Prior to detonation, the causeways were removed to the average high bottom elevation, not including isolated coral heads, and materials were returned to the borrow stockpile.

Drilling began after the completion of the causeways on 29 September 1969. The emplacement holes for the 1-ton charges were to be 3 ft in diameter; the holes for the 10-ton charges were to be 5 ft, 8 in. in diameter. The emplacement holes were drilled with a truck-mounted bucket auger (see Fig. 18). To prevent caving in of the walls and to aid in the emplacement of the explosive charge container, the holes were cased. The auger method is the most rapid and efficient technique for drilling large-diameter holes of shallow depths (less than 210 ft) in soft and moderately soft materials. Auger drilling destroys the rock by a rotating bit equipped with knife- or blade-like cutting devices. The rock cuttings are retained inside the bit and are removed by pulling the bit to the surface. The type of auger machine used was the truck-mounted fold-over derrick unit, with the following major components: an independent power unit, transmission, rotary table, kelley and digger attachment. The holes were cased the entire length of the hole.

The explosive containers were emplaced in the cased drill hole. Containers were cylindrical in shape and fabricated from steel conforming to Federal

Specification QQ-S-698 and AM-2. Bracing angles of A36 steel (structural carbon steel) were provided for top and bottom plates. A fill line of a standard weight steel pipe conforming to ASTM A120-68a was threaded into the top center of the explosive container and, with extensions, was made to extend to the surface. After cans were placed at the proper depth, they were covered with a 1-ft layer of crusher run material with a 6-in. maximum size. Concrete (3 ft) was placed by the tremie method on the top of the crusher run material and was allowed to "set-up" for approximately 48 hr. Concrete for the stem and grouting had a compressive strength of 3000 psi at 7 days. The casing was extracted to 6 in. below the surface of the concrete during the tremie operation.

Casing removal was difficult in the Alpha and Bravo emplacement holes. The concrete formed a firm bond to the lower portion of the casing. The concrete and the casing had to be jacked apart, by means of two 4-in. diameter pipes resting on the concrete and a 12-in. H-beam welded across the top of the casing. Two 30-ton capacity jacks were used from the inside of the casing.

The access hole was stemmed with crusher run material 6-in. maximum size, graded from coarse to fine. After the explosives were emplaced, the steel pipe fill line was filled to the surface with fine aggregate (100% passing No. 4 sieve size). The causeways were subsequently removed by dragline as illustrated in Fig. 19.

Phase II

The drilling work for Phase II was accomplished from a floating barge equipped with a bucket auger machine suspended from a track-mounted crane. Casing was again used to insure the integrity of the excavation. However, the casing did not extend the entire depth of the hole; it was required only from above water to a few feet into the coral bottom. A telescoping three-sectional casing, which could be extended to 40 ft, was utilized for this purpose. With the barge anchored over the charge emplacement hole location, hydraulic jacks raised the platform out of

Fig. 19. Removal of Phase I causeway by dragline.

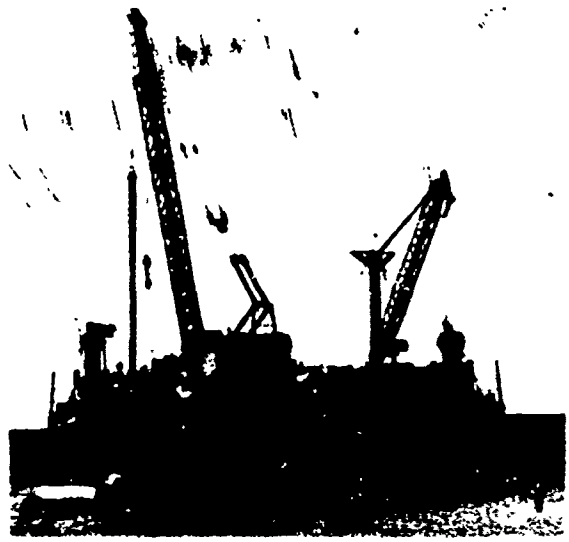

Fig. 20. Drilling platform used during Phase II emplacement construction.

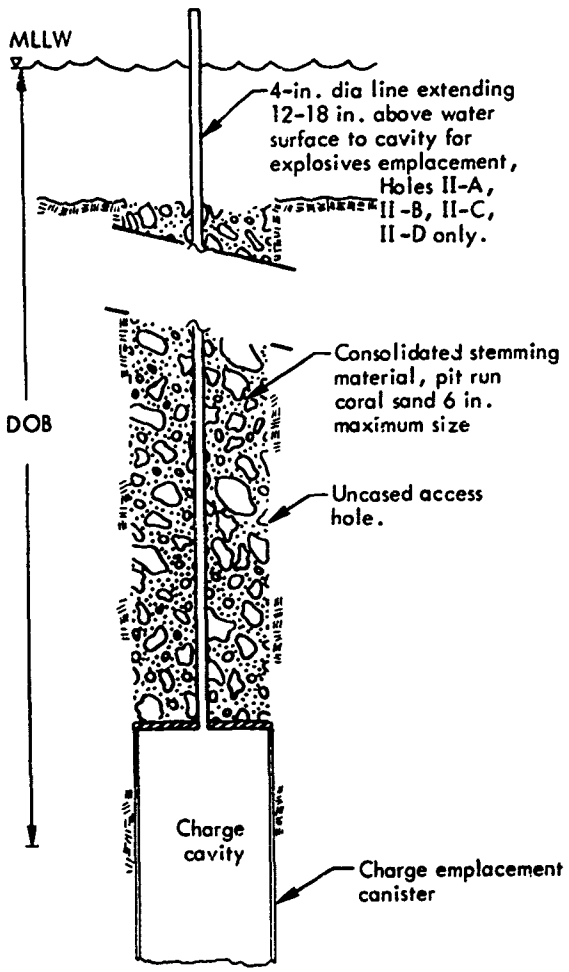

Fig. 21. Charge emplacement design for Phase II.

the water to eliminate the interference of waves, tides, currents, or wind on the drilling platform position. The platform and drilling rig is shown during construction operations in Fig. 20.

The stemming techniques were the same as in Plase I. The material used for stemming the access hole was 6-in. maximum size, well graded from coarse to fine, and was obtained from the Government coral stockpile at the project site. The coral was placed in an initial 10-ft lift and then in 3-ft lifts for the remainder of the fill; each lift was consolidated. Figures 21 and 22 illustrate the typical cratering charge emplacement holes utilized in Phase II.

Explosives

General Procedures

Explosives were stored, handled, and transported in accordance with the applicable portion of the AMCR Safety Manual.[6] The Test Manager had direct responsibility for planning and coordinating project execution. The HE Project Officer (1) supervised all assembly, transportation, handling, emplacement, and preparation for firing of explosive charges; (2) acted as the Explosives Safety Engineer; (3) was responsible for the functional capability of the explosive system, including the electronic timing and firing systems; and (4) served as the senior member of the arming party. Prior to explosive emplacement, a limited access area was established by the Test Manager

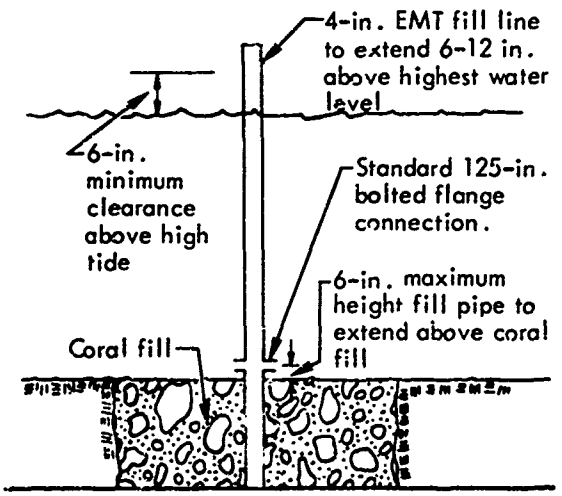

Fig. 22. Flange modification to charge emplacement design for Charges II-E, II-F, II-G, II-H, II-I, II-J, II-K, and II-L.

in consultation with the HE Project Officer.* The size of the area depended upon the amount of explosives to be emplaced, the potential ejecta range, the relative operational hazards, and the practical work problems. During the emplacement operations, a fire control area was also established.†

Prior to D-day, the main firing and control cables were run from the firing point to the CDU (capacitor discharge unit) in the vicinity of the SGZ. A final dry run on all systems including the firing system was made.** All dry runs were completed prior to arming. Upon receipt of authority from the Test Manager, the charges were armed by connecting the detonator leads to the CDU and by connecting other auxiliary devices fired by the CDU. The remote control firing unit was always locked out during arming, and the key was in the possession of the senior member of the arming party. The senior member of the arming party turned on the timing and firing unit and started the count-down to detonation. Following detonation, the detonation site was inspected for evidence of misfire before personnel access restrictions were removed.

Blasting Agent Selection

The blasting agent used in the Phase I safety calibration series and the Phase II entrance channel and berthing basin detonation was an aluminized ammonium nitrate slurry (AANS). The selection of the slurry blasting agent for the job was based upon the following criteria:

(1) Minimum emplacement costs

(2) Minimum explosive costs consistent with prerequisite detonation properties

(3) Compatible with wet environment

(4) Free-flowing during emplacement

(5) Density greater than sea water

(6) High excavation capability per unit volume of explosive

The explosive provided under a competitive bid contract was Dow Chemical Company's Modified MS-80-20. The following specifications characterize the explosive:

(1) The explosive gelled from 5 to 10 min after emplacement to a viscosity of at least 25 poise

(2) The density of the explosive after gelling in the borehole was greater than 1.2 g/cm^3

(3) The total energy of the explosive mixture was more than 1700 cal/g of explosive

(4) The velocity of detonation as measured by arrival was between 4000 and 5500 m/sec

(5) The explosive mixture did detonate at high order in a 4-in. diameter unconfined column and was incapable of being detonated with a No. 8 blasting cap

*Limited access area: that area associated with explosives where entry is restricted to those persons concerned with the job at hand. The purpose of limited access control was twofold: first, to prevent undue interference with necessary workers and, second, to minimize extent of injury in case of explosive accident.

†Fire control area: that area associated with explosives where the possession or use of any flame- or spark-producing equipment or material was prohibited. Normally, this distance extended 50 ft in any direction from any explosive in a fixed location.

**All fire control keys were removed and kept adequately secured except during approved test periods.

(6) The explosive mixture was capable of high-order detonation after being submerged in seawater for 200 hr

(7) The explosive was sufficiently nontoxic and nonirritating to personnel engaged in explosive handling

(8) The explosive was capable of being pumped into the charge cavities when filled with seawater at the rate of 200 lb/min.

Primer System—Phase I

Boosters were a high-strength, nonnitroglycerin explosive, capable of initiation by 50-grain primacord suitable for use in ammonium nitrate slurry and resistant to tropical seawater. They were installed through a fill pipe (3-in. minimum diameter). The detonating cord used was plastic reinforced, 54 grain/ft, 21 lb/1000 ft of PETN cord with a 275-lb tensile strength.

A standard booster system, planned for use in all 1-ton charges of Phase I is shown in Fig. 23. Individual explosives in this booster system were Dupont HDP-1 primers which are 1-lb discs of cast Composition B containing a 200-grain PETN initiator. Each primer has a central detonating cord well (adjacent to the PETN initiator) and a cap well slightly off-center. These are standard primers used in commercial practice for detonating aluminized slurry; one such primer is considered adequate for initiating a charge. An extension of this system using four Dupont HDP-1 primers strung out such that they were interspersed throughout the charge height was used for the 10-ton charge. Dow approved this booster design and furnished the primers under the contract, as well as all other explosive components except caps. The primer blocks were initiated with detonating cord run through both priming wells and primed at the surface with No. 6 caps. Detonating cord lines were run through

(a) Dupont HDP-1, 1-lb booster with primacord.

(b) Completed booster for 1-ton charges.

Fig. 23. Standard Phase I booster arrangement.

1/2-in. plastic tubing for protection against abrasion.

Charge Emplacement—Phase I

The explosive loads for all five Phase I charges were placed by pumping from a truck on the causeway. The explosive fill hose (2-1/2-in. nominal o.d.) was extended through the metal fill pipe (4-in. i.d.) to the bottom of the charge canister and the explosive pumped down the hole (see Fig. 24). An inspector was present to insure that seawater was being displaced continually through the annulus between the 2-1/2-in. fill hose and the 4-in. fill pipe while explosives were being pumped downhole. After verifying that the explosive had been loaded and that the top of the explosive charge was at an elevation corresponding to the load, the fill hose was withdrawn slowly (with the explosives pump still running), to avoid leaving a void space in the charge which could allow seawater intrusion. The charges had boosters in place prior to loading explosives. The plan called for separate detonation of each of five emplaced charges. Phase I was executed without any major problems.

Primer System—Phase II

The plan for Phase II execution called for three detonations of four charges each, starting with the four charges farthest from shore and finishing with the four charges in the berthing basin. The maximum detonation of 40 tons was selected to minimize the danger of damage to adjacent structures, based on ground-motion and air-overpressure measurements taken during Phase I. Detonations 1 and 3 were planned for simultaneous firing of all charges. Detonation 2 was planned for firing with 100-msec delays between successive charges, to determine whether

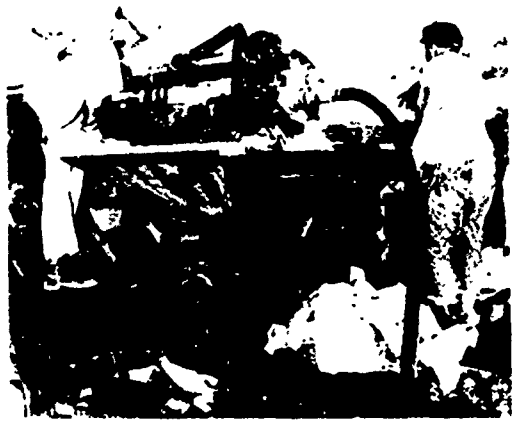

(a) Transferring blasting agent from bags to pumping truck hopper.

(b) Looking down emplacement hole during pumping operations.

Fig. 24. Explosive emplacement operations during Phase I.

this procedure could be used to reduce the severity of ground motion or air overpressure. To accommodate this plan, two different booster systems had to be devised, one for the two simultaneous detonations (II-ABCD and II-IJKL) and one for the detonation with delays (II-EFGH).

The booster system, designed for use in all charges of the first and third detonations, is shown in Fig. 25.

During construction operations the fill pipe into the canister for Charge II-B was bent. It was straightened enough to allow passage of the rubber hose used for explosive loading, but the standard booster string could not be run down the pipe.

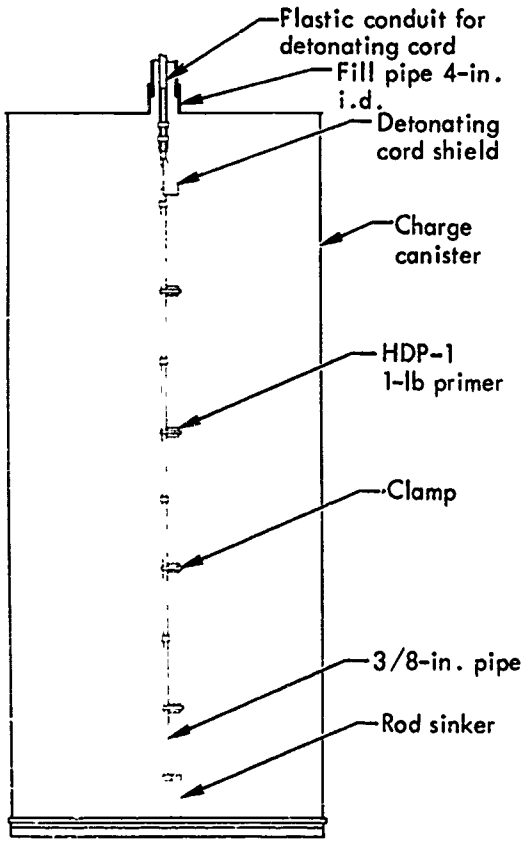

Fig. 25. Booster design for Detonations II-ABCD and II-IJKL.

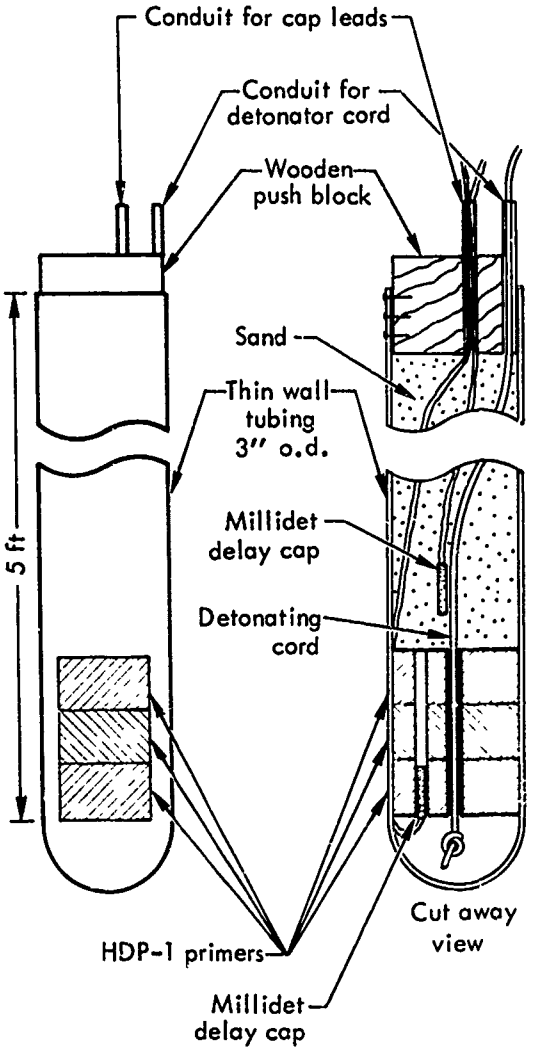

Fig. 26. Booster design for all charges in Detonation II-EFGH.

Consequently, a new booster was improvised, using 10 of the HDP-1 primers strung together on detonating cord and suspended in the center of the canister prior to loading main charge explosives.

A second type of booster, used for the second detonation (II-EFGH), is shown in Fig. 26. This detonation was planned for sequential firing with a delay interval of 100 msec. It was considered desirable to place the delay caps down hole in order to avoid the possibility of damaging caps or detonating cord down lines by debris

or by displacement of fill pipes or charge canisters resulting from the detonation of adjacent charges. Because of safety considerations, boosters with caps inserted could not be placed in charge canisters prior to loading the main charges. Following emplacement of the main charges, the booster container shown in Fig. 26 was forced into the main charge so as to initiate detonation at mid-height of the explosive column. Each of these boosters contained three HDP-1 primers placed in close contact, with the delay cap in the bottom cap well (pointed upward) and detonating cord run through the detonating wells and primed with a cap (same delay time) about 3 in. above the top primer. The detonating cord was then run through plastic tubing to the surface, to provide an alternative means of firing in case of interruption to the electrical circuits to the down hole caps, and to provide a means for firing the charges simultaneously. The cap leads were also run to the surface through protective plastic tubing. Slots cut in the metal tube which formed the body of the booster allowed direct contact between the booster charge and the main charge of explosive.

Charge Emplacement—Phase II

The explosive loads for all 12 charges of Phase II were placed by a pumping truck loaded onto a work barge anchored at the surface (see Fig. 27). The explosive fill hose (2-1/2-in. nominal o.d.) was inserted through the metal fill pipe (4-in. i.d.) to the bottom of the charge canister (about 48 ft below mean sea level), and explosive was pumped down the hole until 10 tons had been loaded. An inspector was present to insure that seawater was

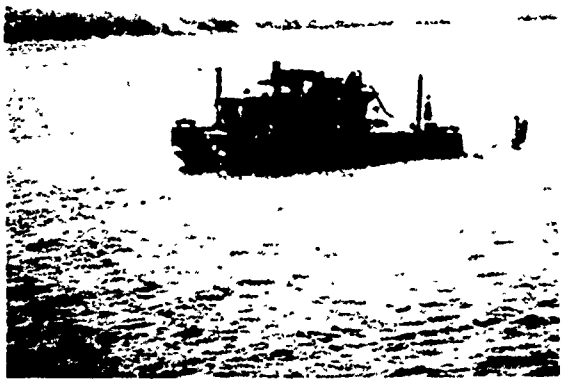

Fig. 27. Explosive emplacement operations during Phase II.

being displaced continually through the annulus between the 2-1/2-in. fill hole and the 4-in. fill pipe while explosives were being pumped downhole. After the inspector had verified that 10 tons of explosive had been loaded and that the top of the explosive charge was at an elevation corresponding to a 10-ton load, the fill hose was withdrawn slowly (with the explosives pump still running) to avoid leaving a void space in the charge which could allow seawater intrusion. The charges scheduled for simultaneous detonation had boosters in place prior to loading explosives: boosters for the four charges in the second detonation were placed after the main charges were loaded.

Explosive loading started closest to shore and progressed seaward as shown in Table 7.

Firing signals for all detonations were initiated by a capacitor discharge unit (CDU). Rated requirements for firing were 0.35 A at 110 V the CDU provided 2.5 to 3.0 A at 275 V.

Table 7. Sequence of charge loading for Phase II.

Charge	Date booster placed	Date explosive loaded
II-A	7 April	17 April
II-B	10 April	16 April
II-C	7 April	16 April
II-D	7 April	15 April
II-E	15 April	15 April
II-F	15 April	14 April
II-G	15 April	14 April
II-H	14 April	13 April
II-I	7 April	13 April
II-J	7 April	8 April
II-K	7 April	9 April
II-L	7 April	11 april

Phase II Misfires

Phase II operations had several problems. The first detonation (II-ABCD) was fired at 0916 hr on 23 April. Charge II-B detonated with full force. Charge II-A hesitated for several milliseconds, then detonated with as much or almost as much energy as Charge II-B. Analysis of surface acceleration data led to estimates that the yields of Charges II-C and II-D were between 2 and 4 tons each. The second detonation (II-EFGH) was already primed, with boosters as shown (see Fig. 26) and caps downhole, prior to the first detonation. It was decided to proceed with the second detonation as planned. The reasoning was:

(1) The booster system already in place was considered adequate to assure detonation, although a 5- to 10-lb booster would be more desirable.

(2) There was no completely safe means of modifying the booster system with the caps already in place.

The second detonation was fired at 0901 hr, 28 April. Visual observation showed that Charges II-E and II-F detonated at full yield with the appropriate 100-msec delay, but that Charges II-G and II-H did not fire at all. Subsequently, investigations found that the fill pipes for Charges II-G and II-H were bent just below the bottom surface and lying at a small angle with the bottom with photography targets still attached. The pipes were bent toward the Charge II-E and II-F locations. The detonating cord line in Charge II-H which extended to the surface of the coral had been fired, indicating that at least the caps in the boosters were destroyed.

The third detonation was postponed from 30 April to 1 May, to allow field testing of explosives as follows:

(1) Samples of slurry explosive were taken from each charge of the third detonation. Material for laboratory analysis was extracted. Enough remained to make up one small charge (3 to 5 lb) which was fired with a small C4 booster. It detonated high-order. On this basis it was assumed that the main charge explosives were in good condition.

(2) Samples were extracted from the rubber hose used during loading operations. This hose had been exposed to direct sun for at least two weeks. One sample was kept for laboratory analysis, one sample was made up into a test charge and fired with a C4 booster, and one sample was first soaked in seawater and then fired with a small C4 booster. Both of these test charges detonated

high-order, giving further evidence of the stability and integrity of the slurry explosive.

(3) An HDP-1 booster, primed with detonating cord, was soaked in seawater and test-fired. It detonated with apparent full design yield.

The general conclusion was that HDP-1 boosters were reliable, but might not have enough brisance to detonate the main charge explosives under the special conditions encountered in this project.

The four charges of the third detonation were primed with new boosters shown in Fig. 28. These boosters were field-fabricated from materials that were available locally. They were formed by packing aluminum tubing with C4 military explosive which was primed with detonating cord. These boosters were designed to provide initiation of detonation for the full height of the main explosive charge. The third detonation (II-IJKL) was fired at 0901 hr, 1 May 1970. All detonated high-order.

Immediately after the 1 May detonation, work on reentry to Charge II-H began. A new 4-in. i.d. fill pipe with a removable point was driven through the back fill material alongside the original fill pipe until the point penetrated the top of the canister. Then the point was knocked loose to sink to the bottom of the canister. Samples of the explosive were taken for laboratory analysis and for test firing, which was successful. Following this the field booster shown in Fig. 29 was inserted.

Material over the bend in the fill pipe of Charge II-G was excavated with an improvised air lift pump until the flange was uncovered at a depth of about 6 ft. The

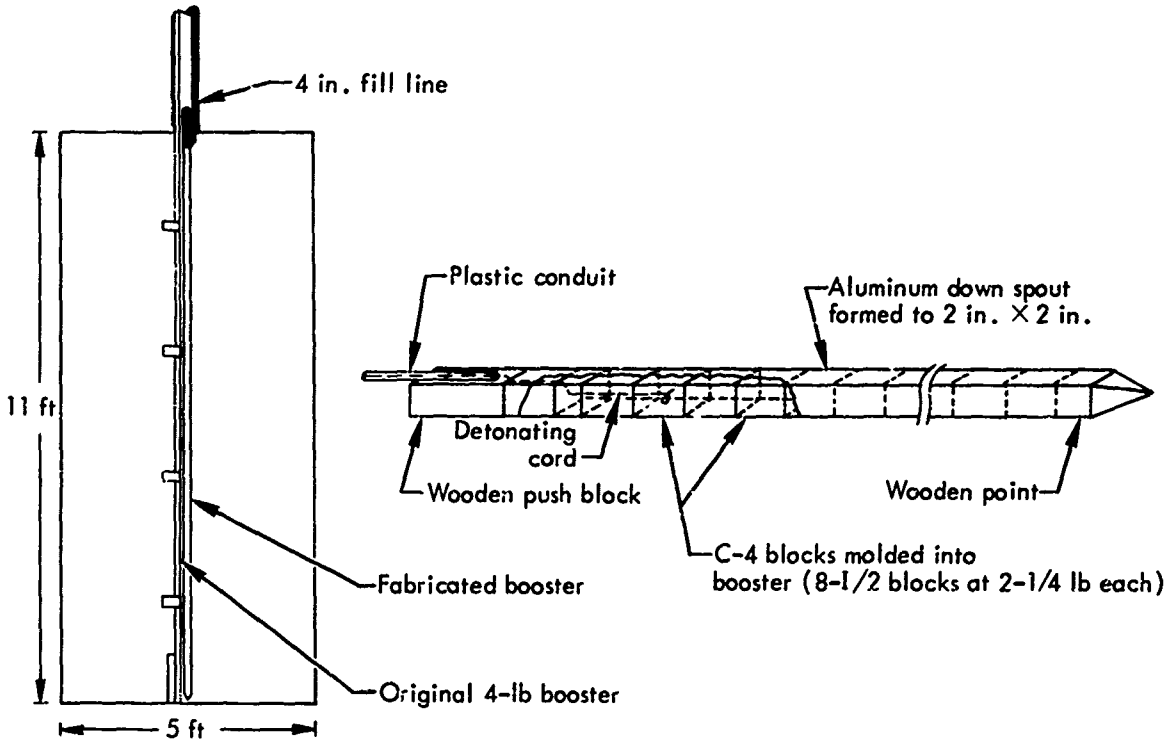

Fig. 28. Field-fabricated booster used to detonate Charges II-I, II-J, II-K, and II-L.

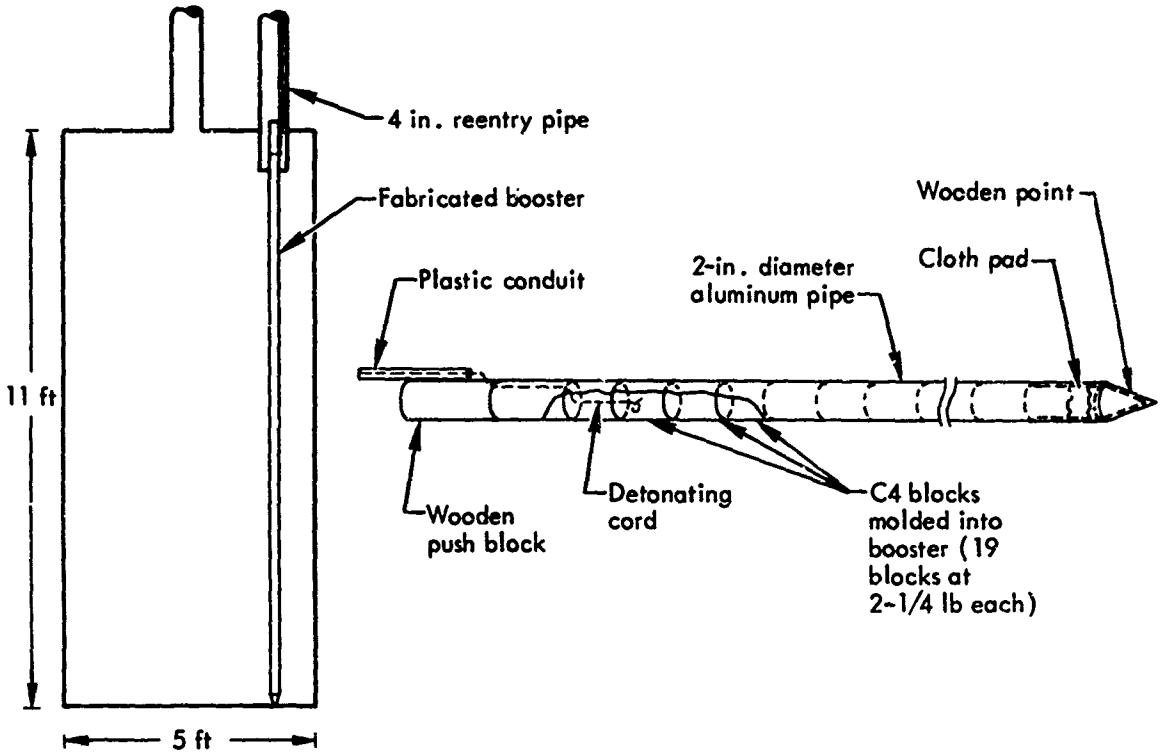

Fig. 29. Field-fabricated booster used to detonate Charge II-H.

Table 8. Drilling equipment used in remedial work.

Drilling rig:
Platform approximately 15 ft × 17 ft, built of 2 × 12 planks and 32 50-gal drums. Hole in center of platform was about 4 ft square. Derrick of 4-in. × 4-in. timbers had about 5.2-ton lift capacity. Derrick stood roughly 18 ft high. Complete drilling rig cost $310.
6-in. airlift:
21 ft long with 4-bladed 12-in. bit and 1-in. diameter line air feed. Ejected chunks approximately 5 in. in diameter and 3 to 4 lb in weight.
160-psi air compressor
Tamper and pipe
300-lb hammer:
An oval-shaped solid about 2 ft long with a hole in the center.
Gasoline-engined winch
Block and tackle

flange was unbolted, revealing that the detonating cord had not fired. Because of the possibility that unfired caps were still present in the charge, it was unsafe to attempt to drive a new fill pipe into this charge canister. Accordingly, a cap was attached to the detonating cord line and circuits were prepared to fire Charges II-G and II-H simultaneously. The fourth detonation was fired at 0901 hr 8 May. Charge II-H detonated at full yield. The water surface above Charge II-G frothed and boiled for almost 90 min after the detonation. The conclusion was that Charge II-G had been destroyed by deflagration.

Remedial Work

Sixteen half-ton charges of the slurry were needed to complete the project in areas where the 10-ton charges had not fully detonated. These charges were placed in thin wall casings which were emplaced by air lift pumping within the casing and intermittent driving of the casing to approximately 11 ft below the coral surface.

The working platform and equipment used to emplace the casings are shown in Figs. 30 through 32. A listing of the equipment is given in Table 8, and a schematic drawing of the air lift pump technique is shown in Fig. 33.

The rig was pulled by the boat to a position over the site and anchored at each corner about 100 ft from the rig. A hole about 1-1/2 to 2 ft in depth was dug prior to emplacement of the casing. Before a casing was placed, an area around each hole was leveled so that a template could be fixed plumb over the hole. The template insured proper alinement as each casing was placed.

A boat was used to transport the casings one at a time from the land fill to each site. The casing was rolled on to the boat with timbers and placed with its length perpendicular to the hull.

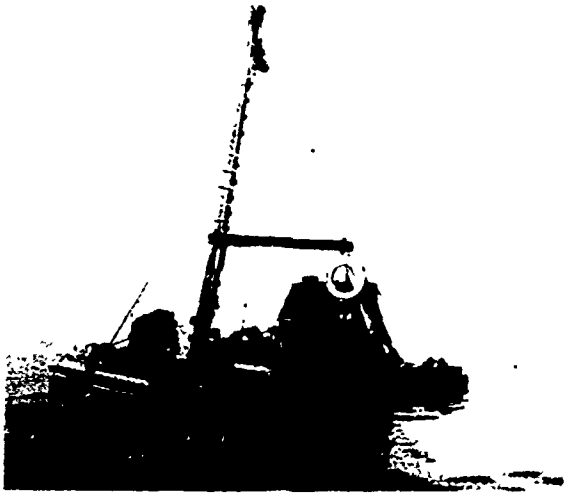

Fig. 30. Remedial work drilling platform (derrick of 4-in. × 4-ft timbers had approximately 5.2-ton lift capacity; 2-in. × 12-in. plank deck was supported by 32 5-gal drums; platform was about 15 ft × 17 ft and derrick stood about 18 ft high).

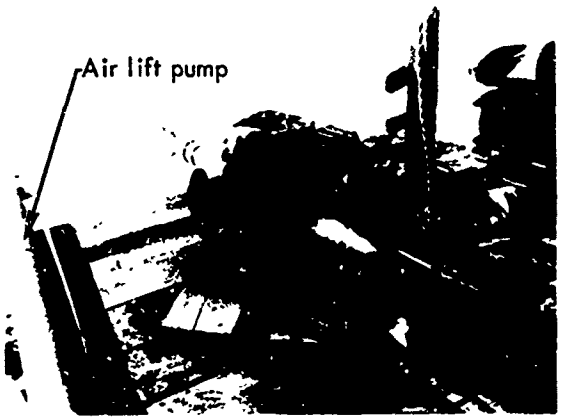

Fig. 31. Air lift used during emplacement of remedial work charge container (thin-wall 6-in.-diameter air lift has approximately 12-in. bit; note 1-in.-diameter pipe along length of air lift for air injection).

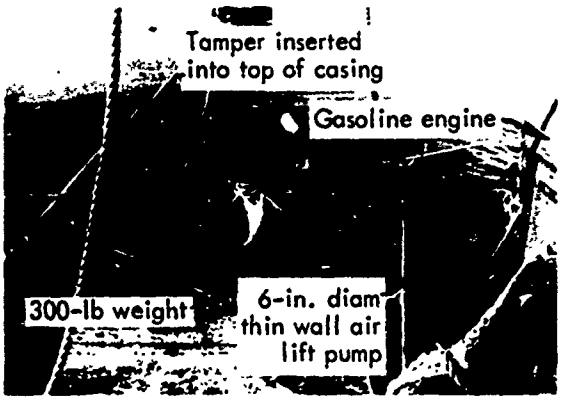

Fig. 32. Remedial work drilling method (tamper shown inserted into top of casing; pipe placed on tamper to aline blows from doughnut-shaped 300-lb weight, which was raised by means of gasoline engine).

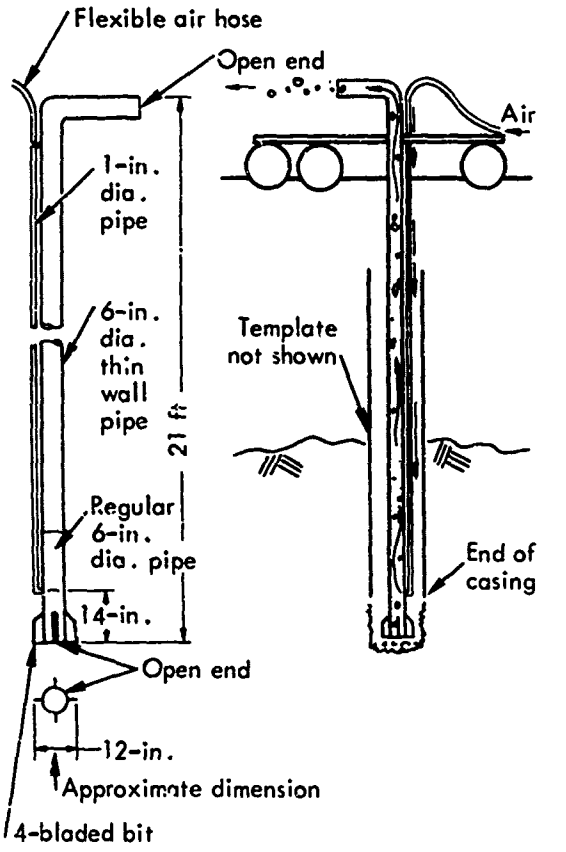

Fig. 33. Thin-wall 6-in.-diameter air lift pump design and use.

Once the template was in place and the casing started, drilling began. The air lift was lifted, dropped; lifted, rotated, and dropped; lifted, rotated, and dropped inside the casing. After the coral was broken, the air compressor was turned on and crushed coral up to about 5 in. in diameter was removed and ejected from the pipe. The air lift was then removed and the tamper was inserted inside the top of the casing. A pipe was placed inside the tamper and the 300-lb weight was then lifted and dropped to drive the casing down inside the drilled hole. When the casing was driven to the excavated depth, the pipe, weight, and tamper were removed and the process began again.

Three men worked to emplace each casing. One operated the friction or slip pulley to raise and lower equipment, one did most of the diving, and the other stood by the air lift or hammer. All three also frequently worked with each other at various tasks.

It took three, four, and sometimes five stages to complete one hole. A hole was advanced about 2 to 3 ft at a time. Once the casing was driven to the desired depth, the top was capped with half of a 50-gal drum and a large rock. An average of one casing was placed each day.

The explosive used in the remedial work was GGA IR-10. It was hand-loaded into the holes in plastic bags that had been split utilizing a tremie after the booster had been placed in the hole (see Fig. 34). Booster design was as shown in Fig. 35. All charges were detonated simultaneously on 8 December and all detonated at high order.

Fig. 34. Loading of explosive used in remedial work.

RESULTS

Phase I

A series of sequential photos of the Phase I, 1e (Echo) detonation are shown in Fig. 36. Profiles of the five Phase I craters are shown in Figs. 37 through 39. The shape of the craters is very different from those previously obtained in dry land cratering detonations. No lips were formed, and the craters are unusually broad and shallow. This is shown graphically in Fig. 40 where the 1e (Echo) crater profile is compared with the profile for the crater dimensions assumed in the preliminary design.

Because the crater radius is so large and does not significantly change over the range of DOB's in the 1-ton detonations, a cratering curve has not been plotted. A new radius, defined as the radius over which a relatively flat bottom occurs, was chosen as the parameter for row and

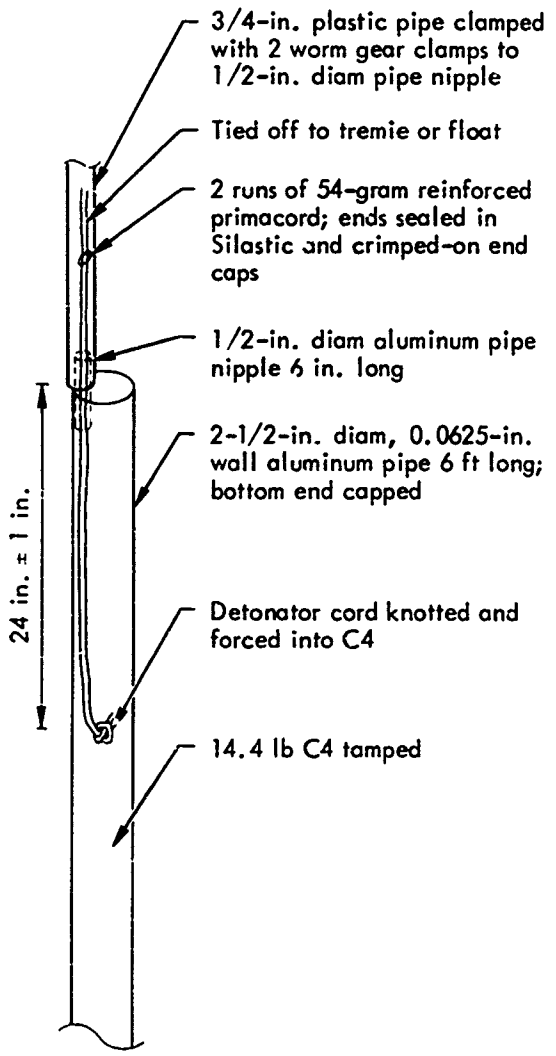

Fig. 35. Booster design used in remedial excavation.

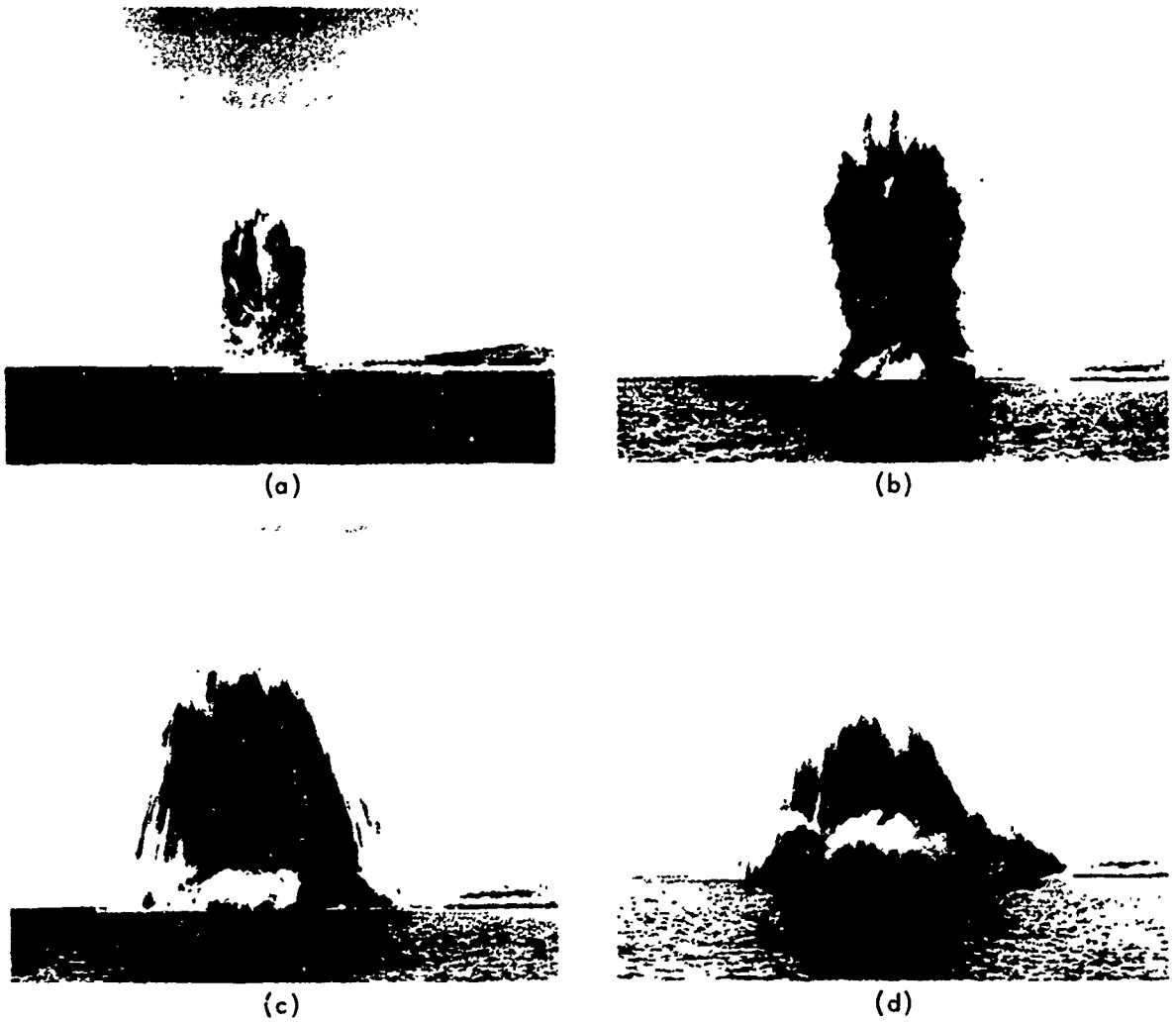

Fig. 36. Sequential photos of Phase I, 1e (Echo) 10-ton detonation.

array charge design. For the 10-ton 1e (Echo) crater this new radius was estimated to be 60 ft (radius over which a minimum 12-ft depth below MLLW occurs). The row and array charge design spacing was chosen as two times this new radius. This multiple was based on some 1-lb model tests in sand under water (Ref. 7). The berthing basin charge layou' was therefore based on the use of 10-ton single charges spaced 120 ft apart. With the wide flat-bottomed crater, a square array of four charges was more than adequate to provide the required berthing space at a minimum 12-ft depth.

Phase II Breakwater Construction and Remedial Excavations

As indicated previously, misfires occurred in Detonations II-ABCD and II-EFGH. Detonation II-IJKL in which all charges detonated properly provides the best illustration of the method of creating a channel and basin in the coral material with explosives. A series of sequential photos of this detonation are

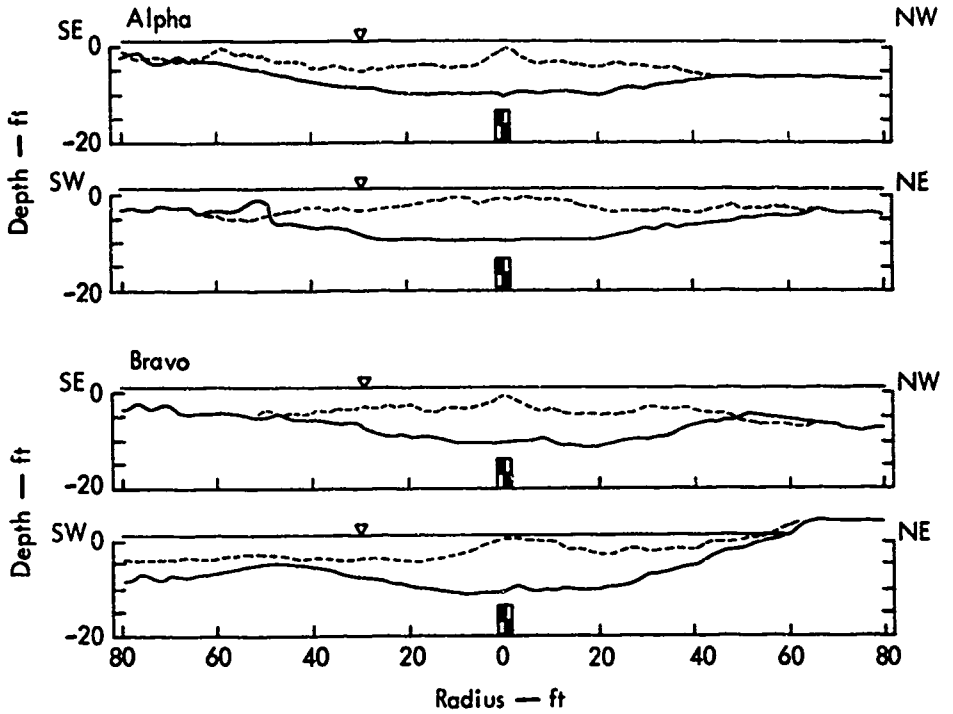

Fig. 37. Project Tugboat Phase I: crater cross sections for 1a (Alpha) and 1b (Bravo) detonations.

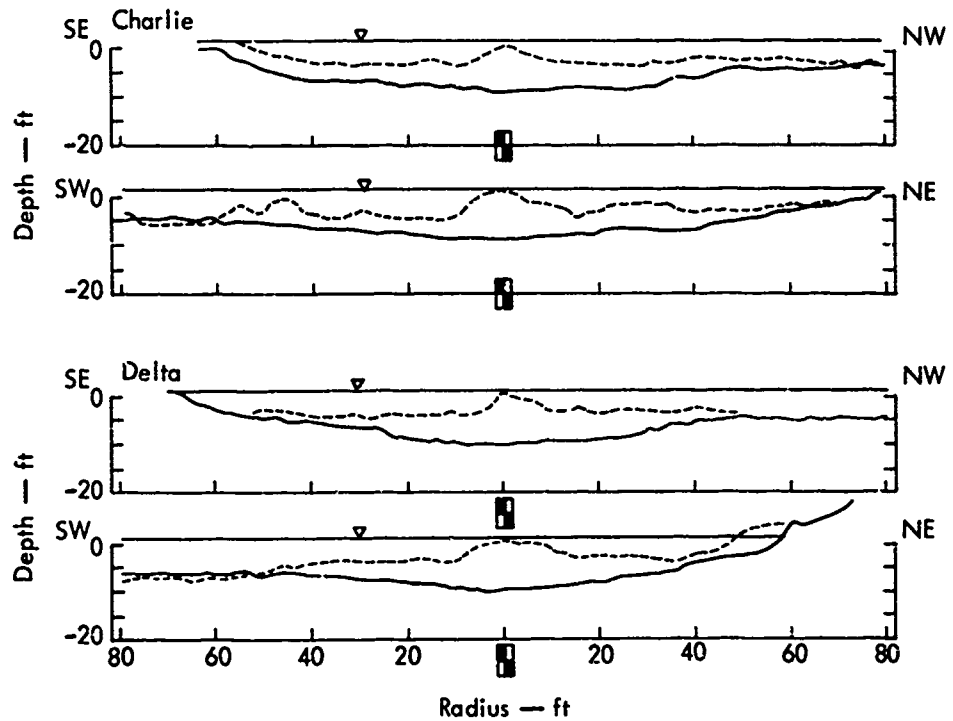

Fig. 38. Project Tugboat Phase I: crater cross sections for 1c (Charlie) and 1d (Delta) detonations.

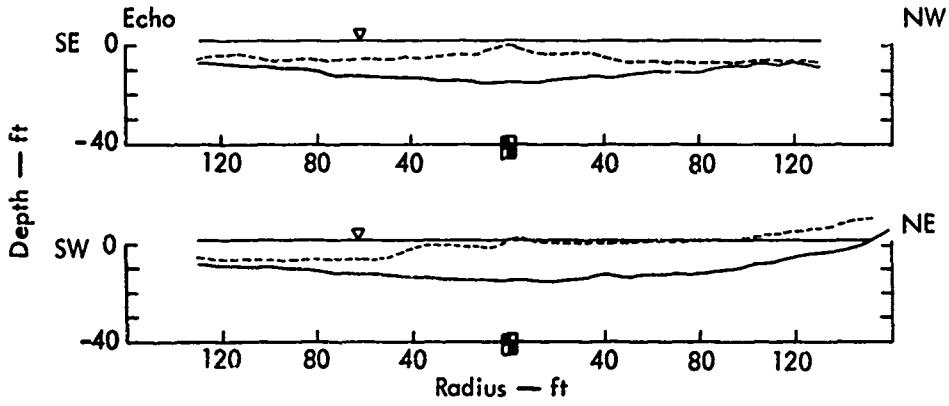

Fig. 39. Project Tugboat Phase I: crater cross sections for 1e (Echo) detonation.

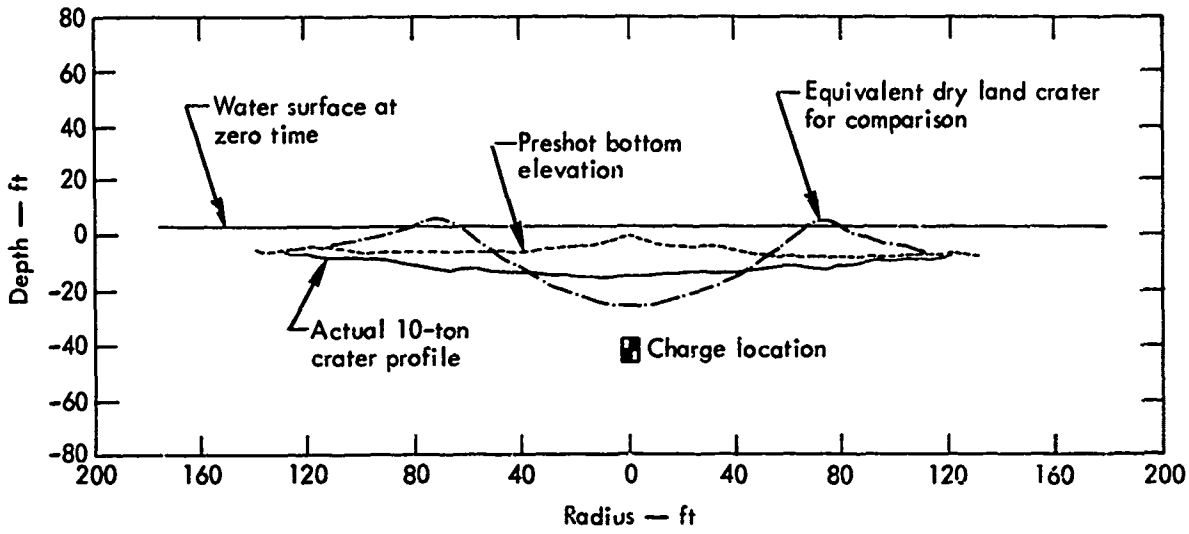

Fig. 40. Comparison of 1e (Echo) crater profile with dry land crater profile having dimensions assumed in the preliminary design.

shown in Fig. 41. An interesting shock wave interaction pattern was observed at the water surface for this detonation. Figure 42 shows the charge markers just prior to the detonation. Three sequential closeup photographs (Figs. 43 through 45) taken from high-speed movies of the SGZ area show a complex successive reinforcement and null pattern that forms a cross between the four charge locations. This phenomenon has been investigated in some detail and can be explained as due

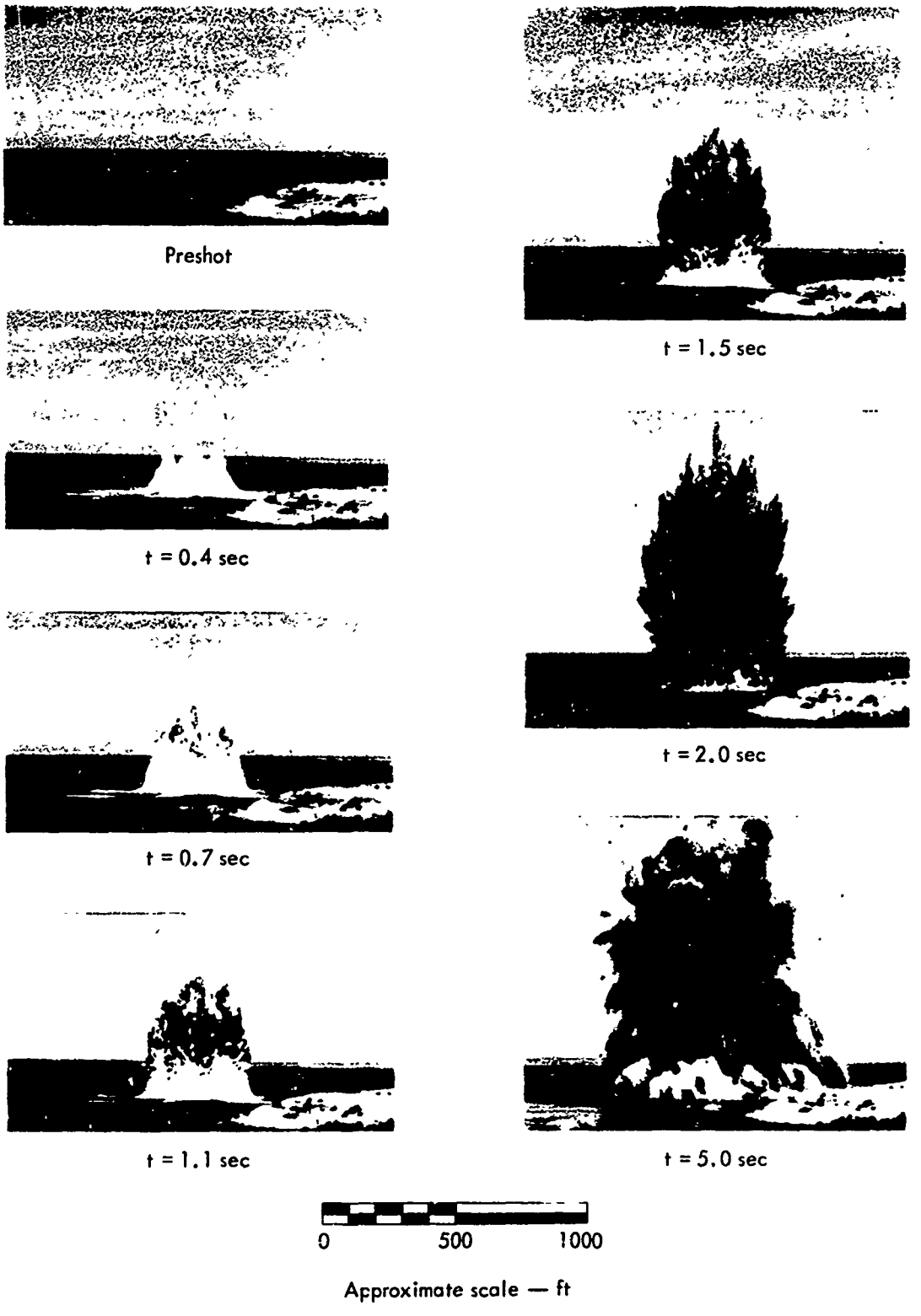

Fig. 41. Sequential photos of Detonation II-IJKL that created the berthing basin.

Fig. 42. Charge layout just prior to Detonation II-IJKL.

Fig. 43. Aerial photo taken just after detonation.

Fig. 44. Detonation II-IJKL showing shock interaction and cavitation phenomena at water surface.

Fig. 45. Changes in shock interaction and cavitation phenomena.

to shock wave interaction in the near surface water cavitated region over the charge locations (Ref. 8).

Following the Phase II detonations, the breakwater was constructed (see Fig. 46). This breakwater was in place during the remedial explosive excavation detonations in December 1970.

The final explosively excavated harbor is shown in Fig. 47 in which the area within the 12-ft water depth contour is shaded and can be compared with the original design. The actual channel and berthing area exceed the design area in all cases. The generally deeper water and sandy bottom of the channel and berthing area can be seen in a picture of the harbor area in Fig. 48.

Surveys

Surveys have been carried out to date at four times: (1) May 1969, (2) April 1970 before the Phase II shots, (3) May 1970 following the Phase II detonations,

Fig. 46. Breakwater construction activity following Phase II detonations.

and (4) December 1970 following the remedial detonations. Surveys were carried out by fathometer with tagline checks at intervals.

Figure 7 is a plan showing the bottom topography revealed by the May 1969 survey. Figure 49 shows the bottom topography from the May 1970 survey which followed the Phase II detonations, and Fig. 50 shows the bottom topography from the survey of December 1970. Figures 51 through 53 are isopach maps showing the thickness of material displaced (removed

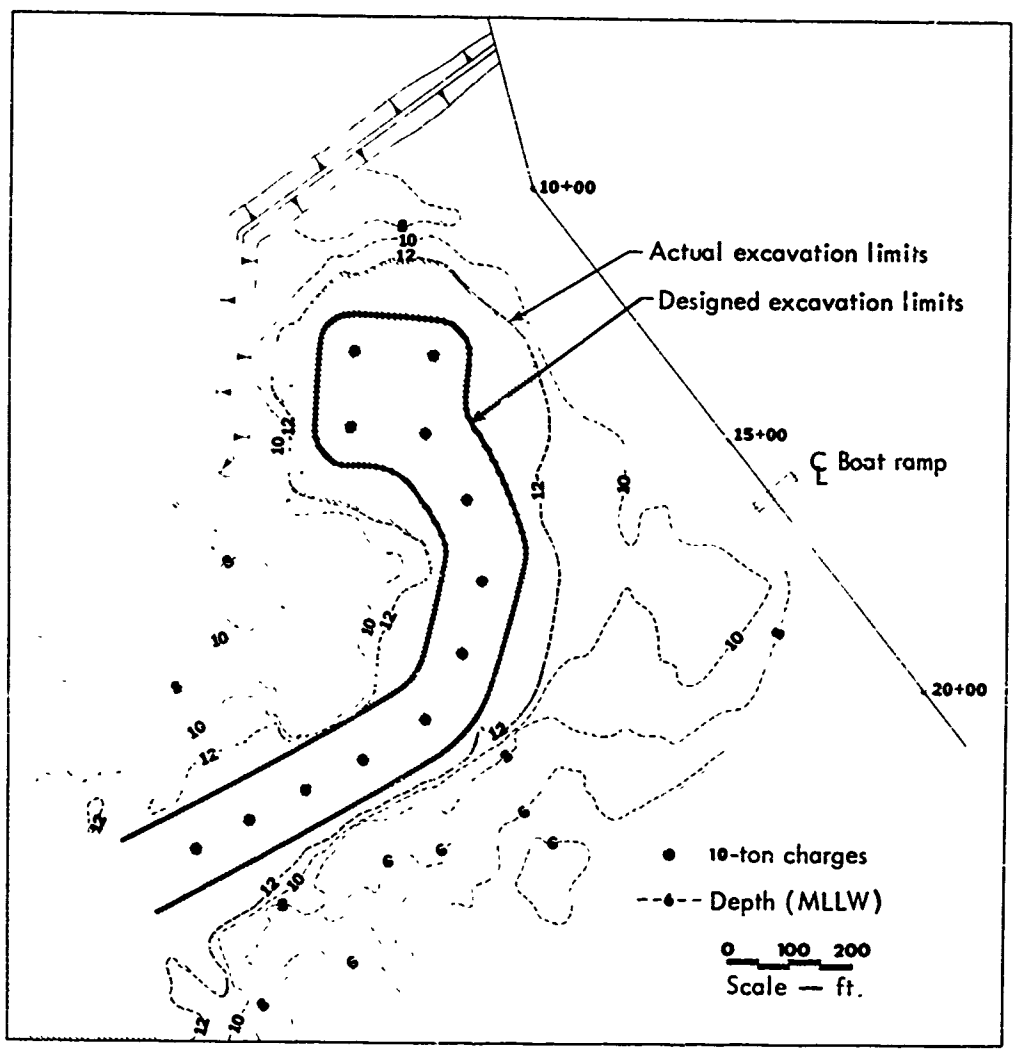

Fig. 47. Final harbor area excavated to 12-ft depth contour compared with required dimension.

or added) by the Phase II detonations, by the remedial blasts, and finally by the entire project, respectively.

The total volume excavated was roughly analyzed from these isopach maps. These analyses show the volume excavated within the 12-ft depth contour to be approximately 100,000 yd^3 and the total volume excavated to be approximately 137,000 yd^3. The project design volume was roughly estimated to be approximately 30,000 yd^3.

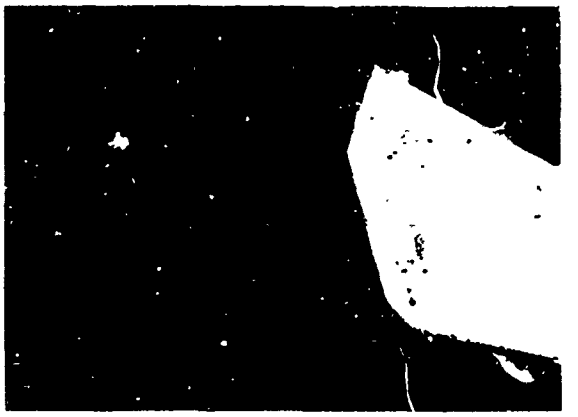

Fig. 48. Final harbor configuration.

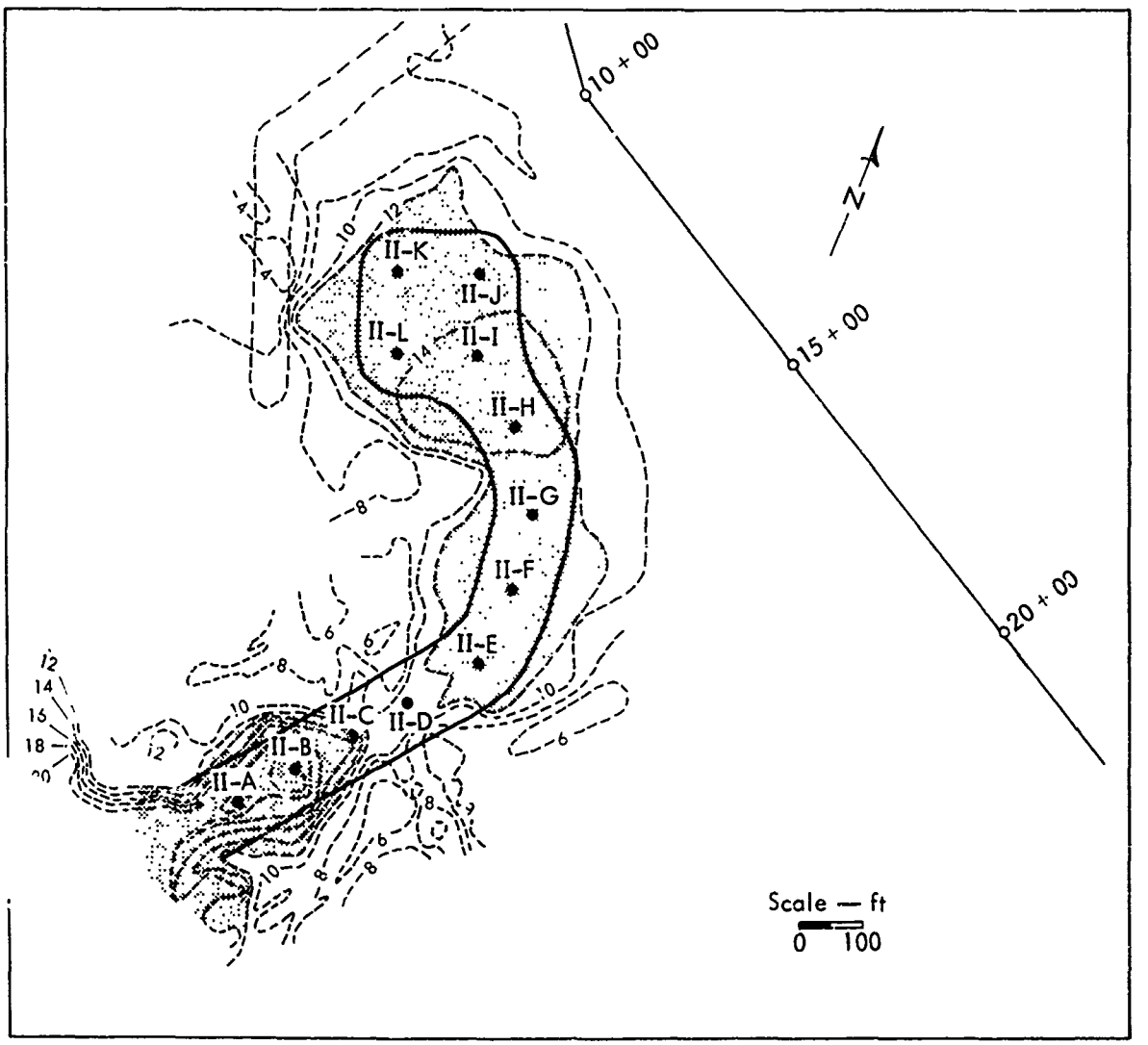

Fig. 49. Sea-bottom topography, May 1970, following Phase II detonations.

Several bottom profiles have been plotted for the project. A longitudinal profile of the channel and basin is presented in Fig. 54. Cross channel profiles were surveyed according to the plan shown in Fig. 55. These profiles were plotted and presented in Figs. 56 through 64.

In examining the profiles, the effects of both series of blasts in creating a channel where none had been are obvious. It is interesting to note, however, the differences between the May 1970 and December 1970 profiles. In the vicinity of Charges II-A, II-C, II-D, and II-G,

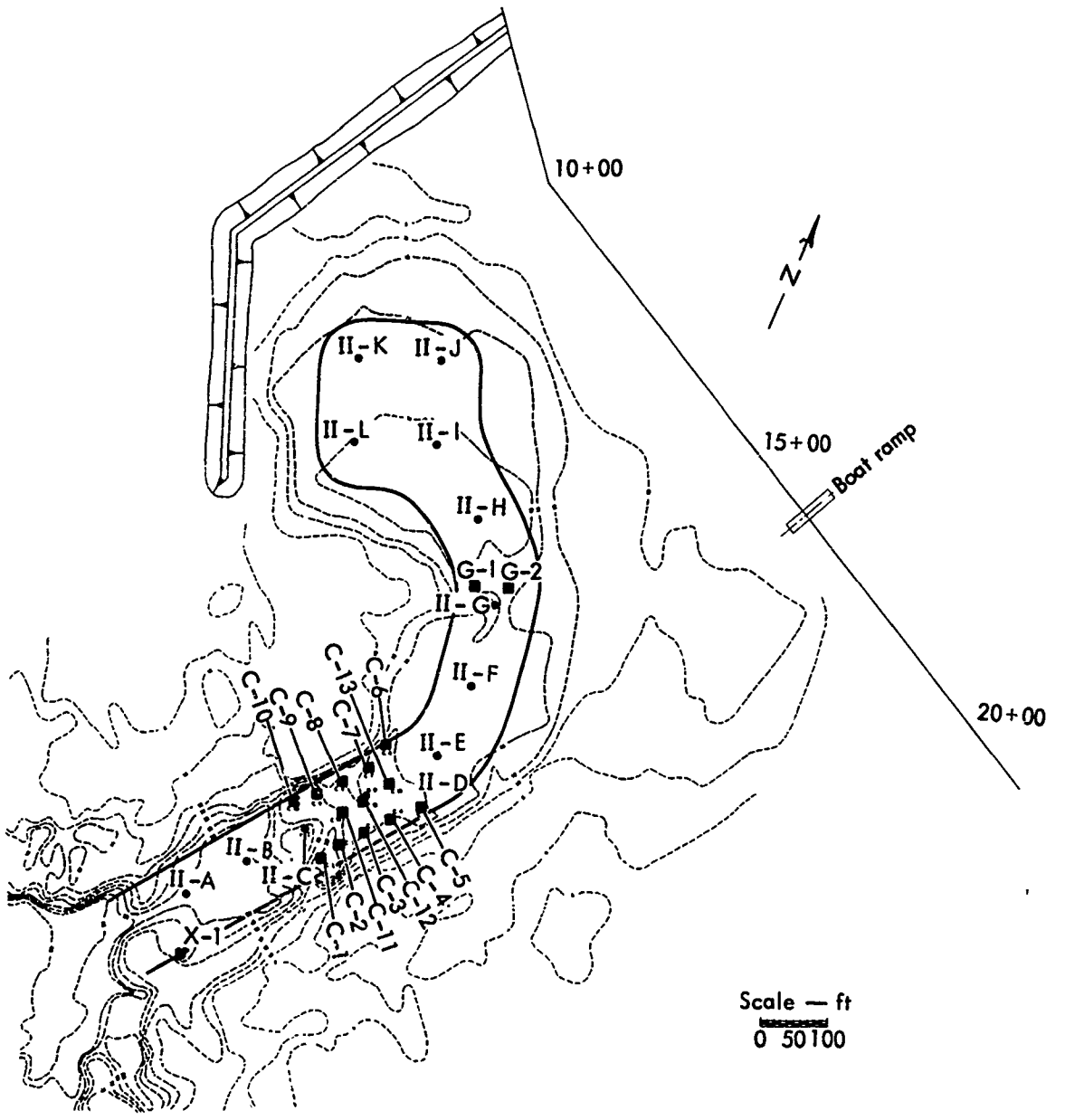

Fig. 50. Sea-bottom topography, December 1970, following remedial blasting.

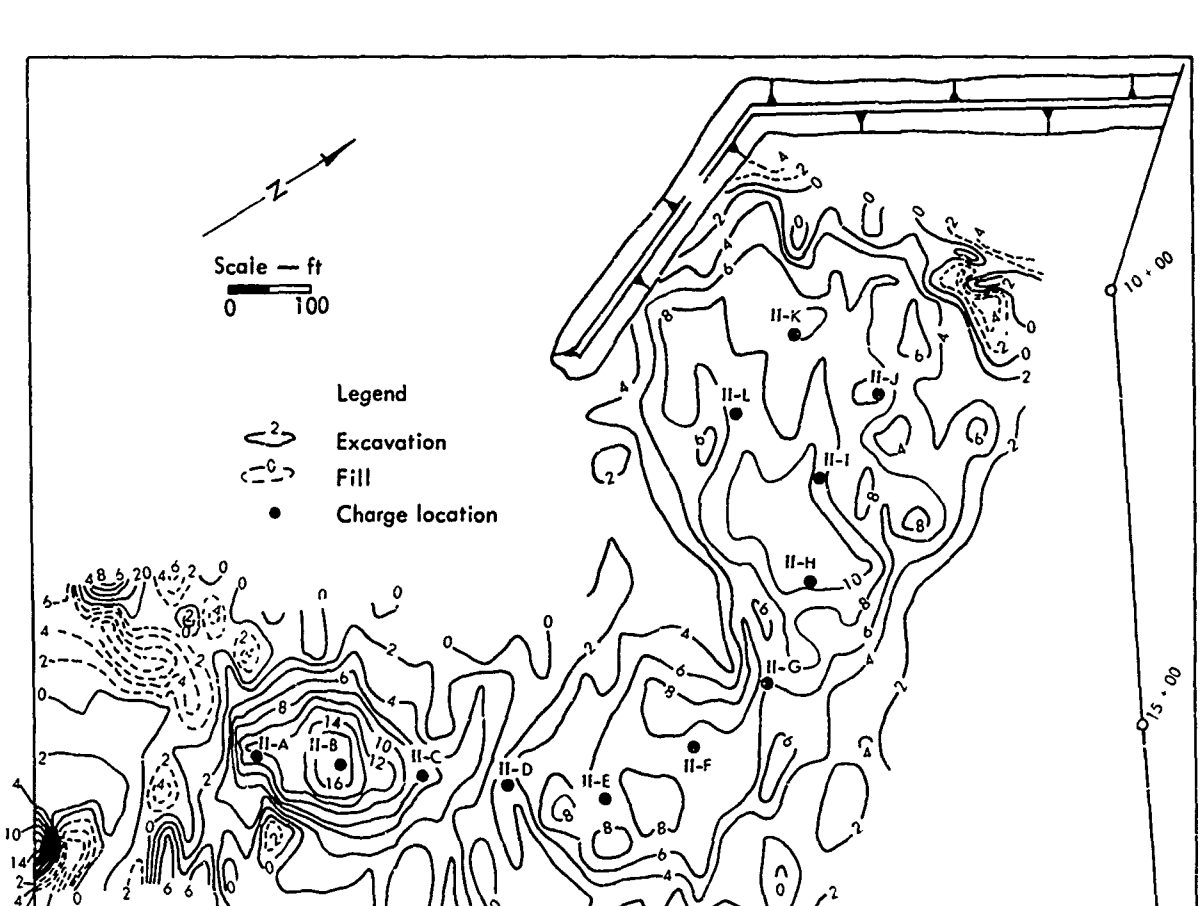

Fig. 51. Isopach map showing amounts of excavation (or fill) produced by Phase II detonations.

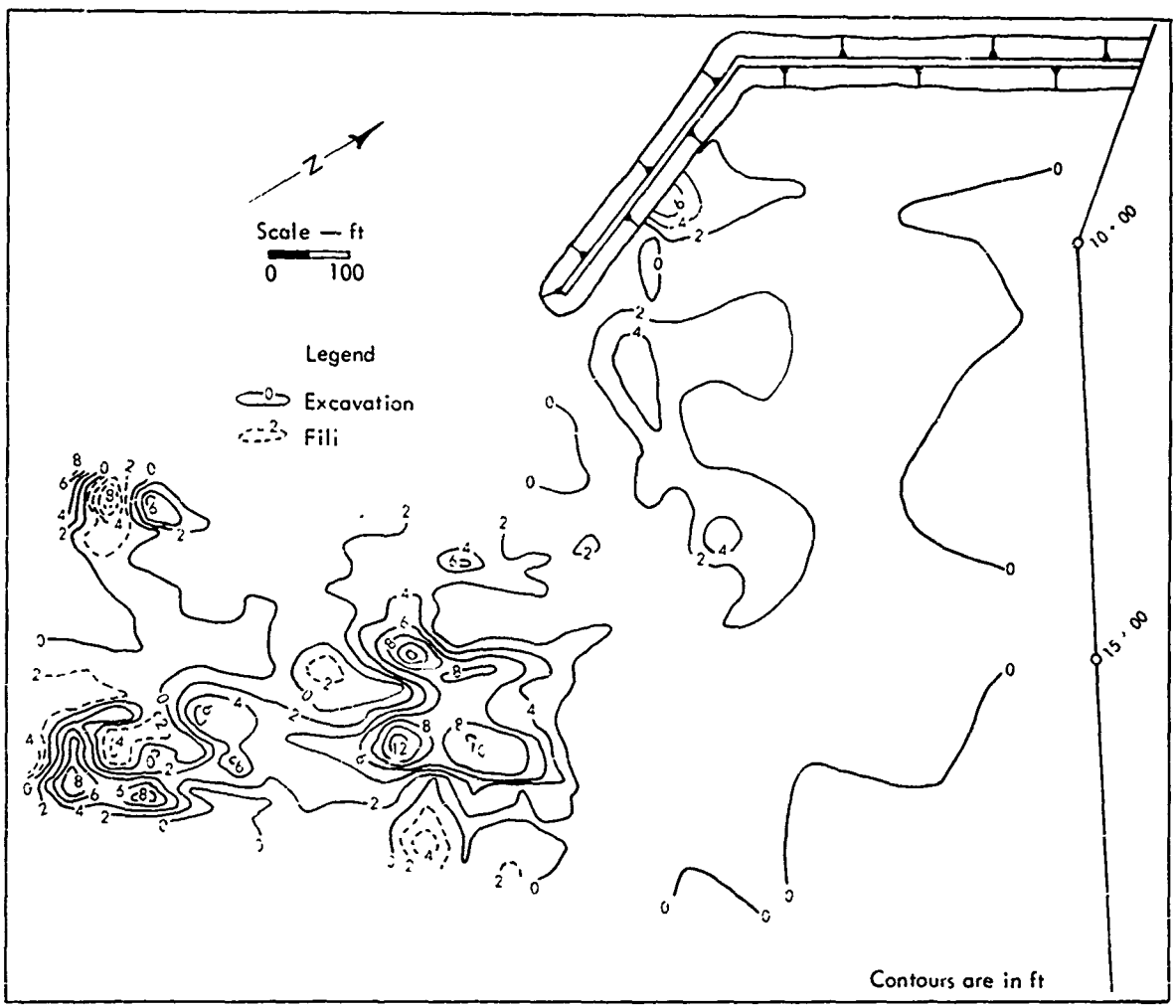

Fig. 52. Isopach map showing material moved by remedial detonations, December 1970.

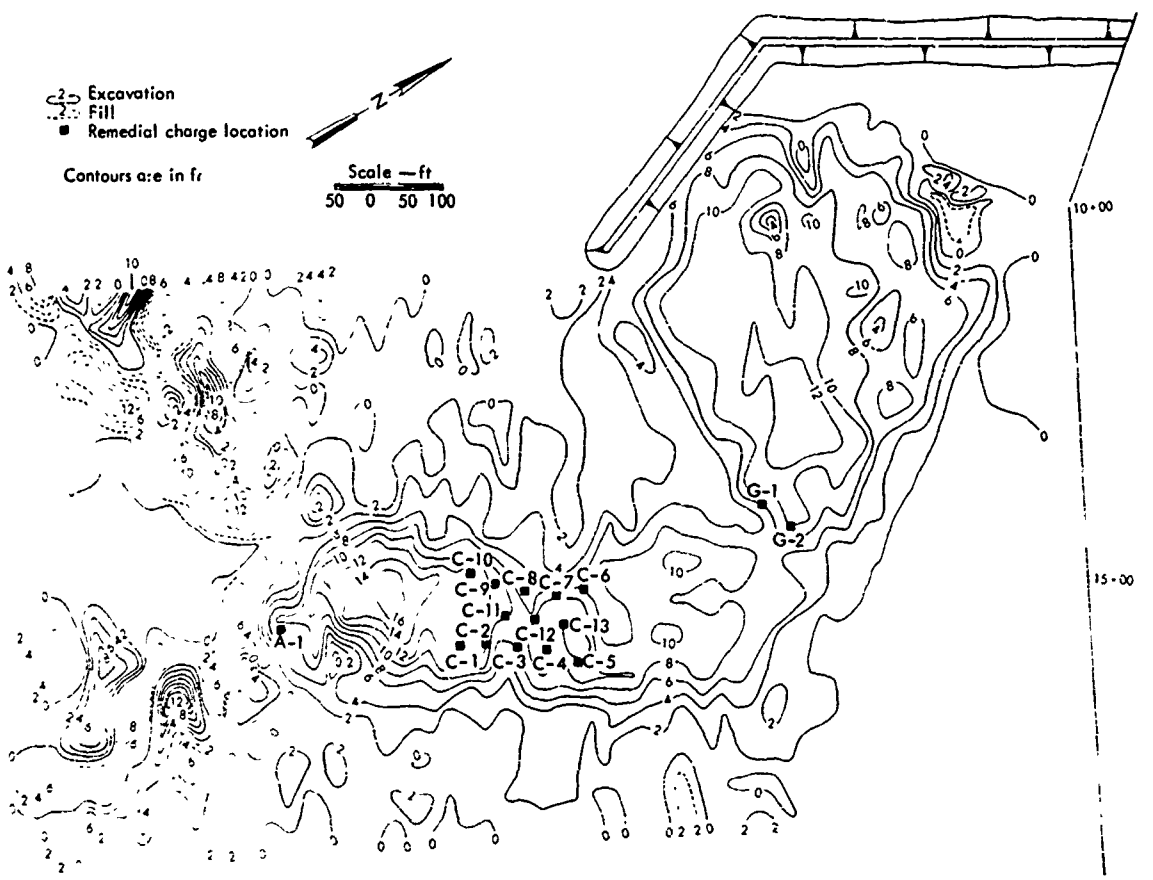

Fig. 53. Isopach map showing amounts of excavation (or fill) accomplished by the entire Project Tugboat program: Phase II and remedial.

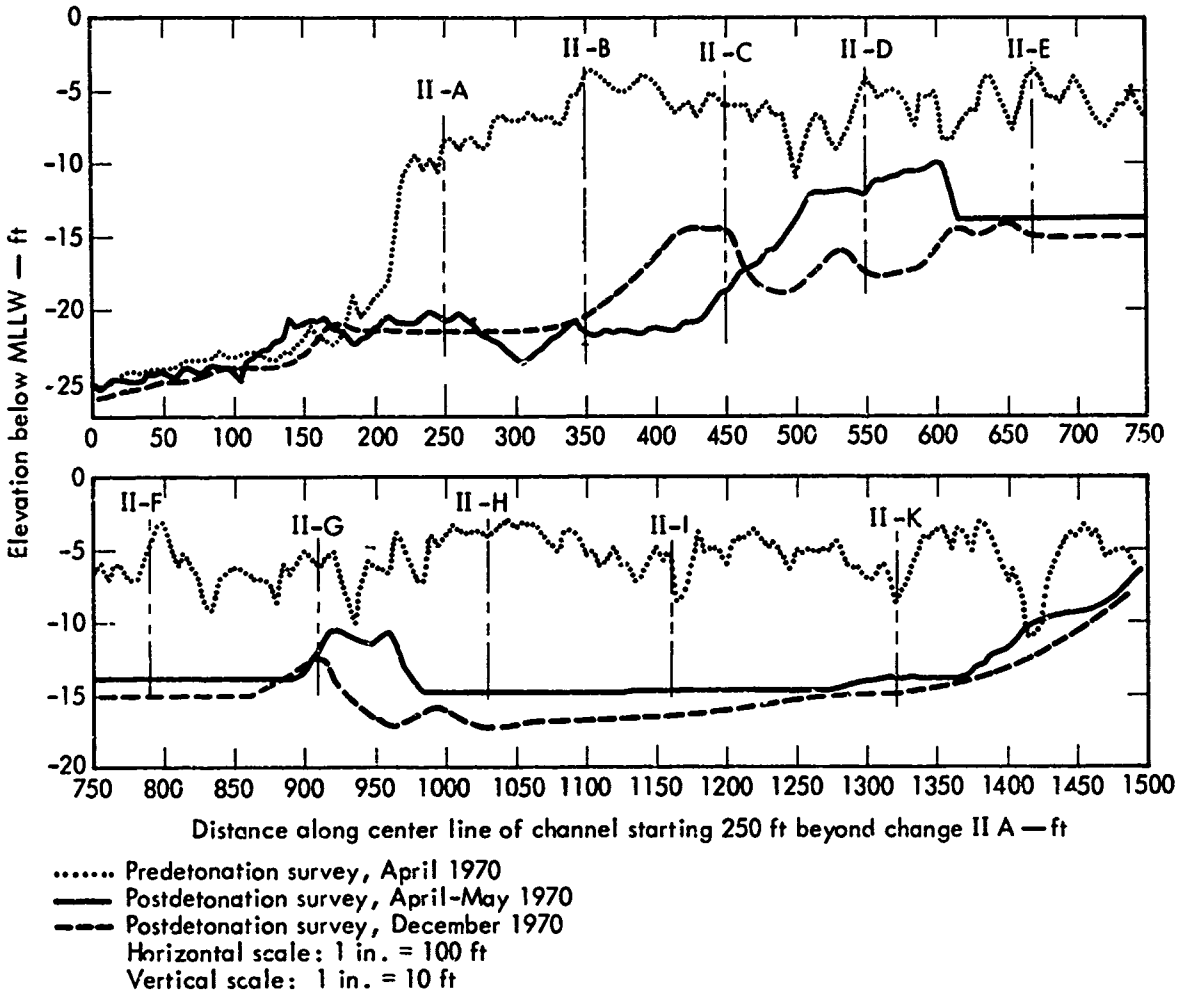

Fig. 54. Longitudinal profiles of Project Tugboat channel.

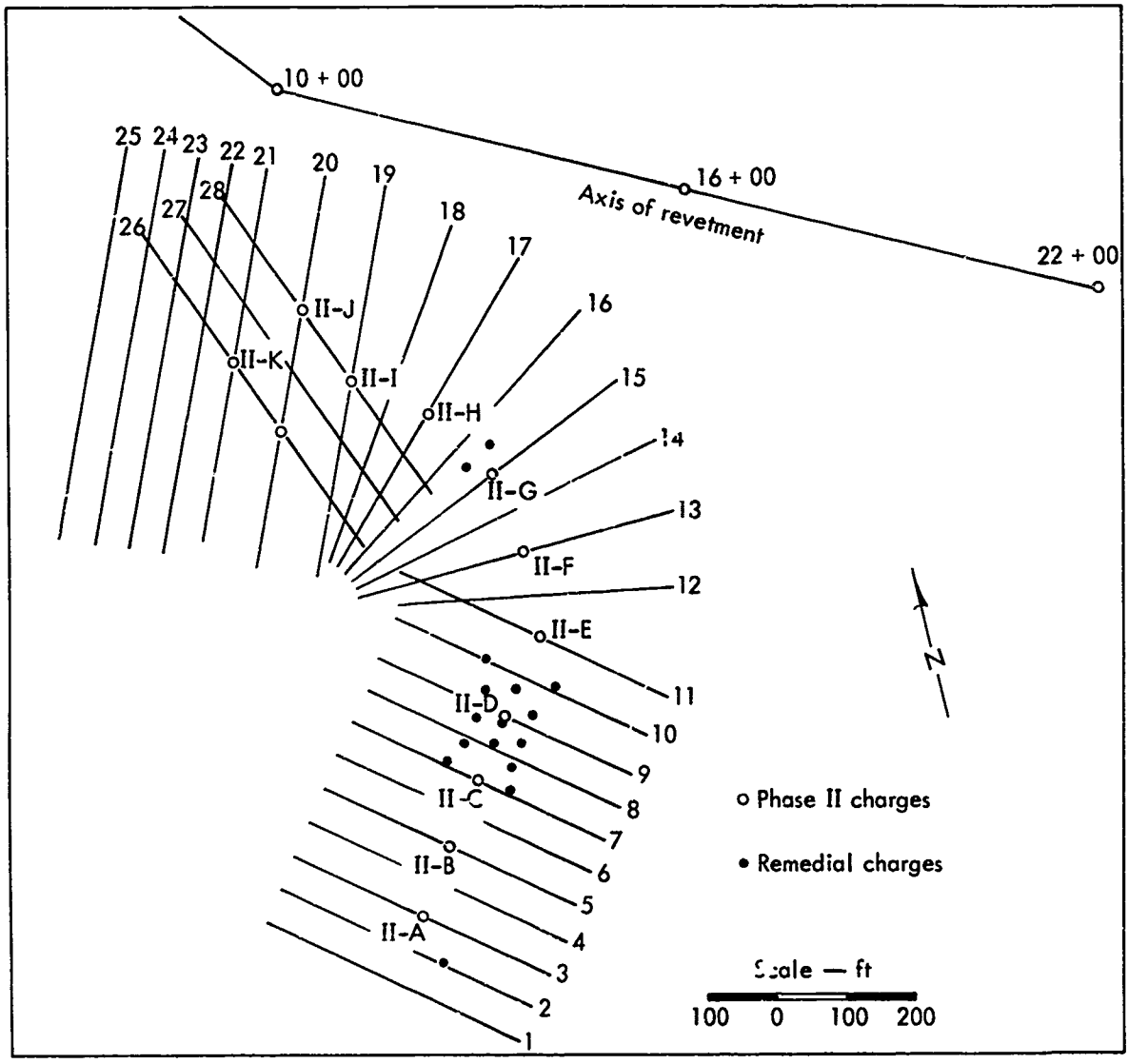

Fig. 55. Locations of survey profiles shown in following figures (in addition longitudinal profile was run—see Fig. 54—from 250 ft seaward of Charge II-A to 170 ft west of Charge II-K).

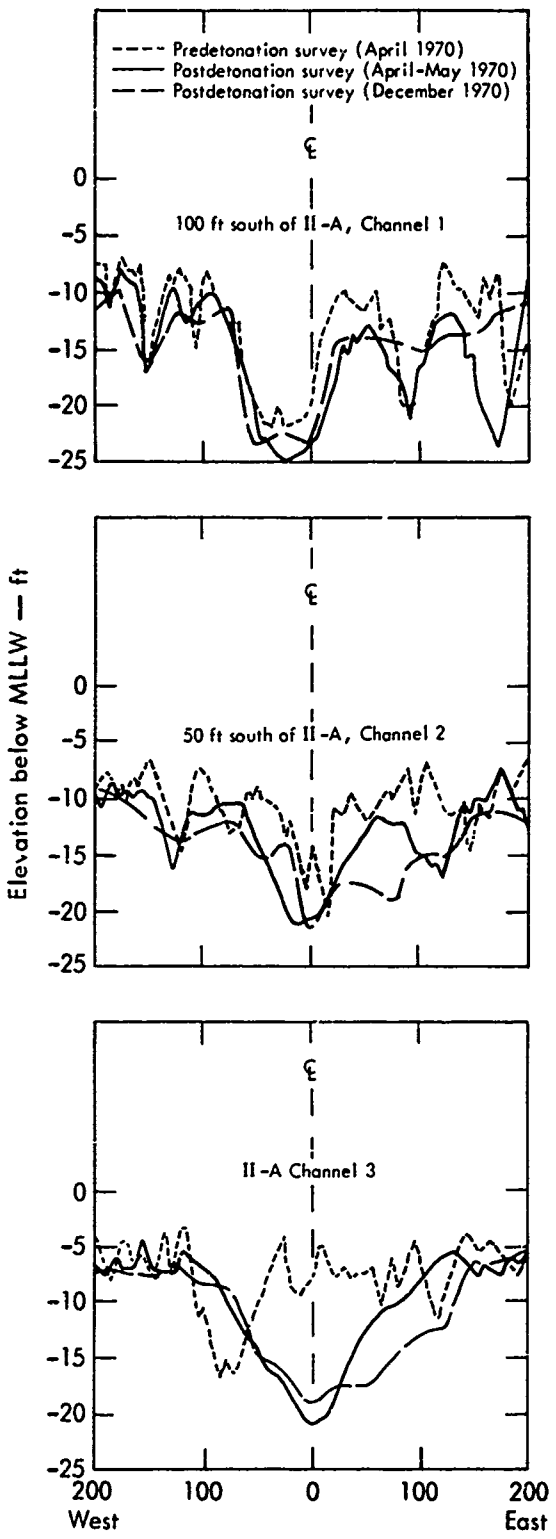

Fig. 56. Transverse profiles, Project Tugboat Channels 1, 2, and 3.

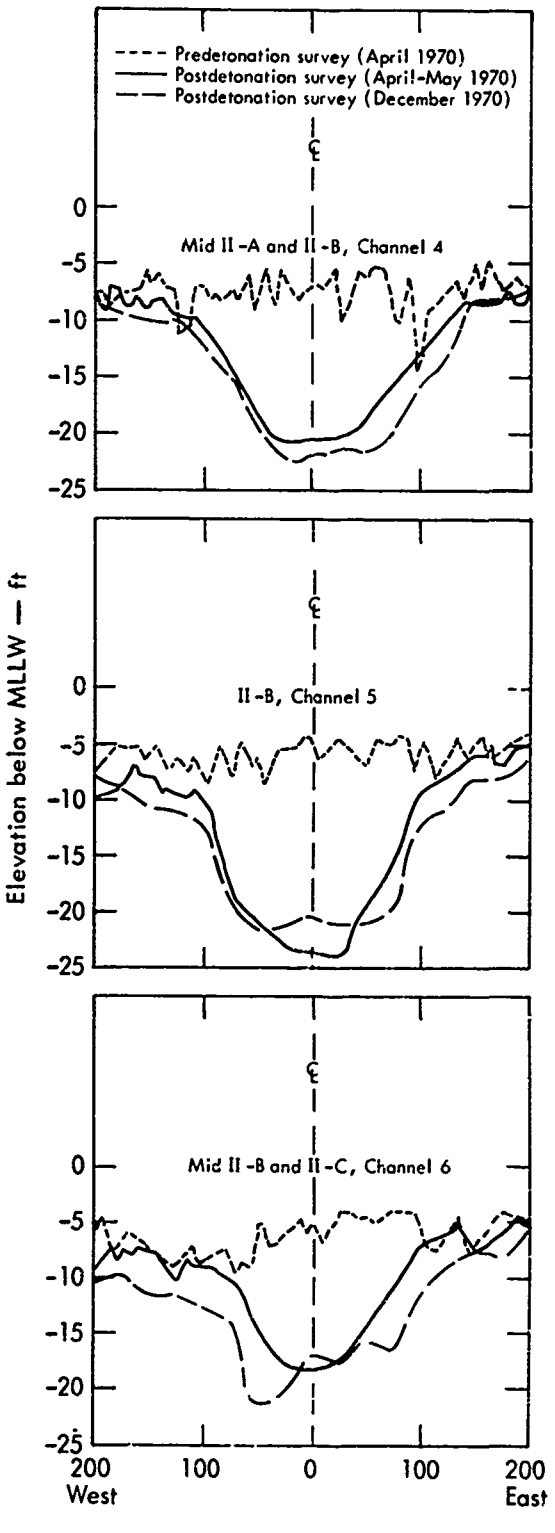

Fig. 57. Transverse profiles, Project Tugboat Channesl 4, 5, and 6.

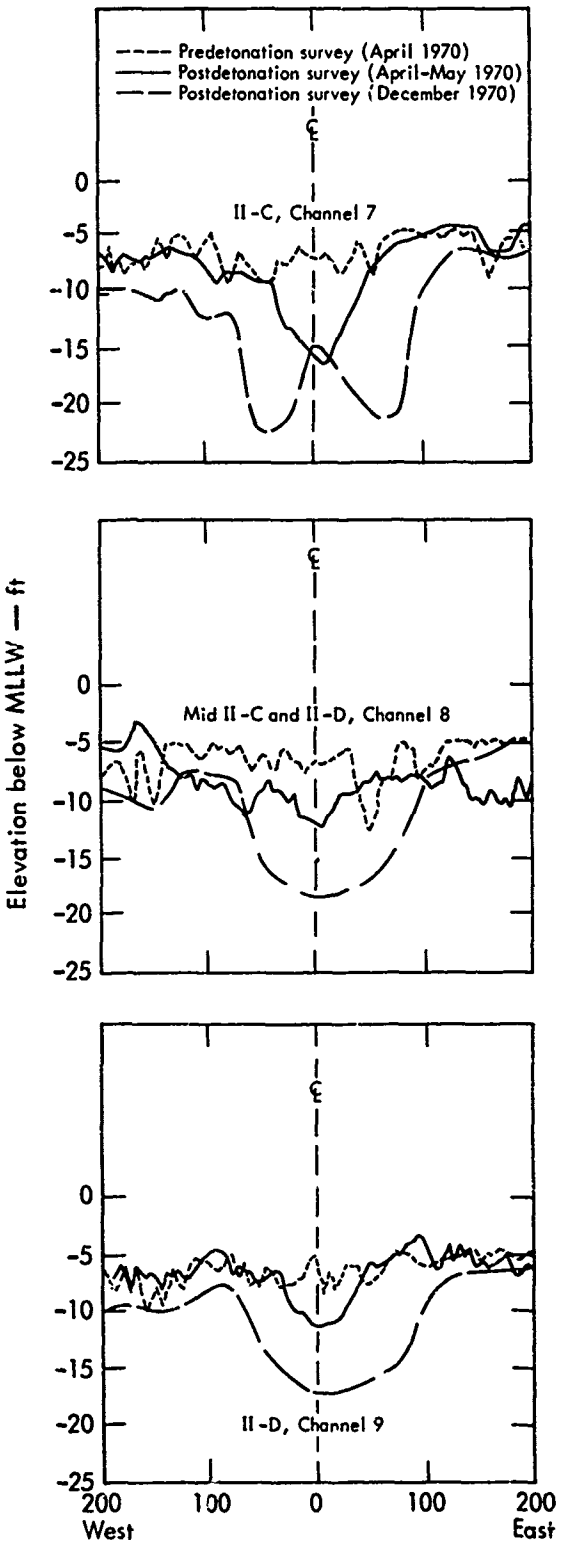

Fig. 58. Transverse Profiles, Project Tugboat Channels 7, 8, and 9.

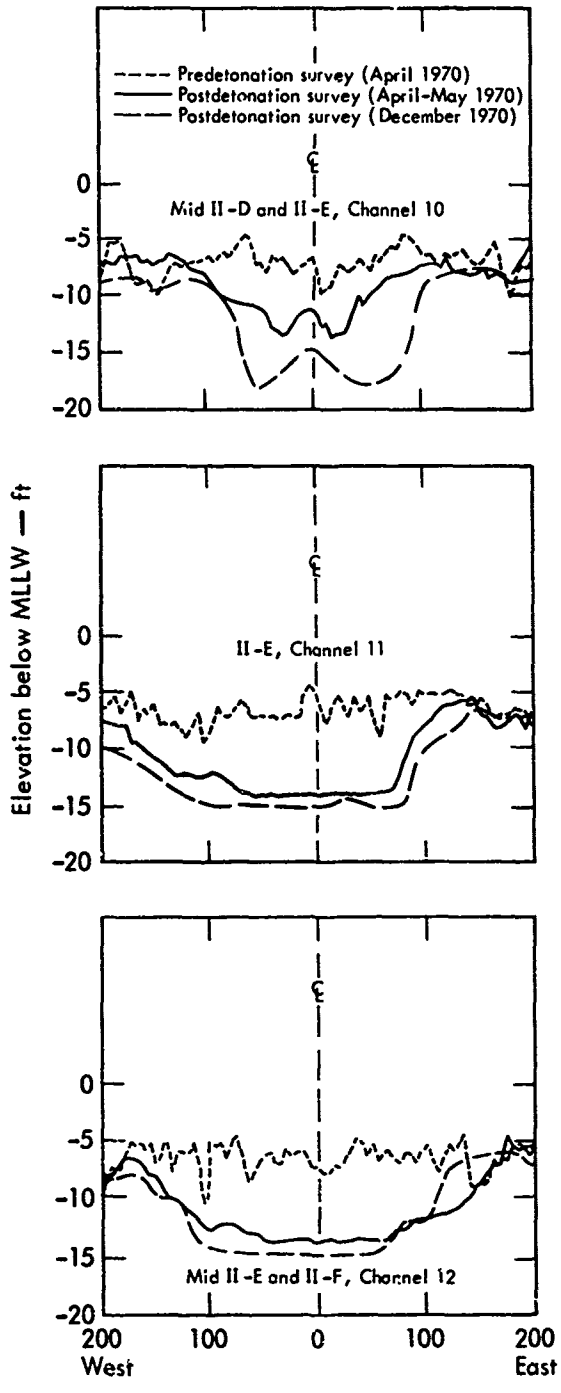

Fig. 59. Transverse profiles, Project Tugboat Channels 10, 11, and 12.

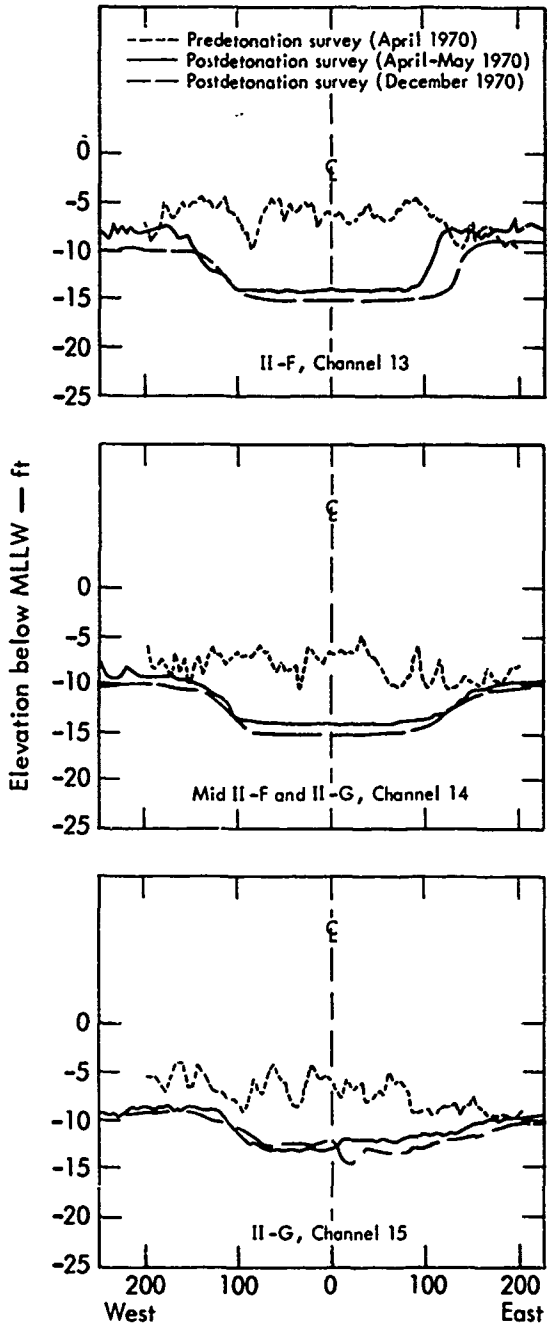

Fig. 60. Transverse profiles, Project Tugboat Channels 13, 14, and 15.

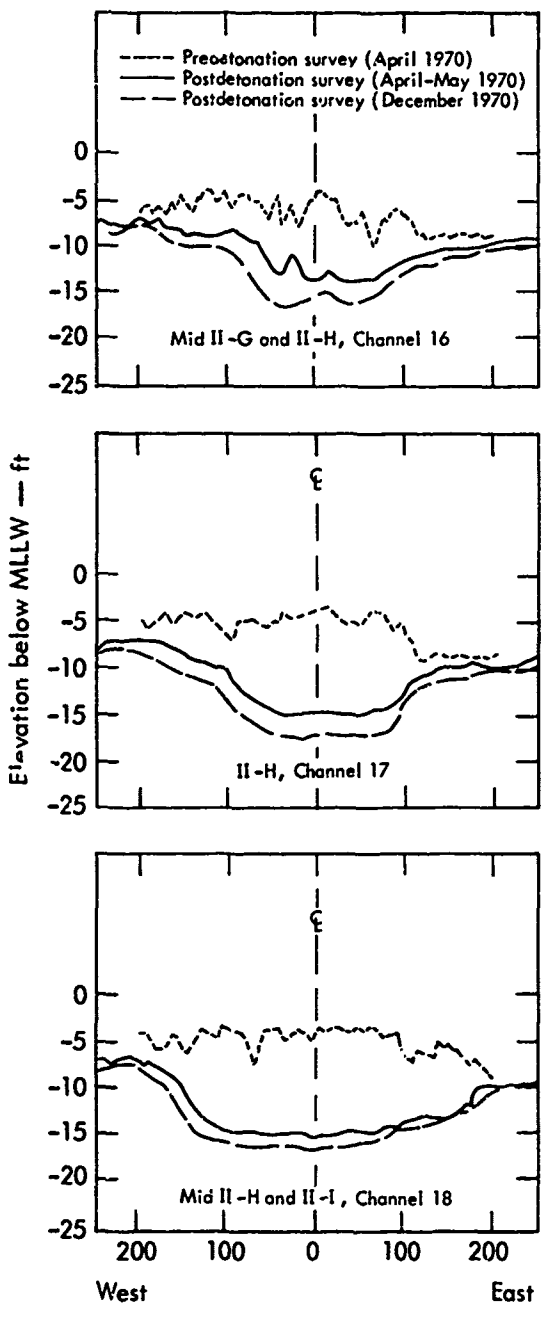

Fig. 61. Transverse profiles, Project Tugboat Channels 16, 17, and 18.

where remedial blasting was done, the surface was noticeably lowered by the blasting, as expected; but at almost all other places a lowering of the ground surface of 1 to 2-1/2 ft on the average was noted. This cannot be ascribed to the remedial blasting but must be a long-term settling effect; i.e., in approximately 7 mo time following the Phase II detonations an average of a little less than 2 ft of settlement occurred. It was in fact noted during the process of emplacement of the remedial explosives that

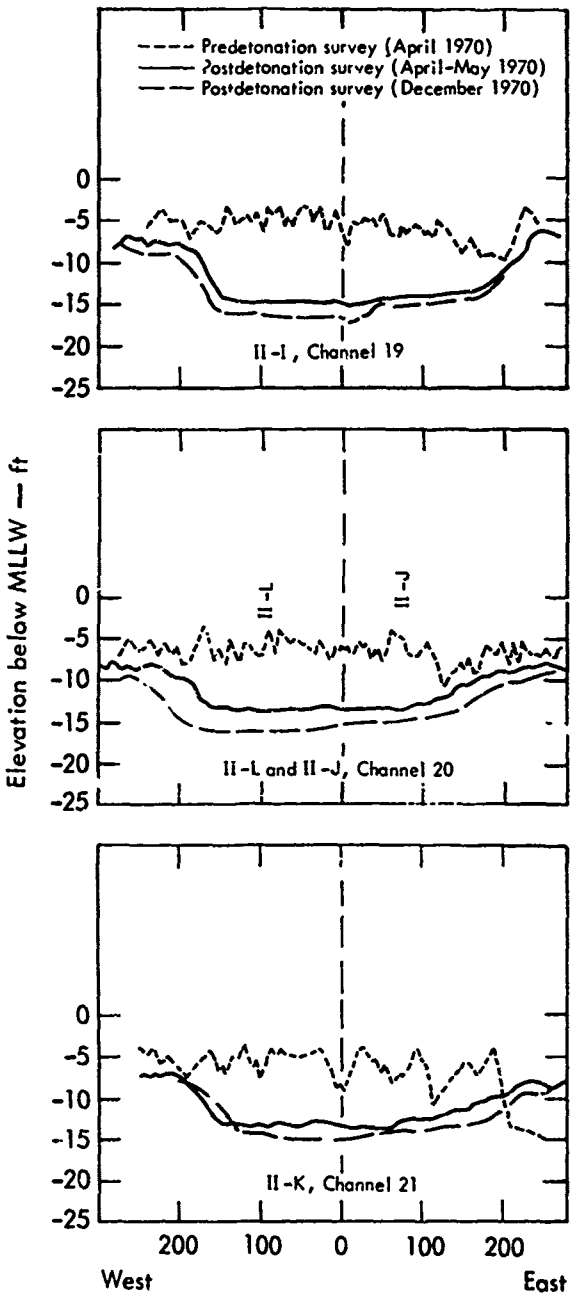

Fig. 62. Transverse profiles, Project Tugboat Channels 19, 20, and 21.

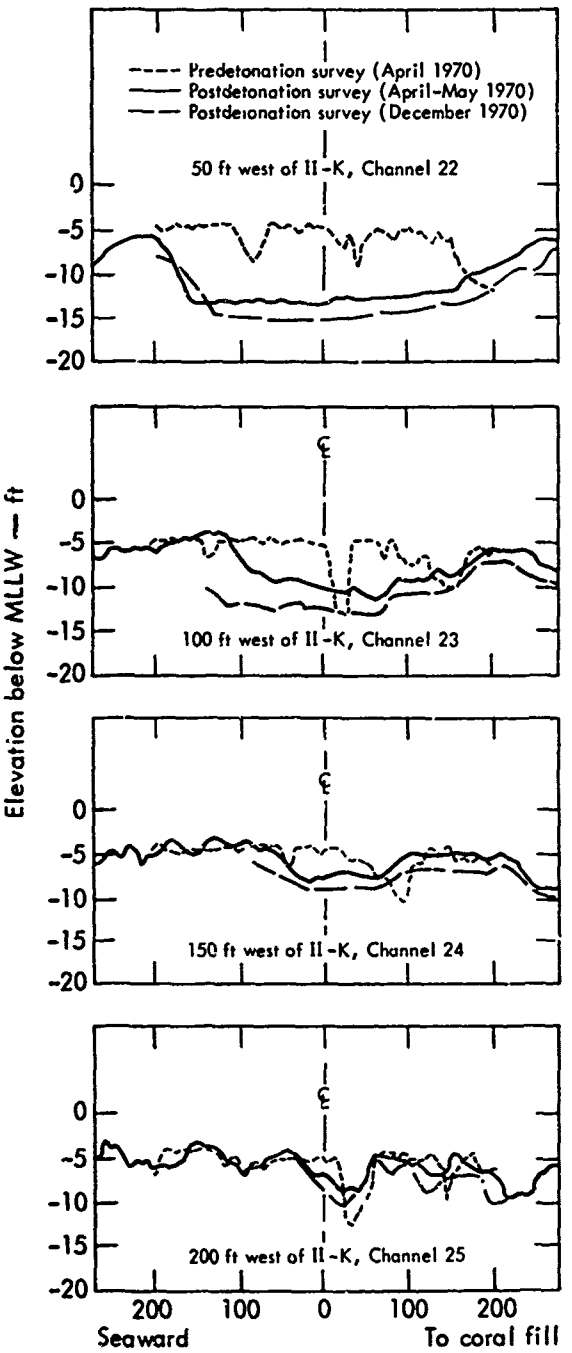

Fig. 63. Transverse profiles, Project Tugboat Channels 22, 23, 24, and 25.

water depths in the channel in the area of Charges II-C and II-D were on the average about 1-1/2 ft deeper than indicated on the working drawings, which were based on the May 1970 survey.

One survey remains to be performed. It is now scheduled to be done during 1972 (one year following the end of construction). An additional survey was planned following a major storm in the Kawaihae area (a storm equivalent to the maximum storm in a 5- to 10-yr interval); however, none occurred in the allotted time period so the survey was cancelled. The purpose of these last surveys was to determine the long-term effects, if any, of time, prevailing wave patterns, and currents in changing the configuration of the Tugboat harbor.

SUBSURFACE INVESTIGATIONS

Several different types of investigations were carried out at the Project Tugboat site after the detonations to measure and to record the postshot condition of the site materials. These investigations included acoustic subbottom profiling, probing, drilling, and underwater photography.

Acoustic Subbottom Profiling

Acoustic subbottom profiling was carried out following the detonations. The profiling was conducted in two surveys: a survey was carried out in December 1969 following the Phase I detonations, and a second survey was carried out in May 1970 following the Phase II detonations. Locations and results of the surveys are discussed in the following paragraphs.

The acoustic subbottom profiling technique is essentially a reflection seismic technique. A repetitive sound signal is transmitted downward through the water into the bottom sediment, and return signals are detected by an acoustic receiving system and recorded by a continuous recorder. Any interface in the ground between layers of two materials with differing acoustic properties may act as a

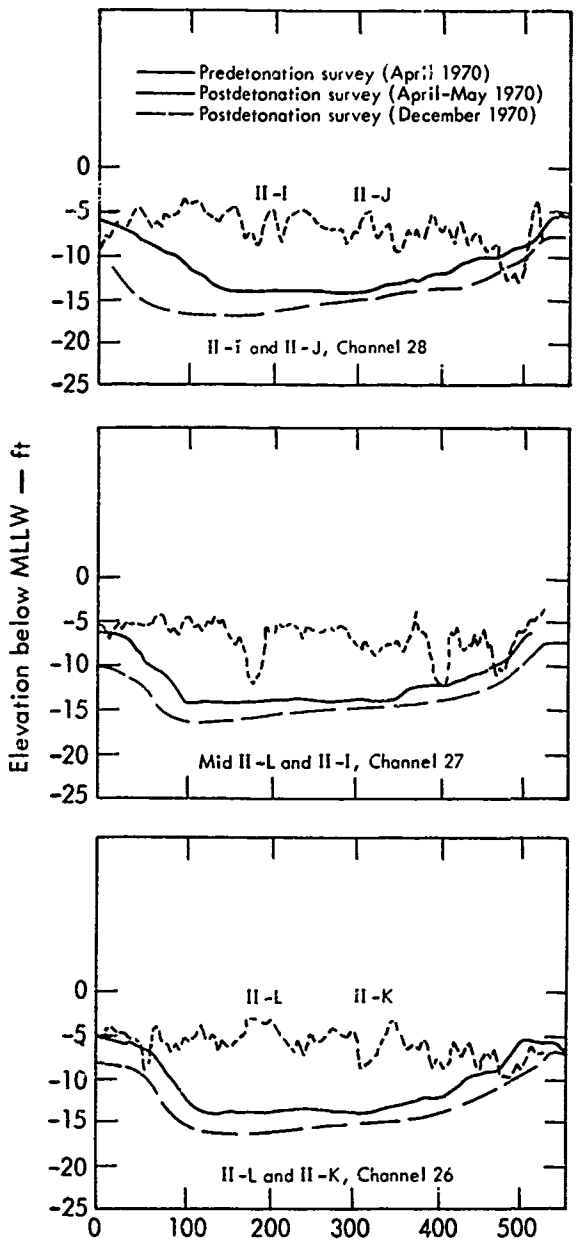

Fig. 64. Transverse profiles, Project Tugboat Channels 26, 27, and 28.

reflecting horizon. The repetitive sound signal may be produced by any of a variety of techniques; e.g., spark, gas, compressed air, etc. The penetration and resolution of the signals are inversely related functions of the frequency of the sound. High-frequency sound gives a signal with high resolution, but has poor penetration; low-frequency sound has higher penetration and thus can detect deeper reflecting horizons, but with poorer resolution, and hence less detail. As with all seismic results the nature of the materials producing the recorded signals is not given directly by the technique; the interpretation of the records is thus a matter of judgment. The materials can be identified with certainty only by drilling through them.

At Project Tugboat two separate types of acoustic systems were used: an 8.5-kHz (high-frequency) high-energy

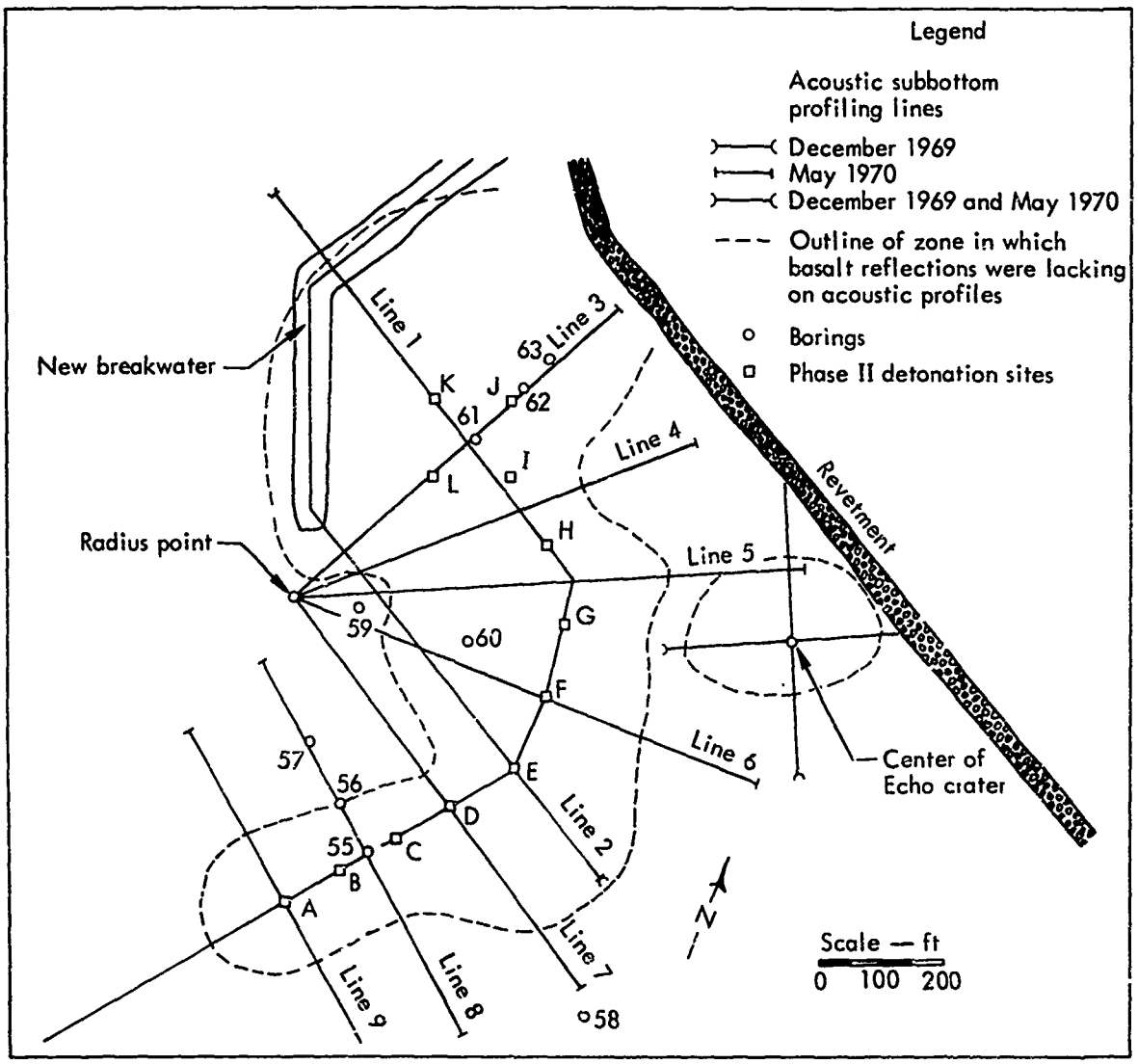

Fig. 65. Locations of acoustic profiling lines and postshot borings.

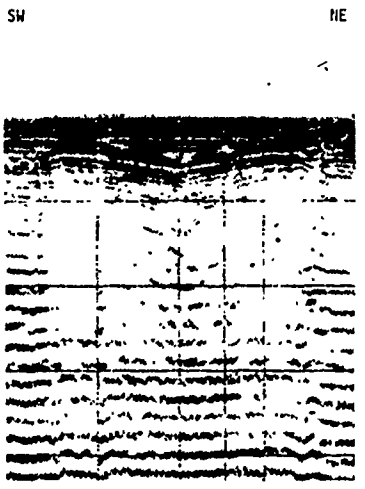

(a) SW-NE line.

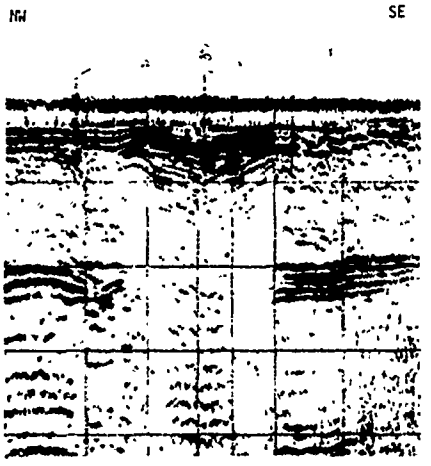

(b) NW-SE line.

Fig. 66. Pulser records for Echo crater, December 1969 (each horizontal line represents approximately 50 ft of depth; dipping strata give probable indication of extent of true crater; note basalt reflection at about 100-ft depth, in (b) especially).

sonar and a 250-Hz center frequency (low-frequency) 16-joule pulser system. The pulser records were the most useful.

The first survey, December 1969, consisted of two perpendicular profiles across Echo crater and two linear traverses, one along the centerline of the proposed breakwater and the other along the centerline of the future channel. The second survey, May 1970, consisted of linear traverses, as above, along the future breakwater and the newly excavated channel, and seven profiles transverse to the channel and berthing basin. The specific locations of these lines are shown in Fig. 65.

Figure 66 shows the pulser records (low-frequency technique) of the two passes over Echo crater in December 1969. Figures 67 through 69 show pulser records of both the longitudinal and the transverse profiles surveyed in May 1970. Interpretations of these records were furnished by the acoustic profiling contractor.

In the December 1969 survey, a strong reflecting horizon was detected along the future breakwater centerline at a depth of about 95 ft near the revetment and sloping down to 125 ft at the outer end of the breakwater. This was interpreted as being the top of the basalt underlying the coral. Along the channel alinement a similar strong reflecting horizon, somewhat irregular, was detected at a depth of 95 ft in the berthing basin area, shoaling to 135 ft at the outer end of the channel. This was likewise interpreted as being the top of the basalt.

In the two lines across Echo crater, the same strong reflection at about 100-ft depth was present (Fig. 66), but only at the ends of the lines; it was missing over the crater itself. The probable reason for the lack of the basalt reflection in the crater area was that the acoustic signal was attenuated in the discontinuous fractured coral in and adjacent to the crater.

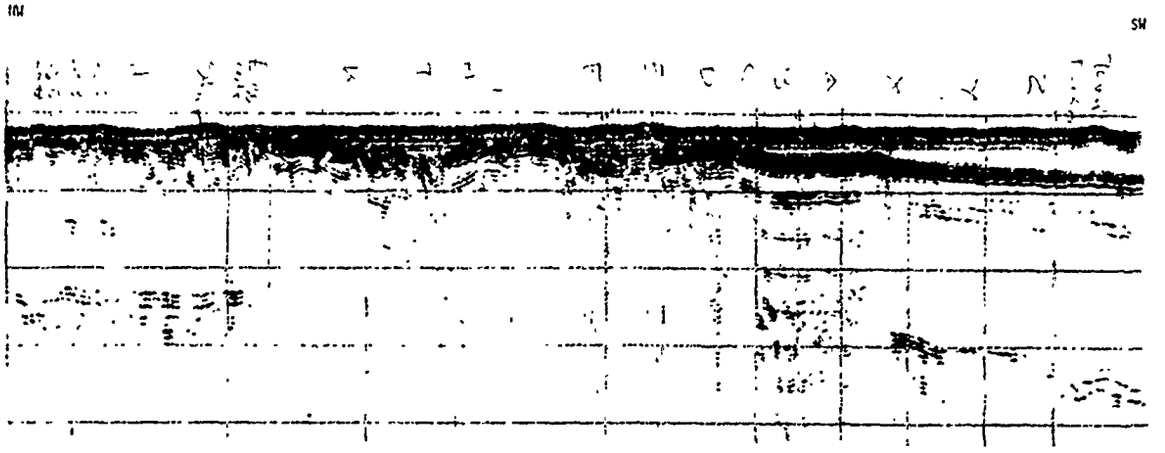

(a) Line 1, along axis of channel.

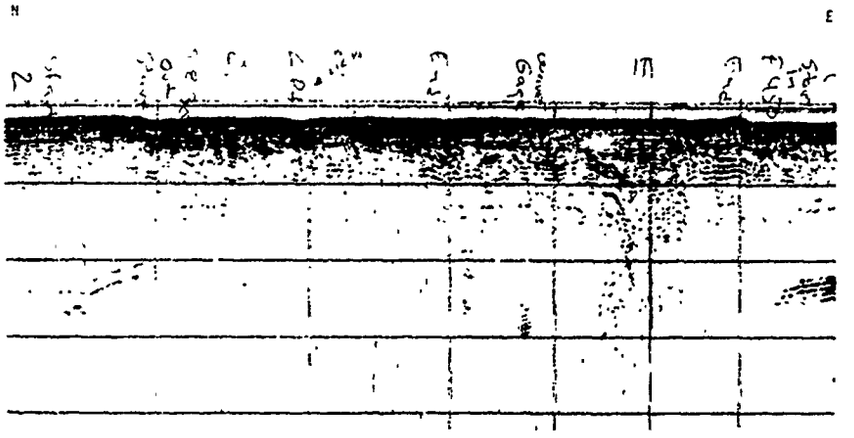

(b) Line 2, along centerline of future breakwater.

Fig. 67. Pulser records, May 1970 (each horizontal line represents approximately 50 ft of depth; letters in (a) correspond to Phase II charge sites; letter "E" in (b) corresponds to charge site II-E; note basalt reflection between 100- and 150-ft depth at ends of both lines).

The presence or absence of the basalt reflection thus offers a clue to the boundary of the rupture zone.

The two lines across Echo crater showed three separate strong reflecting horizons defining the crater itself, the deepest one at about 45 ft with a small "pit" at the precise crater center. The upper reflections, which slope gently toward the crater center, evidently represent sedimentary beds of material redeposited into the crater following the blast (fallback and washback). The outer edge of the dipping reflections suggests the position of the boundary of the true crater.

In the second survey, May 1970, the basalt reflection showed up consistently at the ends of the transverse lines, but failed to show up in the central area (the crater). In the three outboard lines (near the channel entrance) the basalt reflection did show up in the crater area, though weakly. In the profile along the centerline

of the future breakwater, Fig. 67 (b), the basalt reflection was lacking except for a short interval immediately adjacent to the revetment. The reflection had shown up along this line in December 1969. If the cause of the lacking basalt reflection was indeed fracturing of the coral as hypothesized above for the Echo crater profiles, then the coral was apparently fractured out to the location of the breakwater by the detonations in the berthing basin. The basalt reflection also was lacking in the longitudinal traverse along the center of the channel, where it had been present before—except at the ends of the line; see Fig. 67(a).

Inspection of the acoustic records of the transverse lines shows that where Phase II charges detonated, reflections from inward-dipping fallback and washback beds were picked up. In line 5, which passed near the site for Charge II-G, Fig. 68(c), no crater is evident. The true crater boundary is assumed to correspond with the line at which the inward-dipping reflections terminate.

During the May 1970 acoustic survey, a few days after the Phase II detonations,

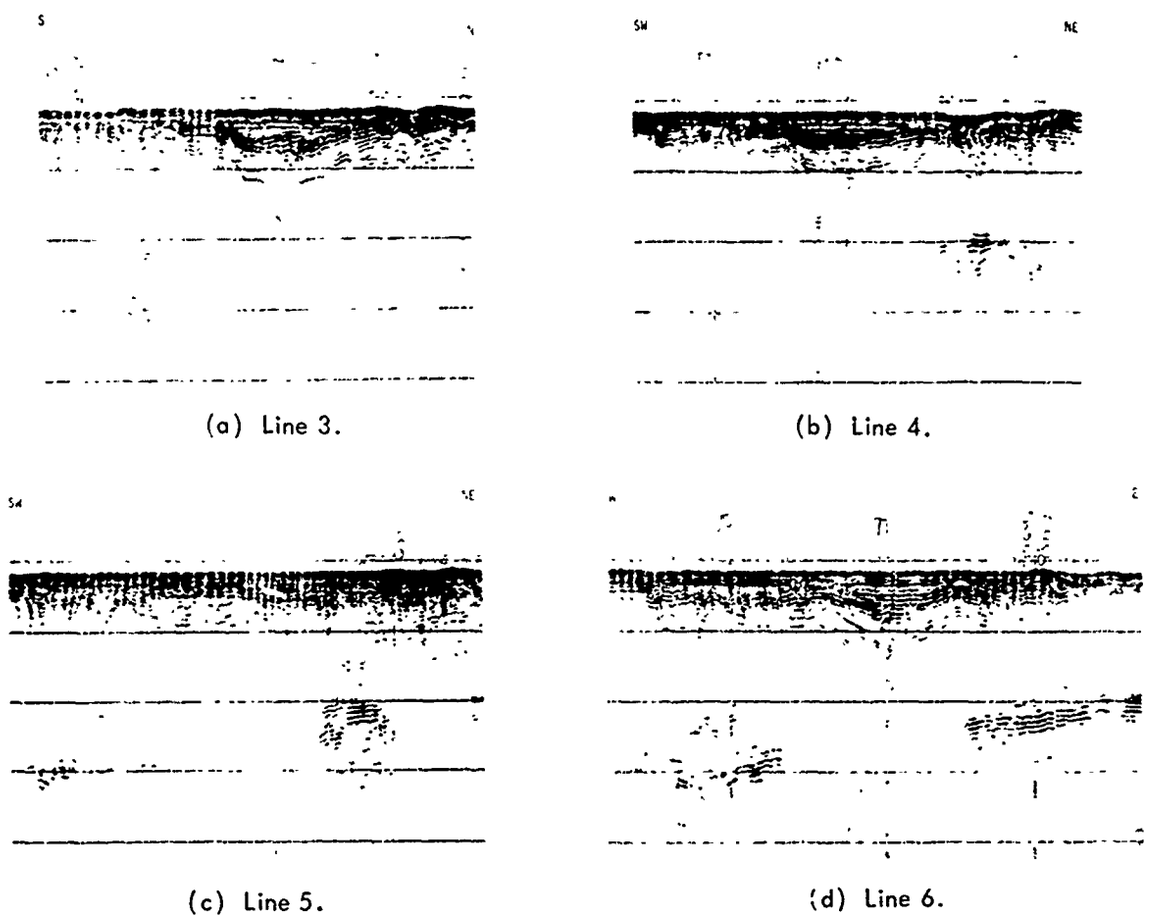

(a) Line 3.

(b) Line 4.

(c) Line 5.

(d) Line 6.

Fig. 68. Pulser records, May 1970 (each horizontal line represents approximately 50 ft of depth; note basalt reflection at depths of 100- to 150-ft in (b), (c), and (d); dipping strata at shallow depths indicate existence of craters, except in (c) where Charge II-G failed to detonate).

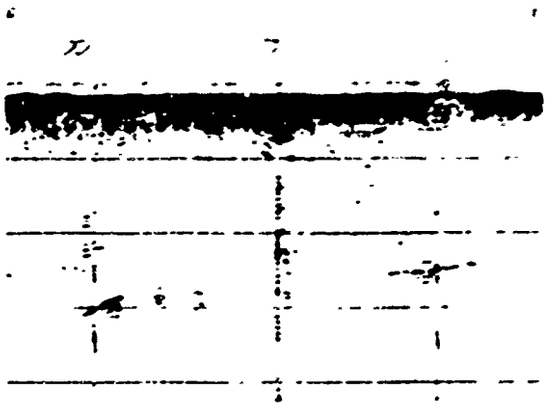

(a) Line 7.

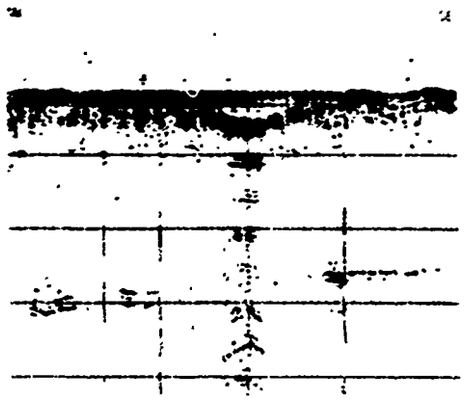

(b) Line 8.

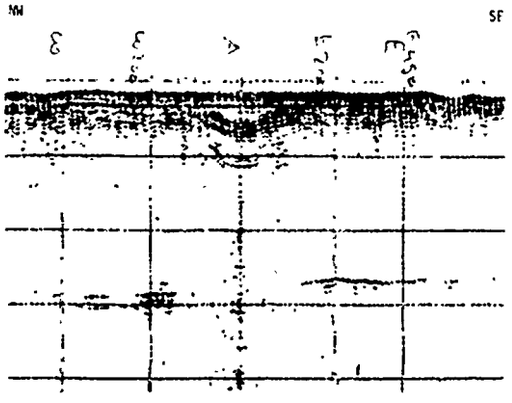

( ) Line 9.

Fig. 69. Pulser records, May 1970 (each horizontal line represents approximately 50 ft of depth; note basalt reflections at depths between 100 and 150 ft; note stronger crater development at Charge II-A, which detonated full-yield in (c), than at Charge II-D, which detonated in (a) low-order).

an anomalous noise condition was noted in the centers of the craters. Hydrophones placed on the sea floor detected sharp clicking and snapping sounds, apparently representing active settlement of crushed coral.

The chief results may be summarized as follows. The pulser records indicate the structure of the craters: very gently inward-dipping layers of material, evidently representing sediment deposited in the crater as fallback and washback. The coral was apparently fractured both in the immediate crater area and as far out as the breakwater foundation, as evidenced by the lack of a reflection from the basalt interface where it had been present before the blasts.

Probing

The Echo crater was probed by hand by swimmers in mid-November 1969 with 40 ft of 1/2-in. pipe. The ocean floor was found to be covered with 4 ft plus of bluish-gray mud, samples of which dried to a cracked condition on exposure. It was possible to probe to 40 ft below MLLW without difficulty. No boulders or large coral fragments were hit.

A second, somewhat more systematic, series of probings was carried out at Echo crater in early December 1969 (Fig. 70). Probing was carried out on two radial lines by hand from a boat with a 1/2-in. pipe using 1-1/2-in. pipe as casing. The maximum depth probed was 33.9 ft below MLLW at the center of the crater. The materials encountered were clay, very fine silt, coral sand, and pea-gravel-sized coral chunks. The inferred profile of the crater is shown in Fig. 71.

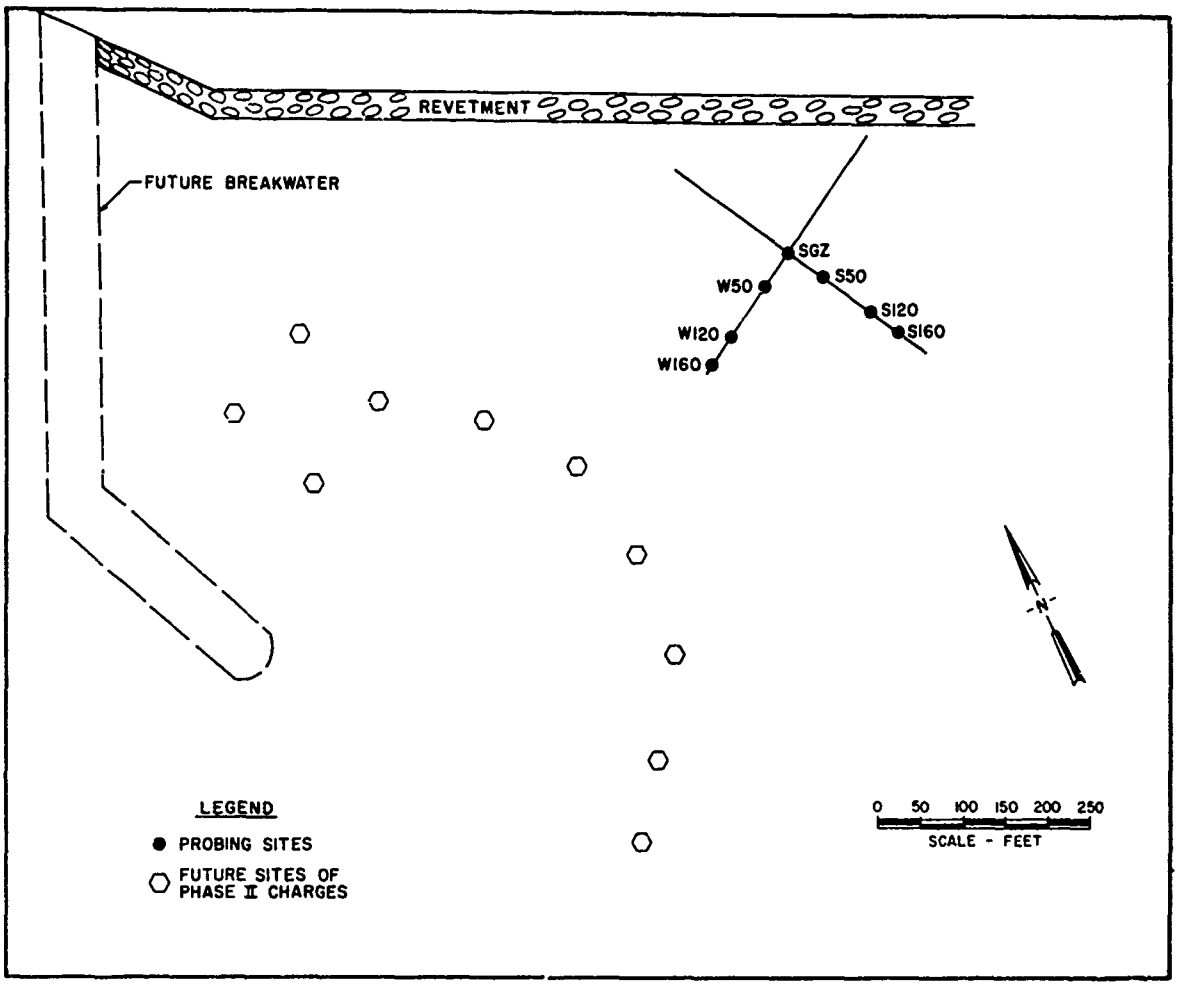

Fig. 70. Location of probings of Echo crater, December 1969.

Drilling

A drilling program was conducted following the construction of Project Tugboat to document the engineering properties of the coral materials after the excavation blasts and to determine if possible the boundaries of the true crater and the rupture zone. The drilling method had to be selected with several facts in mind. The preshot drilling had shown that the material was extremely difficult to core, even in its undisturbed state; and all holes had to be cased to virtually their full depth. Hand probing at the Echo crater had revealed a layer of soft mud several feet in thickness at the surface. Acoustic subbottom profiling, as noted above, had indicated that the coral had probably been shattered both in the immediate crater area and for some distance outward from the crater. Limited funds were available.

Coring was rejected since it was anticipated that core recovery would be even poorer in the fallback, washback, and blast-fractured materials than it had been in the undisturbed coral reef. Coring requires a firmly founded drilling platform, and the soft mud anticipated in the craters would have made for difficult conditions in founding the platform. To

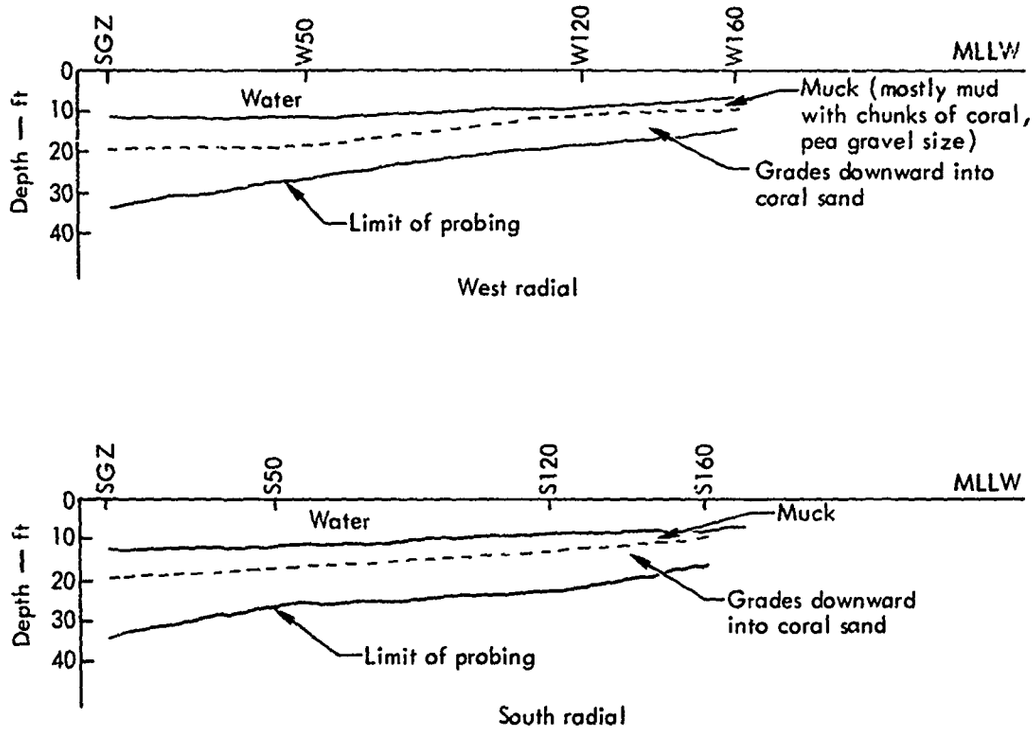

Fig. 71. Profile of Echo crater inferred from probings, December 1969.

be successful in recovering materials in an undisturbed state, larger diameter tools than those used in the preshot borings (4 in.) would have to be used. Probably a specialized core-retaining device would be needed, and would have to be improvised at the site based on experience in the first few holes. Conceivably, undisturbed recovery might not be attained short of such sophisticated techniques as freezing the ground. All these considerations indicated that a successful coring program would be far too expensive for the funds at hand.

Likewise the probability of achieving satisfactory sample recovery with "undisturbed" soil sampling techniques was evaluated and estimated to be low. The same platform foundation problems would exist as for coring. Thin-wall tube sampling was out of the question because of the anticipated hard pieces of coral. The Pitcher sampler[9] was investigated, but based on the types of material in which it had been successfully used, it was judged that it might be successful only if a very large diameter sampler were used, and even then success was not a certainty. Similar considerations applied to the Denison sampler.[9]

In an attempt to obtain some useful information within the scope of a readily attainable program, the drilling method selected was a combination of drive sampling and wash boring, to be performed from a floating platform. By drive sampling, the general nature of the materials might be determined; by standard penetration tests during the drive sampling the penetration resistance of the material

could be measured and some indication of its quality as a foundation could be gained. Since many standard penetration tests had been performed during the preshot borings, a comparison of preshot and postshot penetration resistance would be available.

As a further, more continuous record of the penetration resistance, an improvised sounding method[9] was devised whereby a record was kept of the blows required to drive the 5-in.-diameter drill casing. It was hoped that an indication of the boundary of the true crater might be given by the locus of refusals or of marked changes in blow counts in either the standard penetration tests or the driving of the casing.

Moreover, both the Phase I and the Phase II craters were wide shallow depressions rather than the bowl-shaped or trough-shaped craters that previous experiments on dry land had produced. The cratering process seemed to have produced a net lowering of the ground surface, rather than a shifting of materials from the excavation to lips or to an upthrust zone. Since the process had apparently involved a densification of the coral, it appeared that such densification might be documented if substantially all the material washed from a borehole could be recovered and weighed. A large baffled collecting tank and equipment to weigh the collected washings were therefore specified for this purpose.

The standard penetration test is usually performed in soils. Since the Kawaihae coral has characteristics more like those of overburden than like those of rock, the test could generally be performed. The standard penetration test was performed essentially as specified in ASTM Standard D 1586-67, except that a bottom-discharge chopping bit was used in wash boring and the sampler was driven through intervals varying from 2 to 4 ft.

The 5-in.-diameter casing, with a hardened-steel drive shoe at its base, was driven with a 300-lb hammer, which was dropped through a standardized fall of 15 in. A continuous record of the blows was maintained. This improvised sounding method gave a continuous record of the penetration resistance of the materials. Though crude, the results can validly be compared from hole to hole.

Following a casing drive, the resulting plug of material was washed out with an up-and-down movement of the wash rods to break the coral to a size small enough to wash out. The washings were collected in burlap sacks and in a large baffled cylindrical collecting tank. In this way most of the solid material was recovered, but a certain amount of fines was lost as overflow. The collected solids were then weighed on platform scales, first wet, and again after several days of drying in the sun. Densities were calculated from the casing diameter, the length of a given interval, and the dry weight of the solids recovered from that interval.

Borings were located as shown in Fig. 65. Holes 57, 58, and 59 were in undisturbed coral. The other holes penetrated materials that had been affected to a greater or lesser extent by the blasts. Blast effects were not regularly distributed along and across the channel because of the irregular way in which the Phase II charges detonated. Hole 60 had been partially drilled when bad weather caused an extended layoff. When the casing was found to have been bent, the hole was relocated slightly and completed as Hole 60A.

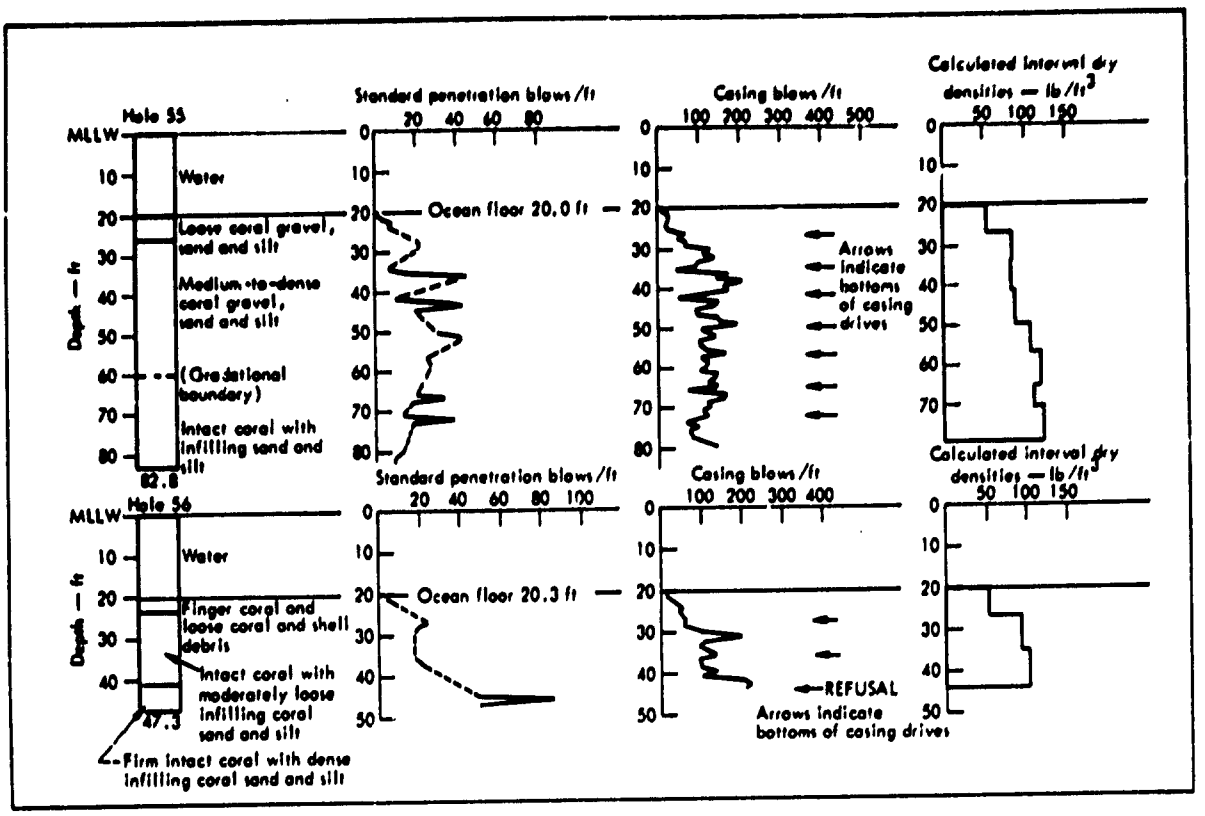

Fig. 72. Penetration and density data, Borings 55 and 56.

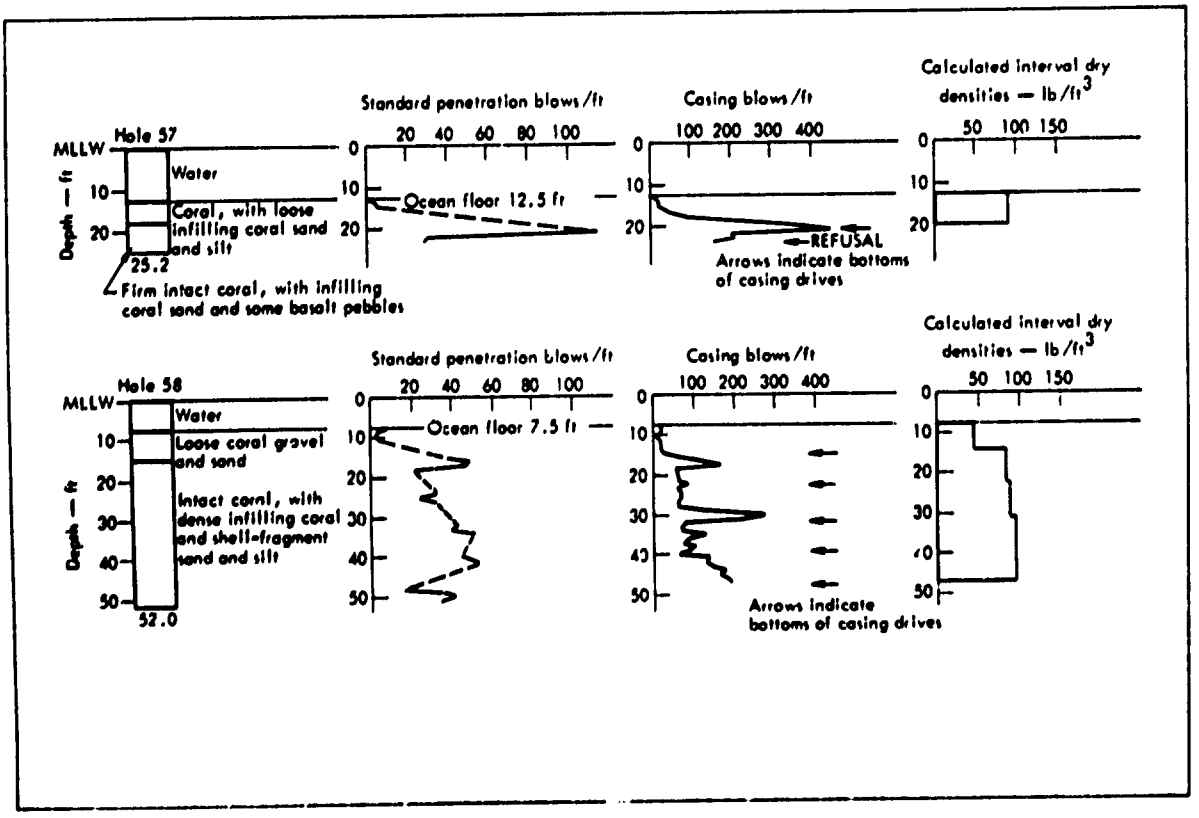

Fig. 73. Penetration and density data, Borings 57 and 58.

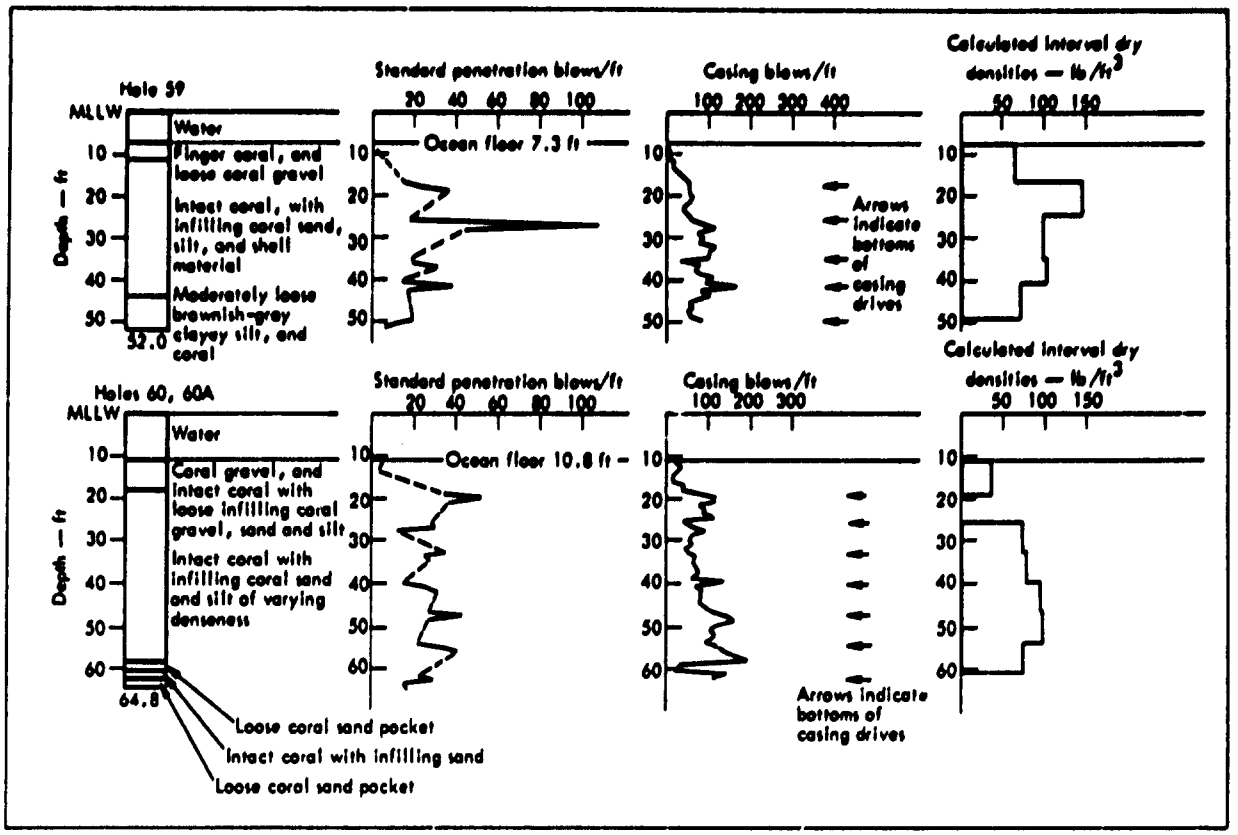

Fig. 74. Penetration and density data, Borings 59 and 60-60A.

The data from the borings are shown in Figs. 72 through 76. A layer of "mud" up to 9 ft thick was found at the surface in the berthing basin area, but not in the outer channel. This layer probably reflects the fact that there was more fine material already in the area of the sediment coral zone, where the berthing basin was situated, and also that ocean scour is inhibited by the new breakwater but can and does take place in the more exposed outer channel. The borings were drilled in the period December 1970 to April 1971, after the completion of the new breakwater.

Unfortunately, it was impossible to tell from the split-spoon drive samples whether the coral materials had been shattered by blasts or whether they had been displaced or reoriented. Hence, the drilling failed to detect either the boundary of the true crater or the extent of the rupture zone. It is doubtful whether any simple drilling program could have demonstrated these zones.

A change in penetration resistance due to blast effects was revealed. The undisturbed coral, represented by the preshot borings (Fig. 77) and the postshot holes farthest from the blasts (Borings 57, 58, and 59), shows a tendency for blow counts to vary markedly from foot to foot. The blow counts in the borings closest to the blast were more uniform. Natural coral conditions exist close outside the channel.

It is impossible to give specific values for the strength of the shattered coral. A general idea, probably sufficient for

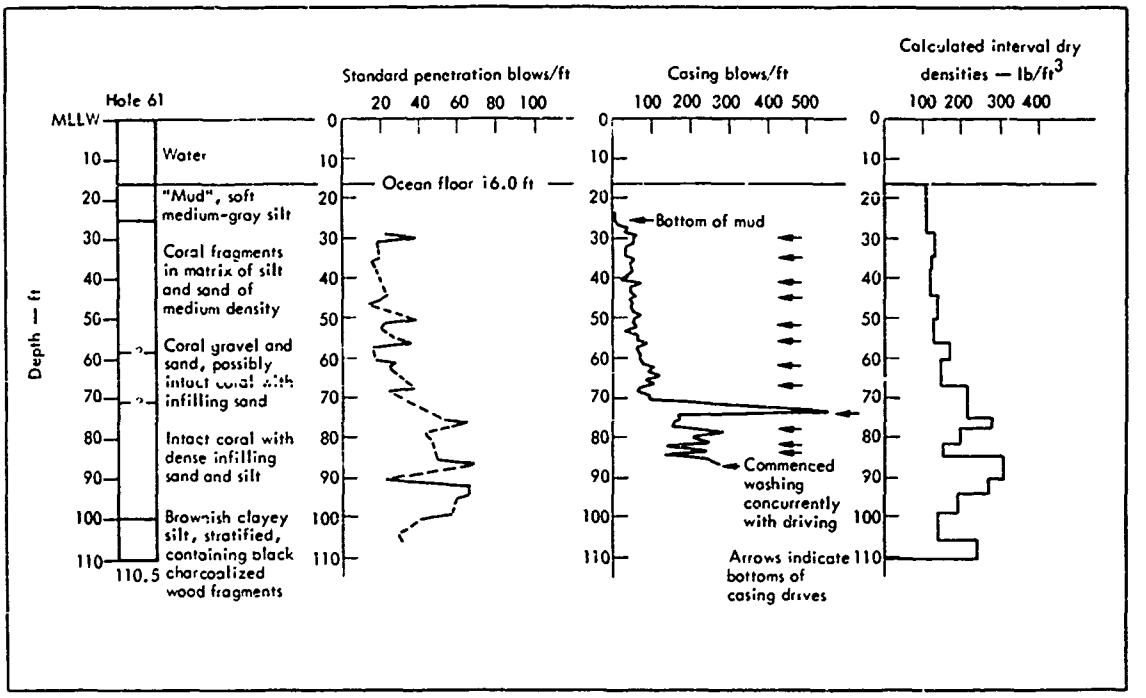

Fig. 75. Penetration and density data, Boring 61.

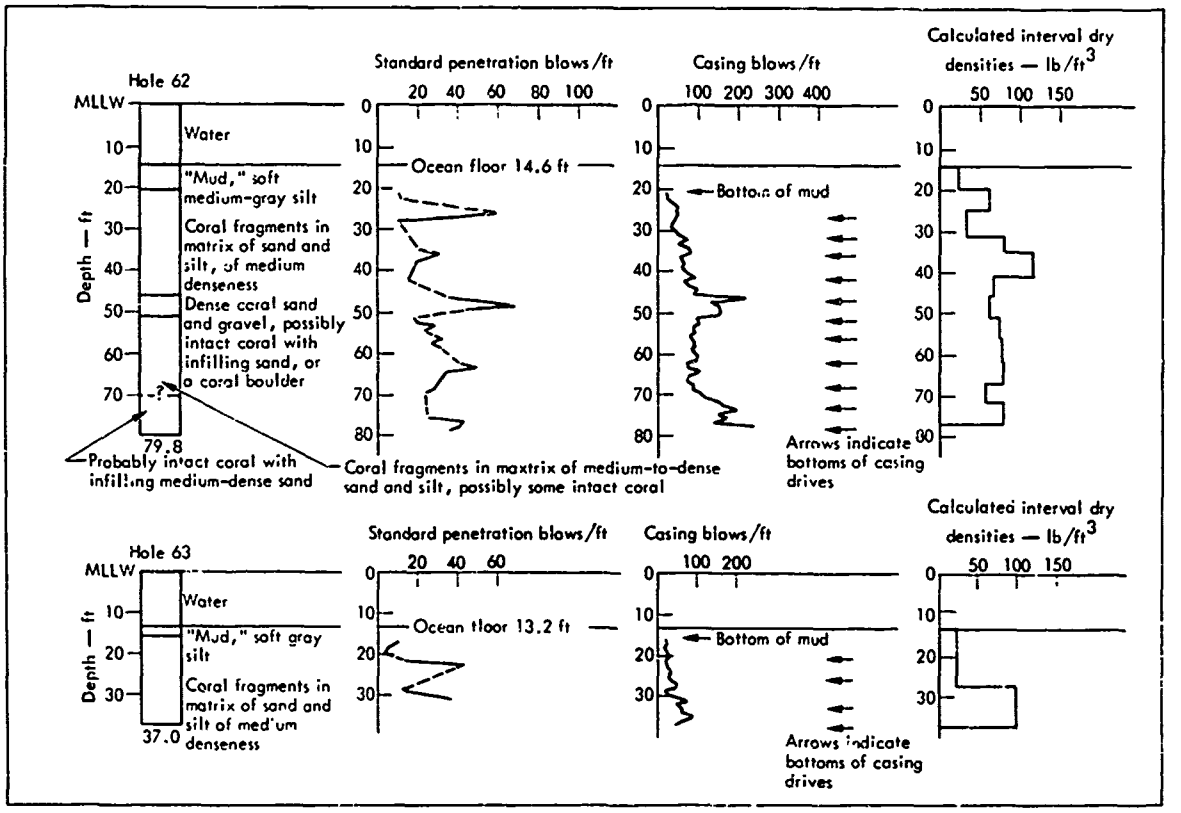

Fig. 76. Penetration and density data, Borings 62 and 63.

foundation engineering purposes, can be obtained from the penetration resistance data. From a foundation standpoint, the materials in and near the channel are similar in consistency to medium-to-dense sand.

The hoped-for increase in density was not clearly shown. Despite the lack of clearly shown densification, the excavation was probably achieved chiefly through a densifying process. Either the increase was not great enough to be detected by the method, or the method was faulty. Part of the excavation may have been achieved by the production of fines and subsequent transporting of them out of the area in suspension.

The results of the drilling program may be summarized as follows: A layer of soft mud is present in the berthing basin area but not in the outer channel. The limits of the crater zones were not satisfactorily defined, nor could they have been defined in any simple drilling program. The effect of the blasts was to render the coral material slightly more homogeneous with respect to penetration resistance than in its natural state. In its consistency, the shattered coral is comparable to medium-to-dense sand. The densification thought to have been responsible for most of the excavation was not conclusively shown, probably because of limitations in the method used.

Underwater Photography

A program of underwater photography was undertaken in May 1971. By this

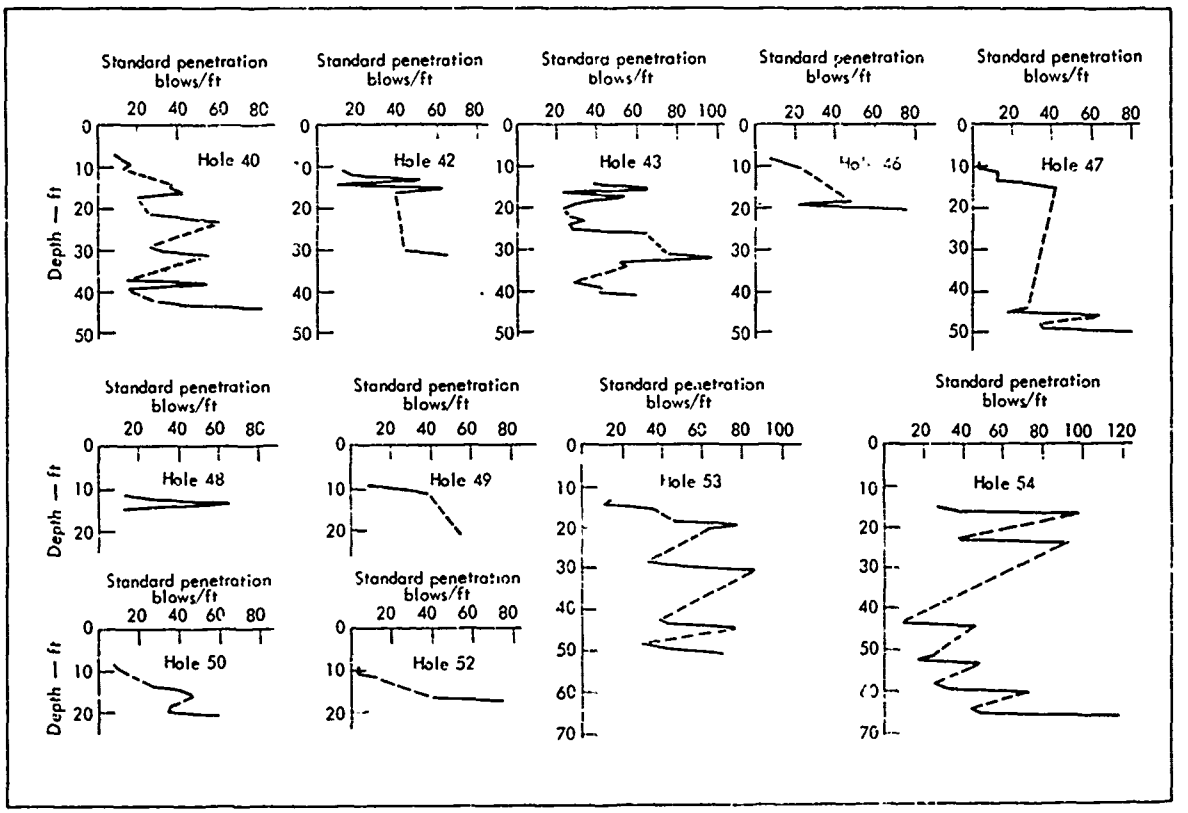

Fig. 77. Standard penetration data from all preshot borings.

time the waters over most of the project were clear enough that good pictures could be obtained. The water in the berthing basin area was too cloudy to permit photography. This condition should slowly improve as the fines settle.

The bottom conditions as photographed are shown in Figs. 78 through 80 showing natural, apparently unbroken coral in the area of Borings 57, 60, and between.

Figure 79 depects intermediate conditions between the natural coral and the smooth bottom in the center of the channel. Some football-sized blocks of coral, broken loose and thrown by the force of the detonations, can be recognized. Visible in Fig. 80(c) is an accumulation of broken coral along the edge of the channel.

Conditions in the central channel area are shown in Fig. 80(a). This area is

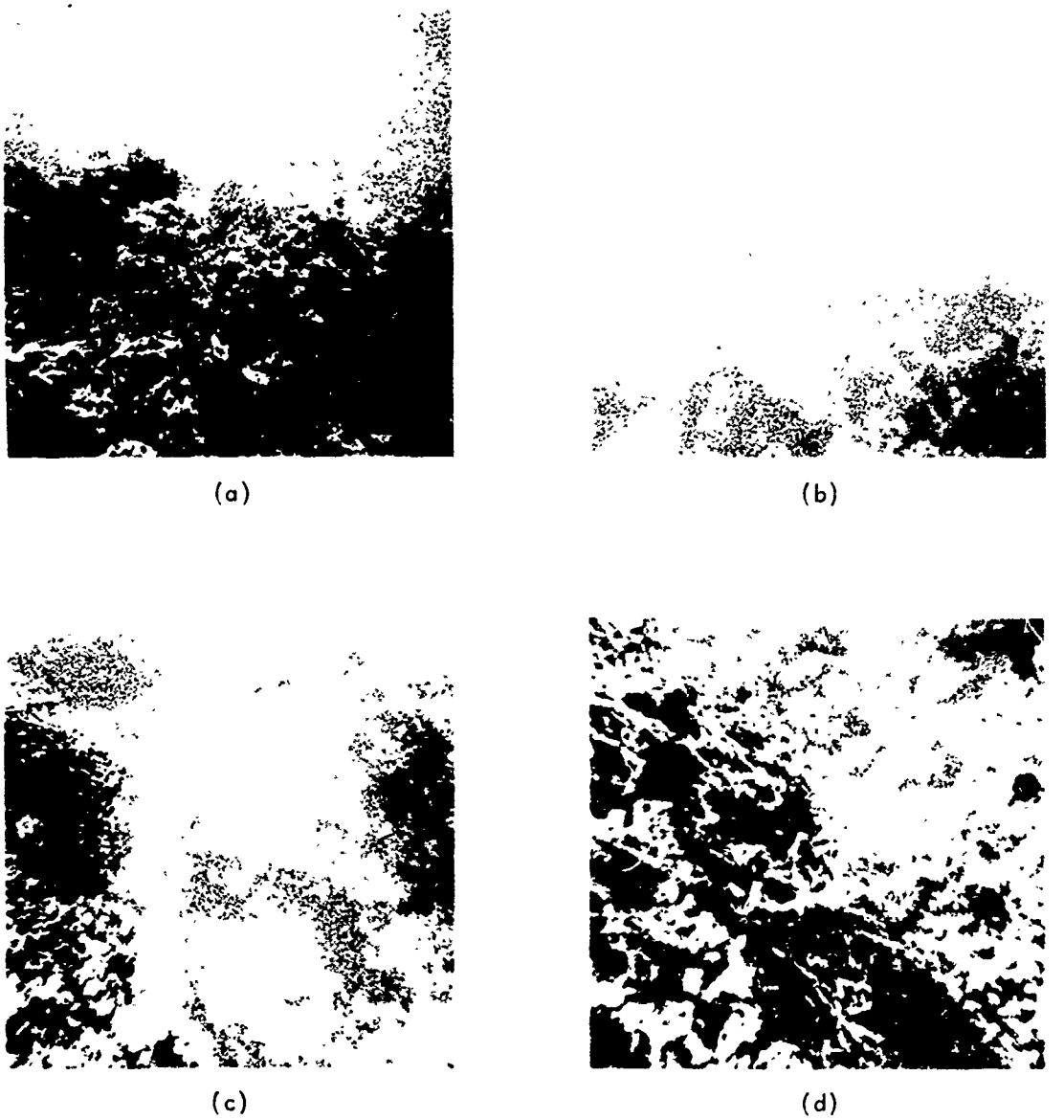

(a) (b) (c) (d)

Fig. 78. Natural coral conditions persisting outside Project Tugboat channel in area between Borings 56 and 60.

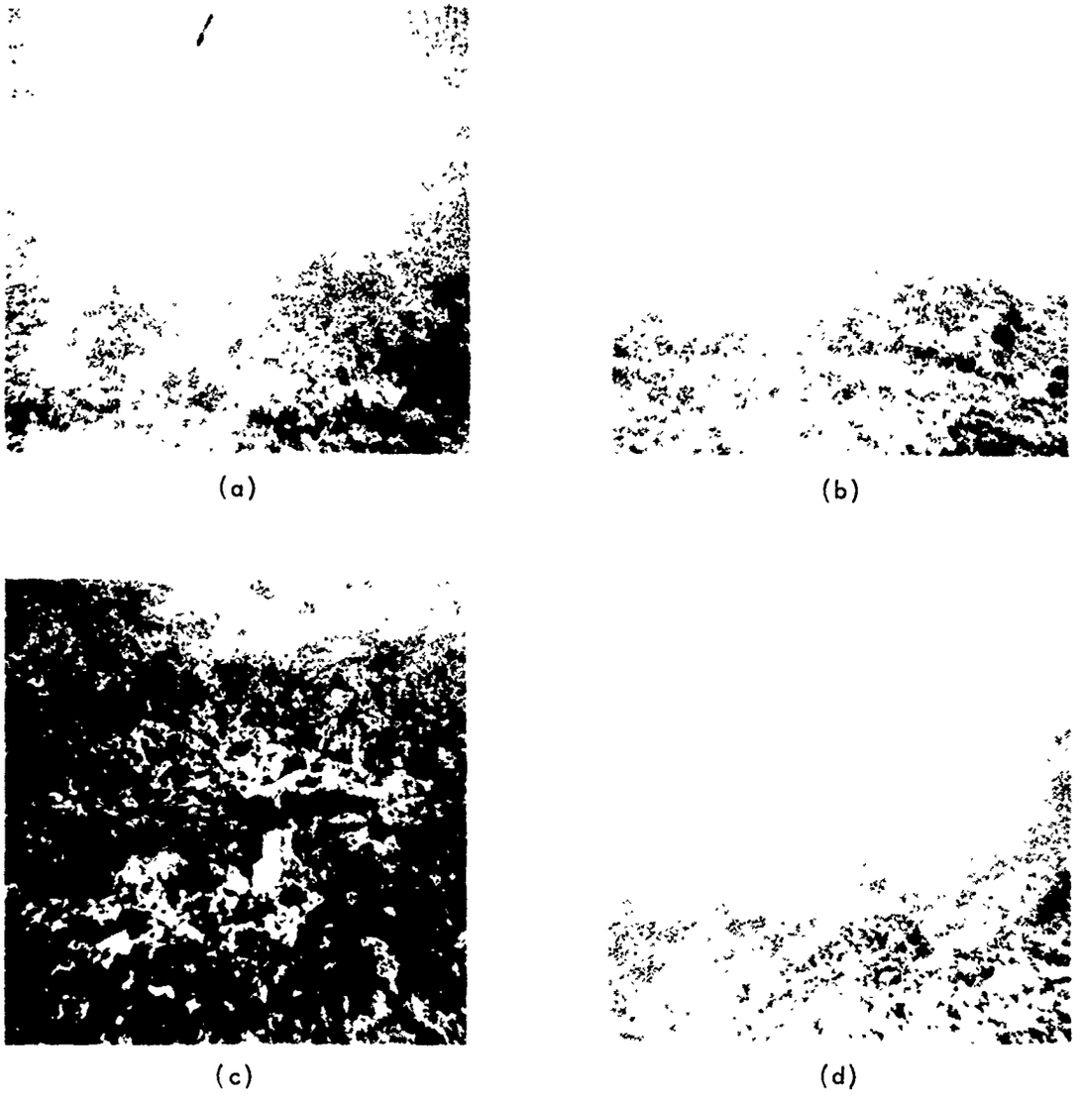

Fig. 79. Broken coral adjacent to Project Tugboat channel in vicinity of Borings 56 and 57.

quite flat and sandy. Baseball-sized chunks of coral are quite common lying on the surface.

DISCUSSION OF UNDERWATER CRATERING IN CORAL

The cratering mechanism observed in this project is quite different from that observed in earlier tests on dry land. In this case it seems to have been one principally of densification of the coral through crushing. Aerial photography of the dynamic cratering process shows that the crater initially resulting from the detonation remains devoid of water for several seconds, and then is filled with crushed coral and water as the crater walls fail radially into the crater. This failure which occurs before the water wave proceeds very far and which affects a large area around the crater causes a turbulence in the water over the crater

area which lasts for some time. In Detonation II-EF, a double whirlpool effect was observed as the water rushed back to the crater area (see Fig. 81).

Further evidence of early failure of the coral medium surrounding the crater is indicated by the movement of a 4-in. diameter pipe that had been placed several feet into the coral bottom and extended above the water prior to Detonation II-IJKL. The pipe was located 200 ft from the nearest charge in the detonation and was being used as a wave height measurement marker or wave staff. A camera was set on shore and filmed the wave as it passed this wave staff. A sequence of pictures showing the movement of the pipe are presented in Fig. 82.

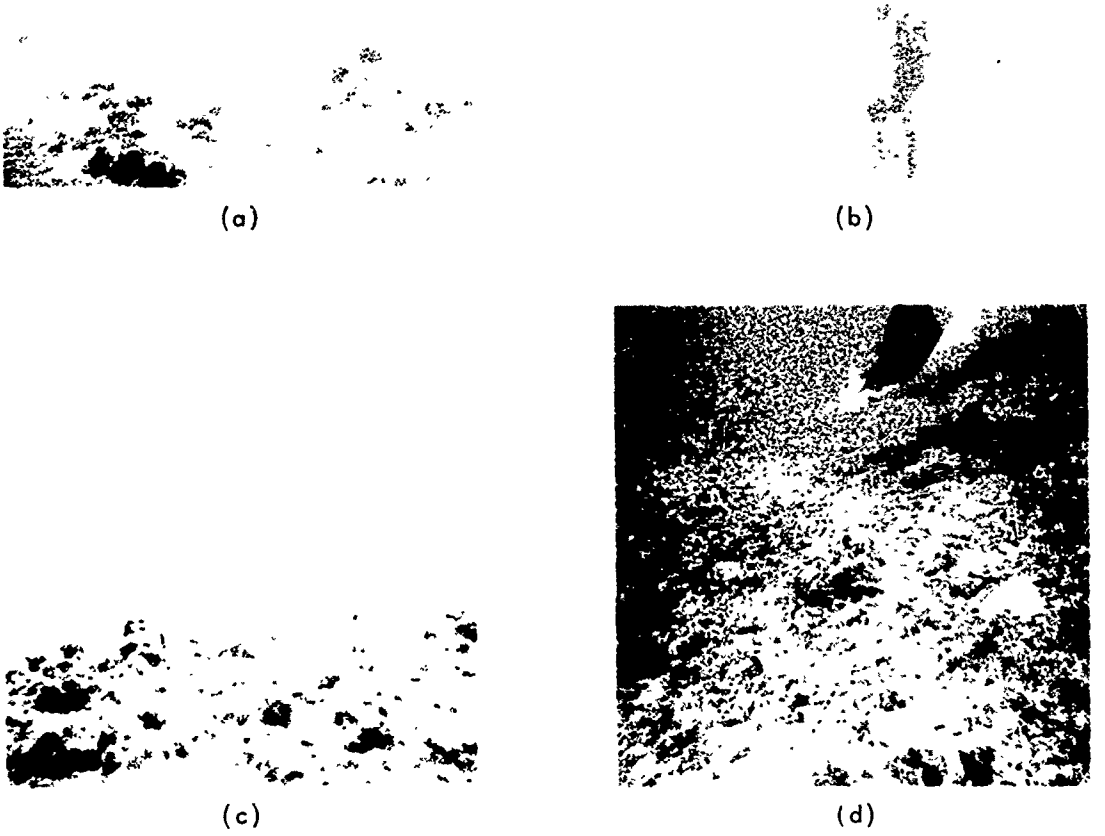

Fig. 80. Typical conditions in Project Tugboat channel, in area between Charge Sites II-B and II-E (visible in (b) is a small marker-stake fouled with rope and in (d) a cruising sting-ray; coral blocks visible range up to baseball size and slightly larger).

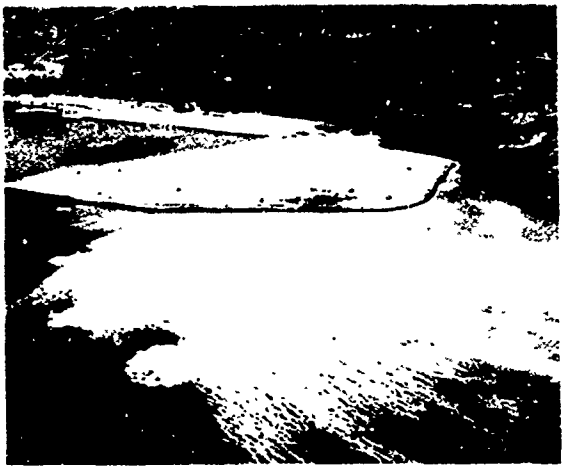

Fig. 81. Whirlpool effect observed following Detonation II-EF.

The pipe is the farthest one from the camera and is on the extreme left in the picture. In this sequence the detonation has just occurred and the spray from surface spalling is just settling when the pipe moves to the left toward the detonation SGZ. Immediately following the last picture in the sequence the outrunning wave and base surge cloud engulf the pipe, obscuring it from further view.

This early failure is probably caused by several factors, the major one being the weak nature of the coral. The coral is crushed by the outrunning shock wave beyond the distance where the majority of the lip-forming material comes to rest, causing the lip material and its nonsupporting base to liquify and flow into the crater void. This process was only partially supported by the postdetonation drilling program because of the difficulty in obtaining undisturbed samples. The best indication of the extent of fracturing was provided by the bubble pulser soundings. It is to be expected that cratering underwater in a higher strength material would show a cratering mechanism more like that observed for land cratering. The question which needs answering is at what strength does the medium resist failure as the crater lip forms and the water rushes back trying to fill the crater void.

SUMMARY AND CONCLUSIONS

Project Tugboat detonations successfully produced a harbor basin and entrance channel which exceeded the design requirements in both width and depth. The detonations resulted in a channel varying in width from about 150 to 260 ft at a minimum project water depth of 12 ft. The berthing basin is almost a square area 400 ft on a side at the 12-ft water depth contour. The minimum channel design width was 120 ft and the berthing basin design requirement was a square 240 ft on a side.

The site medium is a weak coral. Tests on cores recovered in preshot drilling show a compressive strength ranging between 760 and 1738 psi, a mean bulk dry density of 1.37 g/cm^3, a mean saturated bulk specific gravity of 1.76 g/cm^3, and a mean porosity of 49%. The reef mass possesses, by an indeterminate amount, a lower mean strength, a lower mean density, and a higher mean porosity than the tests indicate.

The charge emplacement holes were drilled during Phase I from a causeway which was later removed by dragline. Phase II holes were drilled from a jack-up floating platform. The aluminized ammonium nitrate slurry blasting agent (AANS) was pumped into the canisters containing the charges after the canisters had been placed in the drilled hole and

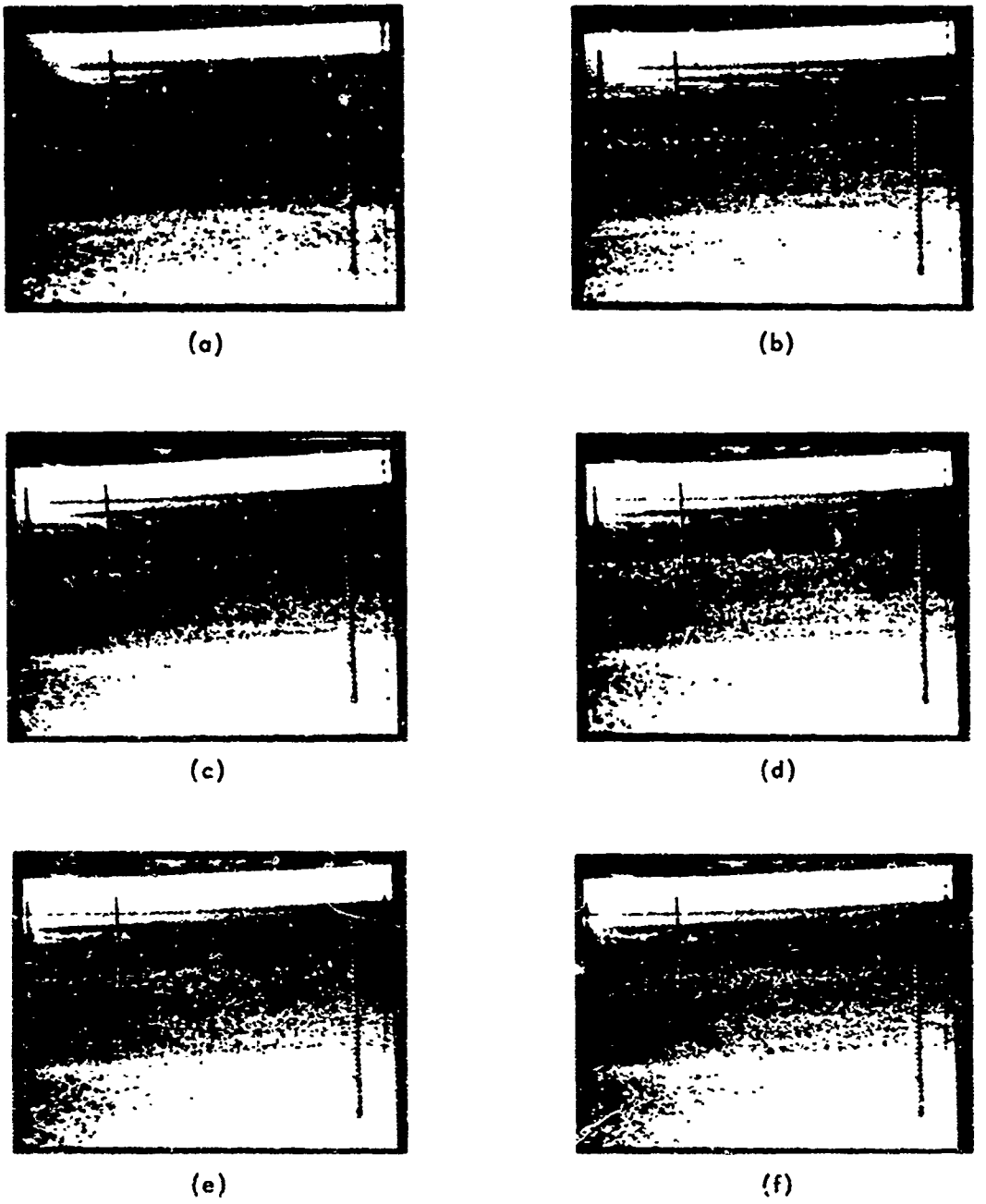

Fig. 82. Photography of wave staffs, Detonation II-IJKL (wave staff on extreme left is 200 ft from nearest charge and is observed to be moving toward it).

stemmed. The slurry was pumped with a truck-mounted pump through a rubber hose down a 4-in. fill line that extended from the top of the canister to the surface.

Calibration tests provided information that permitted a redesign of the harbor excavation using a little more than half the original drill holes and half the quantity of blasting agent estimated to be required in the preliminary design. The craters were broad and shallow with no lips and were actually better suited to

harbor excavation in this situation than the less wide and deeper craters typical of dry land cratering detonations. The cratering mechanism appears to be one of densification of the coral through crushing and subsequent settling. Aerial photography showed that the crater remains devoid of water for several seconds after detonation and then is filled by coral and water as the crater walls fall into the crater. Wave staffs that were placed in the coral near the craters moved toward the crater before being overrun by the outrunning water wave giving further evidence of this failure process.

The 10-ton Echo crater had a radius to the 12-ft depth contour of about 120 ft. This parameter was used to design the harbor detonations. Spacing between charges was set at two times this number.

Low order detonation of Charges II-C and II-D and the deflagration of Charge II-G apparently was due to inadequate boostering. These misfires made it necessary to do some small remedial detonations which were successful in clearing the channel.

The final channel surface is flat, level, and sandy, with scattered small coral blocks lying on it. Foundation conditions in the channel are similar to those in medium-to-dense sand. A short distance outside the channel, natural coral conditions exist. The material in the channel is more homogeneous than that of the natural coral reef. In the berthing basin area, a layer of soft mud from 2 to 9 ft thick lies at the surface. This layer is not present in the outer part of the channel.

Crater zones were not satisfactorily defined by the drilling program. They were crudely defined by the acoustic profiling surveys; the true crater by the limit of dipping beds within the crater, and the rupture zone by the limit of the basalt reflection. To define the true crater specifically by drilling would be very difficult.

A long-term settling effect in both the channel and the surrounding natural coral was detected by the surveys of May and December 1970. On the average the surface was lowered during this 7-mo period by 1 or 2 ft. This effect supports results of the acoustic profiling, which indicate that the natural coral was shattered by the blasts to large distances out from and below the cratered channel.

Though the cratering mechanism seems to have been one principally of densification of the coral reef, this process was only equivocally and partially documented by the drilling program. This partial documentation results from the fact that it was not possible to get undisturbed samples with depth. A small part of the excavation was probably achieved by the production of fines, which were carried away from the site in suspension in the sea water shortly after the blasts.

Section 3
Wave Measurements

INTRODUCTION

Objective

The objective of this wave measurement program was to investigate the generation of shallow water waves by explosions beneath the sea floor. Hopefully a relationship could be developed with this wave data to predict maximum heights in future projects of this type.

The waves generated by both single charges and multiple charge arrays were investigated. The Phase I program was funded by ESSO Production Research Company of Houston, Texas and accomplished by the Baylor Company of Houston. The Phase II program was funded and executed by the Coastal Engineering Research Center (CERC) of the Corps of Engineers. This chapter includes all data collected during both programs.

Background

Previous studies of explosion-generated water waves were conducted primarily to determine the merits of the tactical or strategic employment of nuclear weapons to generate waves large enough to flood and to destroy coastal facilities. In most cases, the surface water waves were generated by a charge detonated either above the water surface or in the water column. The first investigation known to the authors where a study was made of surface water waves generated by an explosion beneath the seabed was conducted by the U.S. Army Waterways Experiment Station in the early 1950's.[10] In this study an experiment was conducted to simulate the blast effects of a 20-kt nuclear explosive in water depths typical of most harbors. Waves were generated by charges up to 256 lb of TNT buried to shallow depths in sand, clay, and loess soil with water overburden.

Project Tugboat is the first large-scale experiment in which the generation of waves by explosions beneath the seabed has been experimentally investigated. The knowledge gained through this program should be useful in planning for future construction of harbors and navigational projects with explosives.

Interpretive Description of Wave Problem

An idealized representation of wave generation in shallow water by an explosive buried beneath the seabed is illustrated in Fig. 83. Initially, the sea floor is impulsively deformed by the shock wave and the expanding explosive gases. In turn, the water column above the deformed sea floor is elevated. As the gases continue to expand, the sea floor disintegrates and the water layer near the edge of the forming crater is elevated and forced aside by the rising gas bubble. By the time the bubble vents, an initial horizontal velocity has been imparted to the displaced mass of water which propagates outward as a turbulent wall of water. During its initial stages, the wave profile is obscured by the disturbances created by falling ejecta debris along the

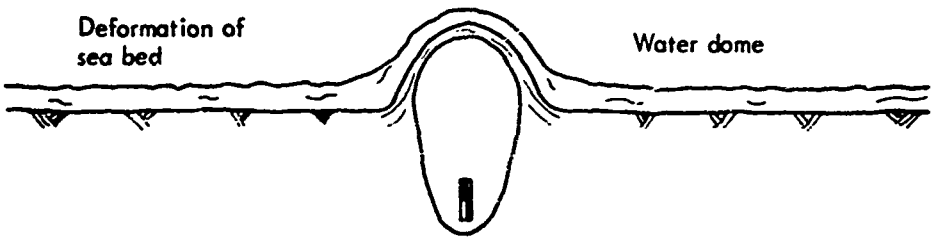

(a) Expansion of gas bubble and formation of water dome

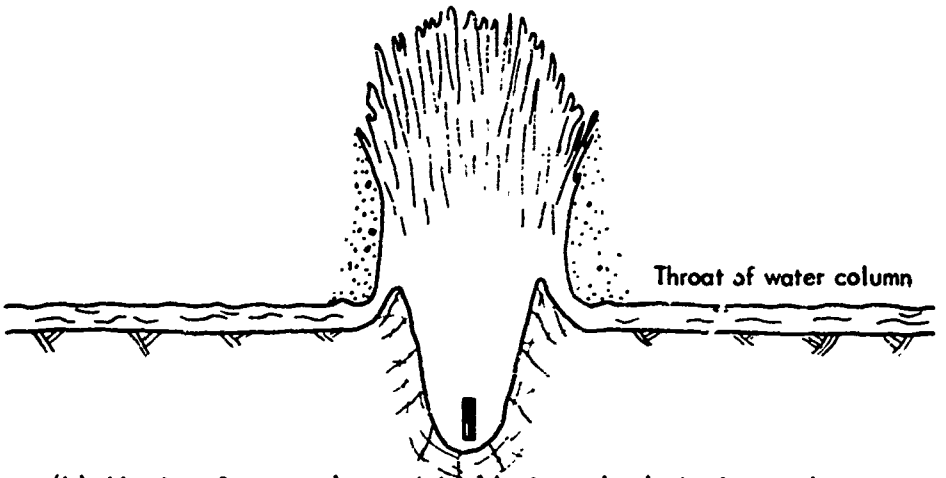

(b) Venting of water column; initial horizontal velocity imparted to water

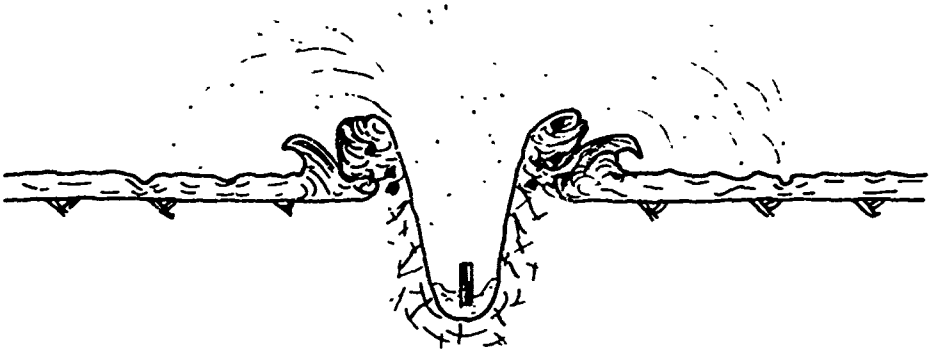

(c) Formation of initial wave and fallback of ejecta

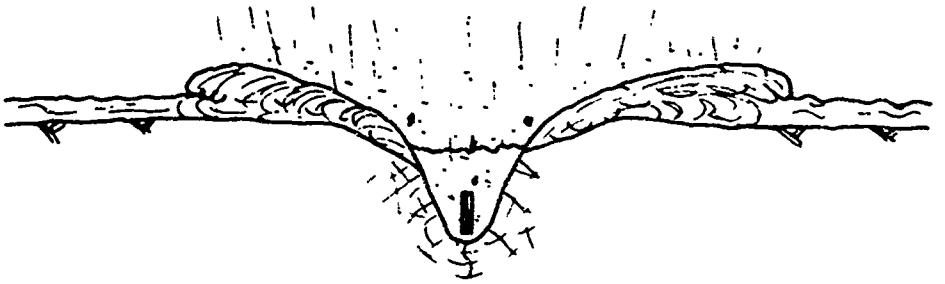

(d) Propagation of explosion-generated wave

Fig. 83. Generation of water wave by explosion beneath the sea floor.

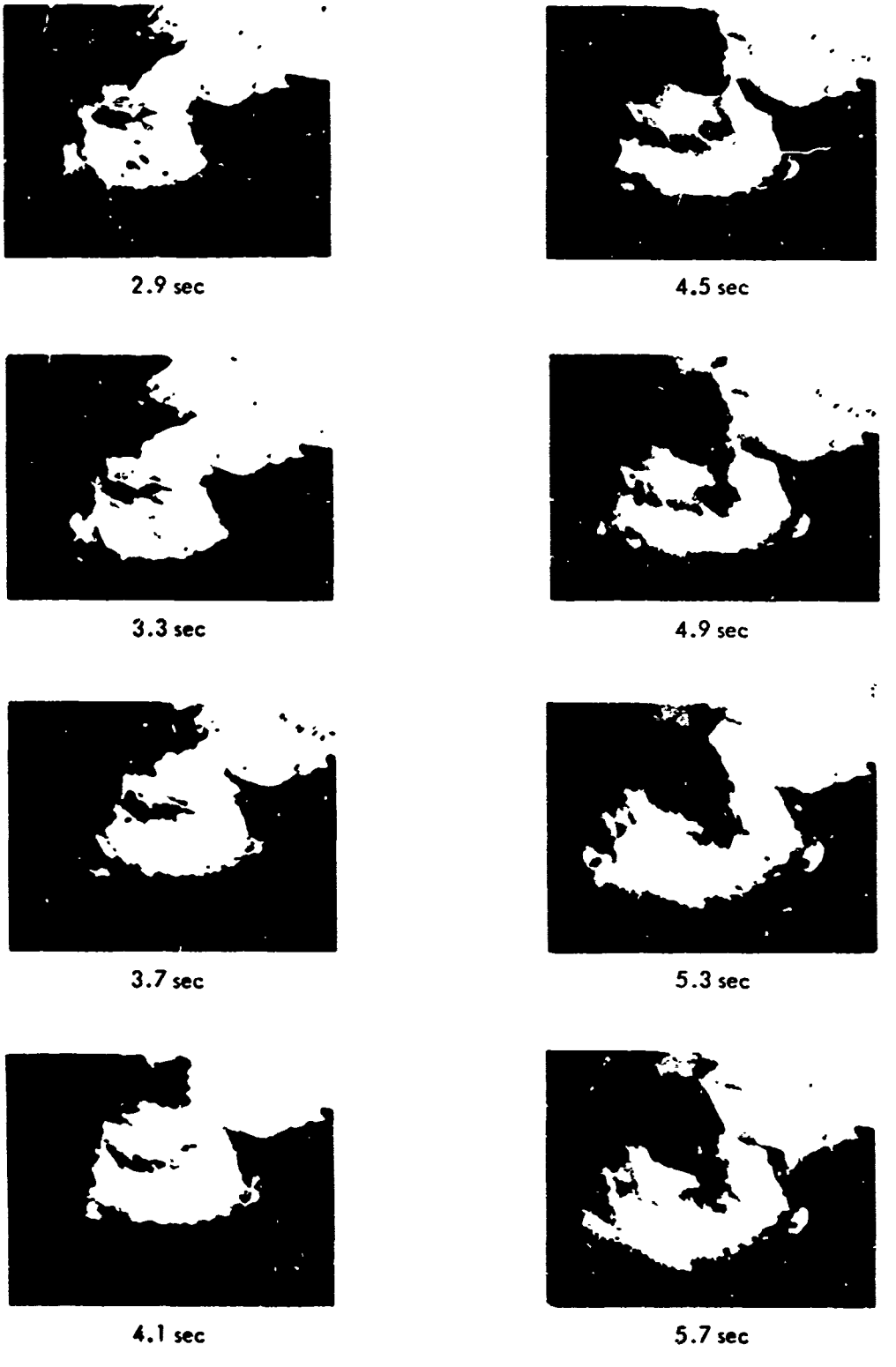

Fig. 84. Aerial photograph of explosion-tenerated wave, Phase I, Detonation Alpha.

crater periphery and the dense dust cloud over the detonation point. A photograph of an explosion-generated wave from above in its initial stage of propagation is shown in Fig. 84.

Kranzer and Keller[11] developed a theory for water waves generated in water of uniform depth by either an axially symmetric initial distribution of impulse or an axially symmetric initial displacement of the water surface. This theory is based on the linear theory of progressive surface waves. Solutions for the explosion-generated waves are given, provided that either the precise impulse distribution or the shape of the initial water surface displacement is known.

However, the test conditions for Project Tugboat did not satisfy several of the assumptions made in the Kranzer and Keller theory. First of all, the bottom topography is not uniform as assumed in developing the theory but very irregular and interspersed with coral heads. These coral heads introduce friction forces which create turbulent flow. This flow conflicts with the theoretical assumption of irrotational, or nonviscous, fluid flow. Wave energy is continually dissipated by these coral heads as the wave propagates outward. In the theory, the sum of the kinetic and potential energy of the wave system is assumed to be constant. Finally, the proximity of the causeway introduces a rigid, vertical boundary to the mathematical model. The solutions presented by the Kranzer and Keller theory are for the case of an explosion in a sea of infinite extent; i.e., no vertical boundaries.

Since there are no known theoretical investigations conforming to the conditions present in Project Tugboat, the empirical approach is taken in analyzing the wave data.

EXPERIMENTAL PROCEDURE

Phase I

The wave measurement program was conducted by the Baylor Company of Houston, Texas. Instrumentation consisted of two gages and a pen and ink recorder. The location of the gages relative to each charge is shown in Fig. 85.

High-speed photography taken from the Command Post and a helicopter supplemented this program.

Phase II

The data collection program utilized three surface wave gages and four ground-based movie cameras looking along four lines of vertical observation poles (CERC was the primary investigator).

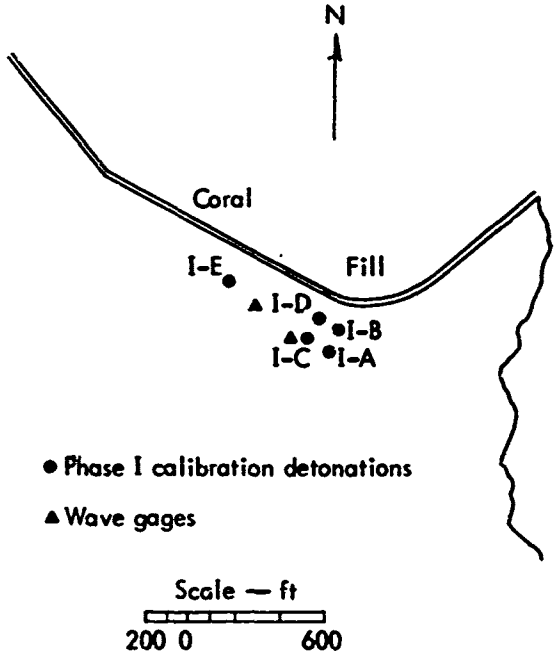

Fig. 85. Map showing location of wage gages, Phase I.

The recording wave gages were identical to those used during Phase I. The data were recorded on four 2-channel recorders. Duplicate recordings were made of each signal to prevent loss of data by recorder failure. The recorders were operated at least 1 hr before and after each blast, during dry runs, and intermittently throughout the project.

Four low-level cameras were positioned at different angles to each detonation to document the complex nature of wave generation, wave propagation, and return flow into the crater. Four lines of observation poles driven into the coral provided a space-and-time coordinate system for investigating wave height and wave celerity. Each line consisted of three or four wave poles extending about 12 ft above the water surface. These poles were constructed of 4-in.-diameter steel pipe and were calibrated with 2-in. wide alternating red and white stripes. The locations of the cameras, wave poles, and wave gages are shown in Fig. 86.

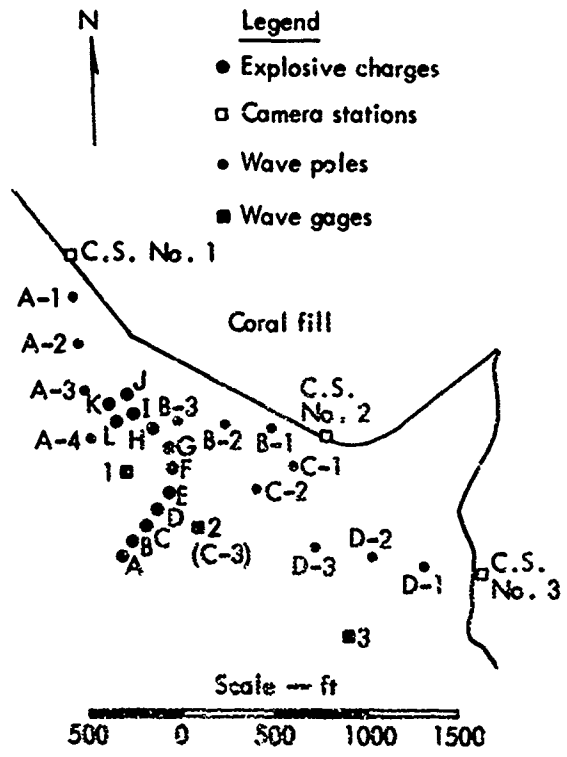

Fig. 86. Location of wave gages and wave poles, Phase II.

RESULTS

Wave Records—Phase I

The wave records for the five detonations, Alpha, Bravo, Charlie, Delta, and Echo, are shown in Figs. 87 through 90.

Only the near wave gage was operational for Detonations Alpha and Bravo, since the cable for the far wave staff was accidently severed by a bulldozer. For Detonation Echo, the region where the nearest wave staff was installed slumped toward the crater before the arrival of the first wave. The wave gage remained operational but true wave heights could not be obtained from the record in Fig. 90 because the gage was displaced from the vertical. However, the time scale was not affected and the times of arrival of the first wave and crests and troughs could be determined.

The heights of the random sea waves at the time of detonation were nearly the same magnitude as the heights of the generated waves at radii greater than 200 ft for Detonations Bravo and Delta. These random sea waves were superimposed on the explosion-generated wave and obscured its height. However, analysis of the random sea record before and after passage of the wave indicated that the heights and periods were consistent. Preshot wave heights were estimated at 0.15 ft from the record while the explosion-generated wave was measured

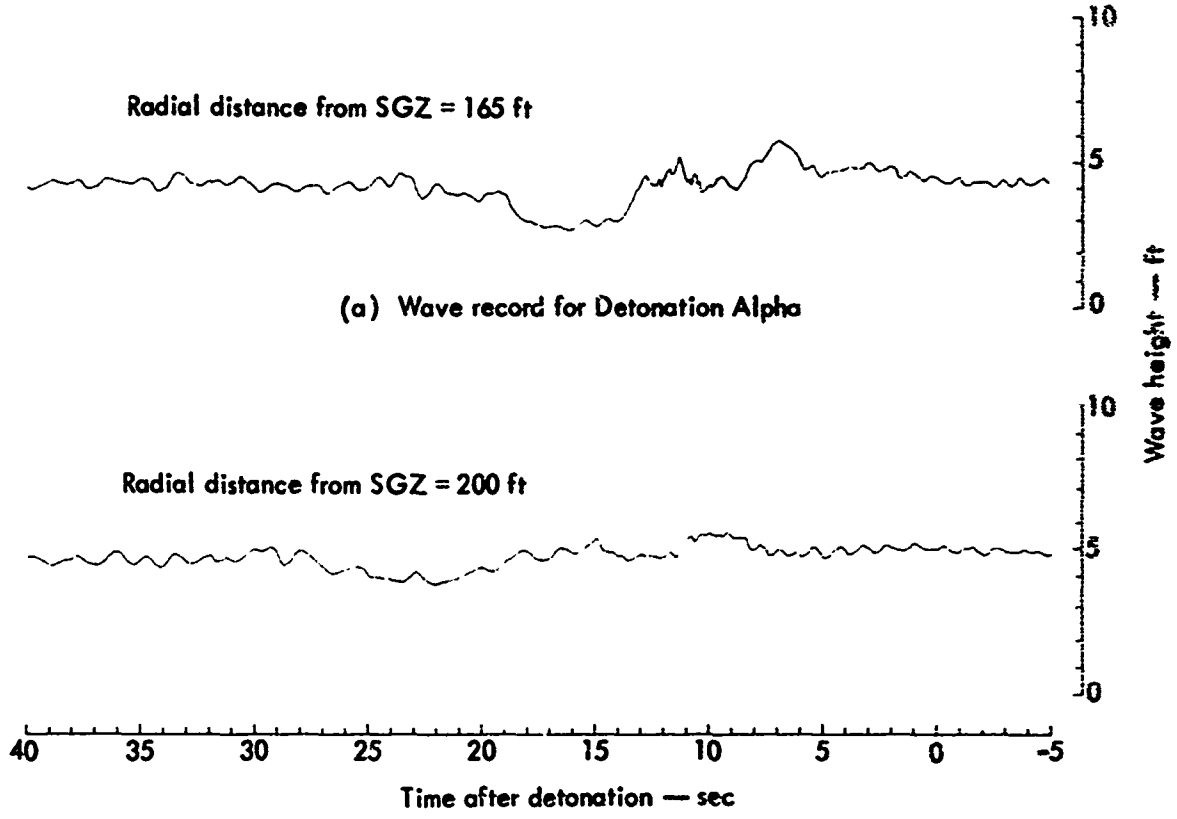

(a) Wave record for Detonation Alpha

(b) Wave record for Detonation Bravo

Fig. 87. Wave records for Detonations Alpha and Bravo, Phase I.

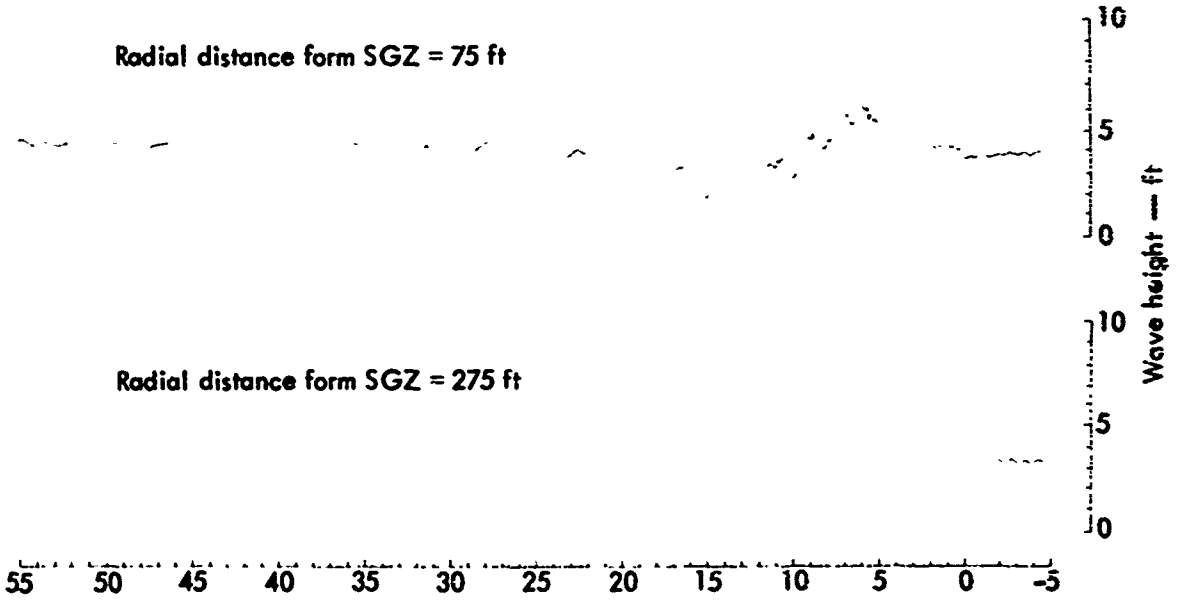

Fig. 88. Wave records for Detonation Charlie, Phase I.

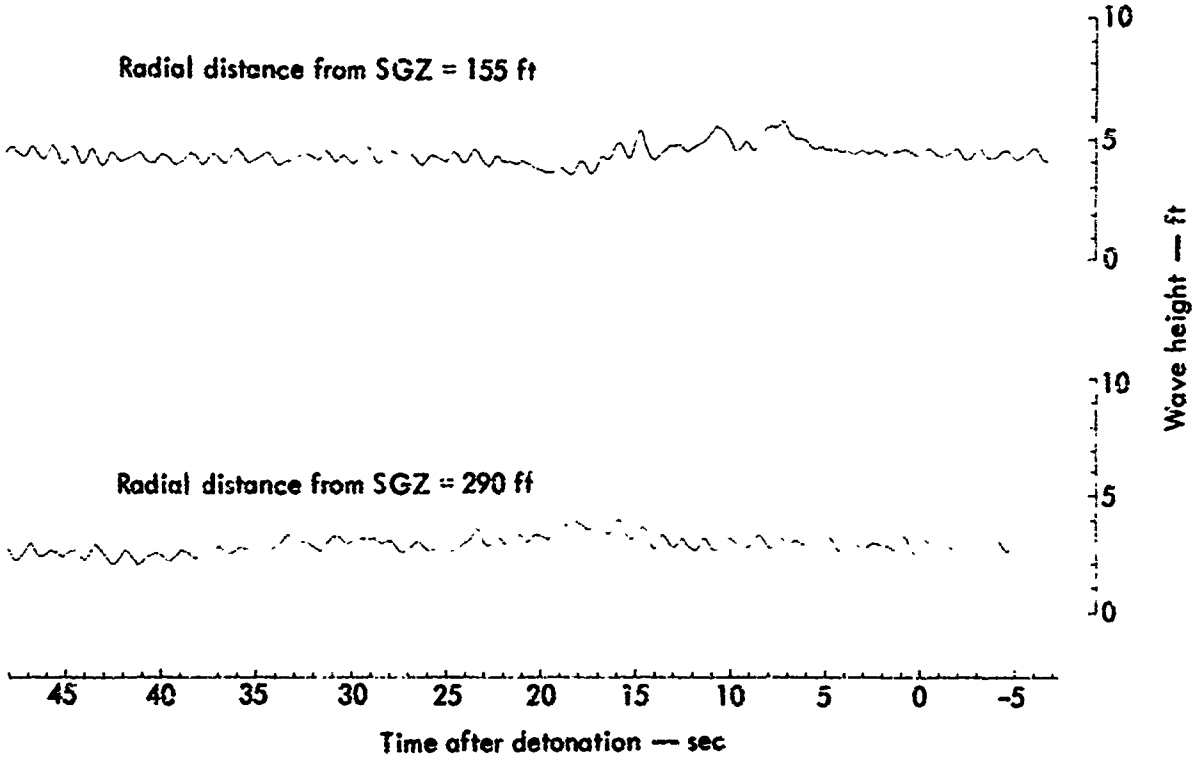

Fig. 89. Wave records for Detonation Delta, Phase I.

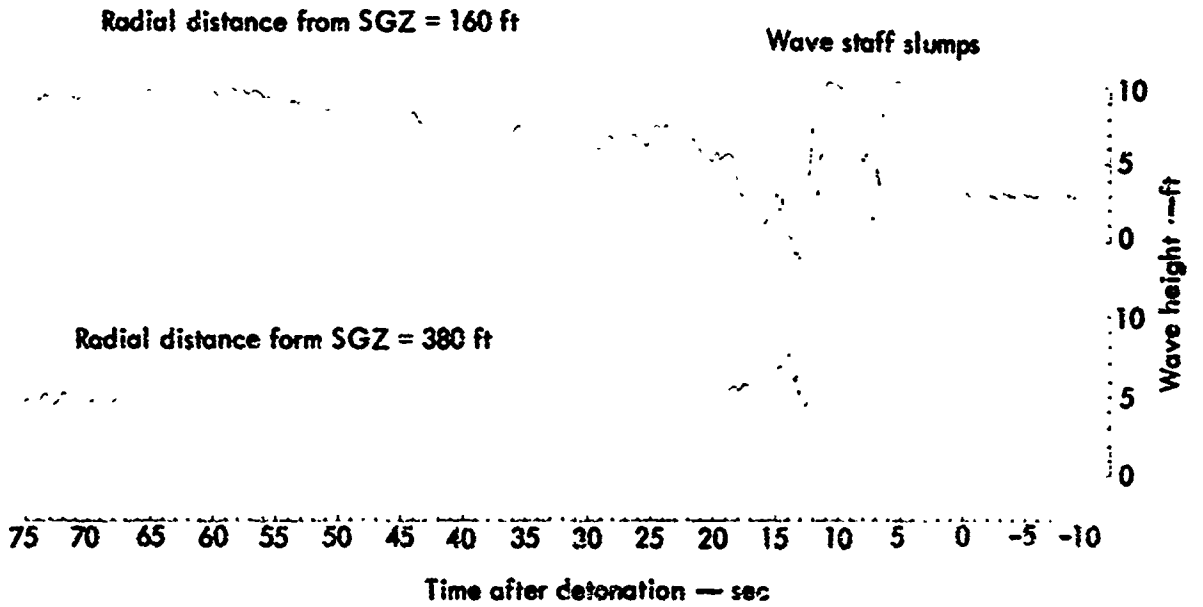

Fig. 90. Wave records for Detonation Echo, Phase I.

Table 9. Summary of maximum wave heights, Phases I and II.

Detonation	Total charge weight, W (tons)	Depth of burial in coral, d_m (ft)	Average water depth, d (ft)	Lithostatic head Z^a (ft)	Distance to wave gage, r (ft)	Maximum wave height, H (ft)
Alpha	1	12.7	4.6	59.4	165	3.4
Bravo	1	13.0	5.0	60.4	200	1.9
Charlie	1	16.6	5.1	66.7	75	4.1
					275	1.6
Delta	1	20.9	5.0	74.0	155	2.2
					290	0.9
Echo	10	36.0	6.5	101.5	160	9.6[b]
					380	4.7
II-ABCD	20-30	36.7	6.6	102.7	360	4.4
					365[c]	4.8
					1425	<0.5
II-EF	20	35.8	6.8	101.4	230	11.1
					300[d]	8.9
					1490	<0.5
II-IJKL	40	36.0	5.8	100.7	340	9.6
					760[e]	5.4
					1940	<0.2

[a] $Z = 33 + d + \frac{110}{64} d_m$, in feet of sea water; saturated unit weight of coral = 110 lb/ft^3.

[b] Estimate only; wave gage slumped during passage of wave.

[c] r measured from SGZ II-B.

[d] r measured from mid II-E and II-F.

[e] r measured from geometric center of square array.

at 4.29 ft. Thus, the true wave height was estimated to be 4.14 ft.

For Detonation Echo, the wave gage displaced by the slumping of the crater lip was located 160 ft from SGZ (Fig. 90). The difference in water level indicated on the wave record before and a very late time after the detonation implied that the angle of displacement of the gage from the vertical was approximately 60 deg. The height of the wave measured from the record was estimated at 11.1 ft. With allowance for tilting of the wave gage, the true height of the initial wave was estimated at 9.6 ft.

The maximum wave height measured at each gage for Phases I and II is tabulated in Table 9 along with the horizontal distance r from the detonation point to each wave gage, the yield W of the charge, the DOB in the coral medium d_m, and the depth of the water overburden d over each charge. Because the height of the wave when it is generated depends on the thickness (depth) of the water layer elevated by the gas bubble (see Fig. 83), the depth d of the water overburden reported in Table 9 is an estimated average preshot water depth of a circular portion of the water layer immediately over the charge

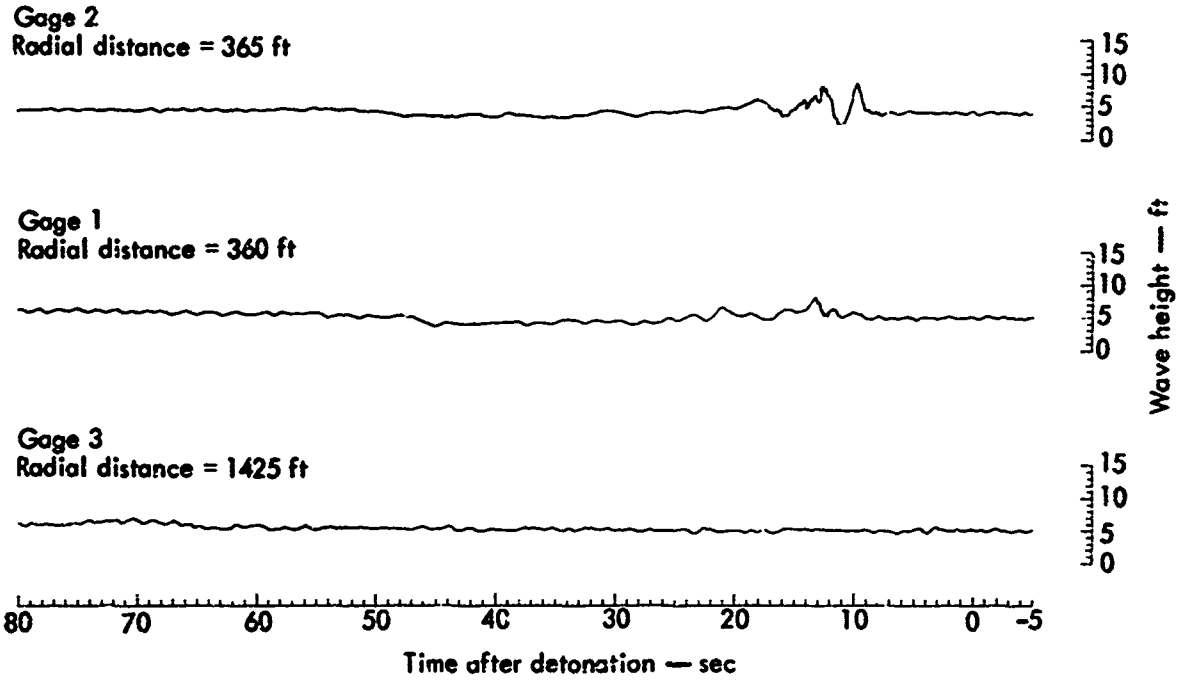

Fig. 91. Wave records for Detonation II-AECD.

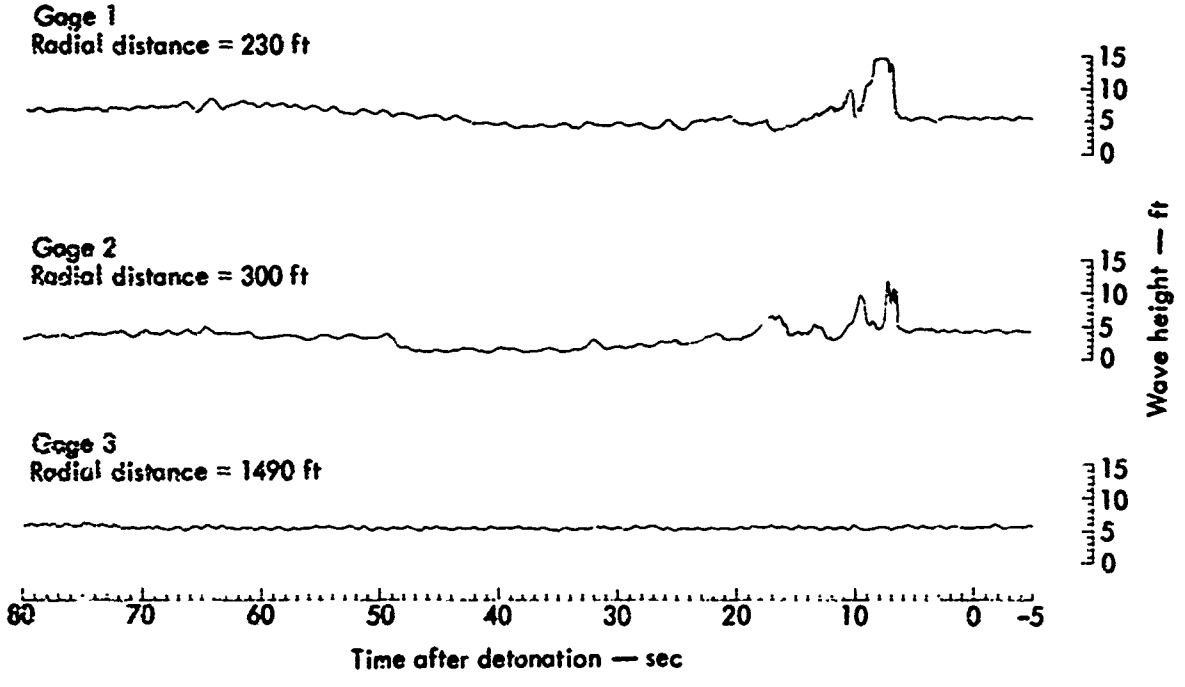

Fig. 92. Wave records for Detonation II-EF.

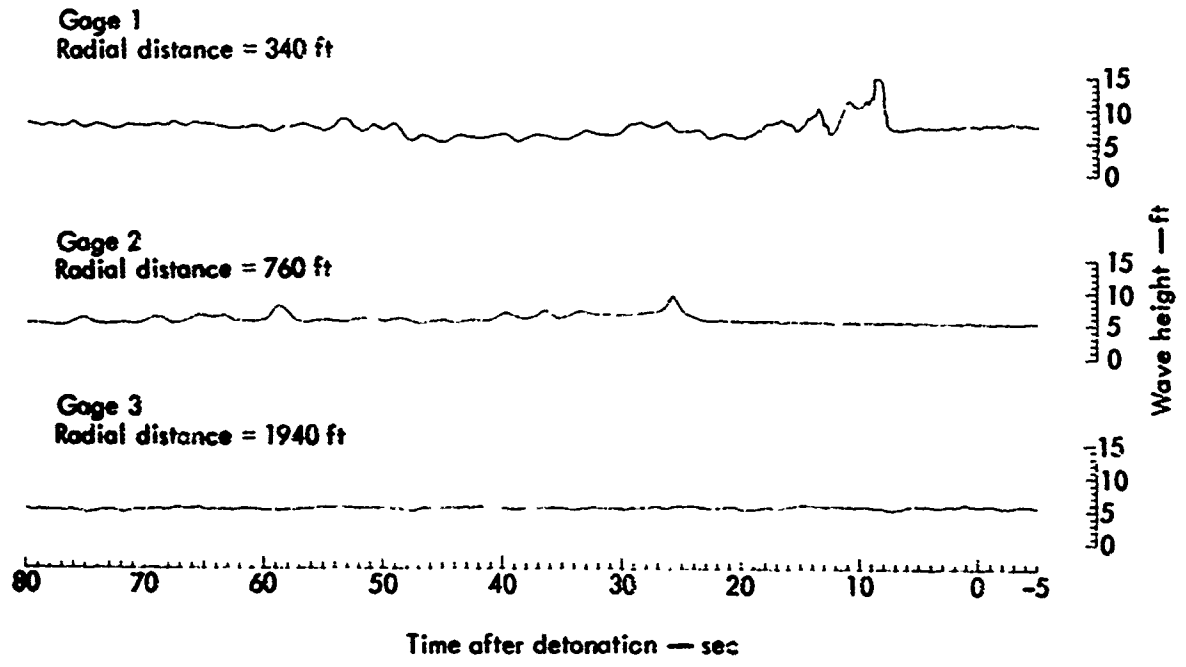

Fig. 93. Wave records for Detonation II-IJKL.

(diameter of circular layer approximately equal to the diameter of the mound observed in documentary photography) which is elevated by the rising gas bubble. These average depths were obtained from preshot topographic surveys and include the tide elevation at the time of detonation.

Wave Climate During Phase II Execution

The sea waves in the vicinity of the harbor area during each detonation for Phase II were generally less than 0.5 ft. The waves moved out to sea in the early morning hours under the influence of a land breeze which is believed to be the result of the radiational cooling of the island during the night. By 0900 hr, a sea breeze replaced the land breeze, and the wind waves reversed direction. The waves continued to build until 1300 to 1400 hr and then slowly decreased during the late afternoon and evening. During the late evening and early morning hours, the wave heights tended to be the same at all gages. During the day, and especially in the afternoons, Gage 3 (see Fig. 86) recorded the highest waves, sometimes by a factor of 2.

Wave Records—Phase II

Surface profiles of the generated waves are presented in Figs. 91 through 93. Maximum wave heights and other pertinent information are summarized in Table 9. Since Phase II consisted of three multiple-charge array events, the depth of burial d_m given for each event is an average of the depths of burial of the individual charges in the array. The charge weight W is the sum of the individual charges in the array and the water depth d is an average preshot depth of the water layer elevated by the explosion bubble. The horizontal distance r to each wave gage is measured from the centroid

of the explosive mass for each array. The first event (II-ABCD) was a low-order detonation and the centroid was assumed at the II-B shot point. The centroid for Detonation II-EF was taken at the midpoint between Charges II-E and II-F. For Detonation II-IJKL the centroid was taken at the geometric center of the square array.

Because the bay was quite calm before and after each detonation, filtering the wave records to delete the random sea waves was not necessary. In all of these detonations the arrival of the explosively generated wave at Gage 3, the farthest of the three gages from SGZ, could not be clearly determined from the wave record since the wave was about the same magnitude as the wind waves at this gage. Generally, the waves recorded at this gage were less than 0.5 ft high for the three events.

Photographic Results with Ground-Level Cameras—Phase II

The low-level photography provided an excellent documentation of the migration of the dust cloud and the propagation of the generated waves.

The falling ejecta created some large splashes, some as high as 50 ft or more. Toward the end of the falling ejecta phase, the dust and water-laden air in the ejecta column began to sink and spread out over the water surface in all directions. The dust cloud moved with peak velocity at an elevation of 5 to 10 ft above the water surface. The cloud obscured the middle portion of the wave poles but the tops and bottoms were readily observable.

A patch of very agitated water accompanied the front of the cloud as it moved shoreward. Complete obscurity was achieved in the photographs as the dust cloud passed the camera station. As the dust began to clear, a breaker or bore could be seen moving outward from the SGZ toward the camera. Visibility did not clear up enough for quantitative estimates from the film until this breaker was near the shoreward wave pole in each line. Two series of photos (Figs. 94 and 95) show this breaking wave as it passes the shoreward wave staffs. Two breakers and one or more nonbreaking waves could be recognized in most films. In general, the breaker strength did not appear to be constant across its crest. The horizontal velocity of the breakers was quite high, since an enormous splash, which was as high as the breaker itself and a foot or two in radius, was created as the breaker passed the 4-in.-diameter wave pole. In comparison, the effect of the poles on an ordinary 2-ft high, 3-sec wind wave was hardly detectable more than a few inches from the staffs. It is not possible to determine with the available data the effect these splashes may have had on the wave records.

After the passage of the initial breakers considerable heaving of the water surface was observed, but quantitative measurements could not be obtained. In some cases the agitated movements of floating debris gave an indication of the turbulence over the crater area. Horizontal shears in both waves and currents were apparent within a distance of a few hundred feet. The water motions were much more complex than those suggested by any of the available theories of impulsively generated waves. An example of the complex water motions is shown in

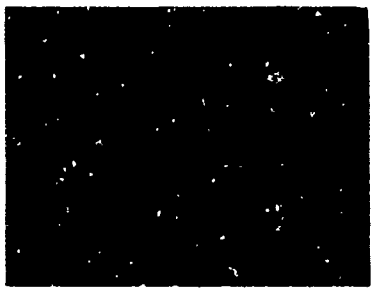

31.6 sec

35.0 sec

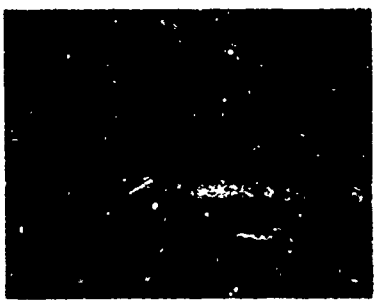

32.5 sec

35.8 sec

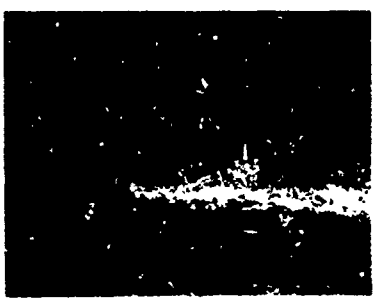

33.3 sec

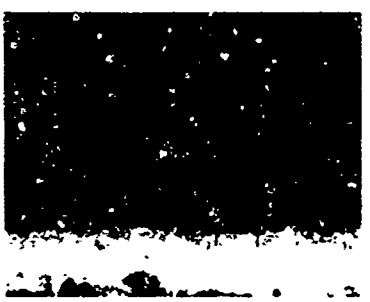

36.6 sec

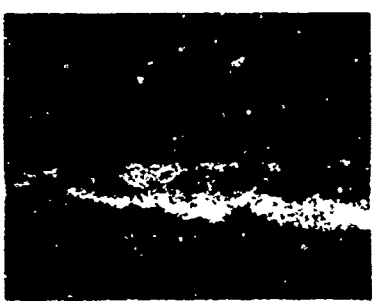

34.2 sec

37.5 sec

Fig. 94. Breaking wave propagating past shoreward wave staff, Camera Line B, Detonation II-IJKL.

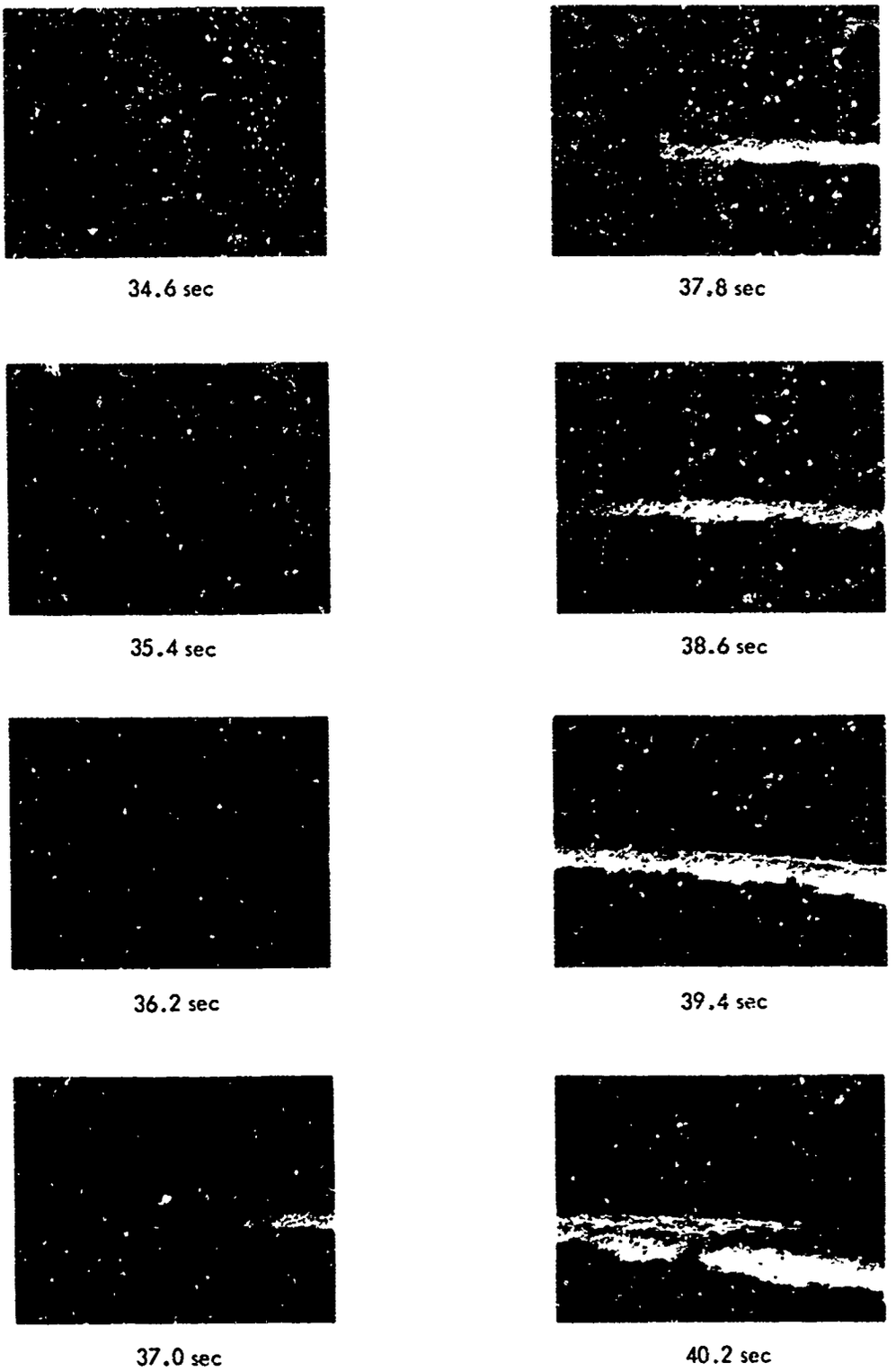

Fig. 95. Breaking wave propagating past Camera Line C, Detonation H-IJKL.

Fig. 96. This sequence is the SGZ area of Detonation II-EF after the cloud has cleared away (118 to 164 sec). The large vortices shown here are rotating in opposite directions.

High-Speed Aerial Photography

High-speed photography taken by helicopter presented a dramatic view of the sea state once the dust cloud had lifted, as indicated in Fig. 96. The qualitative data obtained during Phases I and II by this method were invaluable toward a better understanding of the wave problem.

The actual phenomenon of wave generation was obscured by the spray and dust cloud, but the outward propagation of the wave and the return flow of water into the crater were observable. The time and distance from SGZ at which the initial wave originated could not be observed.

One significant observation obtained by studying these films is that a void in the crater area existed at a fairly late time. The rush of water and fractured coral material back into this void can be seen in Fig. 97 for Detonation II-IJKL. There was a large circular area that could be seen failing toward the central void in this detonation.

The water rushing into the void and crater for the five single charges of Phase I created complex oscillations over the crater that persisted for several minutes before equilibrium was restored. Whether these oscillations generated any waves could not be detected in the aerial photographs or distinguished from the random sea waves on the wave record.

The flow of water back into the crater for the multiple charges of Phase II differed from the case for a single charge. In the case of the row craters, the return flow created two vortices with radii on the order of 50 to 75 ft (see Fig. 96). The resulting sea state was very turbulent—with waves and currents traveling in apparent random patterns.

A study of these films indicated the variation of the generated wave type around the periphery of the void. In the case of Detonation II-EF where the dust cloud lifted quite rapidly, two bores were observed propagating toward Samuel Spencer Beach Park while on the opposite side of the void a train of three or four waves was being generated (see Fig. 98). On the shoreward side of the void, a single bore propagated shoreward, reflected off the causeway, and headed out to sea. The effects of refraction and shoaling on the waves were evident in the film, especially on the train of three or four waves.

ANALYSIS AND INTERPRETATION OF WAVE DATA

Maximum Wave Height Scaling Relationship

As stated earlier, the empirical approach is taken to analyze the wave data in the absence of an adequate theory. The Buckingham-Pi Method,[12] a dimensional analysis technique, was used to derive the basic relationship between the maximum wave height, water depth, DOB in the medium, charge weight, and horizontal distance from SGZ.

The following dimensionless Pi terms were obtained from the analysis:

$$\frac{H}{d} = \int\left(\frac{d_m}{d}, \frac{r}{d}, \frac{d^3\rho}{E}, \frac{\rho g d^4}{E}, \frac{\rho_m g d_m^4}{E}, \frac{gt^2}{d}\right) \quad (1)$$

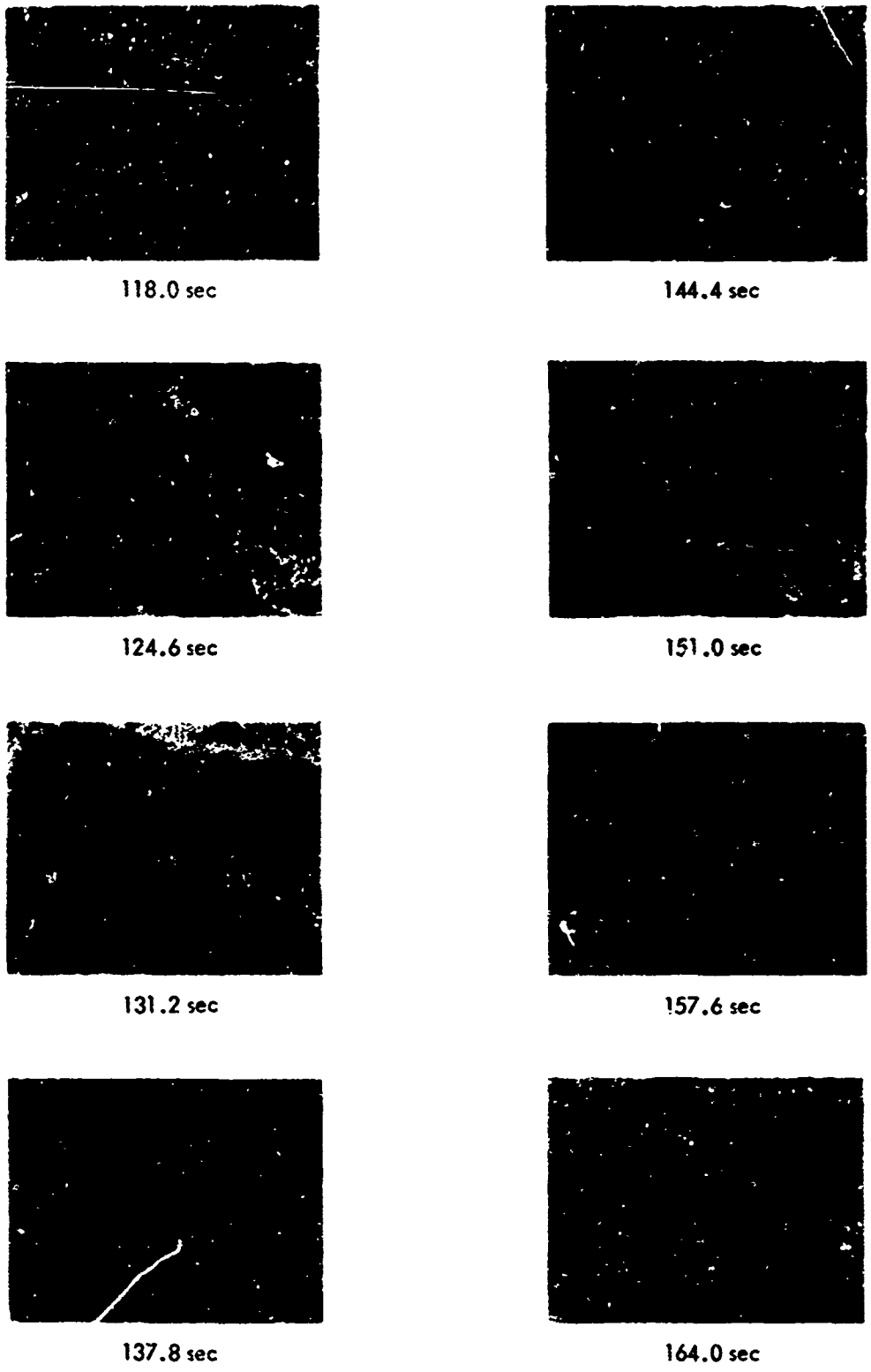

Fig. 96. Complex surface motions and vortices over crater area, Detonation II-EF.

32 sec

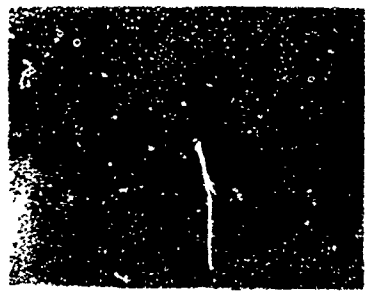

48 sec

36 sec

52 sec

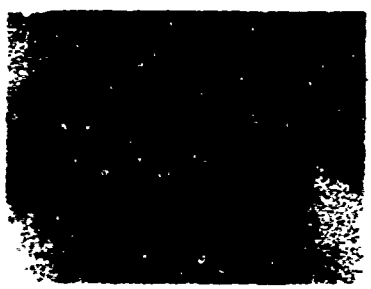

40 sec

56 sec

44 sec

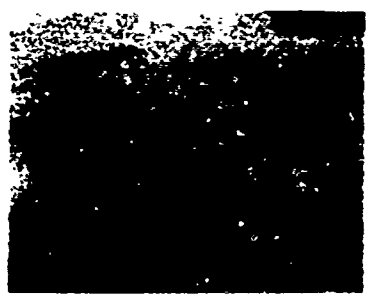

60 sec

Fig. 97. Rush of water and fractured coral into dewatered crater area, Detonation II-IJKL.

35 sec

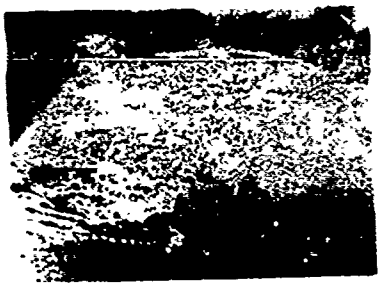

39 sec

36 sec

40 sec

37 sec

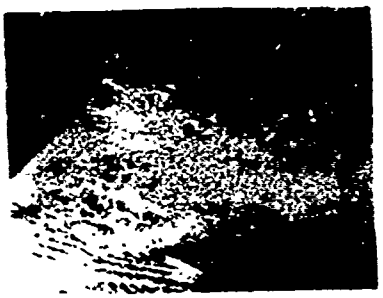

41 sec

38 sec

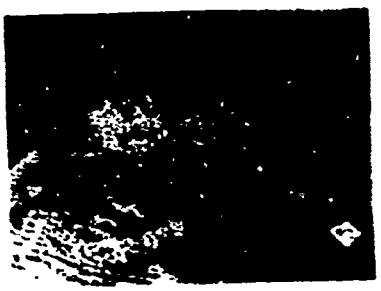

42 sec

Fig. 98. Propagation of wave outward from Surface Ground Zero, Detonation II-EF.

where

H = maximum wave height, crest to following trough

d = average water depth over crater area

d_m = depth of burial in coral medium

ρ = density of water

ρ_m = saturated density of coral medium

g = gravitational acceleration

p = atmospheric pressure

r = horizontal distance from centroid of explosive mass to wave gage

t = time, after detonation

E = energy released by explosive

The dimensionless terms:

$$\frac{d^3(p)}{E}, \quad \frac{d^3(\rho g d)}{E}, \quad \frac{d_m^3(\rho_m g d_m)}{E}$$

are similar in the sense that each bracketed term has units of overburden pressure; i.e., force per unit area. Thus, one useful dimensionless term can be determined:

$$\pi_1 = \frac{z d^3}{E}, \tag{2}$$

where

$$z = p + \rho g d + \rho_m g d_m. \tag{3}$$

Equation (3) can be rewritten as:

$$Z = \frac{z}{\rho g} = \frac{p}{\rho g} + d + \frac{\rho_m}{\rho} d_m, \tag{4}$$

where Z is the lithostatic head on the charge expressed in terms of feet of sea water.

Since E = QW, where Q is the energy per unit mass of explosive and W is the weight of the explosive, π_1 can be written as:

$$\pi_1 = d\left(\frac{Z}{W}\right)^{1/3}, \tag{5}$$

where $\rho g/Q$ = constant for Project Tugboat and has been omitted for convenience.

Since the energy in an idealized wave which propagates axisymmetrically is proportional to $(Hr)^2$, another useful dimensionless term is

$$\pi_2 = \frac{H}{d} \times \frac{r}{d} = \frac{Hr}{d^2}, \quad r \geq R \tag{6}$$

where R is the maximum throat radius of the water dome formed by the explosion bubble. The relationship between π_1 and π_2 is shown in Fig. 99. The equation of the line of least squares fit is

$$\frac{Hr}{d^2} = 11{,}930 \left[d\left(\frac{Z}{W}\right)^{1/3}\right]^{-2.21}. \tag{7}$$

The two data points for Detonation II-ABCD are indicated with error bars because the exact total charge which detonated is indeterminate but appears to be between 20 and 30 tons.

It should be noted that no effort has been made to consider the effects of wave refraction, shoaling, and friction losses because of insufficient topographic detail of the site before and after each shot and theories of refraction available are not valid for the Kawaihae case anyway. In general, the first wave is the maximum of the system. This maximum wave is characterized by a large crest followed by a shallow but long trough.

Wave Travel Times

The time $t = t_0$ for the crest of the maximum wave generated by the underwater explosions to travel a distance

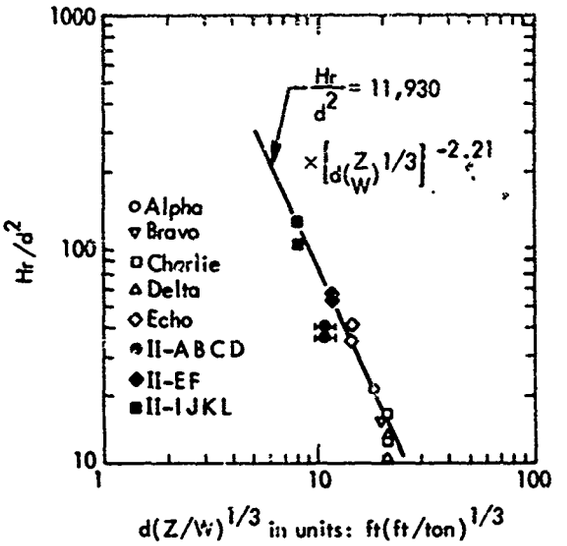

Fig. 99. Maximum wave height scaling relationship.

r - R can be scaled by the two nondimensional terms:

$$\pi_3 = \frac{g(t - t_0)^2}{D}, \quad \pi_4 = \frac{r - R}{D}, \qquad (8)$$

where

- t = time after detonation
- t_0 = time for water dome to attain its maximum throat radius R
- R = maximum throat radius of water dome
- r = distance from centroid of explosive mass to point of measurement
- D = average water depth from point of wave formation to point of measurement
- g = gravitational acceleration

Data from the wave records and low-level photography are tabulated in Table 10. Data for Detonations II-ABCD and II-EF are not included, because the throat radius R of the domes could not be measured accurately from the high-speed photography. A plot of r - R/D vs $g(t - t_0)^2/D$ is shown in Fig. 100.

Again, no effort was made to consider the effects of wave refraction, shoaling, friction losses, or changes in water depth. These factors influence the celerity and path of propagation of the wave and contribute to the scatter in the data points in Fig. 100. The equation of the line of least fit through the data points is:

$$\frac{g(t - t_0)^2}{D} = 1.37 \left(\frac{r - R}{D}\right)^{1.8}. \qquad (9)$$

Solving for $t - t_0$, the time required for the crest of the maximum wave to travel a distance r - R is:

$$t - t_0 = 0.205 (r - R)^{0.9} D^{-0.4}. \qquad (10)$$

If the exponent in Eq. (9) is taken to be 2.0 instead of 1.8, this reduces to

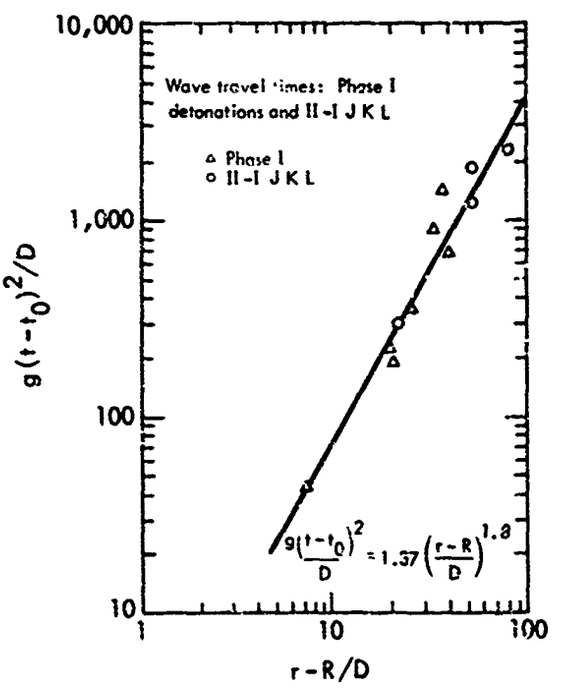

Fig. 100. Travel time for crest of maximum wave.

Table 10. Travel time of crest of maximum wave.

Detonation	Average water depth, D (ft)	Maximum radius of water dome, R (ft)	Time for water dome to attain R t_0 (sec)	Radial distance, r (ft)	Travel time of crest t (sec)	$\frac{r-R}{D}$	$\frac{g(t-t_0)^2}{D}$
Alpha	5.5	55	1.08	165	6.8	20.0	191
Bravo	5.8	54	1.14	200	9.1	25.2	356
Charlie	5.6	58	1.30	75	5.3	3.0	92
	6.6	58	1.30	275	15.9	32.9	916
Delta	5.2	53	1.31	155	7.2	19.6	216
	6.5	53	1.31	290	18.6	36.4	1472
Echo	7.3	108	1.50	160	4.7	7.1	45
	6.8	108	1.50	380	13.5	40.0	682
II-IJKL	5.2	230	1.41	340	8.4	21.2	304
	8.0	230	1.41	650	19.0	52.5	1247
	10.0	230	1.41	760	25.7	53.0	1900
	7.0	230	1.41	809	23.0	81.4	2350

$$c = \left[\frac{(r-R)^2}{(t-t_0)^2}\right]^{1/2} = 0.95\,(gD)^{1/2}, \quad (11)$$

where c = wave celerity. This expression for celerity is of the same form as the solitary wave and other shallow water expressions.

CONCLUSIONS

1. A scaling relationship has been developed for waves generated in shallow water by a chemical explosive detonated in a weak coral medium from Project Tugboat data. This relationship is:

$$\frac{Hr}{2} = 11{,}930\left[d\left(\frac{Z}{W}\right)^{1/3}\right]^{-2.21}.$$

This relationship should be used with caution for cratering detonations in a more dense medium than coral where the crater formation process and consequent wave generation would be different.

2. The travel time for the crest of the maximum wave can be determined according to the following relationship:

$$t - t_0 = 0.205\,(r-R)^{0.9}\,D^{-0.4}.$$

3. The wave of maximum height is usually the first wave of the explosively generated system and is characterized by a high crest followed by a long shallow trough.

RECOMMENDATIONS FOR FUTURE EXPERIMENTS

The following two recommendations are made for future experiments or projects where it might be possible to get additional data on explosively generated waves:

1. Floats should be set out so that water movements at late time could be observed in aerial photos.

2. Laboratory model tests should be conducted to get a feel for the problem prior to field operations.

Section 4
Fish and Wildlife Studies

OBJECTIVES

The objective of this program was to determine the effects of the Project Tugboat detonations on the marine environment in Kawaihae Bay, Island of Hawaii. Studies were restricted to the marine environment because it was felt that the detonations would have little effect on the limited terrestrial wildlife present at the project site. The following make up the scope of this program:

1. To record the species composition and densities of marine life that existed at the project site through underwater observations and counts by divers with emphasis being placed on fishes

2. To determine the effects of the detonations in relation to (a) the distances from the blast centers to which fish kills and injuries are effected, (b) the total area affected by the blasts, and (c) the total number and/or poundage of fishes that were killed or injured

3. To determine the time required for and the nature of repopulation of the affected area

MATERIALS AND METHODS

Species Composition and Densities of Marine Life

The species of marine life inhabiting the project site were initially determined through underwater fish counts. Information obtained through the collections of dead and injured fishes after each detonation was used to supplement the fish count data.

Fish counts were conducted by using a method that was described by Brock.[13] Divers using Scuba or snorkeling gear (Fig. 101) swam along a 600-ft length of weighted cotton transect line that was laid over a selected section of the reef. The divers carried a plastic slate on which they recorded the species, numbers, and estimated lengths of all fishes that were encountered within a 20-ft wide band extending 10 ft to the right and left of the line. Estimates of fish weights were then calculated by multiplying the cube of the

Fig. 101. Underwater fish counts to record the densities and species composition of marine life at project site.

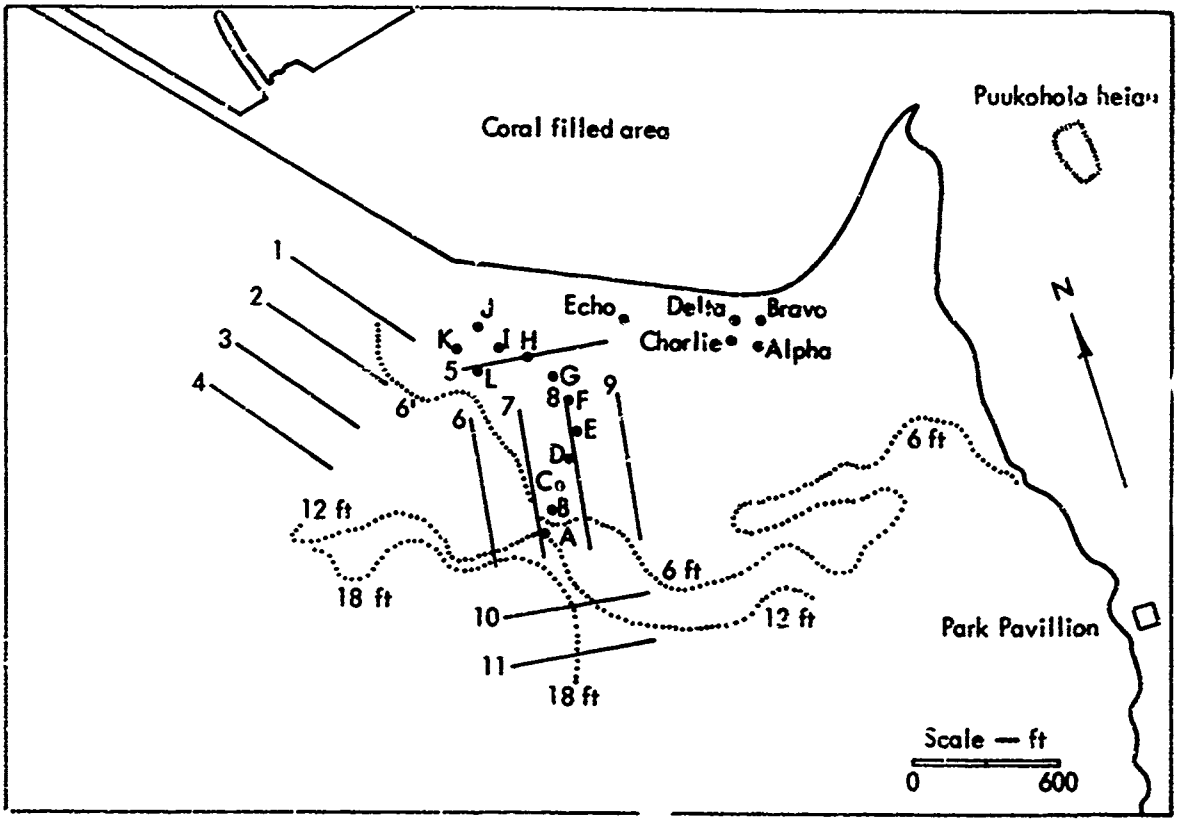

Fig. 102. Approximate locations of 11 fish-counting stations in relation to Surface Ground Zeros of Phase I and Phase II detonations.

fish length by a species constant previously determined from known length-weight relationships for each of the species involved.

Predetonation fish counts were made at 11 stations during the period of 22-25 September 1969 and at three stations on 3 November 1969. Postdetonation counts were made at two stations on 27 April 1970 and at seven stations on 4 June 1970. Fish counting stations were established only in the vicinity of the Phase II detonations (Fig. 102) because turbidity at the Phase I site precluded diver observation of fishes as is required using Brock's method. In order to obtain some information of fish composition and densities at the Phase I site, two attempts were made to fish gill nets in September 1969 (Fig. 103). The netting efforts, however, were not successful; only two fishes were caught in a 6-hr daylight set, and only one fish was caught in an overnight set. The nets were damaged beyond repair by large predators and by snagging on submerged coral heads, and no further netting attempts were made.

Effects of Detonations on Marine Life

Test cages, each containing four or five live fishes, were placed at varying distances from the SGZ's of Phase I Detonations Alpha, Delta, Echo and Phase II Detonations II-ABCD, II-EF, and II-IJKL.

Fig. 103. Gill nets were fished in areas that were too murky for fish counting by divers (only limited information was obtained through this method).

Fig. 104. Lantern basket containing live fishes being set out to determine the distances to which fishes were affected by detonations.

Lantern baskets, or fish-holding bags, served as test cages and were attached to anchored floats in a manner that permitted the test animals to be suspended some 3 to 4 ft below the surface. Lantern baskets are basically mesh bags held open by galvanized wire rings of varying diameters. The No. 16 size basket with 1-in. stretch measure cotton mesh was used; the basket measured 24 in. in height and tapered from a 7-in.-diameter opening at the top to 15-1/2-in.-diameter at the base (Fig. 104). The necks of the baskets were tied-off with a short length of string to prevent the escape of test fishes while the cages were submerged.

Test fishes used during the Phase I series of detonations consisted of rilapia (Tilapia mossambica), the squirrelfishes, menpachi (Myripristis sp.) and alaihi (Holocentrus sp.), and the cardinal fish upapalu (Apogon snyderi). Tilapia were airshipped from the island of Oahu whereas the last three species were caught by hook and line in Kawaihae Bay. Tilapia was used exclusively during the Phase II series of detonations.

The test animals, ranging between 2 and 7 in. in length, were held in floating ring nets placed in the Kawaihae small-boat harbor until they were needed for the tests. The cages and fishes were setout from 2 to 4 hr prior to the detonations. They were checked from 1 to 2 hr after the detonations when collections for dead fishes were completed.

Searches for dead and injured fishes floating at the surface were made following each of the blasts immediately after clearance to enter the blast zone was obtained (Fig. 105). Besides the Division of Fish and Game boat, skiffs manned by other project personnel participated in the fish collections.

RESULTS AND DISCUSSION

Marine Organisms at Project Site

One hundred eleven different species of fishes representing 34 families were found at the project site (Table 11). Seventy-six species were recorded during the fish counts, including two species that

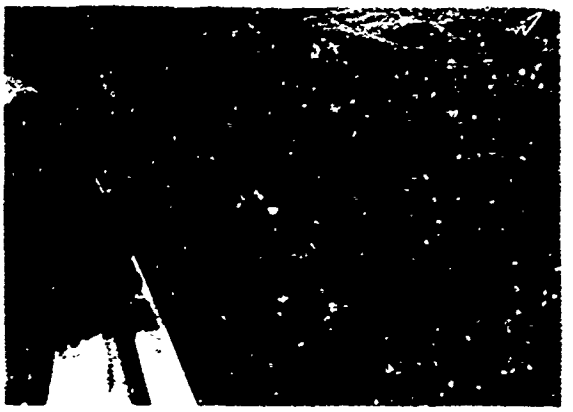

Fig. 105. Spiny puffer, Diodon hystrix, being netted after Detonation 1c (Charlie).

were caught in the gill nets, and 74 species were represented in the collections that were made after the detonations. The majority of the 111 species of fishes may be considered as permanent residents of the project site reef. Many of these, however, are capable of moving over wide areas of the reef. Wandering species, or those fishes that probably enter the project reef only at infrequent and irregular intervals, include the eagle ray, Aetobatus narinari, the mullet, Mugil cephalus, six species of jack crevallys (Family Carangidae) and the snapper, Lutjanus vaigiensis. Several unidentified species of sharks were observed in September 1969 and in April 1970, but they were not included in the list of fishes. Sharks were never observed during the fish counting dives or during postdetonation fish collecting.

The 12 most abundant fishes at the project site in terms of average numbers per acre as determined from fish counts during September 1969 are listed in Table 12. These fishes, except for the damselfish Chromis ovalis and the goatfish, Mulloidichthys samoensis, were among the most widely distributed over the project site reef. They were recorded at 9, 10, or all 11 of the counting stations. The butterfly fishes, Chaetodon ornatissimus and C. trifasciatus, and the wrasse Thalassoma ballieui were three other common species and were observed at 8 of the 11 stations.

Coral species in the Porites, Montipora and Pocillopora genera comprised the major portions of the reef. A few scattered colonies of Fungia scutaria, a mushroom coral were present. Besides the corals, sea urchins were the most prominent and abundant invertebrates. The sea urchins Heterocentrotus mammillatus (slate-pencil urchin), Echinothrix calamaris, E. diadema and Diadema paucispina (three species of long-spined urchins collectively called "wanas"), Tripneustes gratilla (short-spined urchin), Echinometra mathaei and E. oblonga, were very common particularly on the outer half of the reef. Counts of sea urchins at transect stations 6 and 8 in November indicated that there was an average of about 425 slate-pencil urchins, 158 short-spined urchins, and 191 long-spined "wanas" per acre of reef.

A few individuals of the coral eating starfish Acanthaster planci (crown-of-thorns starfish) were seen during the fish counts. Some of these were feeding on the corals, but the damage being inflicted was light. The starfish population level was considered as being normal for the reef. Other invertebrates that were seen on the project site reef but only infrequently were Panulirus japonicus (spiny lobster), Polypus marmoratus (octopus) and Holothuria atra (sea cucumber). The kona crab, Ranina serrata, was seen in

Table 11. Fishes inhabiting project site.

Family and species	Species observed during fish counts				Species collected after detonations	
	September 1969	November 1969	April 1970	June 1970	November 1969	April-May 1970
MYLIOBATIDAE (eagle ray)						
1. Aetobatus narinari	x	—	—	—	—	—
MURAENIDAE (moray eels)						
1. Echidna nebulosa	—	—	—	—	x	—
2. Gymnothorax meleagris	—	x	—	—	—	—
3. G. eurostus	—	—	—	—	—	x
4. G undulatus	—	—	—	—	—	x
CONGRIDAE (white eels)						
1. Conger marginatus	—	—	—	—	x	—
FISTULARIIDAE (cornet fishes)						
1. Fistularia petimba	x	—	—	—	—	—
AULOSTOMIDAE (trumpet fishes)						
1. Aulostomus chinensis	x	x	—	—	—	—
HOLOCENTRIDAE (squirrelfishes)						
1. Holocentrus spinifer	—	—	x	—	—	x
2. H. lacteoguttatus	—	—	—	—	—	x
3. H. diadema	—	—	—	—	x	x
4. Holotrachys lima	—	—	—	—	—	x
5. Myripristis multiradiatus	—	—	—	x	x	x
6. M. berndti	—	—	x	—	—	x
MUGILIDAE (gray mullets)						
1. Mugil cephalus	—	—	—	—	—	x
POLYNEMIDAE (threadfins)						
1. Polydactylus sexfilis	x[a]	—	—	—	x	—
SERRANIDAE (groupers)						
1. Ypsigramma sp.	—	—	—	—	—	x
PSEUDOCHROMIDAE						
1. Pseudogramma polyacantha	—	—	—	—	—	x
KUHLIIDAE (aholeholes)						
1. Kuhlia sandvicensis	—	—	—	—	x	x
PRIACANTHIDAE (aweoweos)						
1. Priacanthus cruentatus	—	—	—	—	—	x
APOGONIDAE (cardinal fishes)						
1. Apogon brachygrammus	—	—	—	—	x	—
2. A. snyderi	—	—	—	—	x	x
3. A. menesemus	—	—	—	—	—	x
CARANGIDAE (jack crevally)						
1. Seriola dumerilii	—	—	—	—	x	—
2. Decapterus pinnulatus	x	—	—	—	—	—
3. Carangoides ajax	—	—	—	—	x	—
4. Caranx lugubris	—	—	—	—	—	x
5. C. sexfascintus	—	—	—	—	x	—
6. Trachurops crumenophthalmus	x[a]	—	—	—	—	—
LUTJANIDAE (snappers)						
1. Lutjanus vaigiensis	—	—	—	—	x	—
MULLIDAE (goatfishes)						
1. Upeneus arge	—	—	—	—	x	—
2. Mulloidichthys samoensis	x	x	x	x	x	x
3. M. auriflamma	x	x	—	—	—	—
4. Parupeneus chrysorydros	x	x	—	x	—	—
5. P. porphyreus	x	x	—	x	—	x
6. P. multifasciatus	x	x	x	x	—	—
7. P. pleurostigma	—	—	—	x	—	—
CHAETODONTIDAE (butterfly fishes)						
1. Centropyge potteri	—	—	—	—	—	x
2. Forcipiger longirostris	x	x	—	x	—	—
3. Chaetodon fremblii	x	x	—	—	—	—
4. C. auriga	x	x	—	—	x	x
5. C. unimaculatus	x	x	—	x	x	x
6. C. lunula	x	x	x	x	x	x
7. C. trifasciatus	x	x	x	x	x	x
8. C. ornatissimus	x	x	x	x	x	x
9. C. quadrimaculatus	—	x	—	—	—	—
10. C. multicinctus	x	x	—	x	—	x
11. C. miliaris	x	—	—	—	x	x

Table 11 (continued)

Family and species	Species observed during fish counts				Species collected after detonations	
	September 1969	November 1969	April 1970	June 1970	November 1969	April-May 1970
CIRRHITIDAE (hawkfishes)						
1. Paracirrhites arcatus	x	—	—	—	—	—
2. P. forsteri	x	—	—	x	—	—
3. P. cinctus	x	—	x	—	—	—
POMACENTRIDAE (damselfishes)						
1. Dascyllus albisella	x	—	—	x	—	x
2. Abudefduf abdominalis	x	x	x	x	—	x
3. Plectroglyphidodon johnstonianus	x	x	x	—	—	x
4. Pomacentrus jenkensi	x	x	x	x	—	x
5. Chromis ovalis	x	x	x	x	—	x
6. C. leucurus	x	x	x	x	—	x
LABRIDAE (wrasses)						
1. Bodianus	—	—	—	—	—	x
2. Labroides phthirophagus	x	x	x	x	—	—
3. Cheilinus rhodochrous	x	x	x	x	x	x
4. Thalassoma duperreyi	x	x	x	x	—	—
5. T. ballieui	x	x	x	x	—	—
6. Gomphosus varius	x	x	x	x	—	—
7. Coris flavovittata	x	—	—	—	—	—
8. C. gaimardi	x	—	—	x	—	—
9. Stehojulis axillaris	x	x	—	—	—	—
10. S. albovittata	x	x	—	—	—	—
11. Novaculichthys taeniourus	x	—	—	—	—	—
12. Anampses cuvieri	x	—	—	—	—	—
SCARIDAE (parrotfishes)						
1. Calotomus sandvicensis	—	x	x	x	—	—
2. Scarus dubius	x	x	x	x	—	x
3. S. perspicillatus	x	x	x	—	—	x
4. S. sordidus	x	—	—	x	—	x
ZANCLIDAE (moorish idol)						
1. Zanclus canescens	x	x	x	x	—	—
ACANTHURIDAE (surgeonfishes)						
1. Acanthurus sandvicensis	x	x	x	x	x	x
2. A. achilles	x	x	—	x	—	—
3. A. leucopareius	x	x	—	x	—	x
4. A. nigrofuscus	x	x	x	x	x	x
5. A. nigroris	x	x	x	x	—	—
6. A. olivaceus	—	—	—	—	—	x
7. A. dussumieri	x	—	—	—	—	x
8. A. xanthopterus	x	x	—	—	x	x
9. A. mata	—	x	x	x	x	x
10. Ctenochaetus strigosus	x	x	x	x	—	—
11. Zebrasoma flavescens	x	x	x	—	—	—
12. Z. veliferum	x	x	x	x	—	—
13. Naso lituratus	x	x	x	x	—	x
14. N. hexacanthus	x	—	—	—	—	—
15. N. unicornis	—	—	—	—	x	x
ELEOTRIDAE						
1. Asterropteryx semipunctatus	—	—	—	—	x	—
BLENNIIDAE (blennies)						
1. Exallias brevis	x	x	x	x	—	x
2. Cirripectus obscurus	x	x	x	x	—	—
BROTULIDAE						
1. Brotula multibarbata	—	—	—	—	—	x
SCORPAENIDAE (scorpion fishes)						
1. Dendrochirus brachypterus	—	—	—	—	—	x
2. Scorpaenodes guamensis	—	—	—	—	—	x
BALISTIDAE (triggerfishes)						
1. Xanthichthys ringens	—	x	—	—	—	—
2. Rhinecanthus rectangulus	x	x	x	x	—	x
3. Melichthys buniva	x	x	x	x	—	x
4. M. vidua	x	—	—	—	—	—
5. Balistes bursa	—	—	—	—	—	x
MONACANTHIDAE (filefishes)						
1. Pervagor spilosoma	—	—	—	x	—	x
2. P. melanocephalus	—	—	—	—	—	x
3. Amanses carolae	x	x	—	—	—	x
4. A. sandwichiensis	—	—	—	—	—	x

Table 11 (continued)

Family and species	Species observed during fish counts				Species collected after detonations	
	September 1969	November 1969	April 1970	June 1970	November 1969	April-May 1970
OSTRACIONTIDAE (boxfishes)						
1. Ostracion lentiginosus	x	x	—	—	x	x
TETRAODONTIDAE (puffers)						
1. Arothron meleagris	x	—	—	—	x	x
2. A. hispidus	—	—	—	—	x	x
CANTHIGASTERIDAE (sharpbacked puffers)						
1. Canthigaster jactator	x	x	x	—	—	x
DIODONTIDAE (spiny puffers)						
1. Diodon hystrix	—	x	—	x	x	x
ANTENNARIIDAE (frogfishes)						
1. Abantennarius analis	—	—	—	—	—	x
2. Antennarius drombus	—	—	—	—	—	x
Total number of species	65	52	35	43	31	64

[a]Caught in gill net.

Table 12. Twelve most abundant fishes at project site as determined from fish counts at 11 stations in September 1969.

Ranking	Species	Average number per acre	Occurrence (number of stations)
1	Scarus dubius	70.2	11
2	Thalassoma duperreyi	64.8	11
3	Chromis ovalis	44.6	6
4	Pomacentrus jenkinsi	34.5	11
5	Ctenochaetus strigosus	34.1	10
6	Gomphosus varius	30.7	11
7	Mulloidichthys samoensis	25.5	5
8	Acanthurus nigroris	18.8	10
9	Parupeneus multifasciatus	18.1	11
10	Acanthurus nigrofuscus	16.1	9
11	Cirripectus variolosus	13.2	10
12	Exallias brevis	13.2	10

the sand channel immediately to the south of the project site. The only invertebrates that were collected after the detonations were two specimens of an unidentified species of nudibranchs.

Standing Crops of Fishes

Estimates of the standing crops of fishes, expressed in pounds per acre, obtained from predetonation fish counts are presented in Table 13. The standing crops derived for the 11 counting stations in September 1969 varied from 17.1 to 101.1 lb/acre and averaged 62.8 lb/acre. An estimate of 196.7 lb/acre was obtained for Station 3, but this estimate was heavily influenced by the inclusion of an eagle ray which was estimated at 30 lb in weight.

Table 13. Results of predetonation fish counts.

Date and station No.	Number of species	Number of fishes counted	Calculated number per acre	Calculated lb per acre
September 22-25, 1969				
1	22	148	537	21.7
2	18	70	254	30.6
3	24	290	1,053	87.8 (196.7)[a]
4	32	228	828	101.1
5	28	159	577	44.4
6	34	239	868	84.4
7	24	347	1,260	93.8
8	32	229	831	97.2
9	19	159	577	50.6
10	25	290	1,053	62.5
11	13	132	479	17.1
Average	24.7	208.3	756.1	62.8
November 3, 1969				
4	42	306	1,111	266.8
6	35	188	682	85.4
8	33	420	1,525	445.2
Average	36.7	304.7	1,106	265.8

[a]Including an eagle ray estimated at 30 lb in weight.

By excluding the weight of the eagle ray from the calculations, the standing crop estimate would be reduced to 87.8 lb/acre which is believed to be a more accurate representation of normal situations. The lowest estimate of 17.1 lb/acre was obtained from station 11 which was situated in a sand bottom channel that bisects the reef immediately to the south of the proposed harbor entrance channel.

Low standing crops were also obtained at the near shore Stations 1, 2, and 5 and at Station 9. This was probably the result of murky water conditions that existed at these stations because of their proximity to the sediment zone lying in a wide band adjacent to the shoreline. Apparently, waters within this sediment zone remain in a constant state of turbidity. This turbidity was increased considerably by project-related activities involving the construction and subsequent removal of crushed coral causeways and the drilling of charge emplacement holes.

The numbers of fishes enumerated at the 11 counting stations in September ranged from 70 to 347 and averaged 208.3 per station (Table 13). Through extrapolation, an overall average of 756.1 fishes per acre of reef was indicated to be present at the project site. As will be discussed in a following section, the fish

collections made after the detonations revealed that several species of fishes, some of which were very abundant in the collections, were missed entirely in the fish counts. Therefore, the estimates that were obtained for the numbers and standing crops based on the fish counts must be considered as underestimates.

Fish counts in November were limited to Stations 4, 6, and 8. During the September survey, data obtained from these three stations showed an average density of 842 fishes per acre and an average standing crop of 94.2 lb/acre (Table 13). In November, the counts indicated that the average number of fishes increased by 31.3% to 1,106 fishes per acre and the average standing crop increased 182.2% to 265.8 lb/acre. These increases were due primarily to an increase in sizes and abundance of parrotfishes and surgeonfishes, and to a lesser extent on the increase in numbers of goatfishes, triggerfishes and spiny puffers. On the assumption that the numbers of fishes and standing crops at the eight other stations surveyed in September but not in November increased at the same ratio as did Stations 4, 6, and 8, an average density of 992.8 fishes per acre and an average standing crop of 177.2 lb/acre were indicated for November.

An attempt was made to conduct fish counts on the day before the initial Phase II detonation in order to obtain data that would have been applicable at the time of the detonations. However, the counts were not made because of a breakdown of the outboard motor on the survey boat. For this reason, the estimates of the average number of fishes and the average standing crop used in later calculations of fishes affected by the detonations were derived by averaging the values obtained from the fish counts in September and November. These averages were 924.8 fishes per acre and a standing crop of 120.0 lb/acre.

Fishes Collected After Detonations

The fish collections made after the Phase I series of detonations may be considered complete in that all fishes observed at the surface were picked up, and most of the fishes collected by other project personnel were made available for examination. After the Phase II detonations, however, it was possible to collect only a representative sample of the fishes because of the large numbers that were affected and because the fishes were dispersed over a very wide area. Also, the samples collected by other project personnel were not examined. Collecting efforts were hampered by the extreme turbidity created by the blasts which limited visibility to within a few inches of the surface, and, because of this turbidity, it was not possible to determine the species and numbers of fishes that sank to the bottom. A thick layer of brownish scum blanketed extensive areas after the Phase II detonations to further hamper collecting efforts (Fig. 106).

The species and numbers of fishes that were collected after the Phase I and Phase II detonations are listed in Table 14. After the first 1-ton detonation (Charlie), 25 fishes comprised of 13 species were found. The butterfly fishes seemed most heavily affected by this blast as 10 individuals of three species were collected. A noteworthy specimen in the collection was the snapper Lutjanus vaigiensis

Fig. 106. Thick layer of brownish scum, resulting from detonations, hampered postdetonation fish collecting efforts.

which was one of the exotic species introduced into Hawaiian waters by the State Division of Fish and Game. Releases of this snapper were made only off the island of Oahu during the period from 1956 through 1961, but it is now well-established around all the Hawaiian Islands.

Dead fishes were not seen after the second 1 ton detonation (Delta). For this blast SGZ was situated only about 100 ft shoreward from the previous blast (Charlie), and it was suspected that most of the fishes not affected by the initial blast may have been scared away, or they may have moved out of the area to escape the extremely silty conditions that were created. Possibly for this same reason, only two dead fishes were found after the third 1-ton detonation (Alpha), and only one was found after the fourth detonation (Bravo). These two detonations were fired on the same day within a period of 2 hr, and both were situated only about 100 ft from the previous two blasts.

The 10-ton detonation (Echo) was situated slightly more than 400 ft northwest of the nearest 1-ton detonation. Seventy-one fishes belonging to 26 species were collected after the blast. The four species were most numerous in the collection, comprising 54% of the fishes collected, included the cardinal fish Apogon snyderi, the squirrelfish Holocentrus diadema, the surgeonfish Acanthurus nigrofuscus, and the puffer Aronthron hispidus. The remaining 22 species were represented by less than three specimens each.

The initial detonation of the Phase II series (II-ABCD) resulted in a collection of 401 fishes representing 50 different species. Seventy-five percent of the fishes in the collection belonged to the squirrelfish, damselfish, and butterfly fish families. Pomacentrus jenkinsi and Myripristis multiradiatus were the two most numerous individual species. The rarest fish found in this collection was a small grouper (Family Serranidae) of the genus Ypsigramma (Fig. 107). As far as is known only one other specimen of this

Fig. 107. A 2-3/4-in. grouper of Genus Ypsigramma (Family Serranidae) killed by Detonation II-ABCD; this specimen was believed to be only the second of species collected from Hawaiian Islands.

Table 14. Species and numbers of fishes collected after Phase I and Phase II detonations.

Family and species	Code No. and date of detonation: Phase I (1969) Charlie 11/4	Delta 11/5	Alpha 11/6	Bravo 11/6	Echo 11/7	Phase II (1970) II-ABCD 4/23	II-EF 4/28	II-EF 4/29	II-IJKL 5/1
MURAENIDAE (moray eels)									
1. Echidna nebulosa	—	—	—	—	1	—	—	—	—
2. Gymnothorax eurostus	—	—	—	—	—	—	—	1	—
3. G. undulatus	—	—	—	—	—	—	—	1	—
CONGRIDAE (white eels)									
1. Conger marginatus	—	—	—	—	1	—	—	—	—
HOLOCENTRIDAE (squirrelfishes)									
1. Holocentrus spinifer	—	—	—	—	—	2	—	—	—
2. H. lacteoguttatus	—	—	—	—	—	3	—	—	2
3. H. diadema	—	—	—	—	8	40	25	8	18
4. Holotrachys lima	—	—	—	—	—	16	—	—	10
5. Myripristis multiradiatus	—	—	—	—	1	82	4	1	25
6. M. berndti	—	—	—	—	—	25	2	—	11
MUGILIDAE (gray mullets)									
1. Mugil cephalus	—	—	—	—	—	—	15	2	—
POLYNEMIDAE (threadfins)									
1. Polydactylus sexfilis	—	—	—	—	1	—	—	—	—
SERRANIDAE (groupers)									
1. Ypsigramma sp.	—	—	—	—	—	1	—	—	—
PSEUDOCHROMIDAE									
1. Pseudogramma polyacantha	—	—	—	—	—	6	—	—	—
KUHLIIDAE (aholeholes)									
1. Kuhlia sandvicensis	—	—	—	—	3	—	—	—	2
PRIACANTHIDAE (aweoweos)									
1. Priacanthus cruentatus	—	—	—	—	—	1	—	—	2
APOGONIDAE (cardinal fishes)									
1. Apogon brachygrammus	—	—	—	—	3	—	—	—	—
2. A. snyderi	2	—	—	—	16	1	3	1	3
3. A. menesemus	—	—	—	—	—	4	1	—	—
CARANGIDAE (jack crevally)									
1. Seriola dumerili	—	—	—	—	1	—	—	—	—
2. Carangoides ajax	1	—	—	—	—	—	—	—	—
3. Caranx lugubris	—	—	—	—	—	—	—	—	1
4. C. Sexfasciatus	—	—	—	—	1	—	—	—	—
LUTJANIDAE (snappers)									
1. Lutjanus vaigiensis	1	—	—	—	—	—	—	—	—
MULLIDAE (goatfishes)									
1. Upeneus arge	1	—	—	—	1	—	—	—	—
2. Mulloidichthys samoensis	2	—	—	—	1	1	—	—	—
3. Parupeneus porphyreus	—	—	—	—	—	—	—	1	—
CHAETODONTIDAE (butterfly fishes)									
1. Centropyge potteri	—	—	—	—	1	—	—	—	—
2. Chaetodon auriga	6	—	—	1	3	3	—	—	—
3. C. unimaculatus	—	—	—	3	5	1	—	—	—
4. C. lunula	1	—	—	2	2	1	—	1	—
5. C. trifasciatus	3	—	—	2	19	7	2	11	—
6. C. ornatissimus	—	—	—	2	5	3		2	—
7. C. multicinctus	—	—	—	—	1	—	—	—	—
8. C. miliaris	—	—	—	1	3	1	—	2	—
POMACENTRIDAE (damselfishes)									
1. Dascyllus albisella	—	—	—	—	—	2	—	—	—
2. Abudefduf abdominalis	—	—	—	—	—	—	—	—	1
3. Plectroglyphidodon johnstonianus	—	—	—	—	—	1	—	—	—
4. Pomacentrus jenkensi	—	—	—	—	—	86	6	1	24
5. Chromis ovalis	—	—	—	—	—	4	—	—	—
6. C. leucurus	—	—	—	—	—	1	—	—	—
LABRIDAE (wrasses)									
1. Bodianus bilunulatus	—	—	—	—	—	1	—	—	—
2. Cheilinus rhodochrous	—	—	—	—	1	—	—	1	—

Table 14 (continued)

Family and species	Code No. and date of detonation								
	Phase I (1969)					Phase II (1970)			
	Charlie 11/4	Delta 11/5	Alpha 11/6	Bravo 11/6	Echo 11/7	II-ABCD 4/23	II-EF 4/28	II-EF 4/29	II-IJKL 5/1
SCARIDAE (parrot fishes)									
1. Scarus dubius	—	—	—	—	—	—	—	5	—
2. S. perspicillatus	—	—	—	—	—	—	—	—	2
3. S. sordidus	—	—	—	—	—	1	—	5	1
ACANTHURIDAE (surgeonfishes)									
1. Acanthurus sandvicensis	—	—	—	—	1	—	1	1	3
2. A. leucopareius	—	—	—	—	—	—	8	2	6
3. A. nigrofuscus	—	—	—	—	7	7	4	8	—
4. A. olivaceus	—	—	—	—	—	2	—	—	—
5. A. dussumieri	—	—	—	—	—	2	—	—	—
6. A. xanthopterus	1	—	—	—	—	2	1	—	—
7. A. mata	2	—	—	—	—	3	2	—	2
8. Naso lituratus	—	—	—	—	—	4	2	—	—
9. N. unicornis	—	—	1	—	—	—	—	—	1
ELEOTRIDAE									
1. Asterropteryx semipunctatus	—	—	—	—	2	—	—	—	—
BLENNIIDAE (blennies									
1. Exallias brevis	—	—	—	—	—	—	—	1	—
BROTULIDAE									
1. Brotula multibarbata	—	—	—	—	—	3	—	5	3
SCORPAENIDAE (scorpion fishes)									
1. Dendrochirus brachypterus	—	—	—	—	—	1	—	—	—
2. Scorpaenodes guamensis	—	—	—	—	—	3	—	—	—
BALISTIDAE (triggerfishes									
1. Rhinecanthus rectangulus	—	—	—	—	—	1	—	—	—
2. Melichthys buniva	—	—	—	—	—	18	3	1	7
3. Balistes bursa	—	—	—	—	—	4	—	—	—
MONACANTHIDAE (filefishes)									
1. Pervagor spilosoma	—	—	—	—	—	4	—	—	2
2. P. melanocephalus	—	—	—	—	—	3	—	—	—
3. Amanses carolae	—	—	—	—	—	8	—	1	3
4. A. sandwichiensis	—	—	—	—	—	1	—	—	—
OSTRACIONTIDAE (boxfishes)									
1. Ostracion lentiginosus	—	—	—	—	1	3	—	1	3
TETRAODONTIDAE (puffers)									
1. Arothron meleagris	1	—	—	—	—	2	1	—	—
2. A. hispidus	2	—	1	1	5	3	3	—	4
CANTHIGASTERIDAE (sharpback puffers)									
1. Canthigaster jactator	—	—	—	—	—	1	1	—	1
DIODONTIDAE (spiny puffers)									
1. Diodon hystrix	2	—	—	—	2	3	1	—	—
ANTENARIIDAE (frogfishes)									
1. Abantennarius analis	—	—	—	—	—	2	—	—	—
2. Antennarius drombus	—	—	—	—	—	4	1	3	1
Total number of specimens:	25	0	2	1	71	401	100	52	152
Total number of species:	13	0	2	1	25	50	25	21	29

species has ever been collected from the Hawaiian Islands,[14] and its specific identity has not yet been determined.

A thorough collection of dead fishes was made after Detonation II-EF. The blast area was searched until every fish at the surface was picked up, and this resulted in a sample consisting of 100 fishes of 25 species. The squirrelfish, Holocentrus diadema, was the most numerous individual species collected. The mullet, Mugil cephalus, an important commercial species, was collected for the first time. According to local residents mullets commonly frequent the area of the project site, and it was somewhat of a surprise that they were not collected after any of the previous detonations. A second search of the blast site on the following morning (29 April 1970) resulted in a collection of 52 additional specimens. These fishes apparently floated to the surface subsequent to the previous days collection and were probably buoyed to the surface by decomposition gases. Among the 21 species that were included, 10 were not represented in the previous days collection. A total of 152 fishes of 35 species was therefore collected after Detonation II-EF.

Detonation II-IJKL excavated the berthing basin of the small-boat harbor and was located closer to shore than the other Phase II detonations. A sample of 154 fishes of 29 species was collected after this blast. As in previous Phase II collections, squirrelfishes, butterfly fishes, damselfishes, and surgeon fishes were well-represented in the sample. Seventy-seven percent of the fishes collected belonged to these families. An ulua, Caranx lugubris, weighing 38 lb was netted as it floundered at the surface. This was the largest fish collected after the detonations.

The differences in species of fishes found after Phase I and Phase II detonations are readily apparent through an examination of Table 14. Ten species found after the Phase I series were not collected after the Phase II series, and, conversely, 43 species collected after the Phase II series were absent in the Phase I collections. To a certain extent, the differences in species composition can be attributed to the different habitats that were available at the two sites. At the Phase I site, the waters were constantly turbid, the bottom was silty and only a few live coral heads were available. On the other hand, a greater part of the Phase II site was characterized by clear water and a hard, live coral bottom containing numerous cracks and crevices. Certain families of fishes, such as the moray eels, squirrelfishes, butterfly fishes, damselfishes, wrasses, surgeonfishes, triggerfishes and filefishes, generally prefer clear water areas free of sediment.[15] These fishes are usually abundant where conditions favor the growth of coral, such as was found at the Phase II site.

The data obtained through postdetonation fish collections suggested that estimates of numbers and standing fish crops derived through fish counts would be lower than that which actually existed. While 37 of the 76 species enumerated during fish counting dives were never found during postblast collecting, 35 of the 74 species found after the blasts were not observed during the fish counts (Table 11). Some of the fishes that were

collected but which were not seen in the fish counting dives belonged to the squirrelfish, cardinal fish, moray eel, and aweoweo families. Species belonging to these families are normally more active during the night and usually spend the day hiding deep within cracks and crevices of the reef. Only a few squirrelfishes were observed by the divers, but they were among the most abundant fishes brought up by the detonations. Some of the other fishes may have been missed during the fish counts because of their small size, their protective coloration, and their relative scarcity, or because they did not occur in the areas where fish counts were conducted.

The sole dependence on postdetonation fish collections as an indicator of the species composition of marine life at the project site would have also proven inaccurate. As previously mentioned, many fishes that were definitely known to be present at the project site were never brought to the surface by the explosions. The species in the wrasse family (Family Labridae) may be cited as an example. Of the 12 labrid species recorded for the project site, 11 were observed during the fish counts and only two species were collected after the detonations (see Table 11). While some of the labrids were not very abundant, which would account for their absence in the postdetonation collections, three species, Thalassoma duperreyi, T. ballieui and Gomphosus varius, were very abundant and occurred throughout the reef. However, not a single one of these three species was collected. The surgeonfish, Ctenochaetus strigosus, and the goatfish, Parupeneus multifasciatus were two other very common and abundant species that were not recovered after the blasts. Although the parrot fishes were among the most abundant fishes at the project site, a total of only 14 specimens was collected, and 10 of the 14 were not found until the day after one of the detonations.

Most of the fishes exhibited no visible external injuries, but a few were severely lacerated (Figs. 108 and 109). Autopsies were not performed on dead fishes.

Fig. 108. Sorting of fishes collected after Detonation II-IJKL (most of fishes showed no sign of external injuries).

Fig. 109. Lacerated damselfish collected after Detonation II-ABCD (only a few of fishes collected after detonation were as severely lacerated).

Although most of the fishes observed at the surface were dead, several were still alive. Some of the injured fishes were capable of only feeble movement of their fins while others were still able to escape from the approaching boat and dip net. A juvenile amberjack, Seriola dumerilii, netted after the 10-ton Detonation Echo, regained equilibrium soon after it was placed in a pail of clear water. This amberjack was taken to Honolulu where it was maintained in an aquarium for a minimum of 12 days at which time it appeared fully recovered and in good health. This recovery would indicate that some of the other injured or stunned fishes would have recovered had they been left in the water after the blasts.

Distances to Which Fishes Were Affected

The effects of Phase I and Phase II detonations on caged fishes placed at varying distances from the SGZ's are summarized in Table 15. The results from Detonations Delta and Alpha indicated that the 1-ton detonations killed or injured all fishes within a radius of about 80 ft and that some fishes were affected to a maximum distance of 185 ft. On the assumption that resident fishes in every direction around the blast center were affected to the same degree as the test fishes, it was estimated that each 1-ton detonation affected fishes within an area of 107,521 ft^2 (2.5 acres), and that all fishes within 20,106 ft^2 (0.5 acres) centered around the blast center were either killed or injured.

Results from Detonation Echo indicated that the 10-ton detonation affected fishes for a maximum distance of 330 ft. The distance to which all fishes were affected was not determined for the reason that at the minimum distance tested (120 ft from the blast center) only 90% of the caged fishes were affected. A comparison of the effects on fishes placed in cages strung-out in two different directions, one to the south and the other to the west, indicated that blast effects were generally more severe in the southerly direction.

The results obtained from the Phase II series of detonations were quite variable (see Table 16). Where Detonation II-EF resulted in a 100% mortality at a distance of 210 ft, only 80% of the caged fishes at a distance of 120 ft from Detonation II-IJKL were affected. The results from Detonation II-ABCD which inflicted a 100% mortality at a distance of 100 ft were not conclusive since cages set at the next two greater distances, at 150 and 200 ft, were not found after the blast.

The effects of Detonations II-ABCD, II-EF, and II-IJKL were evidenced at maximum distances of 300, 300, and 240 ft, respectively. Only for Detonation II-ABCD was there the possibility that the maximum range could have extended beyond the stated distance.

A comparison of blast effects between fishes placed near the surface and those placed deeper were not very conclusive. Fishes placed near the surface at distances of 200 and 300 ft from Detonation II-ABCD were more severely affected than those placed 24 and 30 ft below the surface at the respective distances. On the other hand, fishes in a cage set at a depth of 15 and 210 ft away from Detonation II-EF were more heavily affected than those in the surface cage at the same location.

Table 15. Effects of detonations on caged fishes.

Test cage distance (in feet) and direction (south or west) from SGZ	Condition of fish after blast			Percentage injured and/or dead	
	Number unaffected	Number injured	Number dead		
A. Detonation Delta (5 November 1969)					
100 (s)	1	1	3	80	
120 (s)	1	1	3	80	
150 (w)	4	1	0	20	
155 (s)	2	2	1	60	
185 (s)	3	0	2	40	
205 (s)	5	0	0	0	
235 (s)	5	0	0	0	
270 (s)	5	0	0	0	
B. Detonation Alpha (6 November 1969)					
80 (w)	0	0	5	100	
100 (s)	3	2	0	40	30
100 (w)	4	0	1	20	
130 (s)	5	0	0	0	
160 (s)	5	0	0	0	
190 (s)	5	0	0	0	
220 (s)	5	0	0	0	
250 (s)	5	0	0	0	
C. Detonation Echo (7 November 1969)					
120 (s)	0	1	4	100	90
120 (w)	1	2	2	80	
150 (s)	2	3	0	60	30
150 (w)	5	0	0	0	
180 (s)	3	2	0	40	40
180 (w)	3	1	1	40	
210 (s)	3	1	1	40	50
210 (w)	2	2	1	60	
240 (s)	3	1	1	40	40
240 (w)	3	0	2	40	
270 (s)	3	2	0	40	30
270 (w)	4	0	1	20	
300 (s)	4	1	0	20	
330 (s)	4	0	1	20	
360 (s)	5	0	0	0	

Table 15 (continued)

Test cage distance (in feet) and direction (south or west) from SGZ	Condition of fish after blast			Percentage injured and/or dead
	Number unaffected	Number injured	Number dead	
D. Detonation II-ABCD (25 April 1970)				
100 (w)	0	0	5	100
150 (w)	—[a]	—[a]	—[a]	—[a]
200 (w)	—[a]	—[a]	—[a]	—[a]
250 (w)	3	1	1	40
300 (w)	5	0	0	0
350 (w)	5	0	0	0
400 (w)	5	0	0	0
450 (w)	5	0	0	0
200 (s)[b]	2	1	2	60 } 50
200 (s)[c]	3	1	1	40 }
300 (s)[b]	2	2	1	60 } 40
300 (s)[d]	4	0	1	20 }
F. Detonation II-EF (28 April 1970)				
90 (w)	—[a]	—[a]	—[a]	—[a]
120 (w)	—[a]	—[a]	—[a]	—[a]
150 (w)	—[a]	—[a]	—[a]	—[a]
180 (w)	0	0	4	100
210 (w)	0	0	4	100
270 (w)	2	0	2	50
300 (w)	3	1	0	25
360 (w)	4	0	0	0
420 (w)	4	0	0	0
210 (s)[b]	3	1	0	25 } 38
210 (s)[e]	2	1	1	50 }
F. Detonation II-IJKL (1 May 1970)				
120 (w)	1	1	3	80
150 (w)	3	0	2	40
180 (w)	3	1	1	40
210 (w)	—[a]	—[a]	—[a]	—[a]
240 (w)	4	1	0	20
300 (w)	—[a]	—[a]	—[a]	—[a]
360 (w)	5	0	0	0
420 (w)	5	0	0	0

[a]Cage lost.

[b]Surface.

[c]25 ft below surface.

[d]30 ft below surface.

[e]15 ft below surface.

Table 16. Areas affected by Phase II detonations.

	Phase II detonations		
	II-ABCD	II-EF	II-IJKL
Arrangement of individual charges:	row	row	square
Spacing between individual charges in feet ("x" in equation below)	100	120	120
Radius in feet (R)			
1. Distance to which all fishes were killed or injured:	100[a]	210	120[b]
2. Maximum distance to which fishes were killed or injured:	300	300[c]	240
Equation used to determine area affected:	$A = \pi r^2 + 6rx$	$A = \pi r^2 + 6rx$	$A = \pi r^2 + 4rx + x^2$
Area affected in square feet (A)			
1. Area in which all fishes were killed or injured:	91,416	289,744	117,239
2. Maximum area in which fishes were killed or injured:	462,744	498,744	310,556

Averages. Area in which all fishes were killed or injured: 166,133 square feet or 3.8 acres

Maximum area in which fishes were killed or injured: 424,015 square feet or 9.7 acres

[a]Actual distance may have been greater than 100 ft, but cages placed at the next two greater distances were not recovered after the blast.

[b]Minimum distance tested for this detonation; only 90% of the fishes were affected.

[c]Maximum distance tested; fishes may have been affected beyond this range.

Estimates of Numbers and Poundage of Fishes Affected

Estimates of the numbers and weights of fishes affected by the detonations were obtained only for the Phase II series of detonations since data on densities and standing crops were not obtainable from the Phase I detonations site. Approximations of the areas that were affected by Detonations II-ABCD and II-EF in which the individual charges were arranged in a row were obtained by using the equation $A = \pi r^2 + 6rx$, whereas the equation $A = \pi r^2 + 4rx + x^2$ was used for the determination of the area affected by Detonation II-IJKL in which the individual charges were arranged in a square array. In both equations, "r" represents the radius or distance in feet to which fishes were affected as determined through the tests with caged fishes, "x" represents the spacing in feet between individual charges, and "A" represents the area in square feet affected by the blasts.

The values that were substituted for "r" and "x" and the resulting values of "A" obtained through solution of the equations are listed in Table 16. Estimates of the maximum area affected by each Phase II detonation varied from 310,556 to 498,744 sq ft and averaged 424,015 sq ft, or an equivalent of 9.7 acres. On the

basis that each acre of reef supported an average population of 924.8 fishes weighing 120.0 lb, as was previously determined from fish counts, it was estimated that the 9.7 acres of reef area affected by each blast contained 8,970 fishes weighing a total of 1,164 lb. However, every fish within the maximum area affected by the blasts was not killed or injured. For the three detonations, the area within which every fish was killed or injured varied from 91,416 to 289,744 sq ft and averaged 166,133 sq ft or 3.8 acres. This area contained an estimated 3,514 fishes weighing a total of 456 lb. In the remaining 257,882 sq ft, or 5.9 acres, only an undetermined percentage of the 5,456 fishes were affected.

Postdetonation Fish Counts

Fish counts were made at two stations on 27 April 1970, four days after Detonation II-ABCD but prior to Detonations II-EF and II-IJKL. These counts were made at the approximate locations shown for Stations 6 and 3 in Fig. 102. The count at the approximate location of Station 6 included areas in which the corals were flattened by the force of Detonation II-ABCD. Large chunks of coral were seen laying on their sides and the water was murky from suspended sediment.

The count at Station 6 resulted in the enumeration of 20 species of fishes having a standing crop density of 45.8 lb/acre (Table 17). Nearly 70% of the standing crop was accounted for by small parrot-fishes

Table 17. Results of postdetonation fish counts.

Date and station No.	Number of species	Number of fishes counted	Calculated number per acre	Calculated lb/acre
27 April 1970				
3	30	284	1,030	90.0
6	20	149	541	45.8
Averages	25	216.5	785.5	67.9
4 June 1970				
1	12	120	436	66.5
2	28	686	2,490	292.9
3	23	220	799	57.1
4	26	272	987	76.4
5	—	—	—	—
6	19	255	926	56.2
7	11	31	112	6.5
8	14	240	871	93.8
9	—	—	—	—
10	—	—	—	—
11	—	—	—	—
Average for 7 lines:	19.0	260.6	945.9	92.8

that occurred in large schools. The damselfish, Pomacentrus jenkensi, and two species of blennies were among the fishes that were observed within the coral rubble area created by the blast. This damselfish and the two blennies usually establish themselves within a restricted portion of the reef and do not normally move about as do the other reef fishes, such as the parrotfishes, surgeonfishes, goatfishes and wrasses, to name a few. It appeared improbable, judging from the extent of damage to the reef, that the damselfish and blennies observed were survivors of the blast. It was more probable that these fishes had moved into the coral damaged area subsequent to the blast, and this would indicate that repopulation of affected area would commence almost immediately after the blast even by species that do not move freely about the reef.

The count at Station 3 resulted in the enumeration of 30 species of fishes at a standing crop density of 90.0 lb/acre. The increase in the number of species over the number that was present at this station in September and the almost identical standing crop density, suggested that Detonation II-ABCD had little effect on fishes at this station.

Postdetonation fish counts were also conducted on 4 June 1970 approximately one month after completion of the Phase II series of detonations. New transect lines were laid at approximately the same locations as those in September 1969 and were numbered in the same order. Fish counts were obtained at 7 of the 11 stations, and the findings are also summarized in Table 17. Waters were generally clear over the reef area, but throughout the excavated entrance channel and berthing basin, a 3- to 4-ft thick layer of extremely silty water lay over the bottom. The bottom of the entrance channel was covered over by silt.

The fish counts at Stations 7 and 8 which included areas that were excavated resulted in the enumeration of only 11 and 14 species of fishes, respectively. At both these stations, fishes were not seen in or above the layer of silty water. The fishes were present only along the sides of the newly excavated channel where corals, although damaged and toppled, were still present. A low standing crop of 6.5 lb/acre was obtained for Station 7, whereas at Station 8 the standing crop was estimated to be 93.8 lb/acre. The bulk of the fish weight at Station 8 was from the parrotfish, Scarus dubius, which accounted for 63% of the weight, and the wrasse, Thalassoma duperreyi, which accounted for 14% of the weight.

An average of 19.0 species of fishes were observed at the 7 stations. This represented a considerable decrease from the predetonation average of 26.7 species per station enumerated at the same 7 stations in September 1969. The average number of fishes per acre and the average standing fish crop, however, both increased over the predetonation values. The number of fishes increased from 806 to 946 per acre, and the standing crop increased from 73.8 to 92.8 lb/acre.

SUMMARY AND CONCLUSIONS

A three-part program was carried out on Project Tugboat. This consisted of observing and recording the marine life

at selected locations prior to, during, and following the detonations; determining the distances from the detonations to which fish kills and injuries were affected by the anchored fish cage technique; and collecting the dead and stunned fish following each detonation. The basic objective was to determine the effects of the detonations on the marine environment of Kawaihae Bay.

One hundred eleven different species representing 34 families of marine fishes were found at the project site through underwater observations by divers and through collections of dead and injured fishes after the detonations. Of the 76 species that were recorded by the divers, 37 were not found during postdetonation collections, and conversely, 35 of the 74 species found during postdetonation collection activities were not observed during the underwater observations. These discrepancies were attributed to the limitations inherent in the observation and collection methods that were employed.

For the large detonations of Phase II, the distances to which all fish in fish cages were killed were 100 ft for Detonation II-ABCD, 120 ft for Detonation II-IJKL, and 210 ft from Detonation II-EF. The maximum distance to which any fish were killed or injured probably did not exceed 300 ft on any of the three above detonations.

As estimated from the collections made following the detonations the families of fishes most affected within the area of dead and injured fish were squirrelfish, butterfly fish, damselfish, surgeonfish, cardinal fish, and the puffer. Not all fishes collected following the detonations were dead. Some were just stunned. As a test, a live but stunned

Table 18. Summary of data for four underwater observations in pounds of fish per acre of reef area.

Station	Date of observation			
	Sept 1969	3 Nov 1969	27 Apr 1970	4 June 1970
1	21.7	—	—	66.5
2	30.6	—	—	292.9
3	87.8	—	90.0	57.1
4	101.1	266.8	—	76.4
5	44.5	—	—	—
6	84.4	85.4	45.8	56.2
7	93.8	—	—	6.5
8	97.2	455.2	—	93.8
9	50.6	—	—	—
10	62.5	—	—	—
11	17.1	—	—	—
Average for each observation:	62.8	265.8	67.9	92.8
Average for common stations surveyed during first and last observations	73.8	—	—	92.8

fish that was picked up was kept in a tank for several weeks and appeared to be in good health at the end of that time.

A summary of the data from the four underwater observations conducted is given in Table 18 in terms of total pounds of fish per acre of reef area. As can be seen the data are extremely variable making it impossible to draw definitive conclusions. However, the data do indicate that segments of the project site still containing corals (i.e., immediately adjacent to the blasted channel and berthing basin) are being rapidly repopulated from adjacent unaffected areas. The detonations altered the immediate areas of the channel and berthing basin from one of clear water and hard, coral bottoms to one containing a silt bottom and murky waters similar to what was found at the Phase I detonation site prior to the blasts. It is suspected that the final species composition and density in these areas will reflect the changes that were incurred in the habitat.

Section 5
Seismic- and Structural-Motion Measurements

PROGRAM OBJECTIVES

The objective of this technical program during the Phase I seismic calibration series was to provide seismic-motion and and structural-response data as a function of yield, range, and DOB, specific to the site that could be used to estimate the maximum safe yield for detonations during Phase II.

A comprehensive seismic-motion measurement and structures-response program was also undertaken during Phase II. The objective was to verify safety predictions and to provide seismic-motion and structural-response data as a function of range and firing conditions.

Thirteen locations were instrumented during both phases of the program; i.e., during the period 13 October to 12 November 1969 for Phase I, and 10 April to 5 May 1970, for Phase II. The locations instrumented during Phase II differed slightly from those in Phase I reflecting more definitive predictions for the more vulnerable structures. During the analysis phase of the seismic-motion and structural-response program, the U.S. Army Engineer Waterways Experiment Station (WES) was delegated the prime responsibility for ground-motion data interpretation and John A. Blume & Associates was contracted to analyze structural-response data. WES provided pertinent raw data to John A. Blume & Associates.

EXPERIMENTAL PROCEDURES

Station Locations

Following a survey of structures surrounding the site (see Section 6) and prior to the execution of Phase I, personnel of John A. Blume & Associates, NCG, and WES made a reconnaissance trip to determine the location of the 13 measurement

stations. The criteria for instrumenting a location included the specific structure's vulnerability to possible architectural or structural damage, the predicted motion at the location, and the cost of repairing any possible damage. The project criteria were that no damage would be incurred that could be avoided, and injury to any members of the public was unacceptable. Therefore, all locations were instrumented where predicted motions for Phase II were of such a magnitude as to possibly cause damage or injury, or to incur repair costs.

As a result of data obtained during the Phase I program, a few changes were made in the station locations for Phase II. Actual station locations for Phases I and II, respectively, are shown in Figs. 110 and 111. Those stations identified as GM are ground-motion stations and those identified as SR are structural-response stations. Each station consisted of three sensors oriented in an orthogonally triaxial array resulting in 39 active data channels. The approximate distances of the stations from SGZ are given in Tables 19 and 20. Figures 112 through 123 show some of the instruments in place and their general location and surroundings.

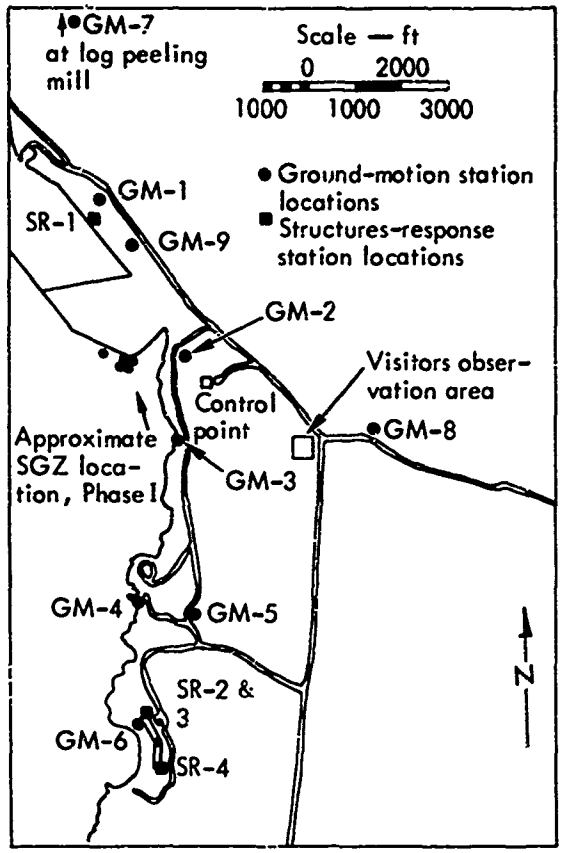

Fig. 110. Seismic station locations, Phase I.

Instrumentation

The three orthogonally triaxial ground-motion transducers at each station were oriented to measure the vertical component of motion and two horizontal components radial and transverse with respect to SGZ. The structural-response transducers measuring motion parallel to the long axis of the specific structure rather than along a radius to SGZ, with the others orthogonal to it to facilitate structure analysis.

All data were recorded on direct-write oscillographs. Selected structural-response stations were also recorded on magnetic tape. All transducers used during both phases of Project Tugboat were of the moving-coil velocity tape. Two sensitivity ranges were used because of the anticipated spread in motion amplitudes. The less-sensitive instruments strategically placed in large-motion areas were MB type 120 sensors with a natural frequency of 2.5 Hz, sensitivity 96.3 MV/in./sec, damping 65%, and a coil impedance of 650 Ω. The highly sensitive units, located in regions of low amplitude, were Type HS-10-1 sensors with a natural

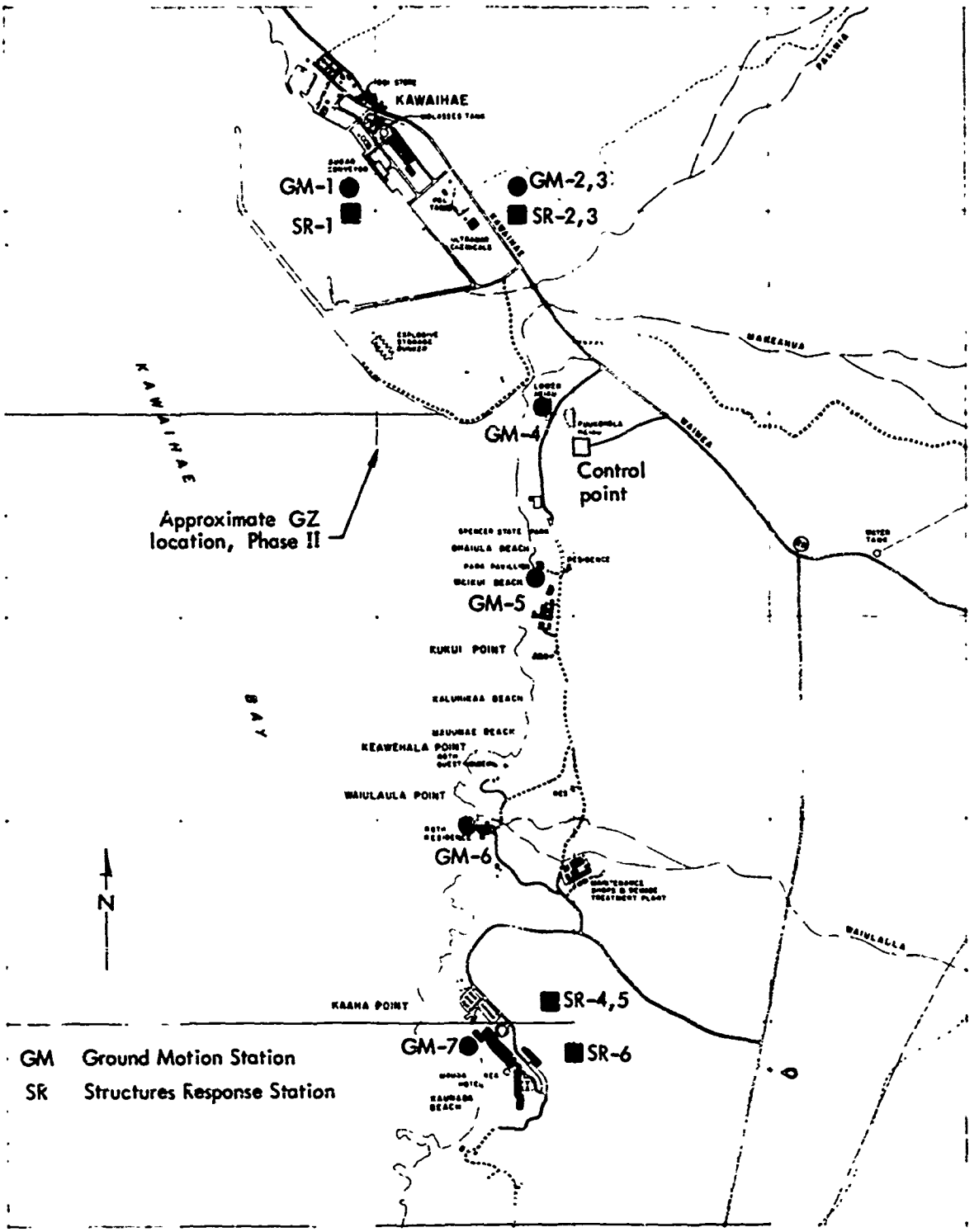

Fig. 111. Seismic station locations, Phase II.

Table 19. Location of Phase I seismic stations.

Station No. and location[a]		Recorder location	Approximate station distance from SGZ: Alpha, Bravo, Charlie, and Delta (ft)	(km)	Echo (ft)	(km)
GM-1	Molasses tank	Terminal warehouse	3,620	1.11	3,360	1.03
GM-2	Puukuhola heiau	Control point	1,460	0.45	1,860	0.57
GM-3	Spencer Park pavilion	Control point	1,940	0.59	2,350	0.72
GM-4	Roth home	Control point	4,860	1.48	5,120	1.56
GM-5	Mauan Kea sewage plant	Control point	5,425	1.66	5,760	1.76
GM-6	Mauna Kea Hotel foundation	Mauna Kea Hotel roof	7,320	2.24	7,540	2.30
GM-7	Plywood mill	Self-contained	8,200	2.50	8,200	2.50
GM-8	Water tank	Self-contained	5,420	1.65	5,880	1.80
GM-9	Ultramar warehouse foundation	Self-contained	2,520	0.77	2,420	0.74
SR-1	Sugar conveyor	Terminal warehouse	3,070	0.94	2,800	0.85
SR-2	Mauna Kea Hotel north roof	Mauna Kea Hotel roof	7,260	2.22	7,480	2.28
SR-3	Mauna Kea Hotel second floor	Mauna Kea Hotel roof	7,260	2.22	7,480	2.28
SR-4	Mauna Kea Hotel south roof	Mauna Kea Hotel roof	7,860	2.40	8,130	2.48

[a]GM denotes a ground-motion station; SR denotes structural-response station.

Table 20. Location of Phase II seismic stations.

Station No. and location[a]		Recorder location	Approximate station distance from SGZ: II-ABCD (ft)	(km)	II-EF (ft)	(km)	II-IJKL (ft)	(km)
GM-1	Terminal facility	Terminal warehouse	3,400	1.04	2,970	0.91	2,760	0.84
GM-2	200 ft from Ultramar	Ultramar warehouse	3,050	0.93	2,620	0.80	2,540	0.77
GM-3	Ultramar warehouse foundation	Ultramar warehouse	3,130	0.95	2,720	0.83	2,620	0.80
GM-4	Puukuhola heiau	Self-contained	2,420	0.74	2,220	0.68	2,500	0.76
GM-5	Spencer Park pavilion	Self-contained	2,360	0.72	2,480	0.76	2,850	0.87
GM-6	Roth home	Self-contained	4,630	1.41	5,000	1.53	5,300	1.62
GM-7	Mauna Kea Hotel foundation	Mauna Kea Hotel roof	7,200	2.20	7,400	2.26	7,680	2.34
SR-1	Sugar conveyor	Terminal warehouse	3,400	1.04	2,970	0.91	2,760	0.84
SR-2	Ultramar warehouse corner roof[b]	Ultramar warehouse	3,080	0.94	2,630	0.80	2,560	0.78
SR-3	Ultramar warehouse center roof	Ultramar warehouse	3,150	0.96	2,700	0.82	2,620	0.80
SR-4	Mauna Kea Hotel second floor	Mauna Kea Hotel roof	6,960	2.12	7,350	2.24	7,620	2.32
SR-5	Mauna Kea Hotel north roof	Mauna Hotel Hotel roof	6,960	2.12	7,350	2.24	7,620	2.32
SR-6	Mauna Kea Hotel south roof	Mauna Kea Hotel roof	7,610	2.30	7,990	2.44	8,300	2.53

[a]GM denotes a ground-motion station; SR denotes structural-response station.

[b]Station SR-2 was relocated from SW to SE roof corner after Detonation II-ABCD.

Table 19. Location of Phase I seismic stations.

Station No. and location[a]		Recorder location	Approximate station distance from SGZ: Alpha, Bravo, Charlie, and Delta (ft)	(km)	Echo (ft)	(km)
GM-1	Molasses tank	Terminal warehouse	3,620	1.11	3,360	1.03
GM-2	Puukuhola heiau	Control point	1,460	0.45	1,860	0.57
GM-3	Spencer Park pavilion	Control point	1,940	0.59	2,350	0.72
GM-4	Roth home	Control point	4,860	1.48	5,120	1.56
GM-5	Mauan Kea sewage plant	Control point	5,425	1.66	5,760	1.76
GM-6	Mauna Kea Hotel foundation	Mauna Kea Hotel roof	7,320	2.24	7,540	2.30
GM-7	Plywood mill	Self-contained	8,200	2.50	8,200	2.50
GM-8	Water tank	Self-contained	5,420	1.65	5,880	1.80
GM-9	Ultramar warehouse foundation	Self-contained	2,520	0.77	2,420	0.74
SR-1	Sugar conveyor	Terminal warehouse	3,070	0.94	2,800	0.85
SR-2	Mauna Kea Hotel north roof	Mauna Kea Hotel roof	7,260	2.22	7,480	2.28
SR-3	Mauna Kea Hotel second floor	Mauna Kea Hotel roof	7,260	2.22	7,480	2.28
SR-4	Mauna Kea Hotel south roof	Mauna Kea Hotel roof	7,860	2.40	8,130	2.48

[a]GM denotes a ground-motion station; SR denotes structural-response station.

Table 20. Location of Phase II seismic stations.

Station No. and location[a]		Recorder location	Approximate station distance from SGZ: II-ABCD (ft)	(km)	II-EF (ft)	(km)	II-IJKL (ft)	(km)
GM-1	Terminal facility	Terminal warehouse	3,400	1.04	2,970	0.91	2,760	0.84
GM-2	200 ft from Ultramar	Ultramar warehouse	3,050	0.93	2,620	0.80	2,540	0.77
GM-3	Ultramar warehouse foundation	Ultramar warehouse	3,130	0.95	2,720	0.83	2,620	0.80
GM-4	Puukuhola heiau	Self-contained	2,420	0.74	2,220	0.68	2,500	0.76
GM-5	Spencer Park pavilion	Self-contained	2,360	0.72	2,480	0.76	2,850	0.87
GM-6	Roth home	Self-contained	4,630	1.41	5,000	1.53	5,300	1.62
GM-7	Mauna Kea Hotel foundation	Mauna Kea Hotel roof	7,200	2.20	7,400	2.26	7,680	2.34
SR-1	Sugar conveyor	Terminal warehouse	3,400	1.04	2,970	0.91	2,760	0.84
SR-2	Ultramar warehouse corner roof[b]	Ultramar warehouse	3,080	0.94	2,630	0.80	2,560	0.78
SR-3	Ultramar warehouse center roof	Ultramar warehouse	3,150	0.96	2,700	0.82	2,620	0.80
SR-4	Mauna Kea Hotel second floor	Mauna Kea Hotel roof	6,960	2.12	7,350	2.24	7,620	2.32
SR-5	Mauna Kea Hotel north roof	Mauna Hotel Hotel roof	6,960	2.12	7,350	2.24	7,620	2.32
SR-6	Mauna Kea Hotel south roof	Mauna Kea Hotel roof	7,610	2.30	7,990	2.44	8,300	2.53

[a]GM denotes a ground-motion station; SR denotes structural-response station.

[b]Station SR-2 was relocated from SW to SE roof corner after Detonation II-ABCD.

Fig. 112. Heiau ground-motion station, Phases I and II.

frequency of 1.0 Hz, sensitivity 7.7 V/in./sec, damping 70% and a coil impedance of 4100 Ω.

Transducers were installed at each seismic station as dictated by the physical characteristics of the specific station. On all of the structures, sensors were affixed using a special type of nonhardening modeling clay to adhere the unit to the structure. This technique has been proven effective on numerous occasions. Some of the ground-motion stations were buried approximately 2 ft below ground surface. In all cases the sensors were sheltered in some way to minimize wind noise. Transducer usage, recording technique, and placement are summarized in Tables 21 and 22.

It was necessary to maintain several recording stations during both test phases, because the seismic instruments were scattered over a wide area. Two of the recording stations monitored twelve transducers or four stations each, one monitored six transducers or two stations, and the remaining three stations were self-contained, portable recording units, each capable of monitoring three transducers.

Radio communications were maintained between the Tugboat control point and each of the recording stations during the test program. A voice channel on the tape recorders was used to record the verbal countdown and all postshot remarks. Tape recorders were started at -1 min and stopped at +2 min. Ocillographs were started at -30 sec and stopped at +1 min at all recording stations. All data channels were calibrated before and after each event.

PREDICTIONS

Predictions for peak amplitudes expected for the Project Tugboat Phase I detonations were based on ground motions recorded during the Dugout[16] 100-ton row-charge event in basalt at the Nevada Test Site and the Pre-Gondola[17] experiments in clay shale at Fort Peck, Montana. A general prediction of peak particle velocity by station was made for three separate yields bracketing the yields anticipated for the entire project. Specific predictions for Phase I are shown in Table 23 and plotted in Figure 124.

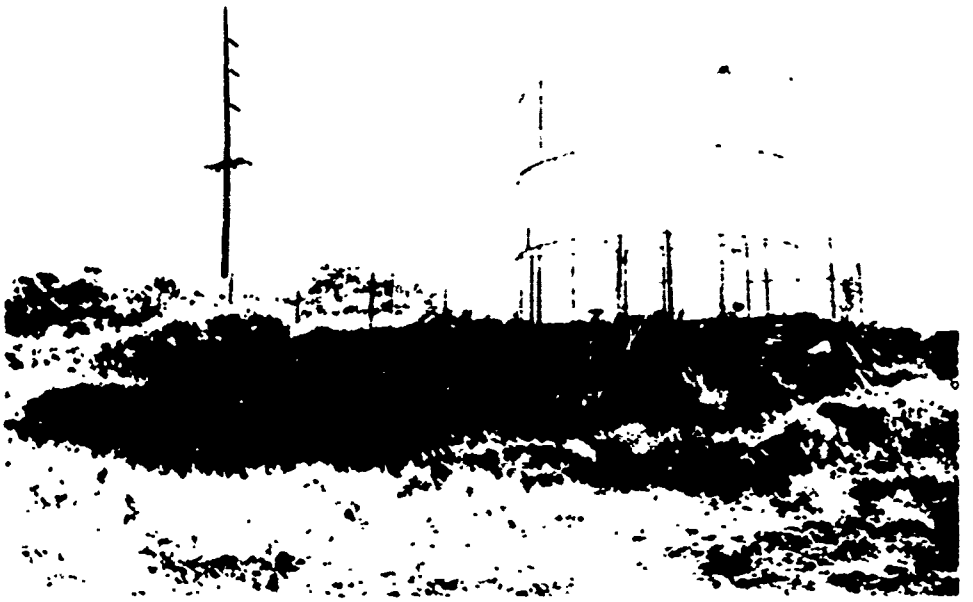

Fig. 113. Water tank ground-motion station, Phase I.

Fig. 114. Roth home instruments, Phases I and II.

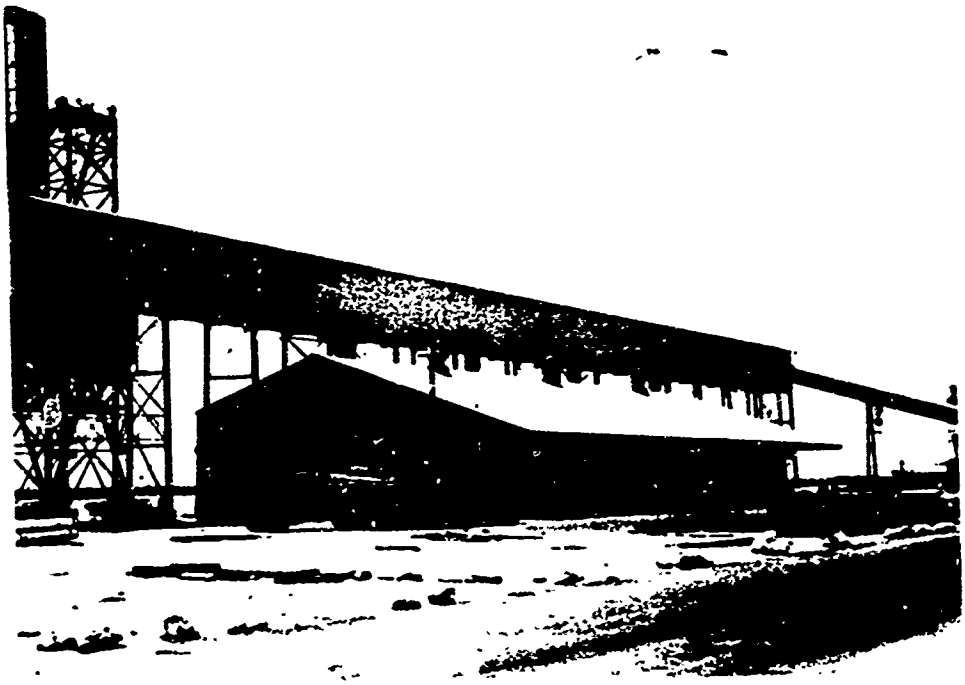

Fig. 115. Sugar conveyor and terminal facility, Phases I and II.

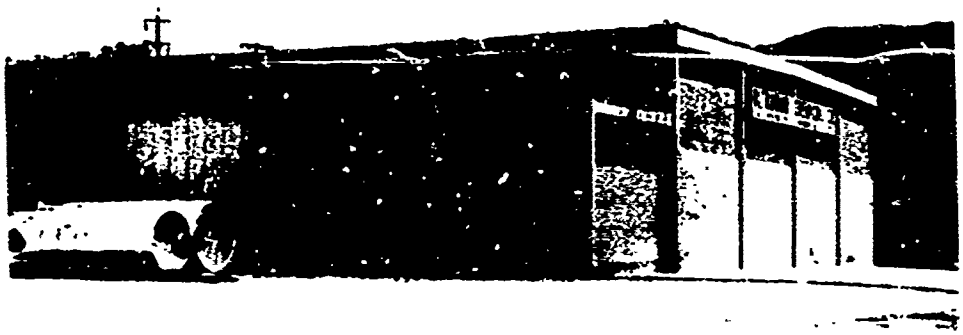

Fig. 116. Ultramar warehouse, Phases I and II.

Fig. 117. Instruments installed at center and corner of roof of Ultramar warehouse, Phase II.

Fig. 118. Spencer Park pavilion instruments, Phases I and II.

After the conduct of Phase I and a new program concept for Phase II was developed, the data obtained during Phase I was used as the sole input for amplitude predictions during Phase II. The predictions shown in Table 24 were made by station and component. These predictions utilized a yield scaling factor of $W^{0.54}$ based upon differences in amplitudes noted during the 1-ton and 10-ton events. This factor proved to be quite accurate as discussed later in this section.

RESULTS

As previously stated, all data were recorded on oscillographs with certain selected stations simultaneously recorded on magnetic tape. Immediately after each event in Phases I and II, the data were

Fig. 119. Close-up of model clay bonding used on lava at Spencer Park pavilion, Phases I and II.

Fig. 120. Promenade of Mauna Kea Beach Hotel (instruments installed behind middle column on right) Phases I and II.

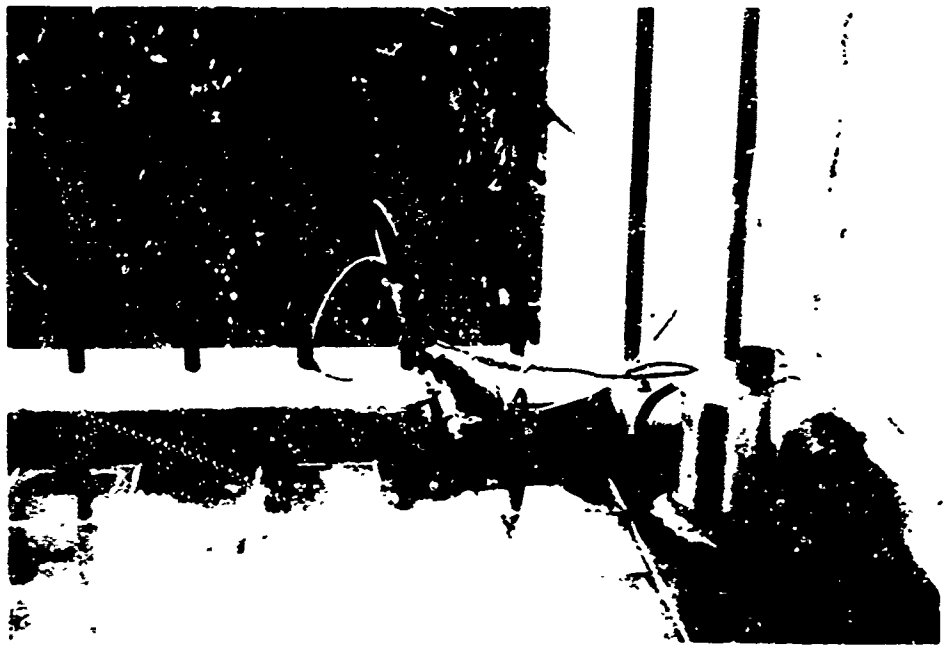

Fig. 121. Second floor station at Mauna Kea Beach Hotel, Phases I and II.

Fig. 122. North roof station at Mauna Kea Beach Hotel, Phases I and II.

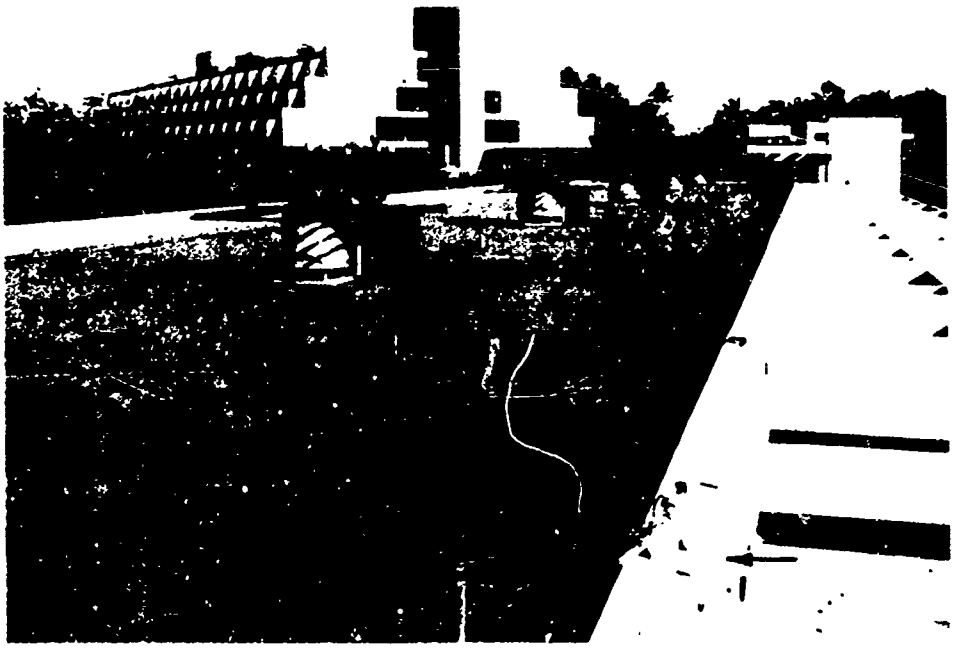

Fig. 123. South roof station at Mauna Kea Beach Hotel, Phases I and II.

Table 21. Installation of sensors for Phase I.

Station location	Recording method	Transducer type: Alpha, Bravo, Charlie, and Delta	Transducer type: Echo	Placement technique
GM-1	Oscillograph	HS-10-1	120	Model clay to concrete slab
GM-2	Oscillograph	HS-10-1	120	Buried at west base of heiau
GM-3	Oscillograph	HS-10-1	120	Model clay to lava
GM-4	Oscillograph	HS-10-1	HS-10-1	Model clay to foundation
GM-5	Oscillograph	HS-10-1	HS-10-1	Buried north side of plant
GM-6	Oscillograph and magnetic tape	HS-10-1	HS-10-1	Buried at column foundation
GM-7	Oscillograph	HS-10-1	HS-10-1	Model clay to foundation slab
GM-8	Oscillograph	HS-10-1	HS-10-1	Buried near tank
GM-9	Oscillograph	HS-10-1	HS-10-1	Model clay to foundation slab
SR-1	Oscillograph	120[a]	120	Model clay to conveyor structure
SR-2	Oscillograph and magnetic tape	HS-10-1	HS-10-1	Model clay to NW corner of hotel roof
SR-3	Oscillograph and magnetic tape	HS-10-1	HS-10-1	Model clay to second floor of hotel
SR-4	Oscillograph and magnetic tape	HS-10-1	HS-10-1	Model clay to south roof of hotel

[a]Type 120 used for Alpha, Bravo, and Delta events; HS-10-1 used for Charlie event (first detonation).

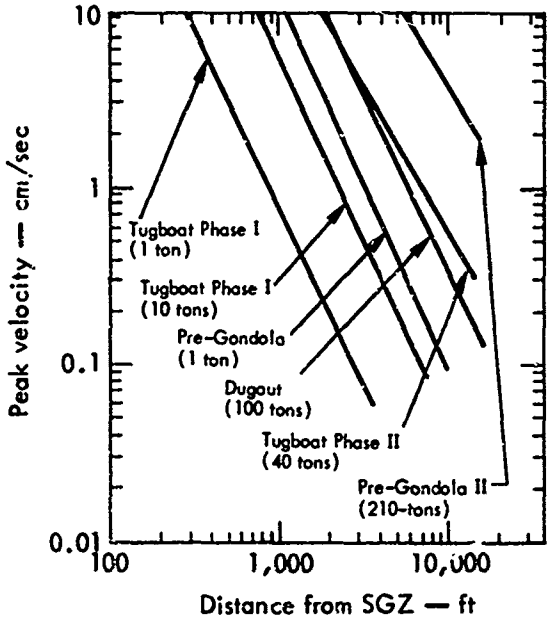

Fig. 124. Project Tugboat ground-motion predictions.

taker om the oscillograph records, tabulated, and plotted for a preliminary data review during the experiment. These data, while reasonably accurate, were yet to be critically reviewed and checked. Visual playbacks of the tape recordings were later made to confirm data quality. Data recovery for the entire series was 100%. It should be stated, however, that after noting that signal levels were higher than predicted, calibration amplitudes and oscillograph paper speed were adjusted following the first event (Charlie) in Phase I to make a more presentable visual display.

All data were reduced from zero to peak amplitude to conform with data collected during previous chemical explosive excavation experiments. This was accomplished by scribing a static trace along the zero axis of each active data channel, then scaling from this reference to the highest amplitude recorded. This results in a transient peak particle velocity.

All data are tabulated in Tables 25 and 26 for Phases I and II, respectively, in both English and metric units. Since WES instrumentation was calibrated in terms of English units, certain values given in this report were more conducive to presentation in English rather than metric units.

ANALYSIS AND INTERPRETATION

The factors of signal attenuation with distance, and yield scaling, as they relate to seismic motion, are discussed in this section. Data from both phases were combined for this analysis. However, ground-motion stations only were considered in the interpretation of seismic-site characteristics. The structural-response analysis is recognized to be dependent upon seismic site characteristics from the standpoint of ground-motion input to the foundation. The structural-response analysis is treated in a separate study in Section 6.

Attenuation

The maximum velocity amplitudes recorded at various ground-motion seismic stations during both Phases I and II of Project Tugboat are shown as a function of distance from SGZ in Figs. 125 through 133. Maximum peak particle velocities recorded during the 1-ton events ranged from about 1.5 cm/sec at a distance of about 1500 ft to about 0.1 cm/sec at a distance of 8200 ft. Data recorded during the 10-ton event ranged from about 4 cm/sec at a distance of about 1800 ft to about 0.4 cm/sec at a distance of about 8000 ft.

Table 22. Installation of sensors for Phase II.

Station location	Record method	Transducer type	Placement technique
GM-1	Oscillograph	120	Model clay to terminal foundation
GM-2	Oscillograph and magnetic tape	HS-10-1	Buried 200 ft SW of warehouse
GM-3	Oscillograph and magnetic tape	HS-10-1	Model clay to foundation in warehouse office
GM-4	Oscillograph	120	Buried at west base of heiau
GM-5	Oscillograph	HS-10-1	Model clay to lava
GM-6	Oscillograph	HS-10-1	Model clay to foundation
GM-7	Oscillograph and magnetic tape	HS-10-1	Buried at column foundation
SR-1	Oscillograph	120	Model clay to conveyor structure
SR-2[a]	Oscillograph and magnetic tape	HS-10-1	Model clay to corner of warehouse roof
SR-3	Oscillograph and magnetic tape	HS-10-1	Model clay to center of warehouse roof
SR-4	Oscillograph and magnetic tape	HS-10-1	Model clay to second floor of hotel
SR-5	Oscillograph and magnetic tape	HS-10-1	Model clay to NW corner of hotel roof
SR-6	Oscillograph and magnetic tape	HS-10-1	Model clay to south roof of hotel

[a]Relocated from SW to SE roof corner after Detonation II-ABCD.

Table 23. Structure- and ground-motion maximum amplitude velocity predictions, Project Tugboat Phase I.

Station No.	Maximum amplitude peak particle velocity				Frequency of maximum amplitude (Hz)
	1-ton events		10-ton event		
	(in./sec)	(cm/sec)	(in./sec)	(cm/sec)	
GM-1	0.026	0.066	0.18	0.460	5
GM-2	0.070	0.178	0.45	1.143	5
GM-3	0.066	0.168	0.46	1.168	5
GM-4	0.014	0.036	0.10	0.254	5
GM-5	0.010	0.025	0.07	0.178	5
GM-6	0.006	0.015	0.04	0.102	5
GM-7	0.007	0.018	0.05	0.127	5
GM-8	0.009	0.023	0.06	0.152	5
GM-9	0.056	0.142	0.39	0.991	5
SR-1	0.057	0.145	0.41	1.041	3
SR-2	0.009	0.023	0.06	0.152	3
SR-3	0.009	0.023	0.06	0.152	3
SR-4	0.009	0.023	0.06	0.152	3

Table 24. Structure- and ground-motion predictions, Project Tugboat Phase II (40-ton event).

Station location	Component	Peak particle velocity, Maximum amplitude (in./sec)	Peak particle velocity, Maximum amplitude (cm/sec)	Prime frequency (Hz)
GM-1	Vertical	1.10	2.79	3-4
	Radial	1.10	2.79	3-4
	Transverse	1.00	2.54	3-4
GM-2	Vertical	1.86	4.72	3-4
	Radial	0.97	2.46	3-4
	Transverse	1.15	2.92	3-4
GM-3	Vertical	1.86	4.72	3-4
	Radial	0.97	2.46	3-4
	Transverse	1.15	2.92	3-4
GM-4	Vertical	3.00	7.62	3-4
	Radial	2.30	5.84	3-4
	Transverse	3.45	8.76	3-4
GM-5	Vertical	0.74	1.88	3-4
	Radial	0.51	1.30	3-4
	Transverse	0.16	0.41	3-4
GM-6	Vertical	0.37	0.94	3-4
	Radial	0.22	0.56	3-4
	Transverse	0.21	0.53	3-4
GM-7	Vertical	0.23	0.58	3-4
	Radial	0.14	0.36	3-4
	Transverse	0.12	0.30	3-4
SR-1	Vertical	0.74	1.88	3-4
	Radial	2.53	6.43	3-4
	Transverse	6.00	15.24	3-4
SR-2	Vertical	3.00	7.62	3-4
	Radial	1.94	4.93	3-4
	Transverse	2.30	5.84	3-4
SR-3	Vertical	3.00	7.62	3-4
	Radial	0.97	2.46	3-4
	Transverse	1.15	2.92	3-4
SR-4	Vertical	0.25	0.64	3-4
	Radial	0.30	0.76	3-4
	Transverse	0.37	0.94	3-4
SR-5	Vertical	0.62	1.57	3-4
	Radial	0.92	2.34	3-4
	Transverse	0.60	1.52	3-4
SR-6	Vertical	0.60	1.52	3-4
	Radial	0.60	1.52	3-4
	Transverse	0.76	1.93	3-4

Table 25. Structure- and ground-motion measurements during Phase I.

Station	Component[a]	Alpha			Bravo			Charlie			Delta			Echo		
		Frequency	Amplitude		Frequency	Amplitude		Frequency	Amplitude		Frequency	Amplitude		Frequency	Amplitude	
		(Hz)	(in./sec)	(cm/sec)	(Hz)	(in./sec)	(cm/sec)	(Hz)	(in./sec)	(cm/sec)	(Hz)	(in./sec)	(cm/sec)	(Hz)	(in./sec)	(cm/sec)
GM-1	V	14 and 4.5	0.063	0.160	14 and 4.5	0.062	0.160	14 and 4.5	0.070	0.174	14 and 4.5	0.087	0.221	14 and 4.0	0.220	0.560
	R	14 and 4.5	0.180	0.457	14 and 4.5	0.190	0.480	14 and 4.5	0.180	0.457	14 and 4.5	0.206	0.524	14 and 4.0	0.450	1.140
	T	14 and 4.5	0.102	0.259	14 and 4.5	0.100	0.250	14 and 4.5	0.110	0.279	14 and 4.5	0.125	0.314	14 and 4.0	0.290	0.740
GM-2	V	20 and 4.0	0.350	0.890	20 and 4.0	0.420	1.070	20 and 4.0	0.300*	0.760*	20 and 4.0	0.460	1.170	20 and 4.0	1.300	3.300
	R	20 and 4.0	0.530	1.350	20 and 4.0	0.490	1.240	20 and 4.0	0.300*	0.760*	20 and 4.0	0.460	1.170	20 and 4.0	1.000	2.540
	T	20 and 4.0	0.410	1.040	20 and 4.0	0.470	1.190	20 and 4.0	0.300*	0.760*	20 and 4.0	0.440	1.120	20 and 4.0	1.500	3.810
GM-3	V	14 and 4.0	0.170	0.430	14 and 4.0	0.165	0.420	14 and 4.0	0.200	0.510	14 and 4.0	0.200	0.510	14 and 4.0	0.320	0.810
	R	14 and 4.0	0.100	0.250	14 and 4.0	0.100	0.250	14 and 4.0	0.110	0.280	14 and 4.0	0.110	0.280	14 and 4.0	0.220	0.560
	T	14 and 4.0	0.035	0.089	14 and 4.0	0.039	0.100	14 and 4.0	0.034	0.086	14 and 4.0	0.036	0.092	14	0.070	0.180
GM-4	V	14 and 4.0	0.049	0.124	14 and 4.0	0.050	0.130	14 and 4.0	0.055	0.140	14 and 4.0	0.060	0.152	14 and 2.5	0.160	0.410
	R	14 and 4.0	0.026	0.066	14 and 4.0	0.027	0.070	14 and 4.0	0.027	0.069	14 and 4.0	0.032	0.081	14 and 2.5	0.095	0.240
	T	14 and 4.0	0.017	0.043	14 and 4.0	0.017	0.043	14 and 4.0	0.027	0.069	14 and 4.0	0.023	0.058	14 and 2.5	0.090	0.230
GM-5	V	14 and 3.0	0.042	0.107	14 and 3.0	0.047	0.119	14 and 3.0	0.045	0.114	14 and 3.0	0.055	0.140	14 and 2.5	0.190	0.480
	R	14 and 3.0	0.022	0.056	14 and 3.0	0.025	0.064	14 and 3.0	0.023	0.058	14 and 3.0	0.027	0.069	14 and 2.5	0.083	0.210
	T	14 and 3.0	0.014	0.036	14 and 3.0	0.017	0.043	14 and 3.0	0.012	0.030	14 and 3.0	0.024	0.061	14 and 2.5	0.070	0.180
GM-6	V	14 and 3.0	0.034	0.086	14 and 3.0	0.033	0.084	14 and 3.0	0.030	0.076	14 and 3.0	0.042	0.107	3	0.100	0.250
	R	14 and 3.0	0.011	0.028	14 and 3.0	0.012	0.030	14 and 3.0	0.013	0.033	14 and 3.0	0.014	0.036	3	0.060	0.150
	T	14 and 3.0	0.011	0.028	14 and 3.0	0.011	0.028	14 and 3.0	0.012	0.030	14 and 3.0	0.015	0.038	3	0.050	0.130
GM-7	V	15 and 3.0	0.025	0.064	15 and 3.0	0.026	0.066	15 and 3.0	0.029	0.074	15 and 3.0	0.035	0.089	15 and 3.0	0.150	0.380
	R	15 and 3.0	0.032	0.081	15 and 3.0	0.044	0.112	15 and 3.0	0.030	0.076	15 and 3.0	0.049	0.124	15 and 3.0	0.210	0.530
	T	15 and 3.0	0.018	0.046	15 and 3.0	0.017	0.043	15 and 3.0	0.024	0.061	15 and 3.0	0.029	0.051	15 and 3.0	0.080	0.200
GM-8	V	14 and 3.0	0.080	0.203	14 and 3.0	0.084	0.210	14 and 3.0	0.086	0.218	14 and 3.0	0.090	0.228	14 and 3.0	0.270	0.690
	R	14 and 3.0	0.050	0.135	14 and 3.0	0.057	0.145	14 and 3.0	0.080	0.203	14 and 3.0	0.060	0.152	14 and 3.0	0.230	0.580
	T	14 and 3.0	0.040	0.102	14 and 3.0	0.042	0.110	14 and 3.0	0.040	0.102	14 and 3.0	0.045	0.114	14 and 3.0	0.150	0.380
GM-9	V	30 and 4.0	0.112	0.284	30 and 4.0	0.145	0.370	30 and 4.0	0.140	0.356	30 and 4.0	0.170	0.432	30 and 4.0	0.810	2.060
	R	20 and 3.0	0.090	0.228	20 and 3.0	0.095	0.240	20 and 3.0	0.098	0.249	20 and 3.0	0.136	0.346	20 and 3.0	0.420	1.070
	T	20 and 3.0	0.190	0.482	20 and 3.0	0.200	0.510	20 and 3.0	0.190	0.483	20 and 3.0	0.200	0.508	20 and 3.0	0.500	1.270
SR-1	V	15 and 3.2	0.080	0.200	15 and 3.2	0.100	0.250	15 and 3.2	0.020[b] 0.090	0.228	15 and 3.2	0.120	0.305	15 and 3.0	0.320	0.810
	R	15 and 3.2	0.360	0.910	15 and 3.2	0.430	1.090	15 and 3.2	0.070 0.300	0.762	15 and 3.2	0.400	1.010	15 and 3.0	1.100	2.790
	T	15 and 3.2	1.400	3.560	15 and 3.2	1.500	3.810	15 and 3.2	0.120 1.000*	2.540*	15 and 3.2	1.500*	3.810*	15 and 3.0	2.600	6.600
SR-2	V	14 and 3.0	0.042	0.107	14 and 3.0	0.042	0.107	14 and 3.0	0.036	0.092	14 and 3.0	0.062	0.157	14 and 3.0	0.270	0.690
	R	14 and 3.0	0.090	0.228	14 and 3.0	0.115	0.292	14 and 3.0	0.096	0.244	14 and 3.0	0.105	0.266	3	0.400	1.020
	T	14 and 3.0	0.066	0.167	14 and 3.0	0.075	0.190	14 and 3.0	0.096	0.244	14 and 3.0	0.070	0.178	3	0.260	0.660
SR-3	V	14 and 3.0	0.038	0.097	14 and 3.0	0.046	0.117	14 and 3.0	--	--	14 and 3.0	0.044	0.109	3	0.110	0.280
	R	14 and 3.0	0.028	0.071	14 and 3.0	0.030	0.076	14 and 3.0	0.029	0.074	14 and 3.0	0.031	0.079	3	0.130	0.330
	T	14 and 3.0	0.037	0.094	14 and 3.0	0.046	0.117	14 and 3.0	0.041	0.104	14 and 3.0	0.052	0.132	3	0.160	0.410
SR-4	V	14 and 3.0	0.034	0.086	14 and 3.0	0.042	0.107	14 and 3.0	0.035	0.089	14 and 3.0	0.060	0.152	6 and 3.0	0.260	0.660
	R	14 and 3.0	0.036	0.097	14 and 3.0	0.036	0.091	14 and 3.0	0.040	0.102	14 and 3.0	0.050	0.127	6 and 3.0	0.260	0.660
	T	14 and 3.0	0.030	0.076	14 and 3.0	0.037	0.094	14 and 3.0	0.040	0.102	14 and 3.0	0.050	0.127	6 and 3.0	0.330	0.840

[a]V = Vertical, R = Radial; T = Transverse.
[b]Amplitude due to wind noise.

Table 26. Structure- and ground-motion measurements during Phase II.

Station	Component[a]	II-ABCD			II-EF			II-IJKL		
		Frequency	Amplitude		Frequency	Amplitude		Frequency	Amplitude	
		(Hz)	(in./sec)	(cm/sec)	(Hz)	(in./sec)	(cm/sec)	(Hz)	(in./sec)	(cm/sec)
CM-1	V	3	0.250	0.635	3	0.350	0.890	3	0.720	1.830
	R	3	0.420	1.070	3	0.360	0.920	3	0.900	2.280
	T	3	0.520	1.320	3	0.570	1.450	3	1.650	4.190
CM-2	V	3.5	0.680	1.720	3.5	0.890	2.260	3.5	2.400	6.100
	R	3.5	1.000	2.540	3.5	1.200	3.050	3.5	1.200	3.050
	T	3.5	0.410	1.040	3.5	1.800	4.550	3.5	2.050	5.210
CM-3	V	3.5	0.400	1.000	3.5	0.720	1.820	3.5	1.500	3.810
	R	3.5	0.560	1.420	3.5	0.750	1.900	3.5	1.150	2.920
	T	3.5	0.420	1.060	3.5	0.490	1.240	3.5	0.820	2.080
CM-4	V	3	1.100	2.790	3	1.500	3.800	3	1.800	4.570
	R	3	0.900	2.280	3	1.150	2.920	3	1.800	4.570
	T	3	0.800	2.030	3	1.000	2.540	3	1.300	3.300
CM-5	V	3	0.340	0.862	3	0.350	0.890	3	0.600	1.520
	R	3	0.300	0.761	3	0.300	0.760	3	0.550	1.400
	T	3	0.120	0.305	3	0.170	0.430	3	0.290	0.730
CM-6	V	3	0.200	0.509	3	0.200	0.510	3	0.450	1.140
	R	3	0.130	0.330	3	0.110	0.280	3	0.300	0.760
	T	3	0.110	0.279	3	0.120	0.305	3	0.240	0.610
CM-7	V	3	0.150	0.381	3	0.150	0.380	3	0.300	0.760
	R	3	0.075	0.190	3	0.070	0.180	3	0.150	0.380
	T	3	0.070	0.178	3	0.058	0.147	3	0.125	0.318
SR-1	V	3	0.320	0.812	3	0.450	1.140	3	0.900	2.280
	R	3	1.200	3.050	3	1.900	4.830	3	4.100	10.400
	T	3	1.300	3.310	3	2.300	5.850	3	3.100	7.880
SR-2	V	3.5	0.500	1.270	3.5	0.620	1.580	3.5	1.500	3.810
	R	3.5	1.800	4.560	3.5	1.300	3.300	3.5	2.100	5.340
	T	3.5	0.900	2.290	3.5	1.200	3.050	3.5	2.300	5.850
SR-3	V	3.5	0.500	1.270	3.5	0.700	1.780	3.5	1.400	3.550
	R	3.5	1.450	3.660	3.5	1.570	4.000	3.5	2.300	5.850
	T	3.5	1.000	2.540	3.5	1.180	3.000	3.5	2.100	5.340
SR-4	V	3	0.160	0.406	3	0.180	0.460	3	0.360	0.910
	R	3	0.150	0.380	3	0.150	0.380	3	0.250	0.630
	T	3	0.210	0.532	3	0.190	0.480	3	0.390	0.990
SR-5	V	3	0.200	0.509	3	0.220	0.560	3	0.550	1.400
	R	3	0.320	0.811	3	0.350	0.890	3	0.640	1.620
	T	4	0.220	0.559	4	0.200	0.510	4	0.580	1.470
SR-6	V	6	0.220	0.559	6	0.200	0.510	6	0.690	1.750
	R	6	0.290	0.737	6	0.150	0.380	6	0.630	1.600
	T	6	0.230	0.582	6	0.290	0.730	6	0.650	1.650

[a]V = Vertical; R = Radial; T = Transverse.

When one compares these values with the preshot predictions in Fig. 124, it will be seen that the predictions were low. Finally, 40-ton amplitudes diminished from about 6 cm/sec at a distance of approximately 2600 ft to about 0.8 cm/sec at a distance of approximately 7600 ft. These figures are in excellent agreement with the revised predictions made after Phase I.

The distance from SGZ was determined by aerial photographs and field surveys. However, distances used to plot data are approximate and were determined as follows:

(1) SGZ for all 1-ton events was assumed to be an imaginary point located in the center of the square formed by the four charges which were located at each corner.

(2) SGZ for all 40-ton row-charge events was assumed to be midway between the two center charges of each four-hole row.

(3) SGZ for the Phase II-JKL four-charge-cluster event was assumed

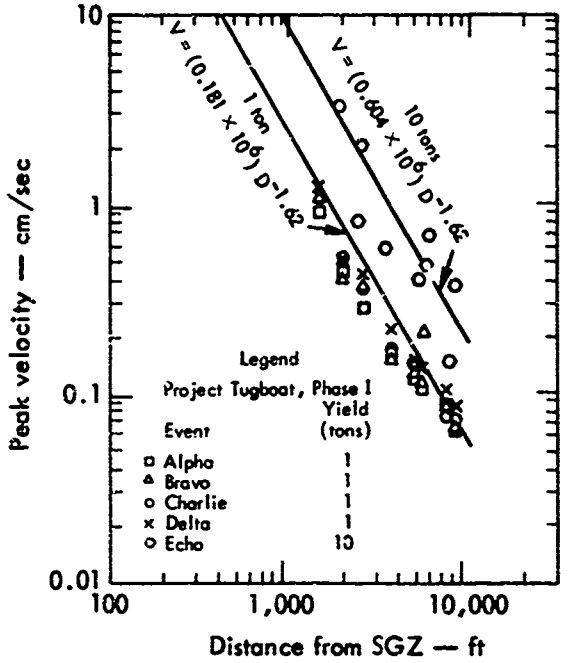

Fig. 125. Vertical peak particle velocity, Phase I.

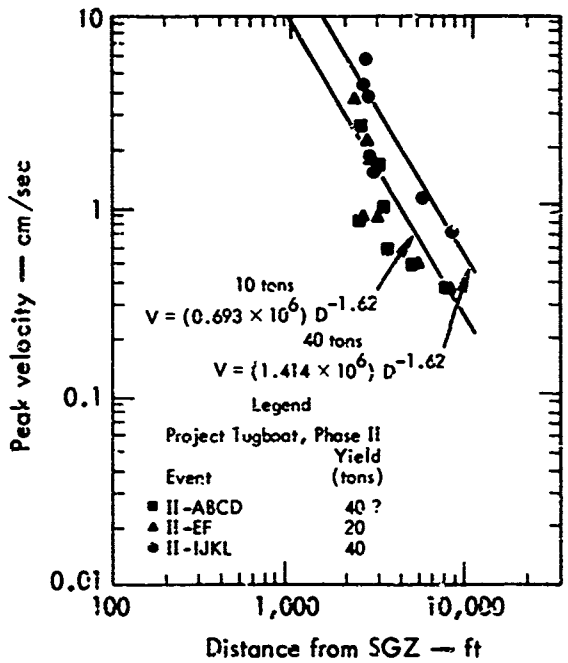

Fig. 126. Vertical peak particle velocity, Phase II.

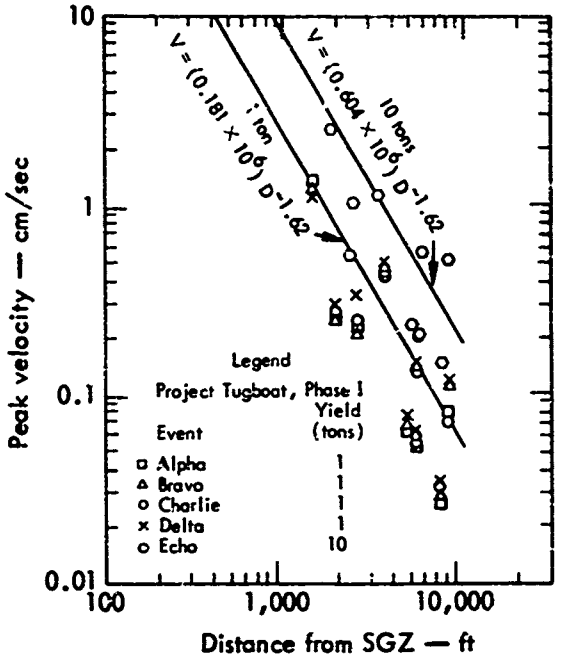

Fig. 127. Radial peak particle velocity, Phase I.

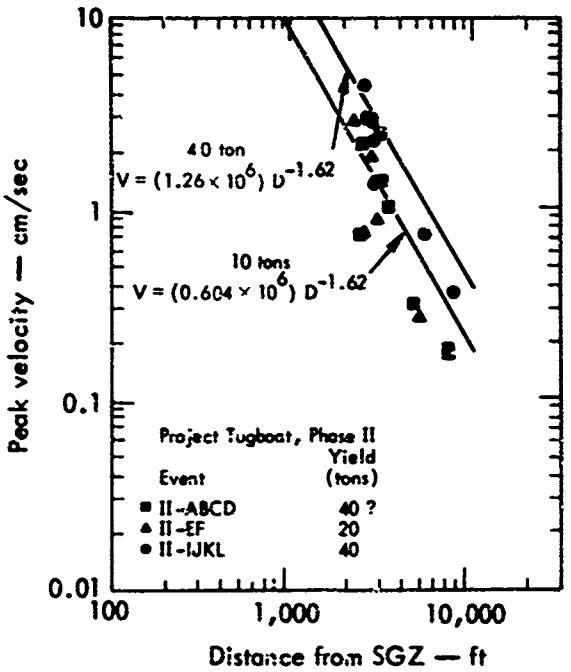

Fig. 128. Radial peak particle velocity, Phase II.

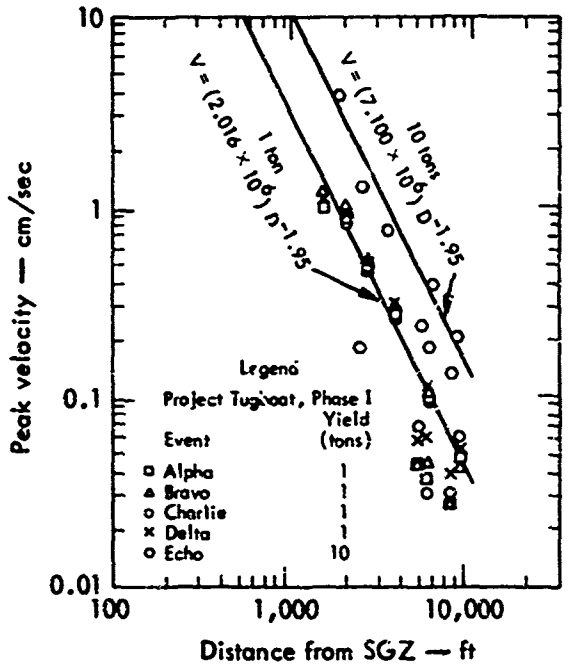

Fig. 129. Transverse peak particle velocity, Phase I.

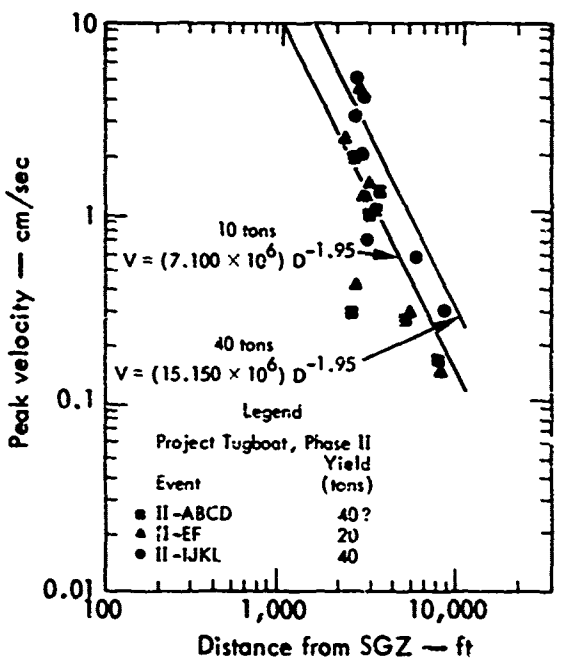

Fig. 130. Transverse peak particle velocity, Phase II.

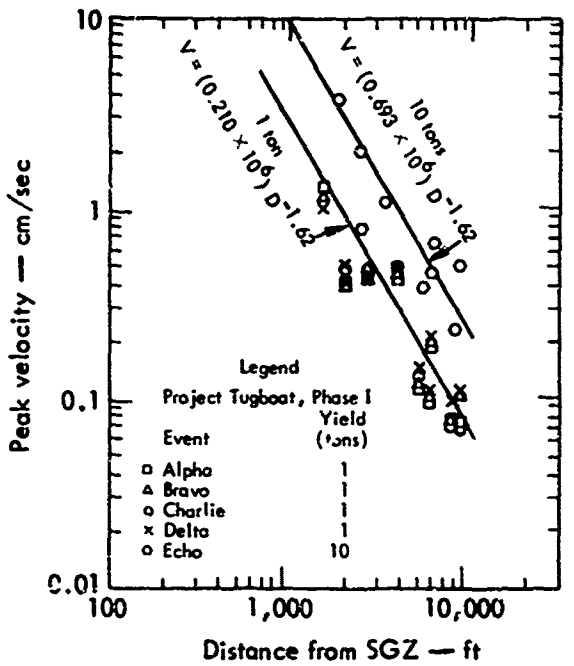

Fig. 131. Maximum peak particle velocity, Phase I.

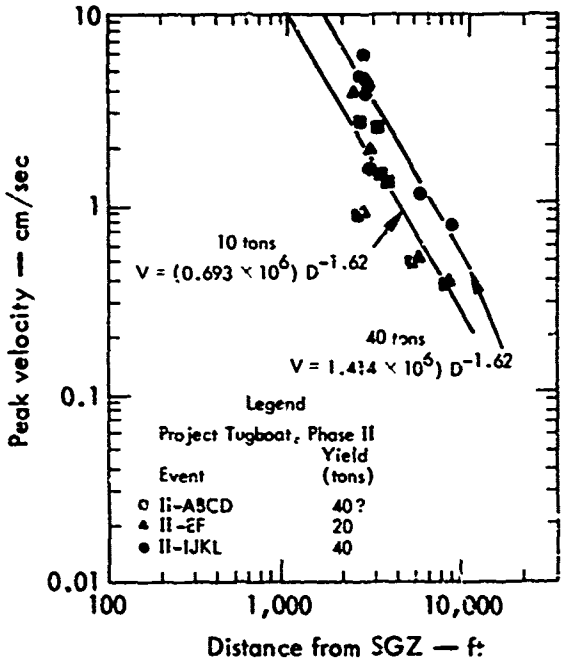

Fig. 132. Maximum peak particle velocity, Phase II.

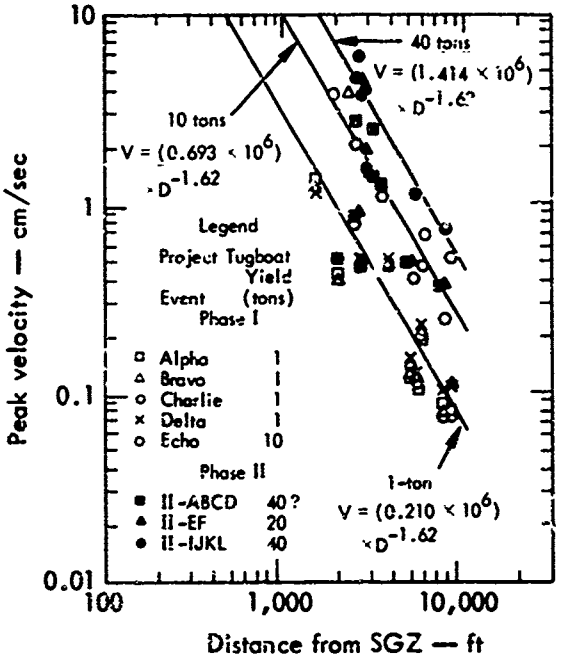

Fig. 133. Maximum peak particle velocity, Phases I and II.

to be an imaginary point located in the center of the square formed by the four charges located at each corner.

By inspection of Figs. 125 through 133, it will be seen that simple exponential decay gives a reasonable description of the attenuation of peak particle velocities with distance. This relationship appears to be descriptive of both individual component (vertical, radial, and transverse) and maximum velocities (largest component) recorded at each station. The amplitudes may be represented by an equation of the form:

$$V = aD^{-b} \qquad (12)$$

where

V = peak particle velocity at a distance D from SGZ

a = constant whose value is particle velocity intercept at unit distance

b = attenuation exponent and is the slope of line through data points on log-log coordinate graph

Vertical and radial mode particle velocities appear to be proportional to $D^{-1.62}$ for all yield levels. The transverse components appear to attenuate at a higher rate; e.e., $D^{-1.95}$. Maximum particle velocity decay also exhibits a slope of $D^{-1.62}$. The following equations of maximum particle velocity are from Fig. 133:

$$\text{(40-tons)}\quad V = (1.414 \times 10^6)D^{-1.62} \qquad (12a)$$

$$\text{(10-tons)}\quad V = (0.693 \times 10^6)D^{-1.62} \qquad (12b)$$

$$\text{(1-ton)}\quad V = (0.210 \times 10^6)D^{-1.62} \qquad (12c)$$

where

V = cm/sec

D = feet

It was observed that the seismic stations located at the Spencer Park pavilion and the Roth home consistently exhibited less motion than the norm defined by the above equations. Conversely, the motions measured at stations located at the molasses tank, 200 ft southwest of the Ultramar building, the water tank, and the plywood mill were usually slightly higher than the norm. These apparent anomalies can possibly be explained by the direction of deposition of the lava flows. Stations along the axis of flow, which is for practical purposes a continuous media, exhibited consistently higher amplitudes than those located normal to the flows. Numerous cracks and voids were visible

from the ground surface between flows and quite likely interrupted the wave traveling toward stations normal to the flows.

Yield Scaling

Several approaches were taken in the evaluation of a yield scaling[17] description of the Tugboat events. Assuming the applicability of an inverse power law attenuation, an expedient approach to the determination of yield scaling could be made on the basis of a cube root scaling applied to the attenuation exponent obtained from a single yield experiment. This method is described in Ref. 18. If it is assumed that:

$$V \propto \left(\frac{D}{W^{1/3}}\right)^{-b}, \tag{13}$$

then, equivalently,

$$V \propto W^{b/3}\, D^{-b}, \tag{13a}$$

where:

W = charge weight, tons,
b/3 = yield scaling exponent

The empirically derived value of b for the entire Tugboat experiment was 1.62, resulting in a yield scaling of 0.54. This method, while recognized as empirical, is presented because of its striking similarity to more conventional analysis approaches.

A second and considerably more reliable approach is to make a direct comparison of the seismic amplitudes (V_1, V_2) from two (or more) different yields (W_1, W_2). If recordings are made at the same location, then the following applies:

$$\left(\frac{V_1}{V_2}\right) = \left(\frac{W_1}{W_2}\right)^Y. \tag{14}$$

Therefore,

$$Y = \frac{\log\left(\frac{V_1}{V_2}\right)}{\log\left(\frac{W_1}{W_2}\right)}. \tag{14a}$$

Project Tugboat Phases I and II showed that the average of the peak particle velocities for the 10-ton event was approximately 3.3 times that for all 1-ton events as demonstrated by the equation coefficients in Fig. 133. Since the yield increase was a factor of 10, the yield scaling would be:

$$Y = \frac{\log 3.3}{\log 10} \approx 0.52.$$

With the 40-ton data, the increase was noted to be 6.7 times the 1-ton events. Again this would show:

$$Y = \frac{\log 6.7}{\log 10} \approx 0.52.$$

When one weighs the merits of both methods while noting the striking similarity of yield scaling results, it would seem logical to conclude that the yield scaling factor is about $W^{0.52}$.

No significant differences appeared to exist in the 1-ton data to suggest seismic amplitude dependence on DOB. The Delta 1-ton event did show some indication of slightly higher amplitudes than the other 1-ton events, but these were considered to be within normal data scatter.

Another phenomenon seems worthy of mention. When one studies Figs. 126,

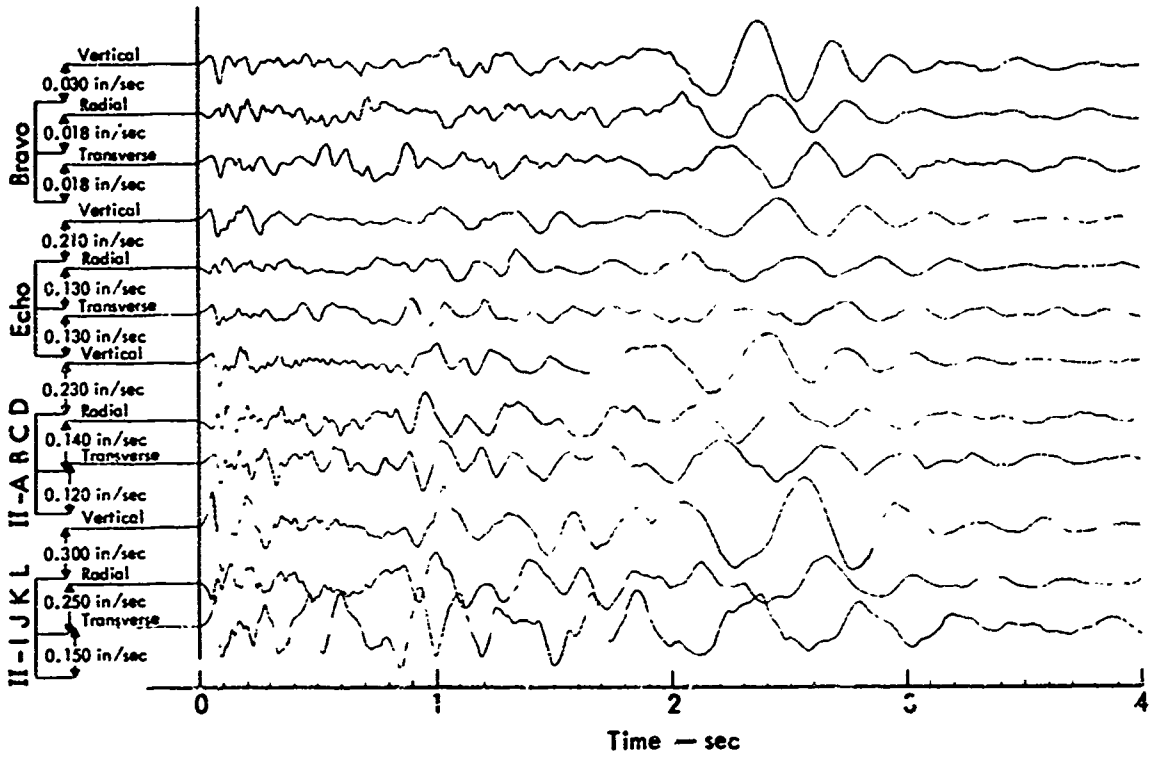

Fig. 134. Selected ground-motion data, Mauna Kea Beach Hotel.

128, 130, and 132, which are representative of Phase II data, it can be seen that a 10-ton equivalent attenuation curve very closely defines the data acquired during the II-ABCD and II-EF events. Of course, neither of these events was intended to have a yield of 10 tons; rather, 40 tons. A possible explanation of this phenomenon could very likely be that it was the result of the accidental sequential detonation and low yield of two charges during the II-ABCD event, and the detonation of only two of the four charges during the intended sequential detonation of the II-EF event. Selected data obtained at the ground-motion station located at the Mauna Kea Beach Hotel (designated GM-6 during Phase I and GM-7 during Phase II) are shown for comparative purposes in Fig. 134. By overlay comparison, and disregarding amplitude differences, one can observe a striking similarity in the characteristic wave shapes of 1-ton Bravo, 10-ton Echo, and the intended 40-ton II-ABCD detonation, which detonated sequentially. The data resulting from the 40-ton II-IJKL show some departure from the established characteristic wave shapes. Specifically, the initial compression (P) wave arrival exhibits a well-defined wave front lasting for about 0.4 sec, and the periods occurring in the Rayleigh wave region of maximum amplitude are slightly longer. Although it was established that II-ABCD was sequentially detonated, definition or interference patterns resulting from the individual charges are not apparent by visual wave analysis. Only one fact is evident: the amplitudes over the entire record are comparable to

the single-charge 10-ton Echo Event. Thus, there is some sparse evidence to indicate that the sequential detonation of multiple charges induces measurably less ground motion than simultaneous detonation.

SUMMARY AND CONCLUSIONS

Instrumented ground-motion seismic stations in the vicinity of Project Tugboat were observed to respond in a fairly uniform manner. Maximum peak particle velocities recorded during the 1-ton events ranged from about 1.5 cm/sec at a distance of about 1500 ft to about 0.1 cm/sec at a distance of 8200 ft. Data recorded during the 10-ton events ranged from about 4 cm/sec at a distance of about 1800 ft to about 8000 ft. Finally, 40-ton amplitudes diminished from about 6 cm/sec at a distance of approximately 2600 ft to about 0.8 cm/sec at a distance of approximately 7600 ft.

Vertical, radial, and maximum peak particle velocities decayed according to $D^{-1.62}$. The transverse component attenuated at the rate of $D^{-1.95}$.

Two yield scaling methods verified one another in defining a yield scaling factor of about $W^{0.52}$. In addition, it was concluded that no reliable seismic amplitude dependence upon DOB could be established.

A final conclusion was associated with the merits of sequential charge detonation. Phase II sequential detonations produced measurably lower ground motions than the expected motion for simultaneous detonation of the same charges.

Section 6
Structural-Response Analysis

OBJECTIVE

The objective of this technical program was to preclude damage to buildings and other structures in the area affected by seismic motion generated by the detonations. The program was performed by John A. Blume & Associates, Engineers, of San Francisco. Ground- and structural-motion records used in the analyses presented in this section were provided by WES (see Section 5).

STRUCTURAL INVENTORY

Prior to the Phase I detonations, a structural inventory was performed in the region surrounding the site. Based on this information several structures were selected as warranting further study and consideration. The following structures, located as shown in Fig. 135, were in this category: sugar conveyor support structure, heiaus, Ultramar warehouse, Plywood mill, Roth house, Spencer Park pavilion, and the Mauna Kea Hotel. Except for the Roth house, residential structures were not considered a problem. All nearby residential construction is of light wood frame construction without masonry chimneys and with a minimum of plaster walls and fragile construction details.

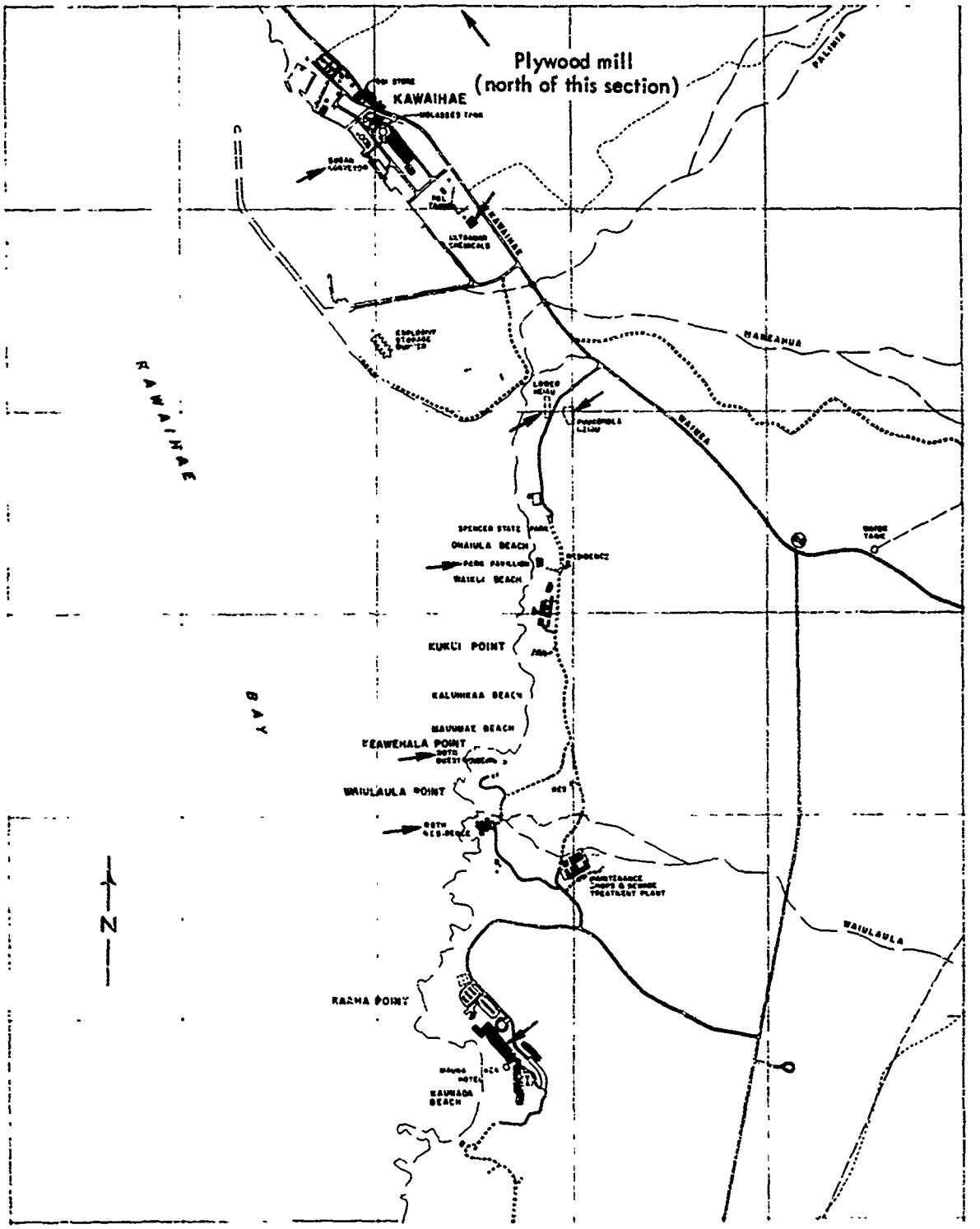

Fig. 135. Plan showing location of structures of interest.

Pre-PHASE I RECOMMENDATIONS

Prior to the Phase I detonations, recommendations were made on the location of the seismic-motion stations. Safe ground-motion damage thresholds of peak particle velocity of 2 cm/sec for residences and 5 cm/sec for harbor structures were also recommended. A firm threshold of damage for the heiaus was lacking, but it was estimated that past seismic activity had reached a level giving a peak particle velocity of at least 1 cm/sec and that temporary restraint of the more critical faces would allow safe levels of 5 cm/sec. Further investigation developed an individual rock stability criteria based on Housner[19] as shown in Fig. 136. As a precautionary measure, temporary bracing was installed on the heiaus as shown in Fig. 137. For all other structures it was anticipated that ground motion would be below the safe damage threshold levels.

POST-PHASE I ANALYSIS

No structural damage from the Phase I detonations could be detected, but preliminary study of the motion records indicated that the sugar conveyor support structure, and the Ultramar warehouse would be the critical structures for the Phase II detonations.

Sugar Conveyor Support Structure

Figure 138 is a cross section of this structure at the structural-response instrument station and shows the temporary bracing installed for the Phase II detonations. Figure 139 shows the motion records for the Phase I Delta and Echo detonations and reveals several interesting features. In the transverse direction the structure is nearly resonant with the long period ground motion (surface waves) and has very low damping. This is indicated by the relatively long duration of the structure's motion and the relatively high amplification when compared to the ground motion scaled from the closest ground-motion station near the molasses storage tank which is about 400 ft farther from SGZ. The structure has two transverse natural periods close to the dominant period of the surface waves. This is shown by the "beat" (alternating addition and attenuation of two wave trains with slightly different frequencies) in the transverse motion which still has considerable amplitude at a period of about 0.37 sec after the ground motion has essentially died out.

There is an abrupt "jerk" in the motion near each point of maximum transverse displacement. At this time the jerk was provisionally explained as a loose joint in the transverse bracing.

A comparison with the 1-ton Phase I detonations showed a much smaller scale effect for the 10-ton Echo detonation in the transverse direction than did all of the other stations. An approximate stress analysis, based on the Echo response records, indicated that the base of the cantilever roof support column might have undergone plastic yield in transverse bending for the peak pulses. Such behavior would be consistent with the motion record, since it would still have been elastic with very little damping for transverse motions causing bending stresses below the yield point. Plastic yielding of the column base would increase

damping and attenuate the peak motion. If such plastic yield did take place it involved very low distortions since no evidence, such as flaked paint or misalinement, was detectable by a close visual examination. The bracing shown in Fig. 138 was designed to eliminate the cantilever action and was installed for the Phase II detonations.

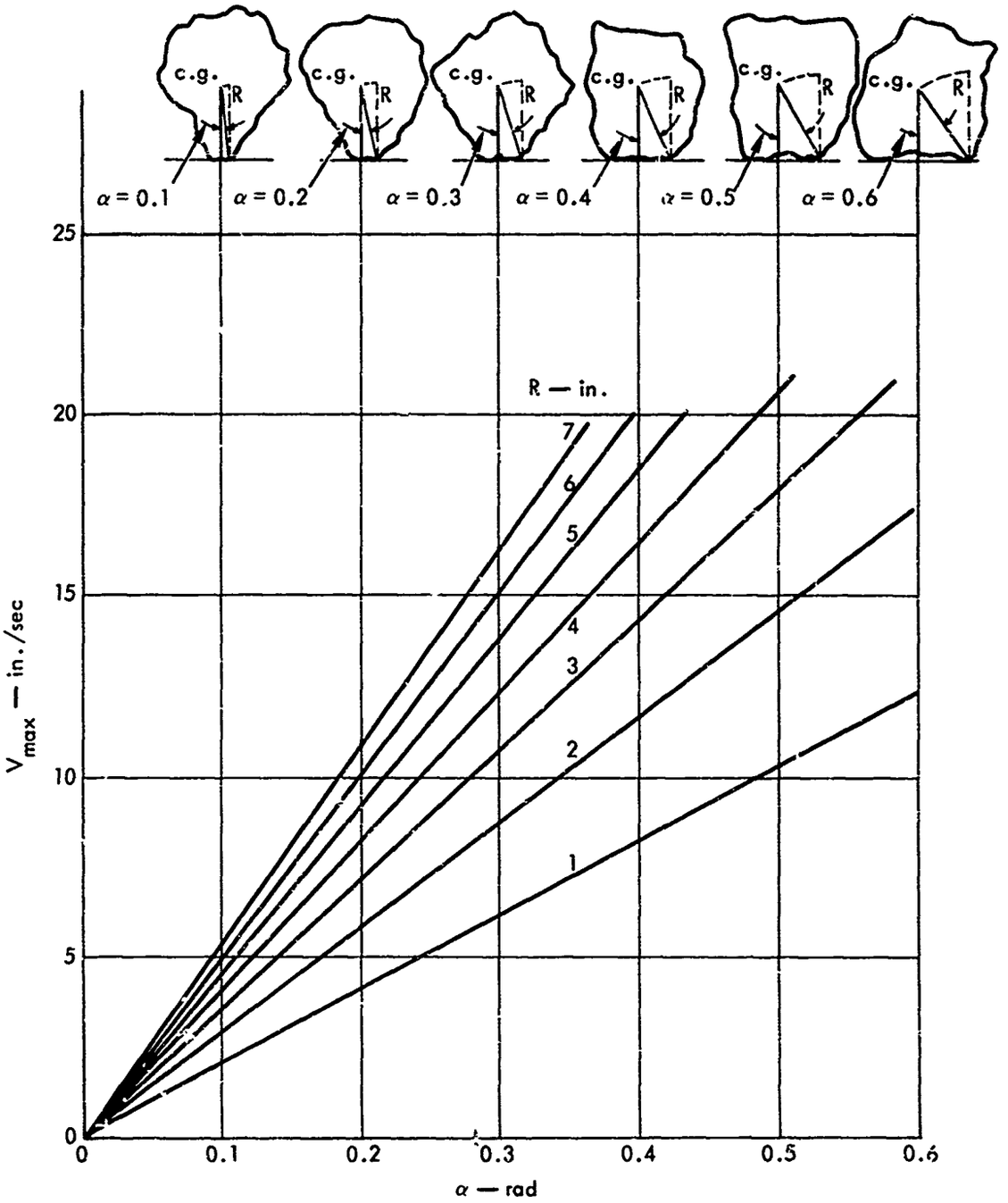

Fig. 136. Seismic motion for 50% chance of tipping a rock.

Fig. 137. Temporary bracing for heiaus.

Ultramar Warehouse

A casual classification of this structure with reference to seismic resistance indicates that it is a modern single-story reinforced concrete structure. This class of structure would be expected to withstand the established damage threshold value of ground motion (5 cm/sec) with no structural problems. A closer analysis, however, revealed the contrary, and this structure's ground-motion resistance became the limiting factor for determining the maximum safe size of the Tugboat detonations.

As shown in Fig. 140a, this structure is a single-story building 100 ft by 100 ft in plan dimension. An 80- by 100-ft portion has a precast concrete roof and concrete and/or concrete block in-fill walls (Fig. 140b) between the perimeter frame columns. The remaining 20- by 100-ft portion is a steel frame lean-to which has essentially no effect on the seismic response of the concrete portion. The two 80-ft sides of the concrete portion act as shear walls and are approximately symmetrical and of equal rigidity. The 100-ft rear wall (column line 1) is a shear wall except for the upper 3-1/2 ft which is a continuous louvered opening. The opposite wall (column line 5) has only the free-standing concrete frame columns for resisting lateral loads, thus creating a pronounced eccentricity for the resistance to lateral loads parallel to these column lines (radial direction on the seismic motion records for this structure). The relatively heavy roof and single-story construction result in resonant periods of the structure close to the ground-motion periods, and relatively large loads from seismic motion. Assuming a dynamic amplification factor of 3 for the roof response vs the anticipated ground motion of 5 cm/sec, preliminary calculations indicated a 100-ton charge would overstress the upper portion of the columns in column line 1. Adequacy of the block portion of the wall could not be determined as precisely, since the strength of a block wall is highly dependent on the quality of the construction. Based on the calculated stresses for a 40-ton detonation, the column stresses would not exceed allowable values based on a one-third increase for seismic loading. The block portion of the wall was judged safe against gross shear failure, but the possibility of minor cracking could not be ruled out.

Based primarily on the behavior of this structure, it was recommended that the initial Phase II detonation should not exceed 40 tons. Response spectra[20] were later calculated for the Ultramar foundation station Echo detonation and are shown in Fig. 141. Based on approximations of the building periods, the assumed amplification factor of 3 for the radial direction appeared reasonable.

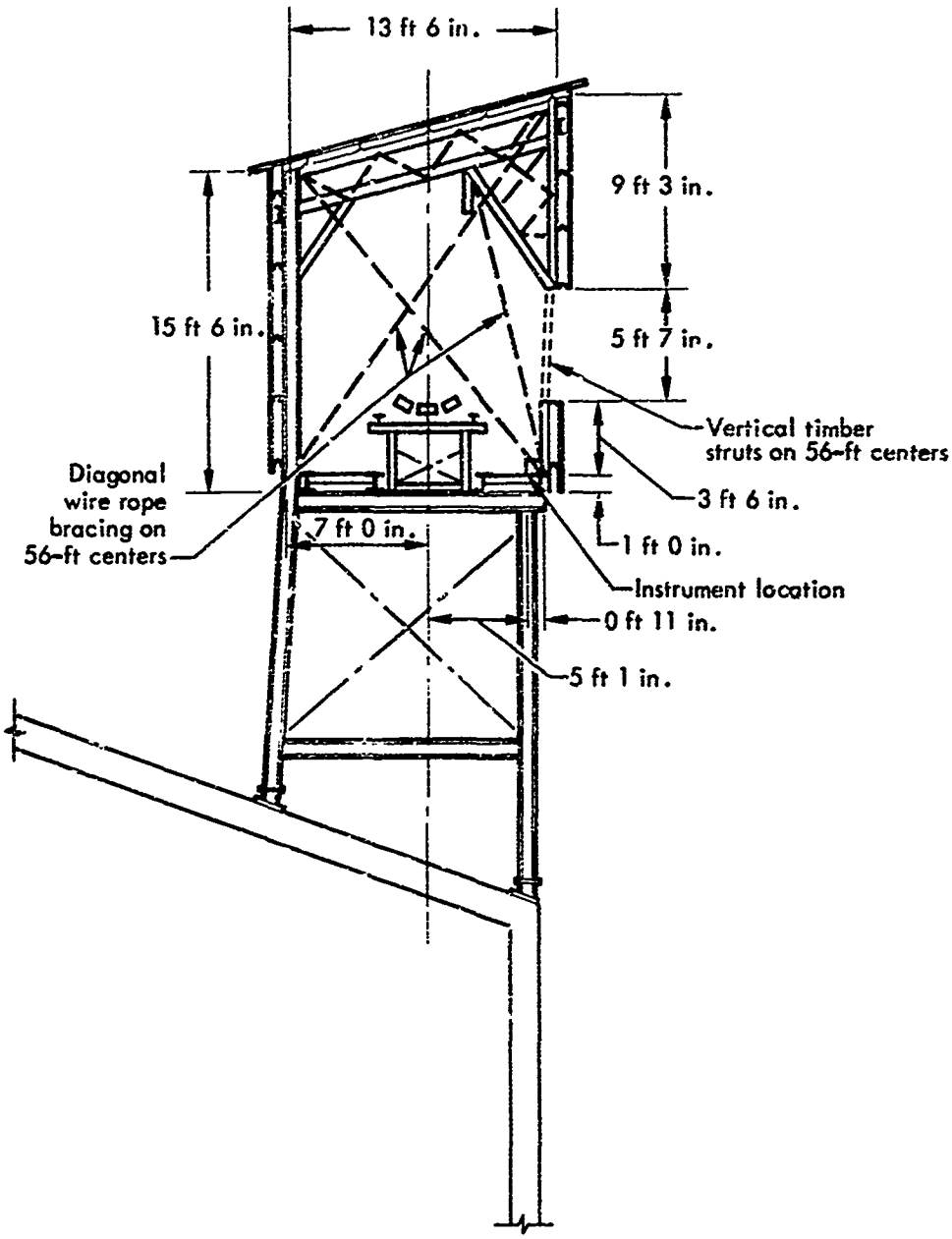

Fig. 138. Typical cross section of sugar conveyor support structure.

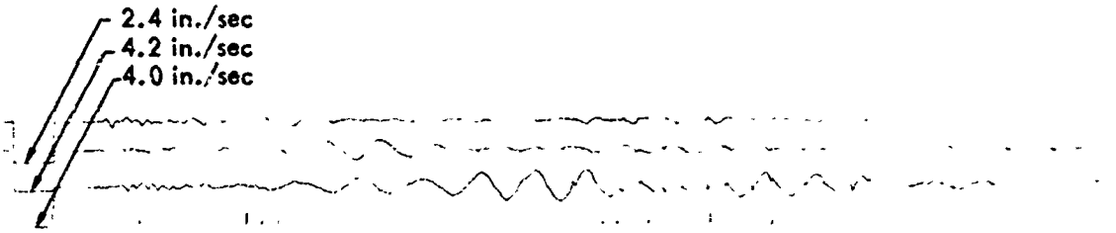

(a) Detonation Echo

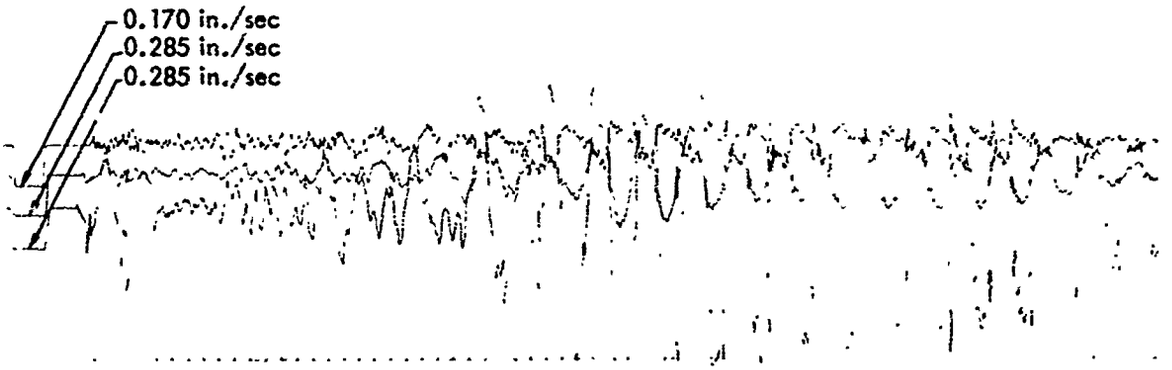

(b) Detonation Delta

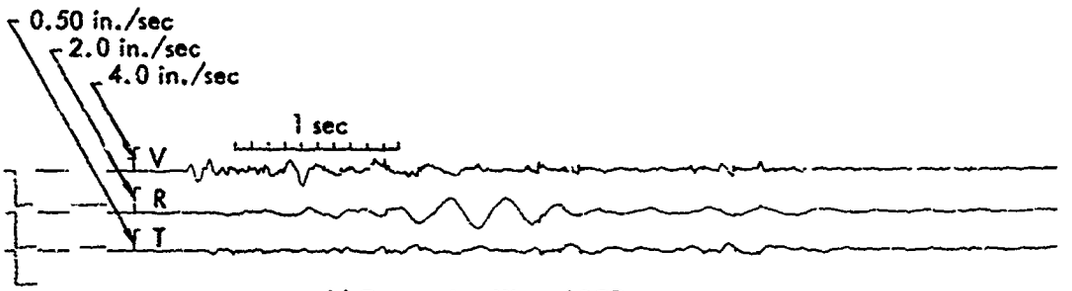

(c) Detonation III — ABCD

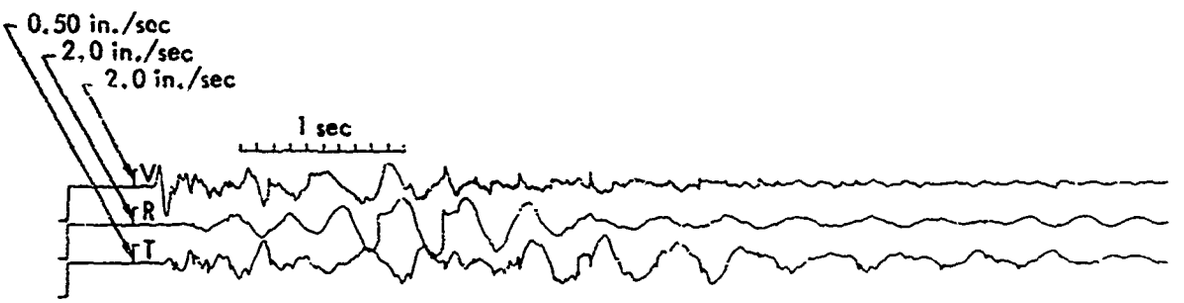

(d) Detonation II — IJKL

Fig. 139. Velocity records at sugar conveyor station, Detonations Echo, Delta, II-ABCD and II-IJKL.

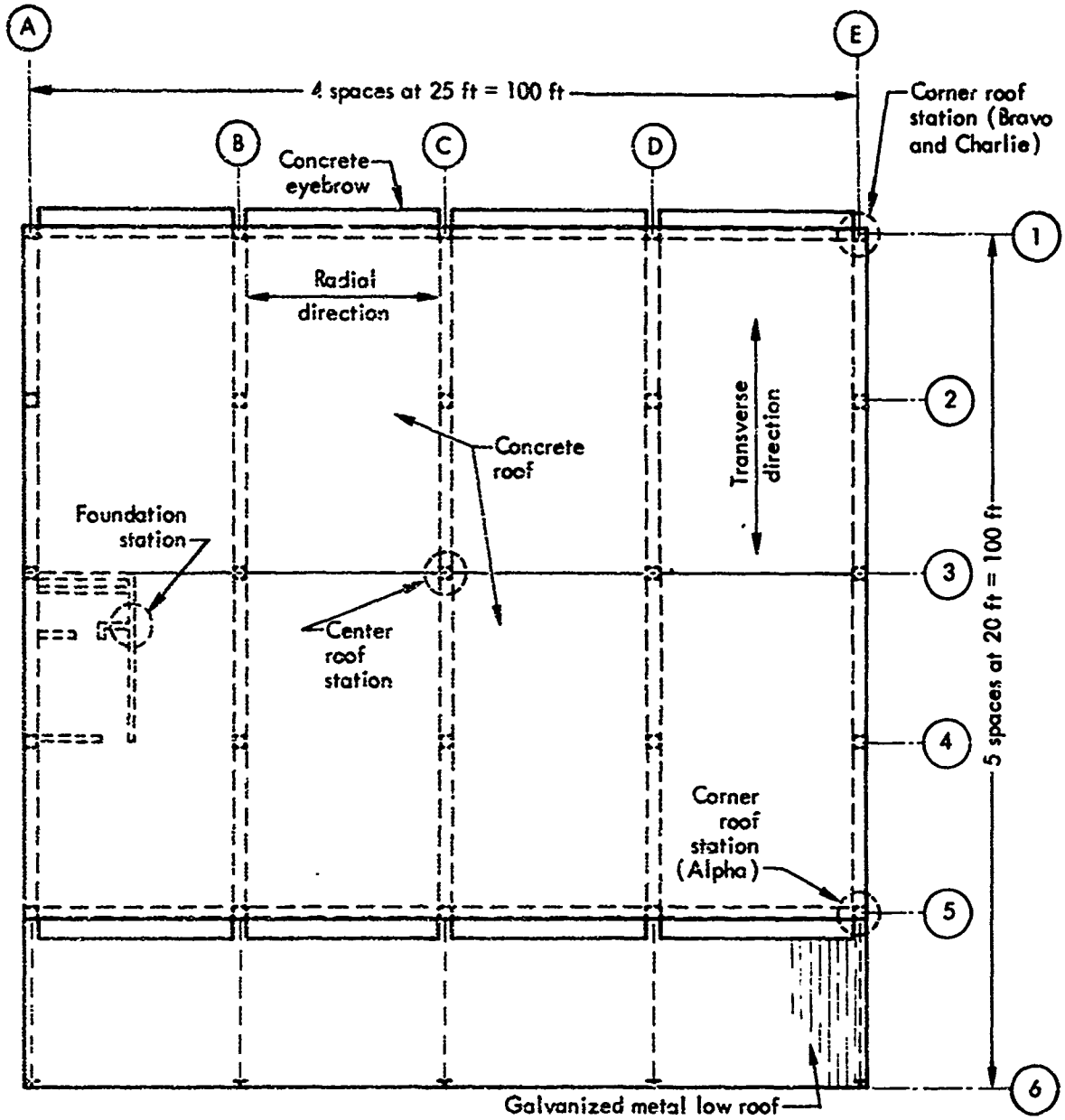

Fig. 140a. Plan, Ultramar Warehouse.

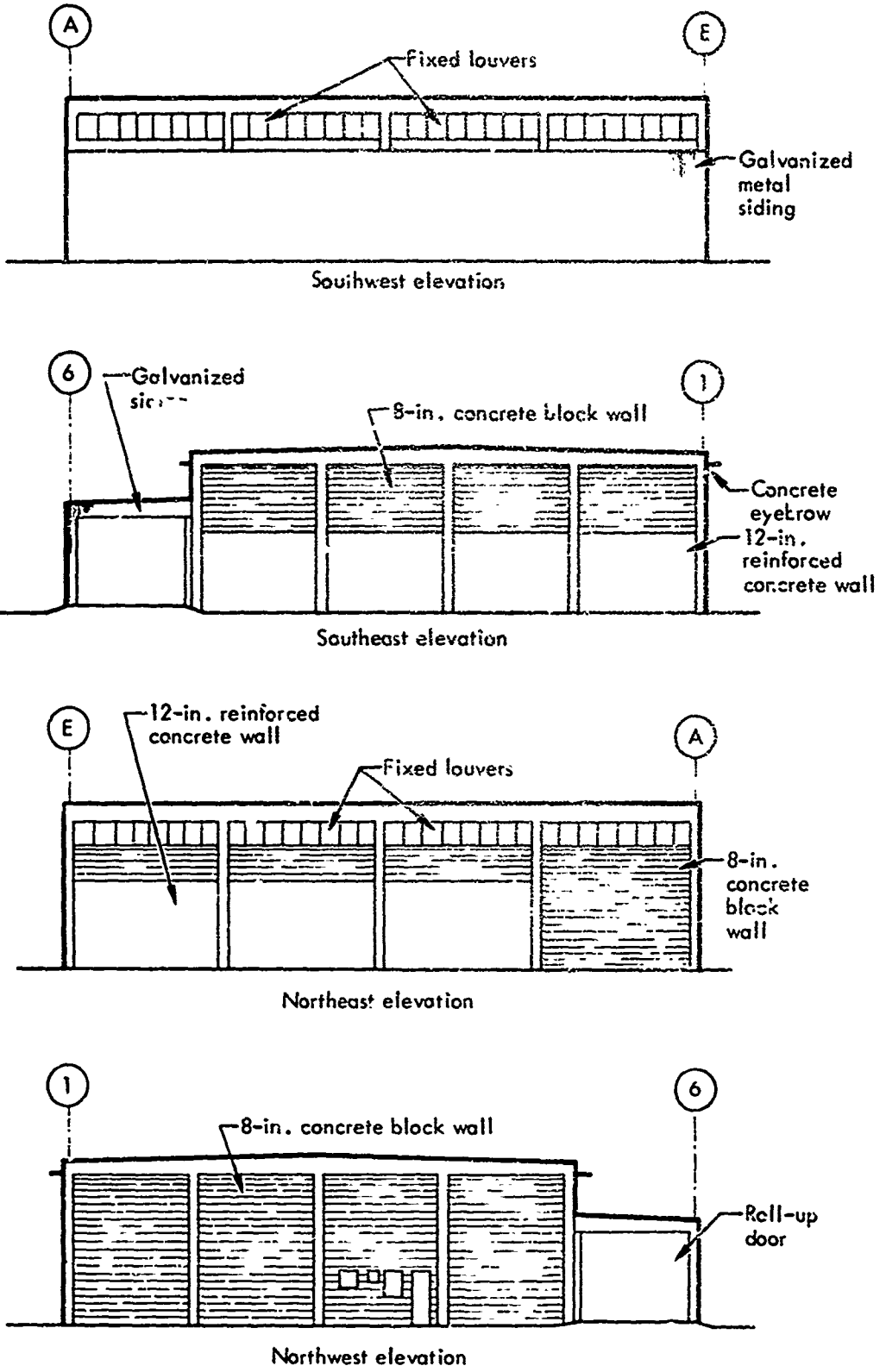

Fig. 140b. Elevations, Ultramar Warehouse.

Other Structures

The Mauna Kea Beach Hotel was not a limiting factor for a 100-ton detonation. Based on a scaling factor of 4 for seismic motion from a 100-ton detonation applied to the Phase I Echo event, peak horizontal accelerations would create inertia forces from one-half to two-thirds of the initial design lateral load. The buildings involved no exceptionally fragile features and construction appeared to have been of high quality throughout. Since this installation was by far the most expensive within the general vicinity, the same instrumentation as used for Phase I was recommended for Phase II.

At the Roth house, Plywood mill, Spencer Park pavilion, and the heiaus, the predicted motion for a 100-ton Phase II detonation appeared to be no problem.

During the period between Phase I and Phase II, a new building for the Hawaiian Telephone Company was completed. An analysis of this building indicated that

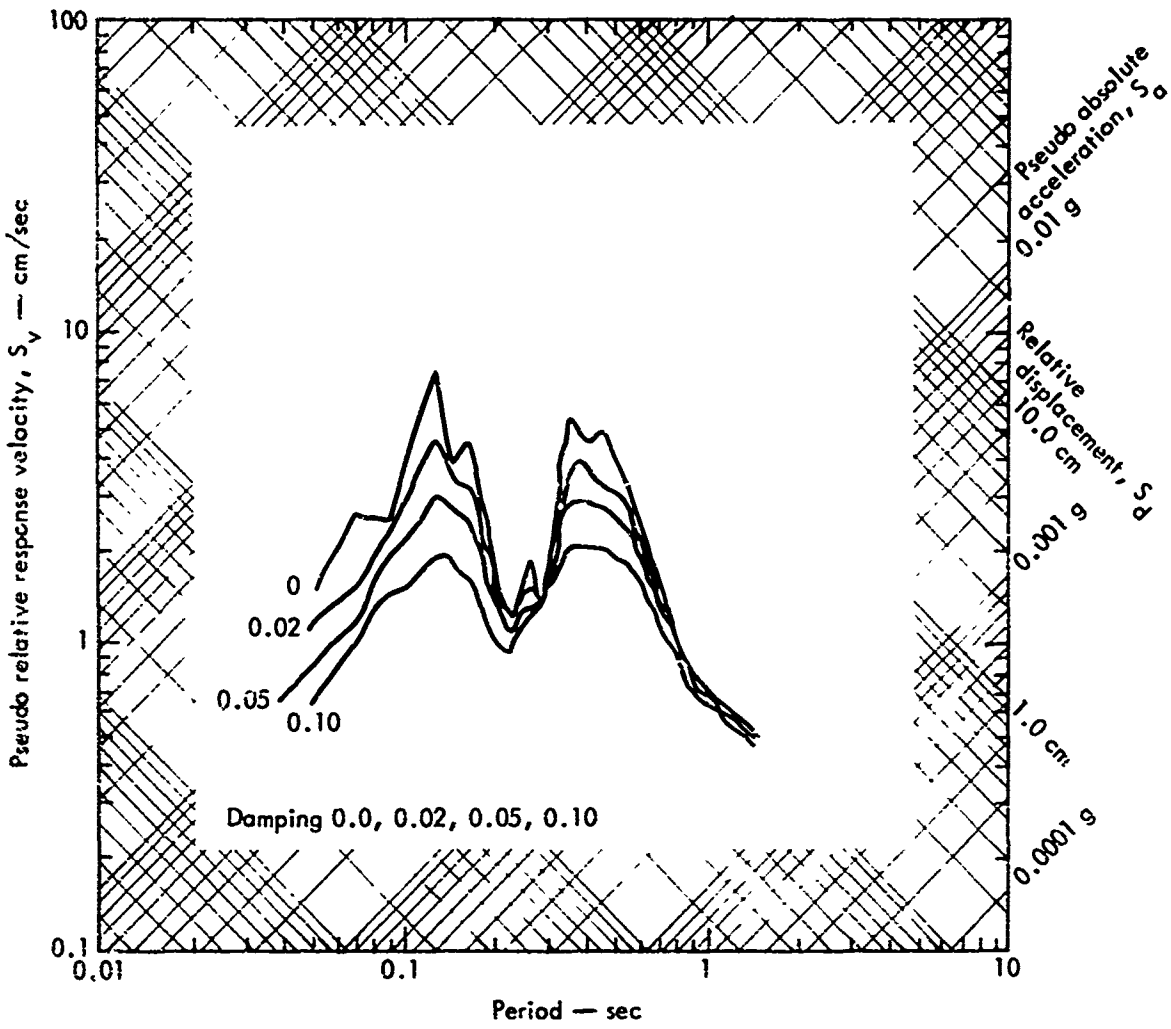

Fig. 141a. Response spectra for Ultramar foundation, Phase I Echo (radial).

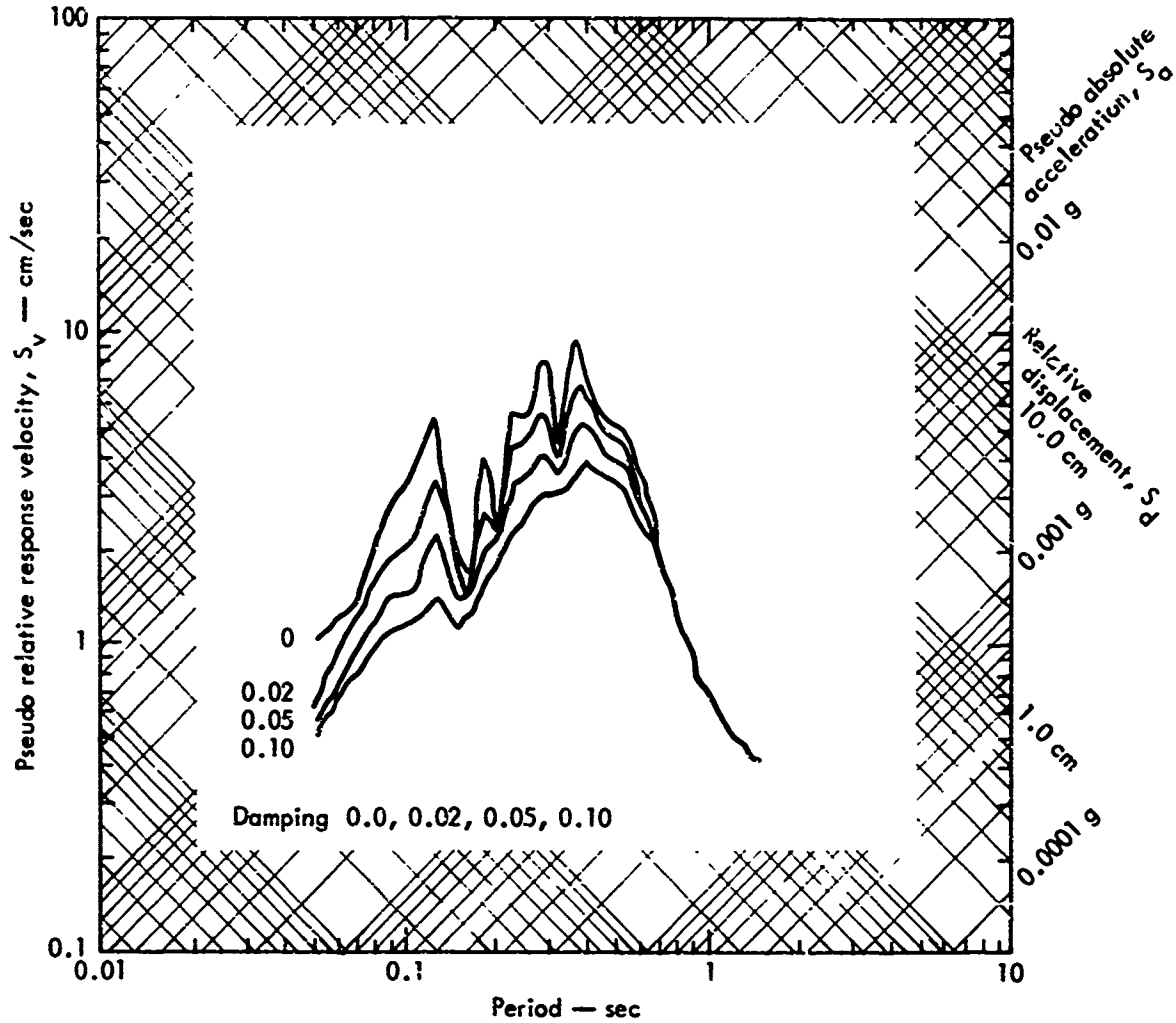

Fig. 141b. Response spectra for Ultramar foundation, Phase I Echo (transverse).

predicted motion from a 40-ton detonation would cause no structural overstressing. The structure has tilt-up concrete walls and a cast-in-place reinforced concrete frame. It appeared likely that the joint filler material separating the top of the wall panel and the concrete frame would show evidence of differential movement between the two, but such movement was not considered to be detrimental.

In order to obtain more data on the Ultramar warehouse and the sugar conveyor structure it was recommended that some of the instrument stations be relocated for Phase II as shown in Fig. 142.

POST-PHASE II ANALYSIS

Ultramar Warehouse

A closer examination of this structure just prior to the Phase II detonations but with the Post-Phase I analysis in mind, revealed minor preexisting damage. As shown in Fig. 143, the concrete coping

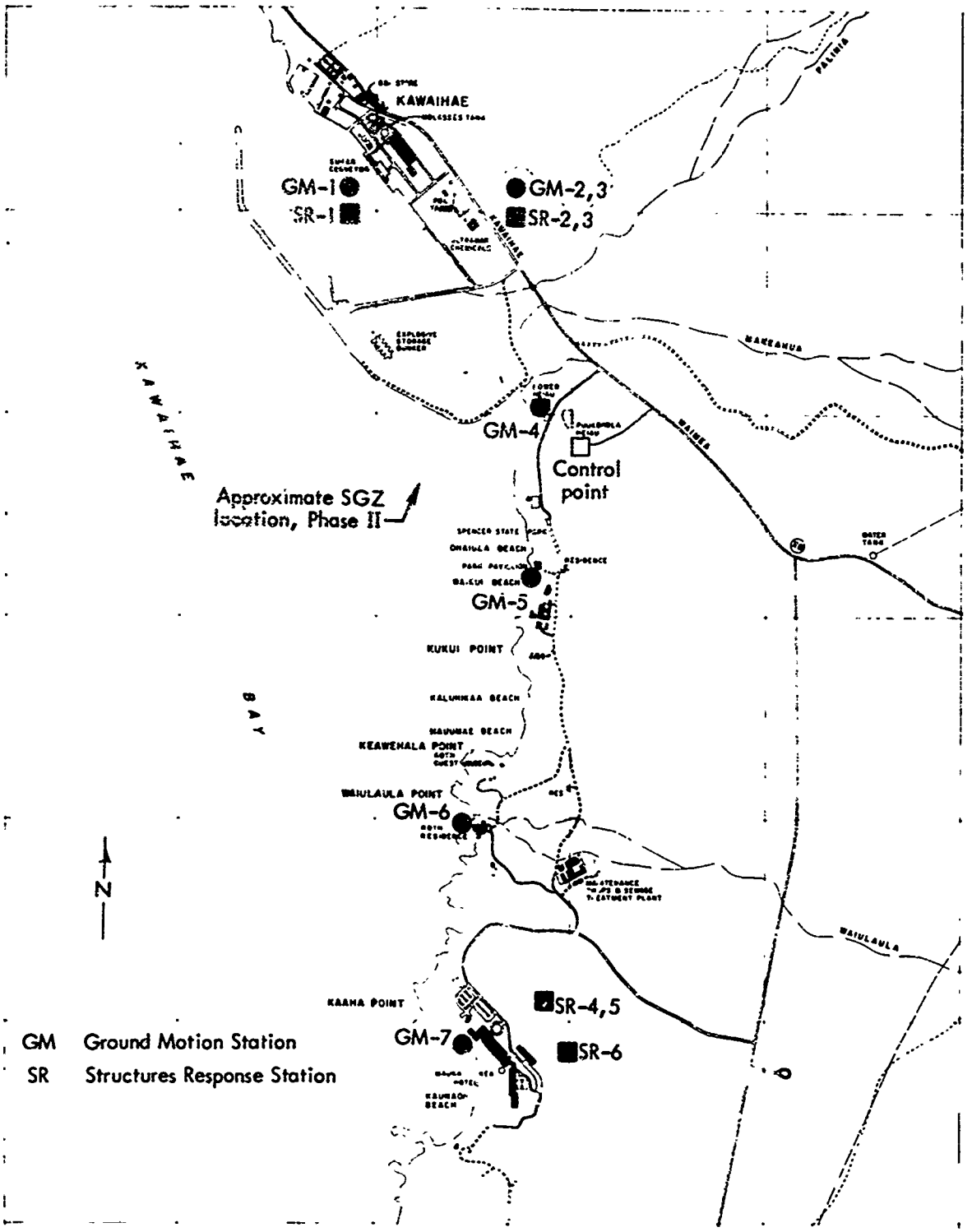

Fig. 142. Plan of seismic instrument locations for Phase II.

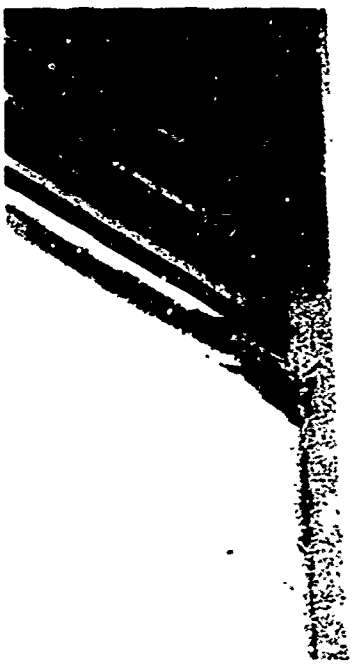

(a) Column A-1 prior to Phase II detonations

(b) Column B-1 (right side) prior to Phase II detonations

(c) Column B-1 (left side) prior to Phase II detonations

(d) Column B-1 after Phase II detonations

Fig. 143. Columns A-1 and B-1, Pre-Phase II Detonations; and Column B-1 Post-Phase II-IJKL Detonation.

beneath the louvers had spalled adjacent to Columns A-1 and B-1. Several vertical cracks in the end wall panel (A-E), extending from the coping to the base of the wall, were also observed. Neither the spalling or the cracks were noted during the Phase I observations. A possible explanation is the fact that bulk fertilizer was stored to a height of about 12 ft against the inside of the wall. This particular wall panel is entirely of concrete block and was not designed for bulk storage against it. The other wall panels along this same wall are constructed of reinforced concrete for the lower 12 ft and designed for bulk storage behind the wall. During the Phase II detonations the two interior panels (B-C and C-D) had no storage load and the other end panel (D-E) had bulk material stored full height (18 ft) against it. At some time in the past, panel B-C had been loaded to a height of about 17 ft, and panel C-D had been loaded to a height of about 14 ft. Horizontal bending of panels A-B and B-C causing the vertical cracks could also produce sufficient rotation of the end of the coping to result in spalling where the rotation was prevented by the concrete column. A random factor which influenced the probability of spalling of the coping was the clearance, if any, between the outer corner of the coping and the adjacent concrete column.

An alternate possibility is that the above minor damage occurred from either the earthquake of 10 May 1969 (magnitude, 4.0; epicenter 11 miles away; focal depth, 26 miles) or the earthquake of 24 September 1968 (magnitude, 5.0; epicenter 60 miles away; focal depth, 26 miles). Estimated peak particle motion at the Ultramar warehouse site from either of these earthquakes, however, is considerably less than the peak motion from the maximum Phase II detonation (II-IJKL). Such estimates are primarily based on data from California earthquakes, and possibly underestimate seismic motion from earthquakes in geologically different areas such as Hawaii.

Neither of the first two Phase II detonations caused any detectable damage to this structure, but the third detonation (II-IJKL) caused a minor spall on the coping block on the opposite side of Column B-1 to the preexisting spall (Fig. 143).

The roof stations for all of the Phase II detonations show a definite resonant period in the radial direction of about 0.26 sec (Fig. 144) that agrees very closely with a calculated period of 0.27 sec for the radial direction. A comparison of the center roof radial motion records and the radial foundation motion records for the Phase II detonations is an excellent example of the application of spectral response analysis. The roof response is primarily in a narrow frequency band close to its natural frequency and filters out most of the higher frequency motion in the first second of the foundation record. The amplitude of the motion is within the elastic range of the structure and the roof "rings" or continues to vibrate at its natural period after the ground motion at this frequency has essentially stopped. The roof corner station was at the southeast corner for Detonation II-ABCD and at the northeast corner for Detonations II-EF and II-IJKL. Essentially its radial motion was similar to the center roof station but both corner

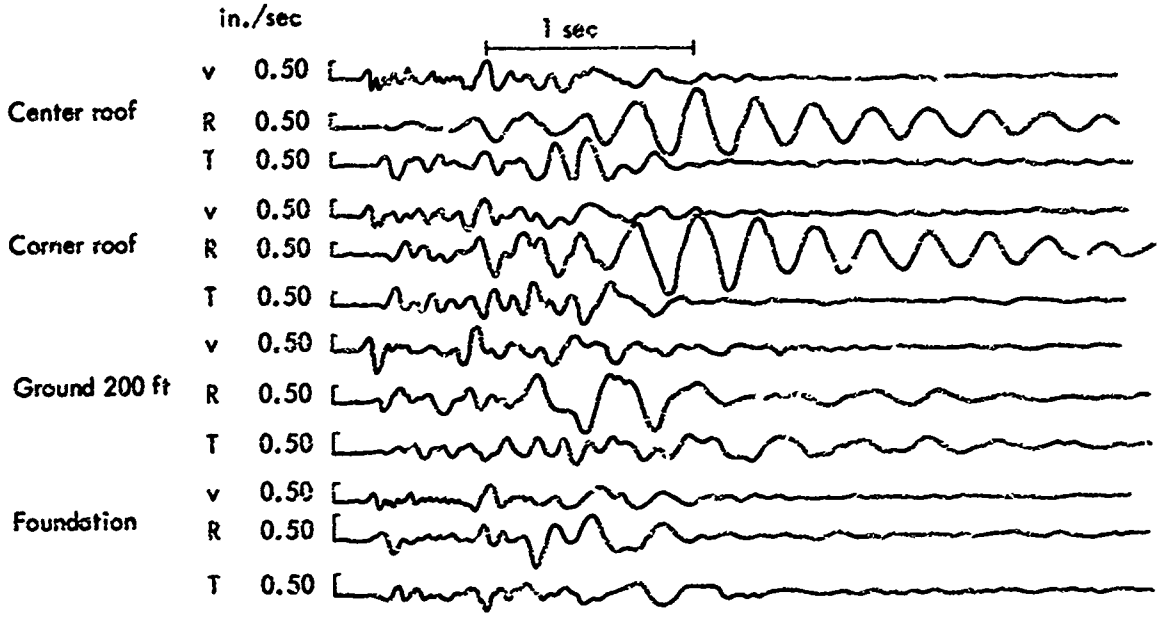

Fig. 144a. Velocity records of Ultramar Stations, II-ABCD.

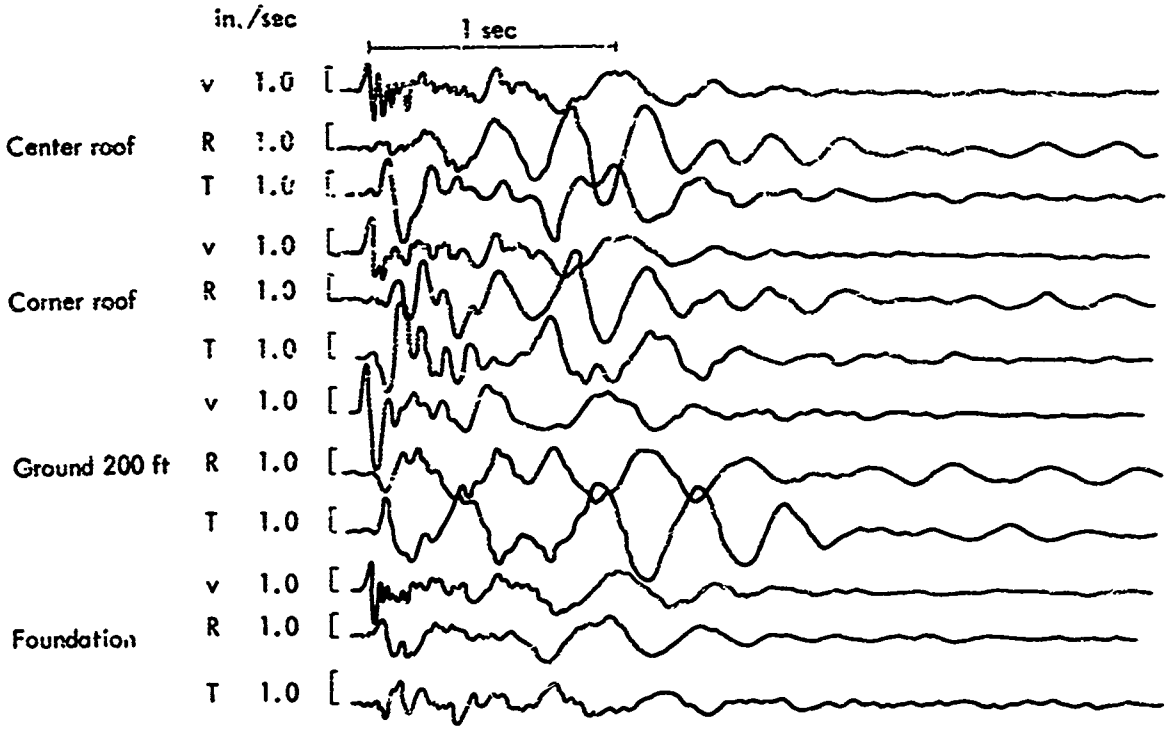

Fig. 144b. Velocity records of Ultramar Stations, II-IJKL.

locations show an added stiffness since the higher frequency foundation motion (about 0.1 sec) was not filtered out as completely as at the center roof station. The calculated period in the radial direction is based on the combined stiffnesses of the concrete frames and the wall along column line 1. The greater stiffness along column line 1 is apparently reflected in the increased response to 0.1-sec radial ground motion by the corner station compared to the center station.

Structural response in the transverse direction does not correlate with the analytical approach as well as in the radial direction, and the discussion of this motion is part conjecture. The calculated fundamental period in the transverse direction is 0.06 sec. In the calculations most of the stiffness derives from the two shear walls along column lines A and E with the E line (southeast wall) being somewhat stiffer than the A line (northwest wall) but both walls being considerably stiffer than the concrete frame. The transverse period is shorter than the periods of the foundation motion; hence, the expected transverse roof motion should be nearly identical to the foundation motion and should show very little amplification. This type of response is well-demonstrated by the vertical records. The roof instruments were all on top of columns; hence, the vertical fundamental period was very short, and the vertical roof motion records are nearly identical to the vertical foundation motion records.

The transverse roof motion records look very similar to the transverse foundation motion records except that the short period (below 0.09 sec) motion is filtered out. Transverse roof motion of the other periods, especially about 0.1 sec and about 0.3 sec, closely follows the foundation motion but shows an unexpected and moderately uniform amplification of the foundation motion. A possible explanation is that the actual response is the result of a combination of frame and shear wall response which for the actual range of amplitudes exhibits a variable natural frequency. There are shrinkage cracks at most of the column-shear wall joints; hence, an initial portion of each cycle of the motion might be due to frame action (resulting in a relatively long period) with the shear walls participating as the joint between the columns and walls closed thereby tending to stiffen the structure and producing a shorter period. Estimated widths of the cracks (a few hundredths of an inch) are consistent with the amplitudes of displacement which occurred. For higher amplitudes the shear wall action would dominate and the structure's transverse response should be more consistent with the calculated response.

Relative displacements between the roof and the foundation of a single mode of vibration structure, such as the Ultramar warehouse, are a direct measure of the stresses in the structure, since a given dynamic displacement would produce the same stresses as a static displacement of the same amplitude. Approximate relative roof displacements for Detonation II-IJKL motion were calculated by two different methods. Figure 145 shows the calculated response spectra for the radial and transverse foundation motion. Reading the 5% damping curve at

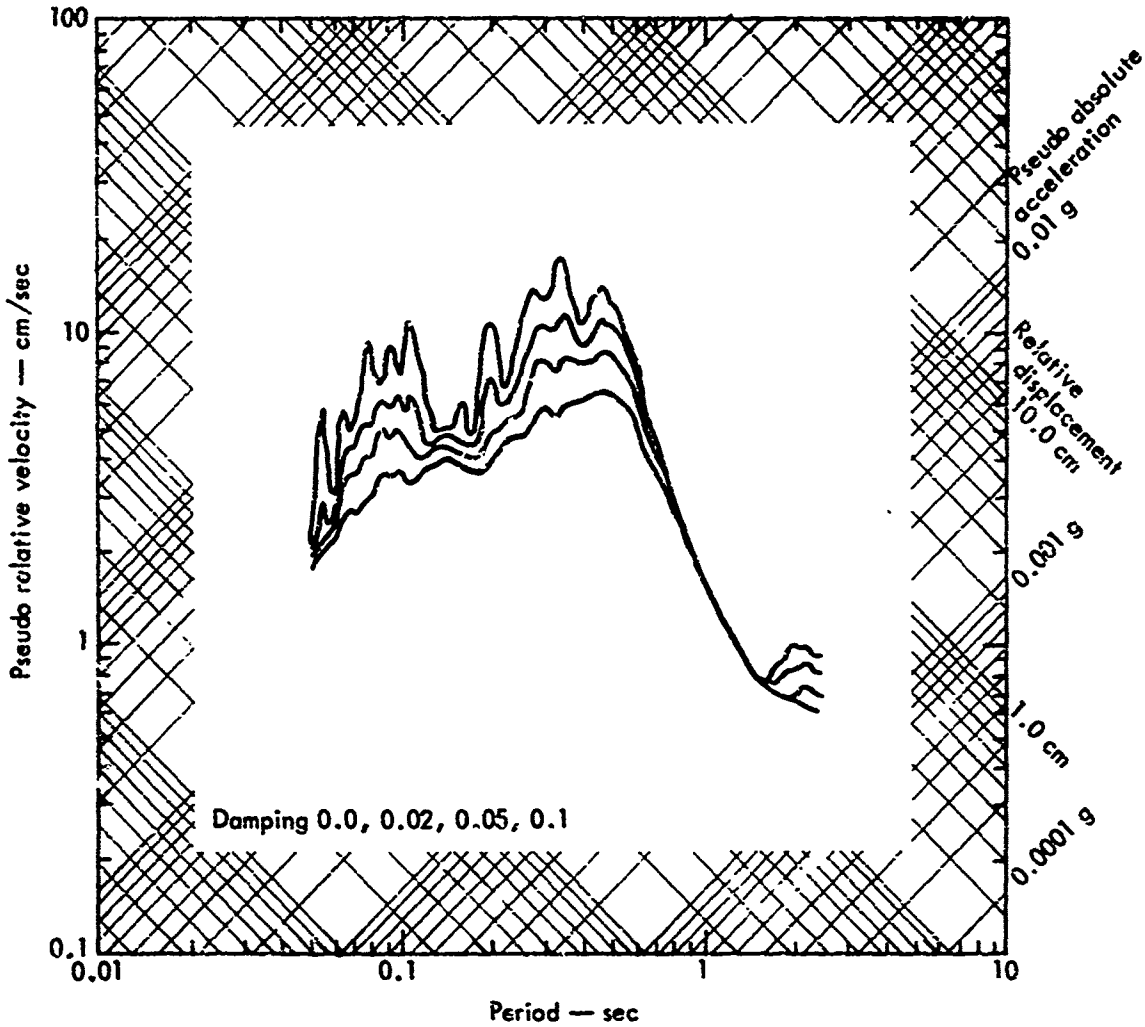

Fig. 145a. Response spectra, Ultramar foundation, Phase II, II-IJKL (radial).

the calculated radial period of 0.27 sec (Fig. 145a) indicates a relative displacement of 0.30 cm. Figure 146 shows a time history plot of ralative displacement obtained by integrating the relative velocities between the foundation station and each of the roof stations. The relative velocity between each pair of stations was obtained by subtracting the foundation velocity record from the corresponding velocity record at each of the roof stations. From the relative displacement plot the peak center roof relative displacement for the radial direction is 0.11 in. (0.28 cm) for the center stations and 0.8 in. (0.20 cm) for the corner roof station (Figs. 146(a) and 146(b).

Similar plots of relative displacements in the transverse direction are not as consistent. With the response spectra (Fig. 145b) for the foundation in the transverse direction, the calculated building period of 0.06 sec indicates a relative displacement of only 0.02 cm. The derived time histories of relative displacement, however, indicate a transverse relative displacement of 0.07 in. (0.18 cm) for the center roof station and 0.06 in. (0.15 cm)

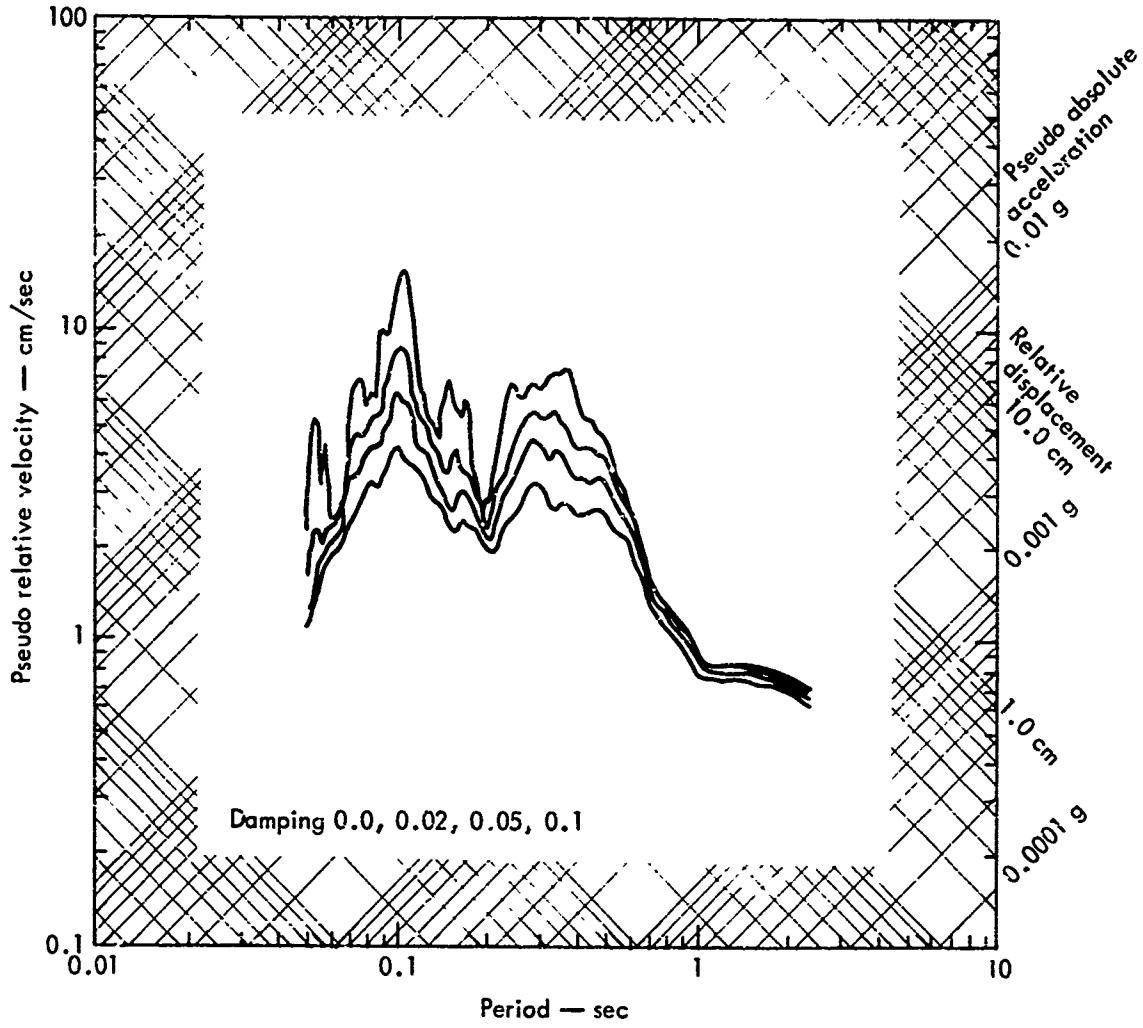

Fig. 145b. Response spectra, Ultramar foundation, Phase II, II-IJKL (transverse).

for the corner roof station—Figs. 146(c) and 146(d). As previously discussed, the building, in the transverse direction, is not responding at its calculated period for the motions experienced, but is behaving as a somewhat less rigid structure.

Another item of interest is the comparison of the ground motion 200 ft from the building and the ground motion at the building foundation (see Fig. 144). There is a definite horizontal resonance in the nearby ground motion at a period of 0.37 sec which shows clearly on the velocity records. It is anticipated that the nearby ground station would have about 20% higher amplitudes since it was closer to SGZ. Actual peak values for horizontal motion averaged about 80% higher. Two explanations are plausible. Due to different soil conditions the ground station was nearly resonant with the surface waves and therefore amplified this frequency much more than the foundation station. A second possibility is that soil conditions were similar at both stations and that the foundation station, without the building in place, would have shown a similar amplification, but the building

had the effect of attenuating the ground motion at the foundation station; hence, it was no longer resonant with the high-energy surface waves. Without detailed soils information no preference for either or both possibilities is offered.

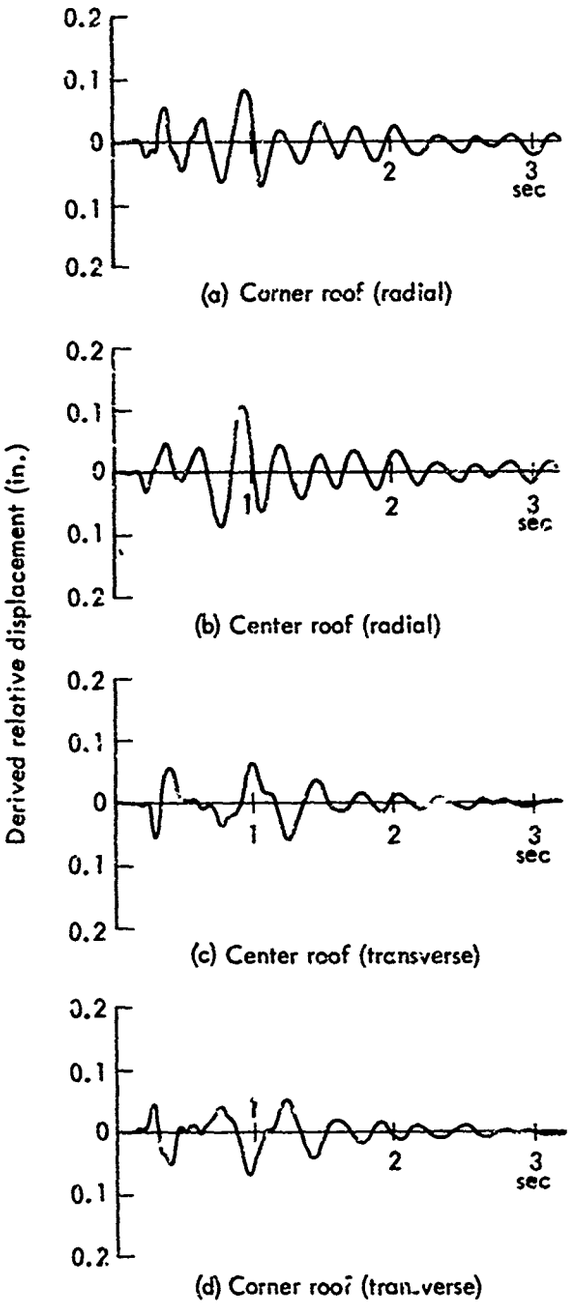

Fig. 146. Derived time histories of relative displacement for Ingomar foundation, II-IJKL.

Sugar Conveyor Support Structure

As shown by the Phase II motion records in Fig. 139, the temporary timber struts radically reduced the transverse response of this structure. The struts were not adequately restrained for the first Phase II detonation (II-ABCD) and about half of the struts fell to the walkway. Prior to slipping out of position, however, the struts had effectively damped the peak pulses which represented the major portion of the energy. Prior to the other Phase II detonations, the struts were adequately restrained and they served satisfactorily for the remainder of the Phase II detonations.

The "jerk" in the motion record near each point of maximum transverse displacement was found to be the movement of the longitudinal conveyor support trusswork at its support points where it is loosely pinned to the primary sugar conveyor structure at each bent. An initial examination of the structure revealed one unwelded bracing joint at the vertical frame where the seismic motion pickup was mounted and was originally considered the probable cause of the jerk. Following the first Phase II detonation this joint was welded, but the "jerk" still appeared in the motion records for Detonation II-EF. Quick-drying spot seals were then placed on three of the longitudinal conveyor support trusswork pinned joints, and movement of two of these joints was noted during the subsequent Phase II detonations.

Other Structures

No residual effects of the Phase II detonations could be detected at the other structures. In Hawaiian Telephone Company's new building the anticipated minor shear movement in the filler material between the top of the precast panels and the cast-in-place frame could not be detected. The joint is not readily accessible, and minor differential movements between the wall panels and the roof framing could not be ruled out although in the one area closely inspected before and after the detonations no break in the paint film over the joint could be detected.

CONCLUSIONS

Predictions of building response to ground motion from cratering detonations can be a determining factor in establishing the feasibility of an explosive excavation project. Pinpointing the critical structure (Ultramar warehouse) and determining the maximum motion the structure could withstand without structural damage, enabled Project Tugboat to be carried out safely and without the threat of large damage claims.

Calibration shots to verify the expected behavior of critical structures and to furnish data for more accurate predictions of structural response are very desirable.

The response of nominally simple structures, such as the Ultramar warehouse, can be very complex. Empirical ground-motion thresholds, which ignore the possible amplification due to the response characteristics of the structure, can be misleading and result in significant structural damage. Techniques are available for interpreting such behavior but the time and effort required will normally limit extensive analyses to only those structures which are critical.

For some structures, such as the sugar conveyor support structure, relatively simple temporary measures can radically change the dynamic response. Typically such structures have high amplification factors because of very little damping and a close match of their fundamental frequency and the peak energy frequencies of the ground motion. Temporary modifications which increase their damping value or shift their resonant frequency to a mismatch with the ground motion are then very effective in reducing the structure's response motion.

Section 7
Air-Overpressure Measurements

OBJECTIVES

A program was set up to measure airblast from the Project Tugboat detonations to determine conditions that might result in damage claims especially at the more substantial installations where claims could be significant.

The objective of this program during Phase I was to provide air-overpressure effects data, as a function of distance and charge weight. The data were used to make a thorough safety evaluation of

proposed larger yield detonations to excavate the berthing basin and an entrance channel in Phase II. It was expected that overpressures in Phase I would be so small that no airblast damage would result.

The principal objective of this program during Phase II was to document airblast for use in the event of claims, and to provide a better understanding of airblast from rows and arrays of charges.

This section is an abstract of a more complete report of the program published by the Sandia Laboratories (Ref. 21).

PREDICTIONS

While airblast measurements have been made on many single-charge chemical-explosive cratering detonations,[22-32] and a few row-charge detonations,[30,31,33-35] and array-charge detonations,[36,37] there were two conditions on Project Tugboat for which there was little experience.

First, the explosive was an aluminized ammonium nitrate slurry (AANS). Most previous airblast data were for TNT and nitromethane (NM) cratering explosions. The AANS has a total heat of detonation of 1700 cal/g, compared with 1093 cal/g for TNT and 1227 cal/g for NM. Detonation velocities for the same three explosives are 13,100 to 18,000, 23,000, and 27,700 ft/sec, respectively.

Secondly, the charges were placed in water-covered coral limestone. There are no reported airblast measurements for charges detonated in coral or other water-covered media, although data have been reported for explosions at various depths in water.[38-40]

Phase I Predictions

With so little precedent on which to base pressure expectations, the predictions for Phase I were made in a simple way. Predictions of peak overpressure as a function of charge burial depth data were available for a series of 1000-lb TNT shots[29] in Albuquerque alluvium. Data were for a scaled distance of 5 ft/$lb^{1/3}$, or 63 ft from a 1-ton charge. A limited number of NM detonations in the same soil showed peaks higher than those for TNT by a factor of 1.57 for the ground-shock-induced peak and a factor of 1.67 for the gas-vent peak. The overpressure predictions for each Tugboat Phase I detonation were based on the more conservative NM data and were as shown in Table 27. All overpressures were assumed to attenuate with distance as R^{-1}

Phase II Predictions

Phase II predictions were made following the Phase I detonations and were based on an analysis of the Phase I data. Each of the three Phase II events involved a planned detonation of four 10-ton charges at burial depths of 42 ft—about the burial depth of the Echo event. Details are given in Table 28. Overpressures produced by the Echo event would be the lowest possible from a Phase II event were there no addition of overpressures from individual charges or were only one of the four charges detonated. Preliminary information indicated that the Echo event gave a peak ground-shock-induced overpressure of 0.022 psi at 3000 ft, the approximate distance to the nearest private property subject to potential blast damage. This overpressure and an R^{-1} attenuation rate constituted the

Table 27. Detonation summary and predicted overpressure for Phase I.

Detonation	Date	Time	Wind direction and velocity (ft/sec)	Charge weight (lb)	DOB[a] (ft)	DOB[b] (ft)	Depth of water (ft)	Scaled DOB ($ft/lb^{1/3}$)	Overpressure predicted at 50 ft/$lb^{1/3}$ (psi)
1a	11/6/69	9:01	ESE 29	2,000	16.33	17.33	5	1.38	0.019
1b	11/6/69	11:01	ESE 23.5	2,000	16.66	17.86	5	1.42	0.015
1c	11/4/69	10:01	ESE 37	1,975	20.12	21.72	6	1.72	0.009
1d	11/5/69	9:01	ESE 29	1,950	24.74	25.84	5	2.05	0.0068
1e	11/7/69	11:01	ENE 22	20,000	41.6	42.9	7	1.58	0.010

[a]Below Mean Low Low Water.

[b]Below actual water surface.

Table 28. Summary of Phase II detonations.

Detonation	Charge	Date	Wind direction and velocity (ft/sec)	DOB[a]	Depth of water	Delay (sec)
II-ABCD		4/23/70	SSW 4-9			0
	II-A			43.2	8	
	II-B			43.2	5	
	II-C			42.6	7	
	II-D			41.0	6.5	
II-EF[b]		4/28/70	WNW 7-10			0.1
	II-E			42.1	6	
	II-F			42.4	7	
II-IJKL		5/01/70	W 9-10			0
	II-I			41.9	6.5	
	II-J			41.7	6	
	II-K			42.1	5.5	
	II-L			41.5	5.5	

[a]Below Mean Low Low Water.

[b]The other two charges in this row (II-G and II-H) did not detonate as planned (see Section 2).

Table 29. Data for five-charge square array detonation, one charge in center, 64 lb TNT per charge, 6-ft burial depth.[36]

Spacing	Ground-shock-induced peak overpressure for 5-charge array (psi)	Equivalent single-charge overpressure (psi)	Ratio of overpressure array/single
10 ft or 2.5 $ft/lb^{1/3}$	0.0131	0.0046	2.85
16 ft or 4 $ft/lb^{1/3}$	0.0081	0.0046	1.75

lower limit of expected overpressures from Phase II events. An upper limit would occur were there simple addition of overpressures from the four charges of each event. Less than simple addition of peak overpressures was to be expected for reasons given in the following paragraphs.

In previous row charge detonations,[28] where 64-lb charges buried 6 ft deep (1.5 ft/$lb^{1/3}$) and spaced 8 ft apart (2.0 ft/$lb^{1/3}$) were detonated simultaneously, the peak ground-shock-induced overpressures measured at the same distance increased with the number of charges as follows:

Off the end of the row:

$$\frac{\Delta p \text{ row}}{\Delta p \text{ single}} = n^{0.05}$$

Perpendicular to the row:

$$\frac{\Delta p \text{ row}}{\Delta p \text{ single}} = n^{0.8},$$

where Δp is overpressure and n is the number of charges in the row. For four charges of Detonation II-ABCD, these expressions give ratios of 1.1 and 3, respectively.

Implicit in the above expressions is the unproven assumption that values of the exponent of n are not also a function of medium, type of explosive, or charge size. It was observed in the five-charge Dugout cratering detonation[31] that values were lower than would be predicted with these assumptions. The spacing proposed for Phase II was larger than any for which airblast data were available; however, data for smaller spacings suggest that the exponent of n decreases with increased spacing, so that expected overpressures would be less than given by the above expressions.

Data from similar nonsimultaneous detonations with about the same scaled delays as planned for Detonation II-EF showed that peak overpressures were below those of simultaneous detonations.

There were no airblast data for square arrays of buried charges. A five-charge square array detonation[34] of 64-lb charges at 6-ft burial depth (1.5 ft/$lb^{1/3}$) gave results at 500 ft as shown in Table 29. These measurements were made perpendicular to only one side of the square. Because of this, azimuthal effects are unknown. Ratio values for four charges should be less. The larger Tugboat spacing (4.4 ft/$lb^{1/3}$ as compared to 4.0 ft/$lb^{1/3}$) would also reduce the peak overpressure expected.

In summary both the row-charge and square-array data suggested peak overpressures should not be more than three times those of the Echo event. Accordingly, predicted overpressures at the approximate distances to the ten stations were as given in Table 30.

INSTRUMENTATION AND STATION LOCATIONS

Ten stations were used for all detonations. Their general locations are shown in Fig. 147. Stations AM-1 through AM-7 were at locations of potential blast damage. Stations AM-8, AM-9, and AM-10 were located on the coral fill area to provide some close-in measurements for establishing good attenuation curves. Specific station locations were the same for both Phase I and II for Stations AM-1 through AM-5. Stations AM-6 and AM-7 were at different locations on the Mauna

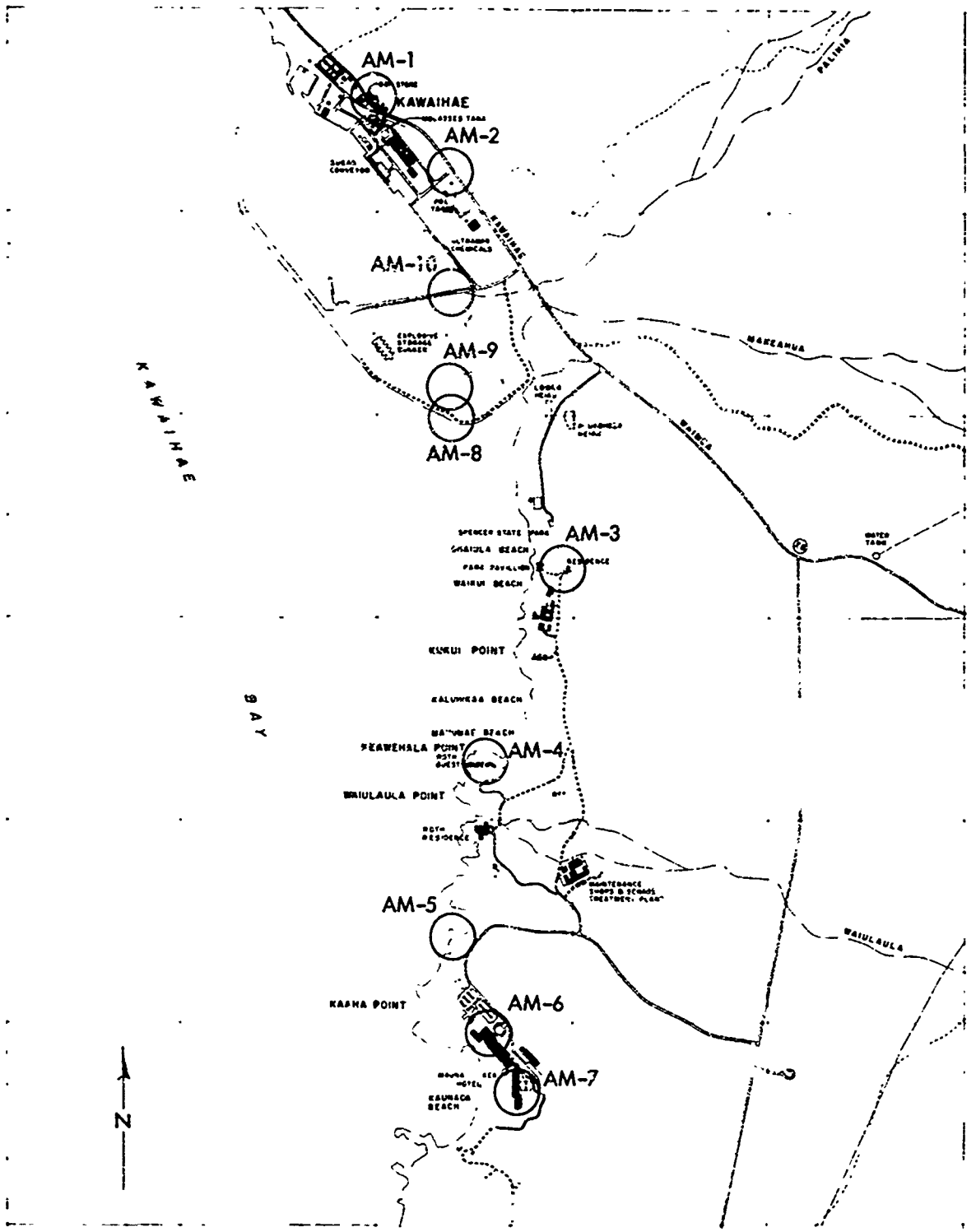

Fig. 147. Map showing locations of air overpressure measurement stations.

Table 30. Tugboat Phase II range of expected overpressures.

Station	II-ABCD Approximate distance (ft)	II-ABCD Low (psi)	II-ABCD High (psi)	II-EF Approximate distance (ft)	II-EF Low (psi)	II-EF High (psi)	II-IJKL Approximate distance (ft)	II-IJKL Low (psi)	II-IJKL High (psi)
AM1	4800	0.015	0.045	4450	0.015	0.045	4200	0.015	0.045
AM2	4000	0.020	0.06	3650	0.20	0.06	3400	0.020	0.06
AM3	2900	0.025	0.075	2800	0.025	0.075	2900	0.025	0.075
AM4	3800	0.020	0.06	4150	0.020	0.06	4400	0.020	0.06
AM5	6150	0.010	0.03	6500	0.010	0.03	6750	0.010	0.03
AM6	7050	0.009	0.03	7400	0.009	0.03	7650	0.009	0.03
AM7	8000	0.008	0.025	8350	0.008	0.025	8600	0.008	0.025
AM8	1200	0.06	0.20	850	0.08	0.25	600	0.12	0.35
AM9	1500	0.045	0.15	1150	0.06	0.2	900	0.075	0.25
AM10	2350	0.030	0.09	2000	0.035	0.1	1750	0.04	0.12

Kea Beach Hotel roof during Phases I and II. Stations AM-8, AM-9, and AM-10 were moved between the 1-ton detonations and the 10-ton Echo detonation on Phase I and again to a slightly different location for Phase II to maintain an almost straight blast line between the SGZ and Station AM-2. The stations are more specifically described in the following paragraphs:

Station AM-1 was about 40 ft in front of the Doi general store. The store and the service station across the street constituted most of "downtown" Kawaihae. Both had plate-glass windows with maximum sizes of about 50 and 30 sq ft, respectively. (A detailed window census is given in Table 31). There were numerous other windows in the store, house, and station, with panes of 2.5 to 5 sq ft. The Chock Hoo store nearby had eight panes, 2-1/2 × 2-1/2 ft, as well as several six-pane casements.

Station AM-2 was across the street from the old school building. Windows were double-hung sash with six small panes each. Most other houses in Kawaihae also had windows with six-pane sash.

Table 31. Window census—Tugboat.[a]

Approximate distance from SGZ (ft)	Number of panes of each size
2,000 to 3,000	30 A,[b] 68 B,[c] 3 C[d]
3,000 to 4,000	434 A, 165 B, 178 C, 2 E,[e] 2 F[f]
4,000 to 5,000	160 A, 100 B
5,000 to 6,000	20 B, 40 C, 40 E
6,000 to 7,000	nil
7,000 to 8,000	20 C
8,000 to 9,000	97 D,[g] 923 E

[a] From John A. Blume & Associates, San Francisco, California.

[b] A size—less than 2 sq ft.

[c] B size—between 2 and 5 sq ft.

[d] C size—between 5 and 16 sq ft.

[e] E size—between 23 and 35 sq ft.

[f] F size—between 35 and 45 ft.

[g] D size—between 16 and 23 sq ft.

Station AM-3 was 35 ft southeast of the home of the caretaker of Spencer State Park. The house was of simple frame construction, with 14 windows containing double-hung sash, six panes per sash.

Station AM-4 was about 40 ft north of a guest house on the property of Mrs. Roth. The property contained a large number of glass picture windows.

Stations AM-5, AM-6, and AM-7 were at the Mauna Kea Beach Hotel. Station AM-5 was about 900 ft from the hotel on a line toward the explosion location. During Phase I Station AM-6 was on the roof of the original (high) section of the hotel at the end nearest the explosions, and Station AM-7 was on the roof of the new (low) section, at the end of the hotel away from the explosions. During Phase II, Station AM-6 was moved from the corner of the hotel roof to a point well back from the leading edge. Station AM-7 was moved from the roof of the hotel to a point near the ground in a garden east of the rooftop location for Phase I. The hotel had 252 rooms, each with four 3 × 7.5-ft sliding glass doors. Glass and frames were heavy and exceptionally well-mounted. The dining pavilion and dining room both had heavy plate-glass windows or sliding glass doors (not included in census) with typical dimensions of 9 × 9 ft for the pavilion and 8 × 9 ft for the dining room. Stores and shops in the hotel contained other glass, most of it facing inside courts.

Stations AM-8, AM-9, and AM-10 were on a coral fill immediately north of the explosion site. Together with Stations AM-1 and AM-2, they constituted an almost unidirectional blast line.

Distances from each of the five detonations to each station are given with the results.* Each station had two gages, one to measure higher-than-expected overpressures and one set to measure the predicted overpressure. The difference was usually a factor of five. Interim adjustments were not made in set ranges but in gage sensitivity. These changes, based on the results of the first two events, were necessary only at the three closest stations.

Gages used were of three types: variable reluctance, unbonded, and bonded.

Table 32 gives gage type and serial number for each station during Phase I. A few changes in the types of gages at each station were made for Phase II. These changes are given in Table 33.

Table 32. Instrumentation for Phase I.

Station	Gage Serial No.	
AM-1S (high)	1670	Transmitter at Station 2
1P (low)	12688	Transmitter at Station 2
AM-2S (high)	1740	Transmitter at Station 2
2P (low)	10771	Transmitter at Station 2
AM-3S (high)	1668	Transmitter at Station 2
3P (low)	17832	Transmitter at Station 3
AM-4S (high)	1665	Transmitter at Station 4
4P (low)	12685	Transmitter at Station 4
AM-5S (high)	1633	Wire to recorder
5 P (low)	17839	Wire to recorder
AM-6S (high)	1635	Wire to recorder
6P (low)	12686	Wire to recorder
AM-7S (high)	1626	Wire to recorder
7P (low)	17844	Wire to recorder
AM-8D (high)	44068	Transmitter at Station 10
8S (low)	1742	Transmitter at Station 10
AM-9S (high)	1744+	Transmitter at Station 10
9S (low)	1667	Transmitter at Station 10
AM-10S (high)	1655	Transmitter at Station 10
10P (low)	11365	Transmitter at Station 10

*See Tables 34a through 34h.

Table 33. Changes in instrumentation for Phase II.

Station	Gage Serial No.
AM-2 (high)	1632
(low)	1745
AM-3 (high)	44065
(low)	1743
AM-4 (high)	1631
(low)	1634
AM-6 (high)	44067
(low	1741
AM-9 (high)	44068
AM-10 (high)	44059
(low)	1630

Information from one, two, or three stations was transmitted by telemetry from the stations to a recording facility in Room 753 of the hotel. Information from gages near the hotel was transmitted by wire directly to two 7-track tape recorders. One tape of each of the first three detonations was sent daily to a playback facility at Barbers Point, Oahu, to provide information by which gages could be set for the next event.

Final playback provided adequate records for all except Station AM-1 during Phase I although signals at distant stations were degraded by wind noise on most 1-ton detonations.

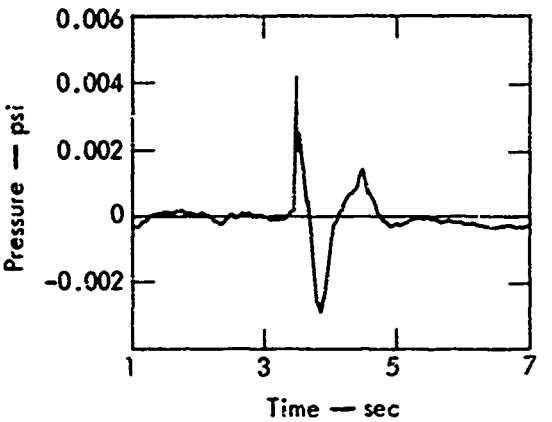

Fig. 148. Air overpressure record at Station AM-4 for 1-ton Bravo detonation of Phase I (1 July 1970).

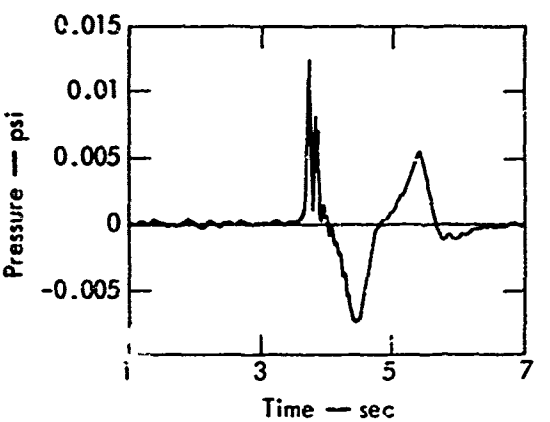

Fig. 149. Air overpressure record at Station AM-4 for 10-ton Echo detonation of Phase I.

RESULTS

Summaries of results including azimuth and distance, set ranges, calibration steps, arrival times, measured peak positive and negative pressures, times of peaks, and measured positive and negative impulses for all stations are given in Tables 34a through 34 h. Peak overpressures were always ground-shock-induced pulses; gas-venting pulses were very small and difficult to identify.

Typical pressure-time waveforms for the detonations are best illustrated by comparing those at one station for all of the detonations. Station AM-4 records provide a good sample. Figure 148 is a waveform observed at Station AM-4 for the 1-ton Bravo detonation. It is typical of the 1-ton detonation records at all stations. The waveform for the 10-ton Echo detonation at Station AM-4 (Fig. 149)

Table 34a. Summary of results—Detonation Alpha.

Station	Azimuth (deg)	Distance (ft)	Set range (psi)	Calibration step (psi)	Arrival time (sec)	p+ (psi)	Time of peak (sec)	p- (psi)	Time of peak (sec)	I+ (psi-sec)	I- (psi-sec)
AM-8D (high)	5.38	401	0.30	0.12	0.062,[a] 0.295	0.098	0.324	0.066	0.602	0.602	0.0143
8S (low)			0.06	0.0206	0.062[a]	[b]	[b]	[b]	[b]	[b]	[b]
AM-9S (high)	1.71	694	0.15	0.0224	0.550	?	0.564	0.03	0.921	0.0041	0.0062
9S (low)			0.03	0.0215	0.127,[a] 0.527	0.042	0.559	0.028	0.818	0.0032	0.0063
AM-10S (high)	2.33	1761	0.08	0.0192	1.432	0.0155	1.455	0.0118	1.792	0.00145	0.00255
10P (low)			0.015	0.008	[c]	[c]	[c]	0.0057 (?)	1.795	[c]	[c]
AM-3S (high)	136.45	2286	0.045	0.019	1.912	0.0097	1.992	0.00775	2.311	0.00142	0.00186
3P (low)			0.009	0.010	1.911	0.0095	1.992	0.0084	2.313	0.00132	0.00206
AM-2S (high)	1.52	3435	0.03	0.02	2.782	0.0078	2.810	0.0062	3.140	0.00068	0.00177
2P (low)			0.006	0.0107	2.786	0.008	2.811	0.0064	3.140	0.0008	0.0015
AM-4S (high)	172.14	4042	0.02	0.0191	3.412	0.00475	3.497	0.00425	3.793	0.0005	0.00088
4P (low)			0.004	0.010	3.411	0.00325	3.496	0.003	3.802	0.00034	0.00063
AM-1S (high)	345.40	4319	0.02	0.024	[d]	[d]	[d]	[d]	[d]	[d]	[d]
1P (low)			0.004	0.0118	[d]	[d]	[d]	[d]	[d]	[d]	[d]
AM-5S (high)	179.28	6417	0.01	0.01	5.470	0.0032	5.552	0.0028	5.862	0.000445	0.000705
5P (low)			0.002	0.0057	5.433	0.0031	5.547	0.0025	5.875	0.00043	0.00068
AM-6S (high)	176.50	7307	0.01	0.009	6.254	0.00265	6.335	0.00385	6.680	0.00026	[d]
6P (low)			0.002	0.0067	6.255	[d]	6.302	[d]	6.547	[d]	[d]
AM-7S (high)	174.08	8274	0.01	0.011	7.165	0.00182	7.227	0.00187	7.510	0.00031	0.00051
7P (low)			0.002	0.0101	7.073	0.00192	7.250	0.00195	7.550	0.00031	0.00058

[a] Arrival of ground-transmitted surface wave.

[b] Limited.

[c] Poor record.

[d] No record.

Table 34b. Summary of results—Detonation Bravo.

Station	Azimuth (deg)	Distance (ft)	Set range (psi)	Calibration step (psi)	Arrival time (sec)	p+ (psi)	Time of peak (sec)	p- (psi)	Time of peak (sec)	I+ (psi-sec)	I- (psi-sec)
AM-8D (high)	358.63	310	0.12	0.12	0.073,[a] 0.219	0.127	0.248	0.07	0.604	0.0108	0.0183
8S (low)			0.025	0.0206	0.074[a]	[b]	[b]	[b]	[b]	[b]	[b]
AM-9S (high)	357.69	604	0.06	0.0224	~0.468	?	0.539	0.033	0.858	<0.0051	<0.0079
9S (low)			0.012	0.0215	0.103,[a] 0.455	0.0405	0.506	0.031	0.850	0.0048	0.00315
AM-10S (high)	0.91	1671	0.03	0.092	1.360	0.014	1.408	0.0127	1.816	0.017	0.00318
10P (low)			0.006	0.008	[c]	[c]	[c]	0.0107(?)	1.763	[c]	[c]
AM-3S (high)	138.77	2321	0.02	0.019	1.893	0.0139	1.967	0.0083	2.316	0.0013	0.00204
3P (low)			0.004	0.010	1.852	0.0135	1.967	0.0092	2.319	0.00125	0.00226
AM-2S (high)	0.30	3345	0.012	0.02	2.739	0.0081	2.780	0.0056	3.167	0.0008	0.00147
2P (low)			0.0025	0.0107	2.707	0.00835	2.781	0.00565	3.167	0.00087	0.00151
AM-4S (high)	172.93	4124	0.008	0.0191	3.424	0.0064	3.499	0.004	3.802	0.000551	0.000576
4P (low)			0.002	0.010	3.437	0.00415	3.500	0.003	3.857	0.00033	0.00062
AM-1S (high)	345.01	4244	0.008	0.024	[d]	[d]	[d]	[d]	[d]	[d]	[d]
1P (low)			0.002	0.0118	[d]	[d]	[d]	[d]	[d]	[d]	[d]
AM-5S (high)	179.69	6505	0.004	0.010	5.475	0.0038	5.552	0.00385	5.901	0.00048	0.00092
5P (low)			0.0008	0.0057	5.472	0.0038	5.552	0.0037	5.902	0.00045	0.001
AM-6S (high)	176.89	7394	0.004	0.009	6.223	[d]	6.285	[d]	6.685	[d]	[d]
6P (low)			0.0008	0.0067	6.235	[d]	6.274	[d]	6.700	[d]	[d]
AM-7S (high)	174.45	8358	0.004	0.011	7.065(?)	?	7.190(?)	?	?	?	?
7P (low)			0.0008	0.0101	6.500(?)	0.004	6.640(?)	?	7.653(?)	?	?

[a] Arrival of ground-transmitted surface wave.

[b] Limited.

[c] Poor record.

[d] No record.

Table 34c. Summary of results—Detonation Charlie.

Station	Azimuth (deg)	Distance (ft)	Set range (psi)	Calibration step (psi)	Arrival time (sec)	p+ (psi)	Time of peak (sec)	p- (psi)	Time of peak (sec)	I+ (psi-sec)	I- (psi-sec)
AM-8D (high)	19.28	356	0.06	0.12	0.072,[a] 0.205	0.083	0.280	0.042	0.665	0.0072	0.0135
8S (low)			0.012	0.0206	0.072[a]	—[b]	—[b]	—[b]	—[b]	—[b]	—[b]
AM-9S (high)	0.03	537	0.03	0.0224	0.468	0.041	0.520	0.0235	0.919	0.004	0.007
9S (low)			0.006	0.0215	0.105,[a] 0.460	0.0383	0.520	0.022	0.922	0.0037	0.0067
AM-10S (high)	3.10	1704	0.015	0.0192	1.330	0.0143	1.424	0.0083	1.907	0.00174	0.0028
10P (low)			0.005	0.008	—[c]	—[c]	—[c]	—[c]	—[c]	—[c]	—[c]
AM-3S (high)	136.10	2386	0.009	0.019	1.969	0.0078	2.031	0.0064	2.519	0.00112	0.00192
3P (low)			0.002	0.010	1.951	0.0078	2.032	0.00675	2.478	0.00117	0.00212
AM-2S (high)	2.99	3379	0.006	0.020	2.705	0.0055	2.764	0.0042	3.266	0.00072	0.00126
2P (low)			0.0012	0.0107	2.711	0.00575	2.765	0.0041	3.286	0.00075	0.00127
AM-4S (high)	171.12	4116	0.004	0.0191	3.464	0.00438	3.520	0.00345	3.955	0.00044	0.00068
4P (low)			0.001	0.010	3.454	0.0038	3.520	0.0024	3.966	0.00025	0.00060
AM-1S (high)	346.74	4239	0.004	0.024	—[d]	—[d]	—[d]	—[d]	—[d]	—[d]	—[d]
1P (low)			0.001	0.0118	—[d]	—[d]	—[d]	—[d]	—[d]	—[d]	—[d]
AM-5S (high)	178.38	6481	0.002	0.010	5.470	0.003	5.525	0.0022	5.941	0.00040	0.00058
5P (low)			0.0004	0.0057	5.439-5.462	0.0029	5.560	0.0021	5.956	0.00041	0.00056
AM-6S (high)	175.91	7376	0.002	0.009	6.120	0.0028	6.303	0.0032	6.861	0.000205	0.00054
6P (low)			0.0004	0.0067	?	—[d]	?	—[d]	?	—[d]	—[d]
AM-7S (high)	173.53	8345	0.002	0.011	6.589	—[d]	7.230	—[d]	?	—[d]	—[d]
7P (low)			0.0004	0.0101	6.983	0.0036	7.220	0.0019	8.035	?	?

[a]Arrival of ground-transmitted surface wave.

[b]Limited.

[c]Poor record.

[d]No record.

Table 34d. Summary of results—Detonation Delta.

Station	Azimuth (deg)	Distance (ft)	Set range (psi)	Calibration step (psi)	Arrival time (sec)	p+ (psi)	Time of peak (sec)	p- (psi)	Time of peak (sec)	I+ (psi-sec)	I- (psi-sec)
AM-8D (high)	16.37	258	0.03	0.12	0.051,[a] 0.149	0.104	0.185	0.042	0.738	0.00745	0.01548
8S (low)			0.006	0.0206	0.047[a]	—[b]	—[b]	—[c]	0.740	—[b]	—[b]
AM-9S (high)	5.88	543	0.015	0.0224	0.377	0.038	0.428	0.021	0.980	0.003	0.0083
9S (low)			0.003	0.0215	0.082,[a] 0.397	0.033	0.427	0.02	1.060	0.0029	0.0079
AM-10S (high)	3.79	1612	0.008	0.0192	1.295	0.0112	1.325	0.007	1.946	0.00112	0.00186
10P (low)			0.0015	0.008	—[c]	—[c]	—[c]	—[c]	—[c]	—[c]	—[c]
AM-3S (high)	138.33	2421	0.0045	0.019	2.027	0.0068	2.092	0.0041	2.650	0.000825	0.00160
3P (low)			0.001	0.010	2.027	0.0066	2.095	0.0045	2.650	0.00081	0.00173
AM-2S (high)	2.20	3281	0.003	0.020	2.636	0.0042	2.720	0.0038	3.243	0.00044	—
2P (low)			0.0005	0.0107	2.646	0.0042	2.721	0.00425	3.291	0.000475	—
AM-4S (high)	171.95	4197	0.002	0.0191	3.532	0.0034	3.635	0.0022	4.145	0.00037	0.00076
4P (low)			0.0005	0.010	3.500	0.0023	3.638	0.0015	4.143	0.00027	0.00056
AM-1S (high)	345.85	4163	0.002	0.024	—[d]	—[d]	—[d]	—[d]	—[d]	—[d]	—[d]
1P (low)			0.0004	0.0118	—[d]	—[d]	—[d]	—[d]	—[d]	—[d]	—[d]
AM-5S (high)	179.00	6569	0.001	0.010	5.570	0.00263	5.674	0.00183	6.250	0.00032	0.00058
5P (low)			0.0002	0.0057	5.567	0.00254	5.673	0.0016	6.251	0.00032	0.00060
AM-6S (high)	176.30	7461	0.001	0.009	6.350	—[d]	6.472	—[d]	7.307	—[d]	—[d]
6P (low)			0.0002	0.0067	6.125(?)	—[d]	6.430(?)	—[d]	7.164(?)	—[d]	—[d]
AM-7S (high)	173.95	8429	0.001	0.011	—[e]	—[e]	—[e]	—[e]	—[e]	—[e]	—[e]
7P (low)			0.0002	0.0101	—[e]	—[e]	—[e]	—[e]	—[e]	—[e]	—[e]

[a]Arrival of ground-transmitted surface wave.

[b]Limited.

[c]Poor record.

[d]No record.

[e]Signal from wind only.

Table 34e. Summary of results—Detonation Echo.

Station	Azimuth (deg)	Distance (ft)	Set range (psi)	Calibration step (psi)	Arrival time (sec)	p+ (psi)	Time of peak (sec)	p- (psi)	Time of peak (sec)	I+ (psi-sec)	I- (psi sec)
AM-8D (high)	18.53	285	0.20	0.12	0.079,[a] 0.170	0.259	0.274	0.163	1.031	0.0033	0.0793
8S (low)			0.04	0.0206	0.079[a]	—[b]	—[b]	—[b]	—[b]	—[b]	—[b]
AM-9S (high)	19.80	553	0.09	0.0224	~0.413	—[b]	—[b]	—[b]	—[b]	>0.0145	>0.027
9S (low)			0.02	0.0215	0.110,[a] 0.413	—[b]	—[b]	—[b]	—[b]	—[b]	—[b]
AM-10S (high)	19.41	1554	0.05	0.0192	0.210,[a] 1.213	—[b]	—[b]	0.0267	2.046	>0.005	0.0114
10P (low)			0.01	0.008	0.210,[a] 1.235	—[b]	—[b]	—[b]	—[b]	—[b]	—[b]
AM-3S (high)	134.00	2808	0.0275	0.019	2.247	0.0225	2.366	0.0148	3.070	0.0032	0.0064
3P (low)			0.0053	0.010	2.238	0.0187	2.370	0.0158	3.060	0.00305	0.00693
AM-2S (high)	7.08	3163	0.02	0.02	2.540	0.0185	2.627	>0.013	3.362	0.0029	0.0057
2P (low)			0.004	0.0107	2.540	0.0185	2.629	0.0115	3.362	0.00313	—
AM-4S (high)	166.93	4412	0.012	0.0191	3.632	0.0128	3.744	0.0075	4.451	0.00125	0.00277
4P (low)			0.0025	0.010	3.617	0.0075	3.746	0.0053	4.460	0.00084	0.00194
AM-5 (high)	351.14	3942	0.015	0.024	—[c]	—[c]	—[c]	—[c]	—[c]	—[c]	—[c]
1P (low)			0.003	0.0118	—[c]	—[c]	—[c]	—[c]	—[c]	—[c]	—[c]
AM-5S (high)	175.53	6731	0.006	0.010	5.604	0.0089	5.730	0.0063	6.460	0.00145	0.00279
5P (low)			0.0015	0.0057	5.596	0.00875	5.730	0.0061	6.460	0.00140	0.00272
AM-6S (high)	173.30	7640	0.006	0.009	6.360	0.0085	6.496	0.0055	7.245	0.00127	0.00239
6P (low)			0.0015	0.0067	6.407	—[c]	6.490	—[c]	?	—[c]	—[c]
AM-7S (high)	171.34	8622	0.006	0.011	7.195	0.00435	7.332	—[b]	—[b]	0.0011	—[b]
7P (low)			0.0015	0.0101	7.213	0.0038	7.440	0.0044	8.010	0.00117	0.00198

[a] Arrival of ground-transmitted surface wave.

[b] Limited.

[c] No record.

Table 34f. Summary of results—Detonation II-ABCD.

Station	Azimuth[a] (det)	Distance (ft)	Set range (psi)	Calibration step (psi)	Arrival time (sec)	p+ (psi)	Time of peak (sec)	p- (psi)	Time of peak (sec)	I+ (psi-sec)	I- (psi-sec)
AM-8D (high)	324.54	853[b]-1064[c]-1157[d]	0.20	0.245	0.119,[e] 0.817	0.0647	0.925	0.0773	1.656	0.0167	0.0286
8S (low)	(332.09)[f]	(820-1017-1119)[f]	0.06	0.575	0.118,[e] 0.817	0.0628	0.925	0.0770	1.663	0.0166	0.0286
AM-9D (high)	327.64	1134[b]-1334[c]-1437[d]	0.15	0.205	0.996	0.0469	1.161	0.0586	1.896	0.0130	0.0210
9S (low)	(332.36)[f]	(1089-1286-1387)[f]	0.045	0.063	0.996	0.0491	1.162	0.0605	1.888	0.0135	0.0285
AM-10D (high)	26.98	2076[b]-2273[c]-2374[d]	0.09	0.121	1.883	0.0251	2.030	0.0316	2.749	0.0073	0.0131
10S (low)			0.03	0.0335	1.883	0.0248	2.030	—[g]	—[g]	0.0072	>0.0129
AM-3D (high)	118.67	2853[b]-2862[c]-2900[d]	0.075	0.0776	2.487	0.0243	2.532	0.0242	3.300	0.00640	0.01075
3S (low)			0.025	(+0.027-0.028)	2.361	0.0247	2.532	0.0244	3.314	0.00675	0.01075
AM-2S (high)	13.47	3672[b]-3855[b]-3949[d]	0.06	0.0612	3.160	0.0149	3.316	0.0200	4.061	0.00450	0.00810
2S (low)	(14.34)[f]	(3605-3788-3883)[f]	0.02	0.0198	3.161	0.0153	3.317	0.0202	4.062	0.00450	0.00815
AM-4S (high)	158.17	3945[d]-3966[c]-4099[d]	0.06	0.0591	3.403	0.0150	3.522	0.0160	4.254	0.00495	0.00780
4S (low)			0.02	0.0194	3.404	0.0150	3.521	0.0163	4.251	0.00500	0.00780
AM-1S (high)	358.59	4346[b]-4500[c]-4581[d]	0.045	0.0465	3.821	0.0129	3.978	0.0161	4.698	0.00400	0.00600
1F (low)			0.015	0.0141	3.816	0.0102[h]	3.975	0.0168	4.699	0.00335[h]	0.00607
AM-5S (high)	170.55	6125[d]-6196[b]-6333[b]	0.03	0.0039	5.346	0.00989	5.475	0.0104	6.112	0.00317	0.00540
5P (low)			0.01	0.0092	5.338	0.00983	5.484	0.0099	6.121	0.00317	0.00540
AM-6S (high)	168.81	7059[d]-7126[c]-7258[b]	0.03	0.0367	6.218	0.00753	6.342	0.00838	6.994	0.00259	0.00424
6P (low)		(7098-7165-7297)[f]	0.009	0.0086	6.214	0.00769	6.343	0.00844	6.995	0.00265	0.00431
AM-7S (high)	167.28	8062[d]-8127[c]-8255[b]	0.025	0.0205	7.021	0.00550	7.181	0.00765	7.868	0.00238	0.00373
7P (low)			0.009	0.0077	7.019	0.00472	7.199	—[g]	—[g]	0.00230	>0.00370

[a] To midpoint between Charges II-A and II-D.

[b] To Charge II-D.

[c] To Charge II-B.

[d] To Charge II-A.

[e] Direct ground shock arrival.

[f] Inferred from time of positive peak.

[g] Limited.

[h] Positive phase suppressed by RF band width.

Table 34g. Summary of results—Detonation II-EF.

Station	Azimuth (deg)	Distance (ft)	Set range (psi)	Calibration step (psi)	Arrival time (sec)	p+ (psi)	Time of peak (sec)	p- (psi)	Time of peak (sec)	I+ (psi-sec)	I- (psi-sec)
AM-8D (high)	322.73	643[b]-744[c]	0.20	0.245	0.161,[d] 0.51	0.162	0.656	0.126	1.402	0.0346	0.0616
8S (low)	(335.46)[e]	(590-750)[e]	0.06	0.0575	0.160, 0.519	0.162	0.652	0.127	1.403	0.0341	0.0614
AM-9D (high)	327.38	908[b]-1016	0.15	0.205	0.749	0.118	0.896	0.087	1.650	0.0244	0.0418
9S (low)	(334.87)[e]	(853-973)[e]	0.045	0.063	0.749	0.122	0.896	0.090	1.650	0.0251	0.0434
AM-10D (high)	25.62	1846[b]-1960[c]	0.09	0.121	1.556	0.0494	1.781	0.0394	2.502	0.0115	0.0189
10S (low)			0.03	0.0335	1.566	0.0497	1.781	0.0393	2.502	0.0117	0.0189
AM-3D (high)	122.71	2842[c]-2911[b]	0.075	0.0776	2.405	0.0266	2.656	0.0227	3.255	0.00655	0.01050
3S (low)			0.025	(+0.027-0.028)	2.405	0.0283	2.655	0.0223	3.254	0.00692	0.01169
AM-2S (high)	11.82	3443[b]-3565[c]	0.06	0.0612	2.978	0.0265	3.117	0.0231	3.846	0.00700	0.01090
2S (low)	(12.07)[e]	(3375-3498)[e]	0.02	0.0198	2.973	0.0265	3.118	0.0243	3.859	0.00720	0.01115
AM-4S (high)	161.69	4163[c]-4280[b]	0.06	0.0591	3.506	0.0209	3.842	0.0150	4.490	0.00574	0.00901
4S (low)			0.02	0.0194	3.515	0.0211	3.843	0.0148	4.498	0.00501	0.00824
AM-5S (high)	172.43	6415[c]-6538[b]	0.03	0.039	5.508	0.0132	5.831	0.0097	6.462	0.00332	0.00500
5P (low)			0.01	0.0092	5.506	0.0127	5.833	0.0091	6.465	0.00316	0.00480
AM-6S (high)	170.51	7338[c]-7460[b]	0.03	0.0367	6.260	0.00965	6.671	0.0080	7.230	0.00280	0.00408
6P (low)		(7371-7493)[e]	0.009	0.0086	6.260	0.009	6.683	0.00710	7.290	0.00250	0.00380
AM-7S (high)	168.82	8332[c]-8454[b]	0.025	0.0265	7.210	0.0073	7.490	0.00655	8.120	0.00171	0.00394
7P (low)			0.008	0.0077	7.207	0.0057	7.514	0.0070	8.159	0.00199	0.00413

[a]To midpoint between Charges II-E and II-F.

[b]To Charge II-F.

[c]To Charge II-E.

[d]Direct ground shock arrival.

[e]Inferred from time of positive peak.

Table 34h. Summary of results—Detonation II-IJKL.

Station	Azimuth (deg)	Distance (ft)	Set range (psi)	Calibration step (psi)	Arrival time (sec)	p+ (psi)	Time of peak (sec)	p- (psi)	Time of peak (sec)	I+ (psi-sec)	I- (psi-sec)
AM-8D (high)	284.42	635[b]-702[c]-772[d]	0.20	0.245	0.111,[e] 0.383	0.326	0.593	0.180	1.324	0.067	0.1245
8S (low)	(291.84)[f]	(512-570-633)[f]	0.08	0.0575	0.111,[e] 0.388	>0.236[g]	—	0.184	1.302	>0.065	0.1235
AM-9D (high)	60.85	825[b]-890[c]-959[d]	0.15	0.205	0.156,[e] 0.574	0.20	0.771	0.125	1.460	0.048	0.0845
9S (low)	(55.15)[f]	(721-791-864)[f]	0.045	0.063	0.155,[e] 0.572	0.205	0.793	0.130	1.480	0.0495	0.0875
AM-10D (high)	38.97	1642[b]-1722[c]-1804[d]	0.09	0.121	1.343	0.0804	1.596	0.057	2.300	0.0223	0.0380
10S (low)			0.03	0.0335	1.325	0.0773	1.597	0.0554	2.303	0.0225	0.0363
AM-3D (high)	127.97	3228[d]-3310[c]-3391[d]	0.075	0.0776	2.796	0.0432	2.938	0.0329	3.675	0.0111	0.0194
3S (low)			0.025	(+0.027-0.028)	2.775	0.0363	2.937	0.026	3.676	0.0096	0.0157
AM-2S (high)	17.78	3122[b]-3206[c]-3290[d]	0.06	0.0612	2.632	0.0370	2.788	0.0343	3.507	0.0118	0.0225
2S (low)	(18.16)[f]	(3057-3141-3225)[f]	0.02	0.0198	2.633	0.0362	2.788	0.0318	3.507	0.0118	0.0205
AM-4S (high)	160.10	4601[b]-4662[c]-4724[d]	0.06	0.0541	3.938	0.0413	4.146	0.029	4.314	0.00845	0.0149
4S (low)			0.02	0.0194	3.939	—[g]	—[g]	—[g]	—[g]	>0.00820	>0.0141
AM-1S (high)	359.73	3752[b]-3809[c]-3886[d]	0.045	0.0465	3.237	0.0385	3.454	0.0313	4.045	0.0102	0.0166
1P (low)			0.015	0.0141	3.235	0.0361	3.455	0.0235	4.094	0.0102	0.0145
AM-5S (high)	170.69	6816[b]-6887[c]-6958[d]	0.03	0.029	5.835	0.0266	6.123	0.0160	6.833	0.0573	0.00973
5P (low)			0.01	0.0092	5.936	0.0245	6.120	0.0155	6.833	0.00555	0.00965
AM-6S (high)	169.08	7740[b]-7815[c]-7885[d]	0.05	0.0367	6.763	0.0205	6.997	0.0130	7.687	0.00465	0.00805
6P (low)		(7889-7858-7928)[f]	0.009	0.0086	6.761	0.0210	6.996	0.0135	7.687	0.00485	0.00825
AM-7S (high)	167.64	8746[b]-8814[c]-8883[d]	0.025	0.0265	7.563	0.0161	7.826	0.0124	8.431	0.00438	0.00675
7P (low)			0.008	0.0077	7.560	—[g]	—[g]	—[g]	—[g]	>0.00430	>0.00656

[a] To center of square array.

[b] To nearest charge.

[c] To center of square array.

[d] To farthest charge.

[e] Direct ground shock arrival.

[f] Inferred from time of positive peak.

[g] Limited.

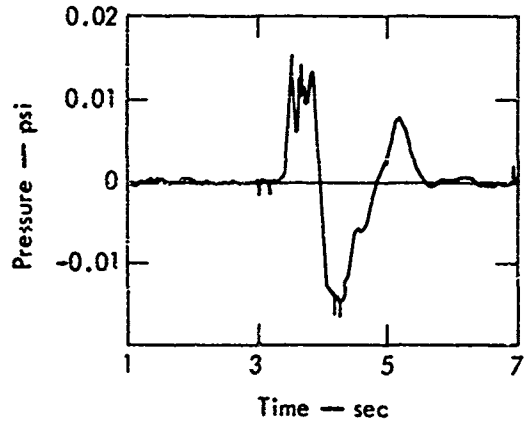

Fig. 150. Air overpressure record at Station AM-4 for Detonation II-ABCD of Phase II (18 August 1970).

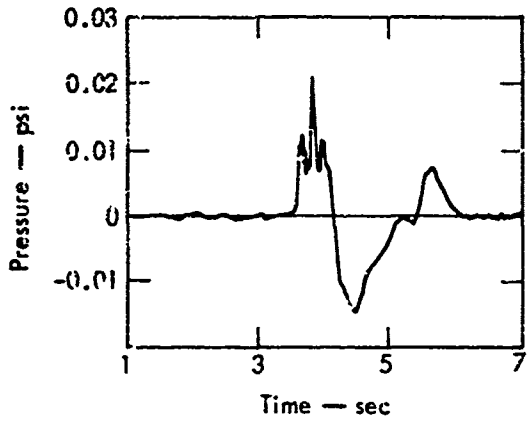

Fig. 151. Air overpressure record at Station AM-4 for Detonation II-EF of Phase II.

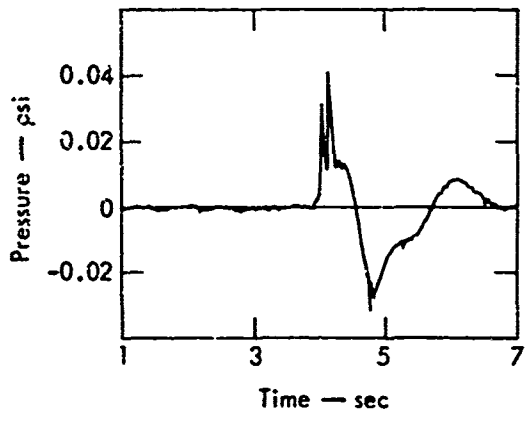

Fig. 152. Air overpressure record at Station AM-4 for Detonation II-IJKL of Phase II (11 August 1970).

indicates better resolution of the individual peaks making up the first positive pulse. Records for the three major detonations of Phase II, II-ABCD, II-EF, and II-IJKL, are shown in Figs. 150 through 152. These records indicate a very complex first positive pulse for each detonation. All records are characterized by a large negative pulse (almost as large as the first positive pulse,, and a second positive pulse.

DISCUSSION OF RESULTS

Arrival Times

Arrival times of the beginnings of the first air-transmitted signals could not always be identified with precision. Times of peak overpressures, because peaks were sharp, ordinarily were identified with an accuracy of ±2 msec.

Ambient pressure and temperature were not measured at detonation times, but, if sea-level pressure and a temperature of 83°F are assumed, sonic velocity would have been 1145 ft/sec. Plotting of the arrival time data gave an estimated velocity of 1180 ft/sec. Differences between this measured shock velocity and ambient sound velocity were within variations attributable to overpressure in the blast wave and to relatively strong winds at shot times.

Peak Pressures

Phase I

Peak overpressures and negative pressures are plotted vs distance in Figs. 153 through 157 for the five detonations of Phase I. A linear least-squares-fit line was drawn for both positive and

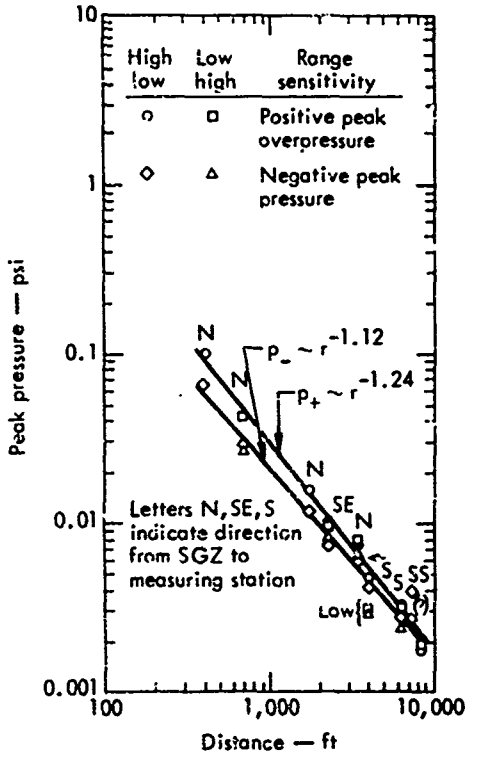

Fig. 153. Measured peak pressure vs distance for 1-ton Alpha detonation of Phase I.

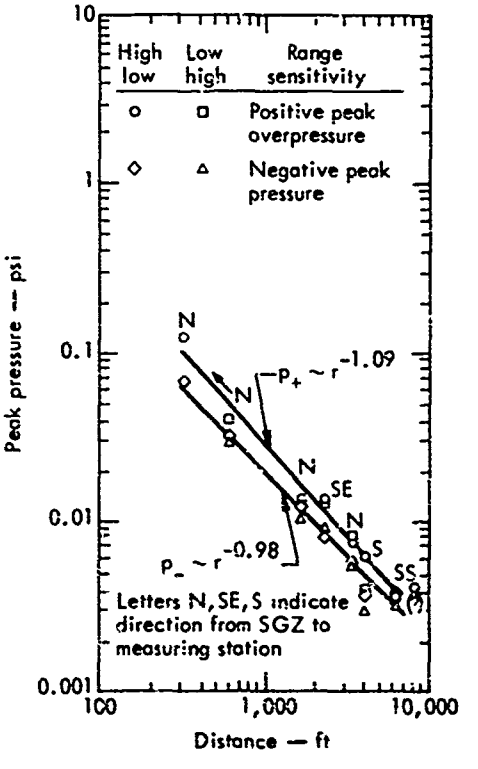

Fig. 154. Measured peak pressure vs distance for 1-ton Bravo detonation of Phase I.

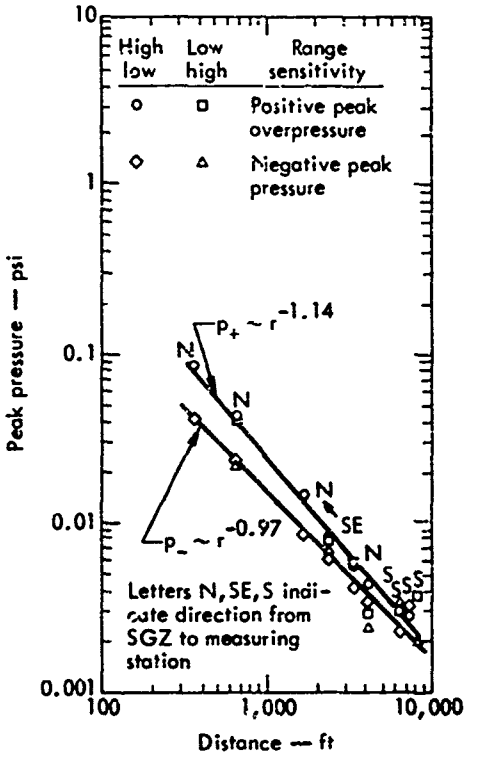

Fig. 155. Measured peak pressure vs distance for 1-ton Charlie detonation of Phase I.

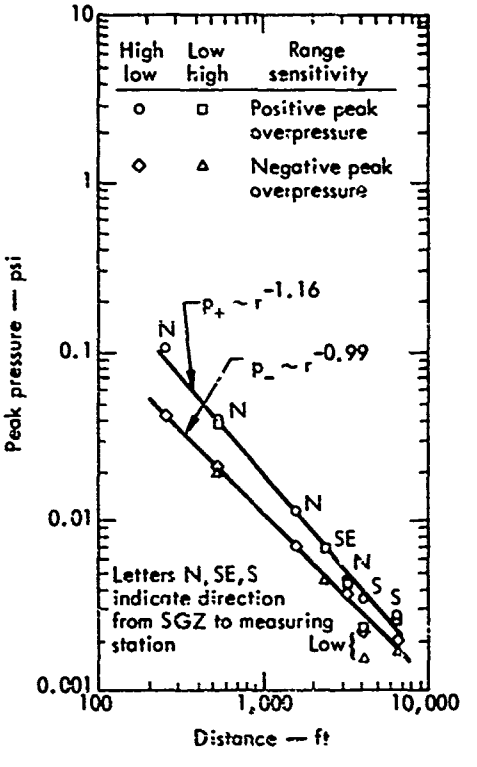

Fig. 156. Measured peak pressure vs distance for 1-ton Delta detonation of Phase I.

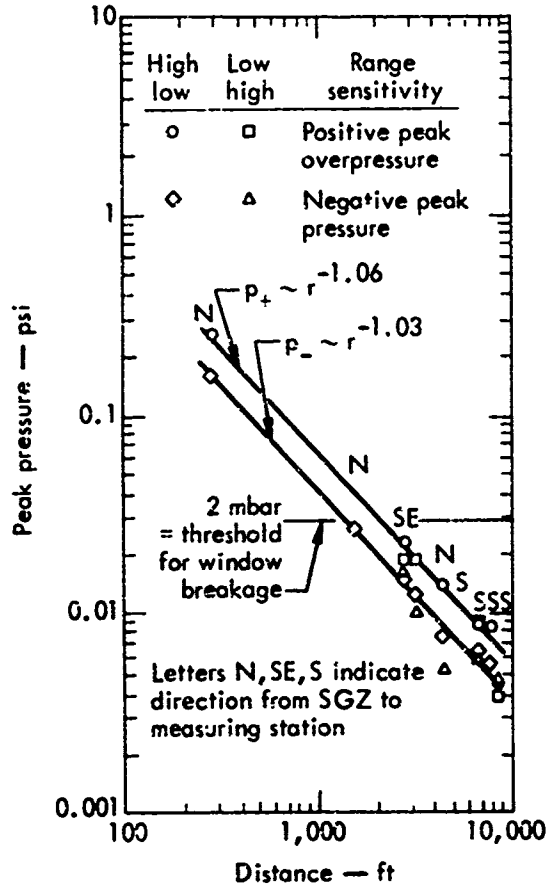

Fig. 157. Measured peak pressure vs distance for 10-ton Echo detonation of Phase I.

negative peaks. There is a slightly greater rate of attenuation of peaks for the higher-frequency positive-phase amplitudes than for those of the lower-frequency negative-phase, implying a change in waveform with distance.

Because high ambient wind velocity affects pressure attenuation with distance, some azimuthal variation was to be expected from the high winds. However, it was difficult to define clearly any trends, and it was concluded that whatever azimuthal effects existed were no larger than the scatter characteristic of the airblast measurements.

Measured peak overpressures are compared with predictions in Table 35 and in Fig. 158. Ground-shock-induced peak overpressures were five times those predicted on the basis of measurements from NM detonations in Albuquerque alluvium. This result suggested especially good coupling of the explosion to the medium, as well as effective shock transmission through the medium. This, in turn, led to the comparison in Fig. 159 with airblast from underwater explosions.[38-40] Agreement of Tugboat peak overpressures with air-transmitted water-shock-induced peak overpressures from other underwater explosions was excellent, attesting that the effect of coral limestone on explosion coupling and shock transmission to the surface was small indeed.

Table 35. Comparison of predicted and measured peak overpressure—Phase I.

Detonation	Scaled dob ($ft/lb^{1/3}$)	Peak overpressure predicted at 50 $ft/lb^{1/3}$ (psi)	Peak overpressure measured at 50 $ft/lb^{1/3}$ (psi)
Alpha	1.38	0.019	0.06
Bravo	1.42	0.015	0.054
Charlie	1.72	0.009	0.046
Delta	2.05	0.0068	0.037
Echo	1.58	0.01	0.050

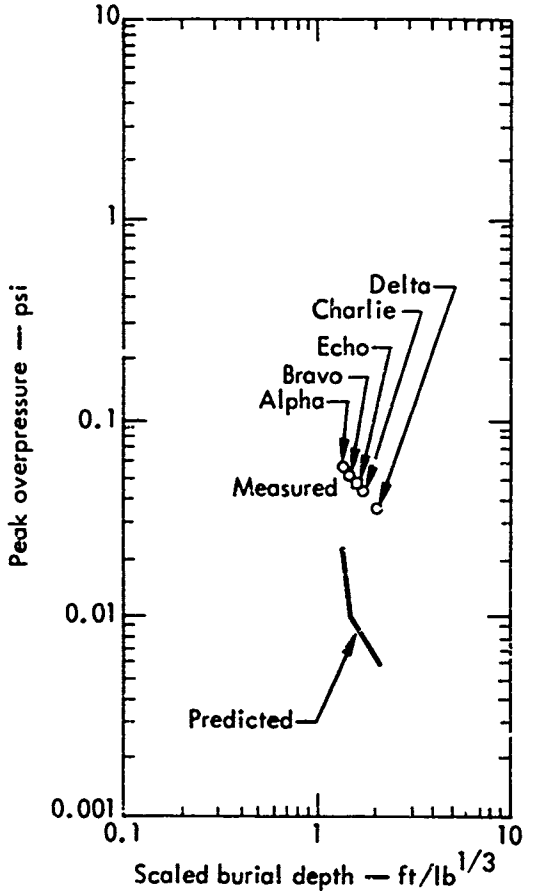

Fig. 158. Phase I peak overpressures predicted and measured at scaled distance of 50 ft/lb$^{1/3}$.

An evaluation of the risk of damage from airblast was made based on the Phase I Echo observed peak pressures. An overpressure of 2 mbar is often accepted as a threshold for breakage of large windowpanes. No structure with glass was closer than about 2800 ft from Detonation Echo. The closest station with windowpanes (Spencer Park) and all more-distant locations were well below this threshold. Actually, such a threshold does not exist. Reed[41] showed that the probability of glass breakage increased as the 2.78 power of overpressure and could be predicted from the empirical relationship:

$$D = 3.71 \times 10^{-3} A^{1.22} \Delta p^{2.78},$$

where D is the number of broken panes per thousand, A is the individual pane area in square feet, and Δp is overpressure in millibars. This relation gives the results shown in Table 36 for he 10-ton detonation.

It was clear that the probability of glass breakage was extremely small and that the Roth estate was the most vulnerable. Windows at the hotel were especially well-mounted and the calculated probability for that location was certainly an overestimate.

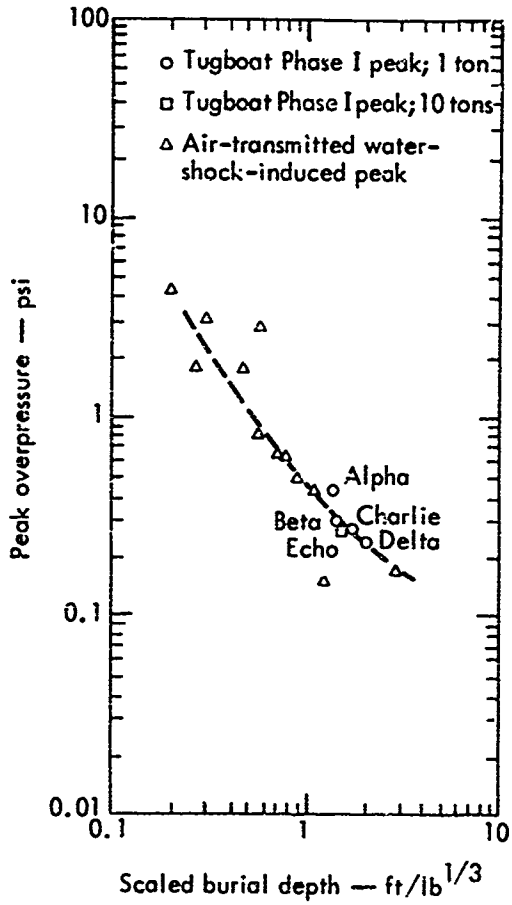

Fig. 159. Comparison of airblast from underwater detonations and Phase I detonations of Project Tugboat at a scaled distance of 10 ft/lb$^{1/3}$.

Table 36. Estimate of risk of damage from airblast for Detonation Echo.

Station	Location	Pane size (sq ft)	Over-pressure (mbar)	Probability of breaking a given pane
AM-3	Spencer Park	1	1.53	0.000012
AM-4	Roth estate	35	0.94	0.00024
AM-1	Doi store	30	0.82	0.00014
AM-7	Mauna Kea Beach Hotel	81	0.52	0.00013
AM-7	Mauna Kea Beach Hotel	22.5	0.52	0.000027

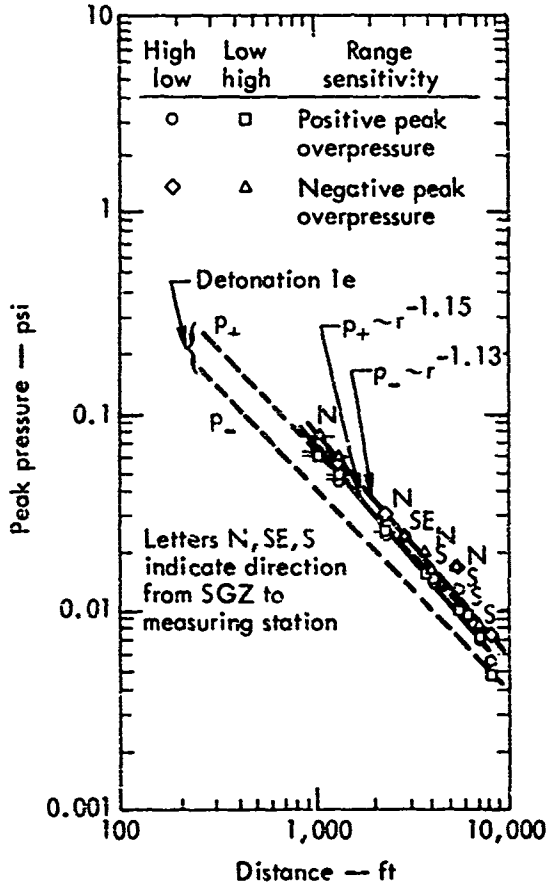

Fig. 160. Peak pressure vs distance for Detonation II-ABCD.

Since four 10-ton charges were planned for each Phase II detonation, the maximum probabilities of breakage from these charges (assuming equal distances perpendicular to the rows and comparable meteorology) were predicted as $22\,[(4^{0.8})^{2.78}]$ times the probability for Detonation Echo, or about 0.005 for the Roth estate.

Phase II

Detonation II-ABCD peak pressures are plotted in Fig. 160. The most unusual aspect revealed by the plot is that negative peaks were about 20% larger than positive peaks. Positive peaks for the station farthest south (AM-8) were low, due probably to the station's location which was on the ground where it was shielded from the direct line of sight to SGZ by the hotel. The negative pulse with its larger duration had a peak not appreciably affected.

In an experiment[30] in dry soil, examination was made of the ratios of pressure perpendicular to a row to pressure off the end of the row as a function of the number of charges in the row. Results showed that the ratio for ground-shock-induced positive peaks was close to 1 for spacing as large as the 100 ft (3.7 ft/lb$^{1/3}$) of Detonation II-ABCD. For Station AM-3, which was nearly perpendicular to the row, the ratio with respect to the rest of the line (most of which was not precisely off the end of the row) was 1.25.

Figure 161 is a plot of peak pressure vs distance for Detonation II-EF. Again,

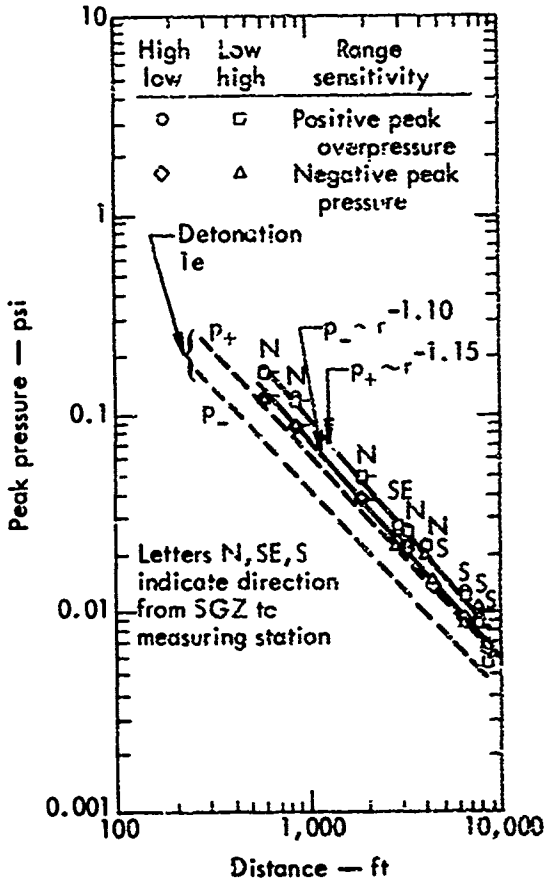

Fig. 161. Peak pressure vs distance for Detonation II-EF.

the results of Detonation Echo have been added for comparison. For Detonation Echo, peak overpressures were 50% greater than negative peaks, while for Detonation II-EF, positive peaks varied from 13 to 39% greater than peak negative pressures. An exception was the record obtained at Station AM-7, where positive peaks were only 80% of the negative peaks, again attributable to shielding by the hotel. The negative peak at Station AM-7 was consistent with those of other stations.

Station AM-3 showed a positive peak which was low by comparison with other stations, as might be the case were the wave propagating upwind. However, the wave was propagating downwind, and wind velocity was quite low.

Measured peak pressures are plotted vs distance in Fig. 162 for Detonation II-IJKL. In this case all four charges detonated satisfactorily and positive peak overpressures were 50% greater than negative peaks.

Probabilities of glass breakage for Detonation II-IJKL were computed as for the Echo detonation, yielding the results given in Table 37.

Maximum probability of breakage shifted from the Roth estate on the Echo detonation to the Doi store on the Phase II, II-IJKL detonation. Again, probabilities at the hotel were certainly overestimates.

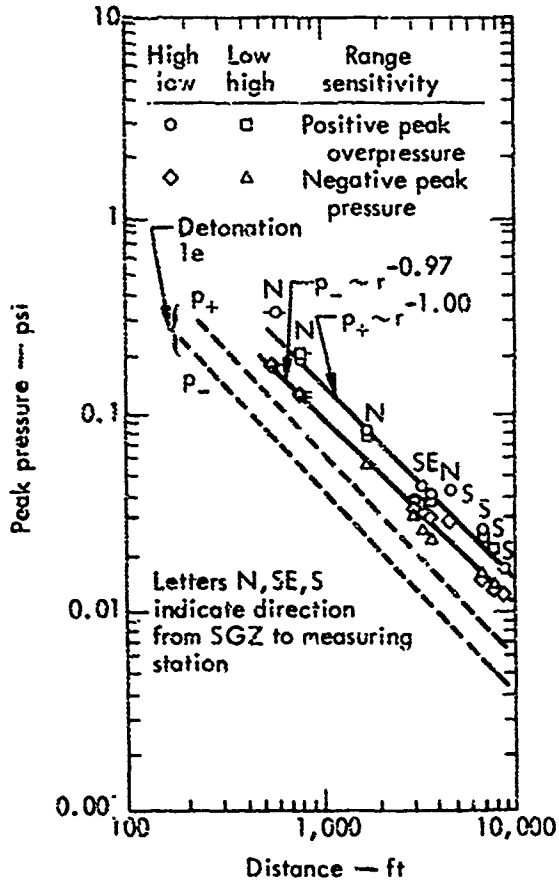

Fig. 162. Peak pressure vs distance for Detonation II-IJKL.

Table 37. Estimate of risk of damage from airblast for Detonation II-IJKL.

Station	Location	Pane size (sq ft)	Over-pressure (mbar)	Probability of breaking a given pane
3	Spencer Park	1	3.05	0.00008
4	Roth estate	35	2.18	0.0025
1	Doi store	30	2.72	0.0038
7	Mauna Kea Beach Hotel	81	1.29	0.0016

Although probabilities of breakage were greater than for the single charge, they were acceptably small for a field operation.

Impulse

Phase I

Even where wind noise is appreciable, positive-phase peak overpressures can be determined with reasonable accuracy if the rise between arrival and the peak is clearly defined. However, the records show that impulse included an effect of wind. Measured impulses, therefore, were adjusted by defining arrival time, fixing zero pressure and impulse at arrival time, and adding or subtracting either a constant or linear pressure variation from the pressure-time record to achieve an impulse-time record of characteristic shape. These adjusted impulse values, both positive and negative, are plotted vs distance in Figs. 163 through 167.

For all detonations, negative-phase impulse was larger than positive-phase impulse. Midrange ratios of negative-phase to positive-phase impulse were 1.7, 1.75, 1.75, 2.25, and 2, respectively, for Detonations Alpha through Echo. In Fig. 168, values for positive-phase impulse are compared as a function of scaled burial depth at a scaled distance of 50 ft/lb$^{1/3}$. When the positive-phase impulse of Detonation Echo was scaled to 1 ton for comparison, it fell below the impulses for the 1-ton detonations. (Agreement was much better for negative-phase

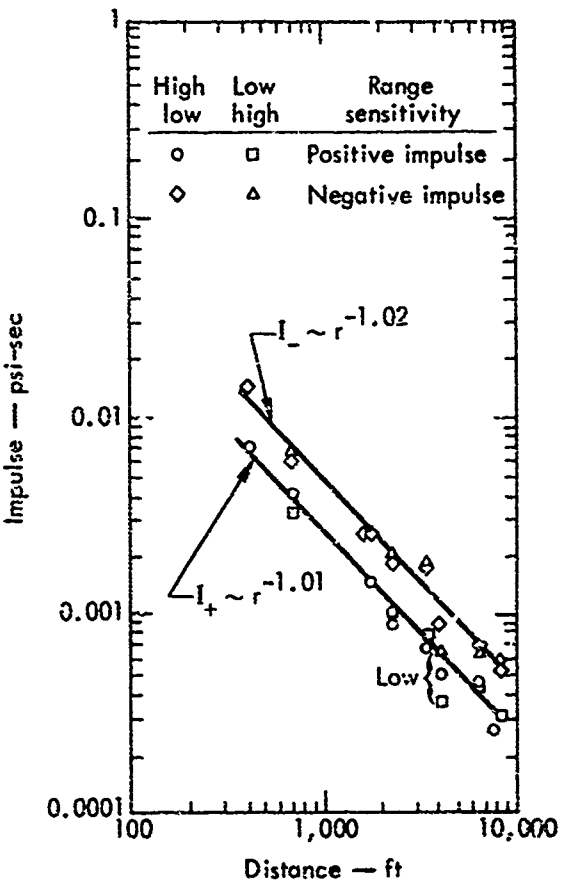

Fig. 163. Impulse vs distance for 1-ton Alpha detonation.

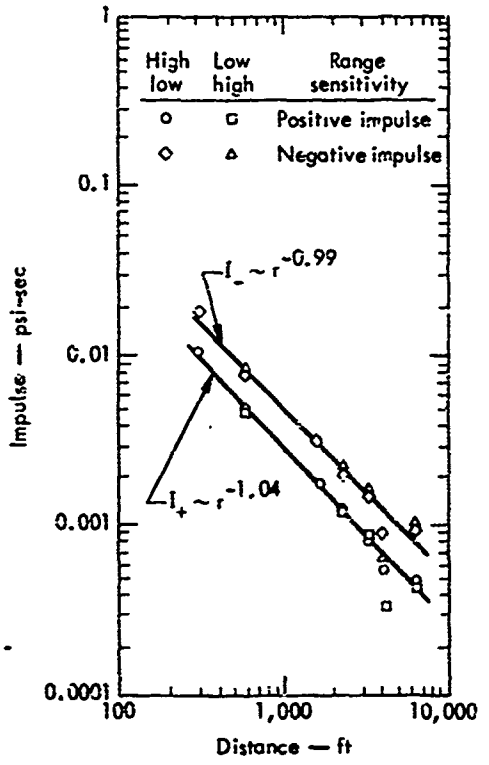

Fig. 164. Impulse vs distance for 1-ton Bravo detonation.

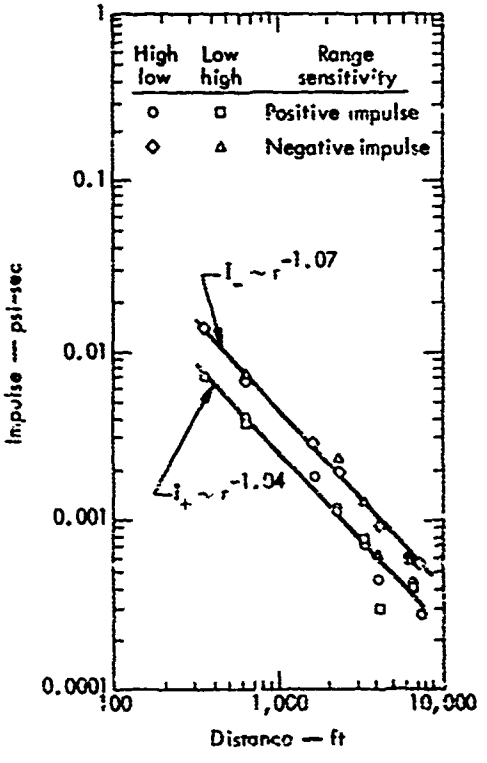

Fig. 165. Impulse vs distance for 1-ton Charlie detonation.

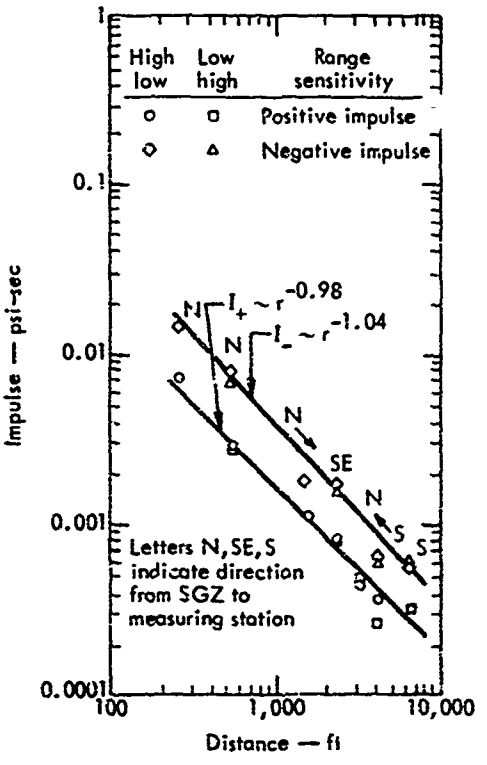

Fig. 166. Impulse vs distance for 1-ton Delta detonation.

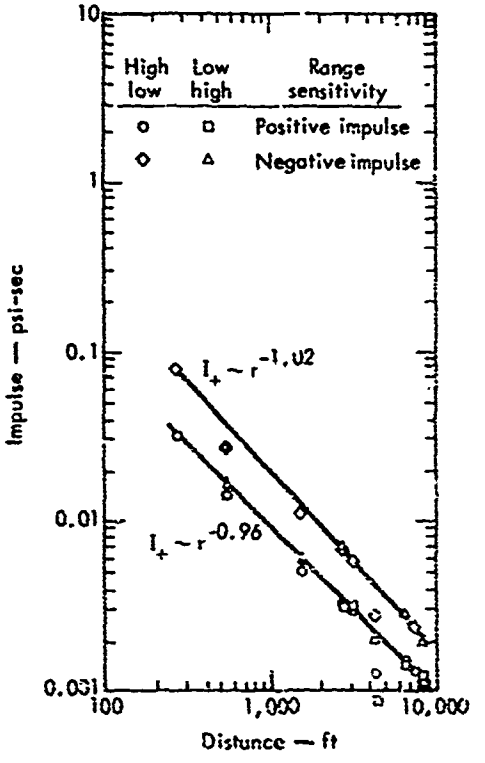

Fig. 167. Impulse vs distance for 10-ton Echo detonation.

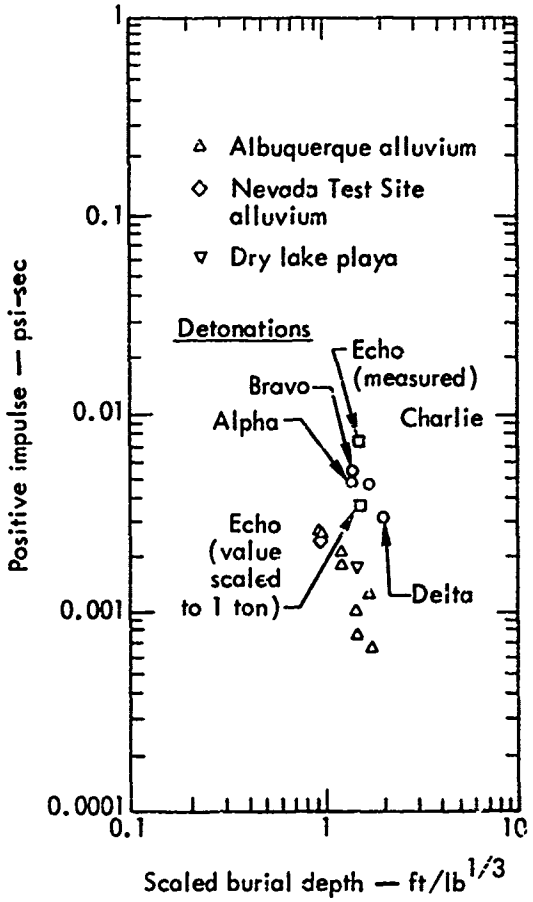

Fig. 168. Positive impulse for Phase I events.

impulse.) This low impulse was probably due to a reduction in pressure between the two pressure spikes which occurred on most Echo records, but a reason for this reduction was not obvious.

Direct airblast measurements have not often been made as far out as 50 ft/lb$^{1/3}$. Unextrapolated data available for comparison with any but the closest Tugboat stations were sparse. Data scaled to 1 ton were added to Fig. 168 for comparison, including one detonation in Nevada Test Site alluvium, one in dry lake playa, and eight in Albuquerque alluvium. Tugboat impulses were roughly five times those from detonation in soil—the same multiple found for peak overpressure. This result was quite unexpected, inasmuch as the positive impulse for shots in soil included contributions of both the ground-shock-induced and gas-venting pulses, whereas no gas-venting pulse was identified in the Tugboat Phase I measurements.

Gas-venting pulses were not discernible in either these Tugboat Phase I records or the Pre-Gondola III records.[37] In both cases motion-picture films showed almost uninterrupted mound growth into a high vertical cylinder. Venting of explosive gases appeared relatively late, by which time the cavity had grown to dimensions permitting cavity pressures to approach ambient pressure. (In dry soils cavity gases vent relatively earlier, while the mound is dome-shaped and cavity pressures are still relatively high.) Venting times for Tugboat Phase I were estimated from motion pictures to be 120, 130, 200, 220, and 200 msec, respectively, for the Phase I detonations. Because positive-phase durations for the 1-ton detonations were about 250 msec, a gas-venting pulse, were it to be observed, would occur just before crossover. It is possible (1) that gas pressure could cause the mound to grow at a higher velocity and (2) that the mound-growth piston could impart some of the gas pressure impulse to the single pulse which was observed.

Phase II

Impulse vs distance is plotted in Figs. 169 through 171 for the three detonations of Phase II. When the entire blast line was considered, rates of attenuation for the three multiple-charge detonations were close to that of the single-charge detonations. Another common

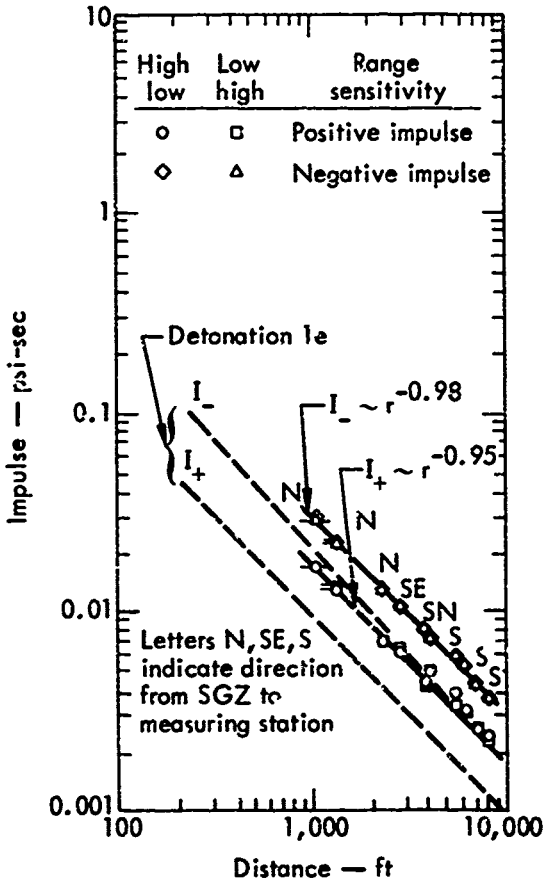

Fig. 169. Impulse vs distance for II-ABCD detonation.

feature was that the difference between positive and negative impulse was always less for the multiple-charge detonations than for the single-charge detonation.

Ratios of the multiple-charge impulse to the single-charge impulse increased from Detonation II-ABCD through Detonation II-IJKL and were roughly equal to the number of charges, if it is assumed the two low-order detonations of II-ABCD made little contribution. The time delay between the two charges of II-EF provided greater impulse than the simultaneous detonation of II-ABCD where the effective number of charges was greater than 2 but less than 4.

Five 64-lb charges in a square array with one charge in the center gave ratios of positive impulse for the array to impulse for a single charge of 3.23 for a charge spacing of 2.5 ft/$lb^{1/3}$ and 3.05 for a charge spacing of 4 ft/$lb^{1/3}$. The corresponding value for the four charges of II-IJKL was larger. Either because of the medium or the type of explosive, the multiple charges of the Tugboat series produced more airblast relative to a single charge than was seen for TNT charges in a dry soil.

Comparison of Waveforms

Four charges were detonated simultaneously in Detonation II-ABCD. Charges

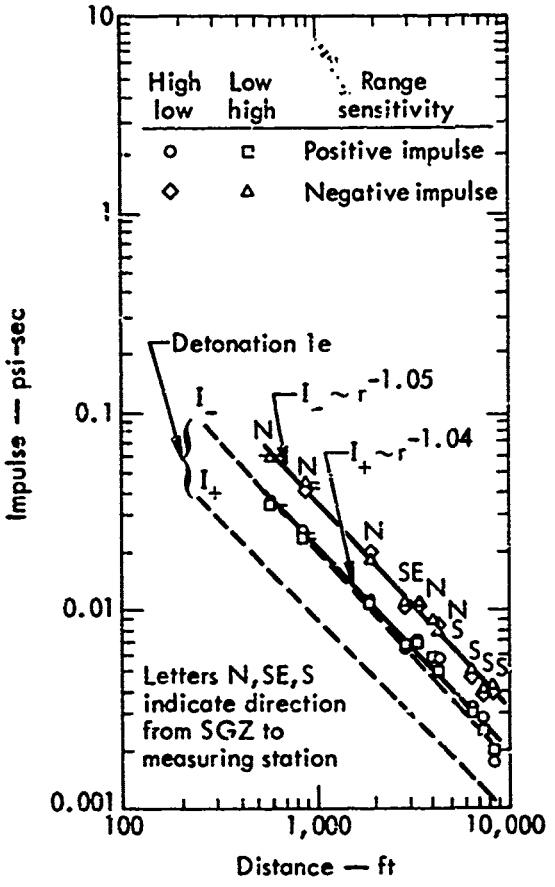

Fig. 170. Impulse vs distance for II-EF detonation.

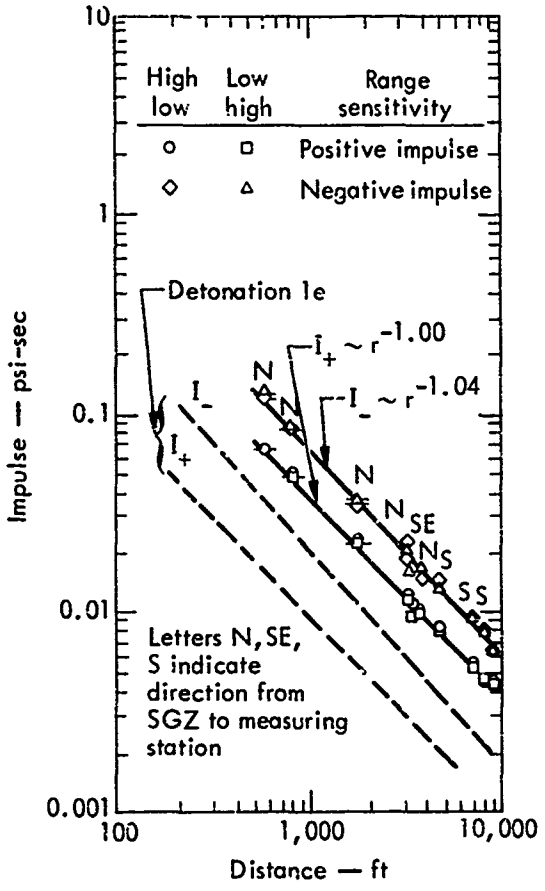

Fig. 171. Impulse vs distance for II-IJKL detonation.

II-A and II-B were high-order detonations with the plume from II-A initially lagging behind that of II-B. Plumes of II-C and II-D were small, indicating low-order detonations even though the shocks from all four charges appeared to reach the water surface at about the same time.

Stations to the north which were off the end of the II-ABCD row of charges showed maximum overpressure shortly after shock arrival, followed by a sharp decay, then rose to a second but smaller peak 120 msec after the first, followed by a third small peak about 140 msec later, and that in turn followed by a still smaller peak about 200 msec after the third (Fig. 172). Thus, although four peaks were identified, for the four-charge event intervals between peaks made it clear that no one peak should be identified with a particular charge.

Station AM-3 (Fig. 173), which was more nearly broadside to the row, also showed the high initial peak followed by a sharp decay and an irregular rise to a final peak of lesser amplitude about 380 msec after the first peak. This time interval was much greater than could be

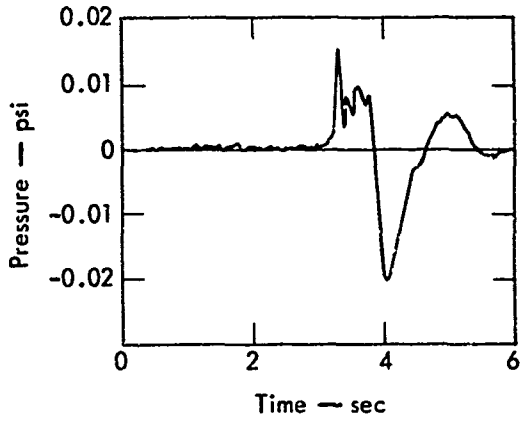

Fig. 172. Station AM-2 record for Detonation II-ABCD, typical of stations to north of SGZ (14 August 1970).

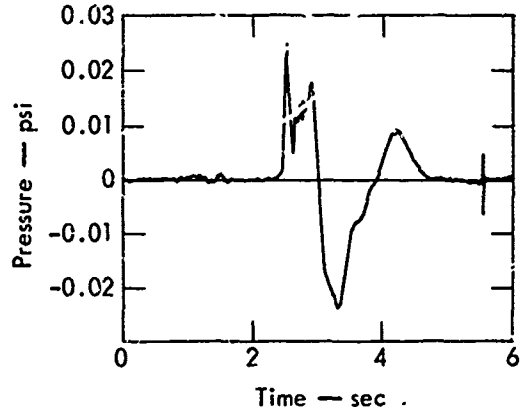

Fig. 173. Station AM-3 record for Detonation II-ABCD showing slightly different wave form broadside to row (14 August 1970).

explained on the basis of the space interval between charges in the row.

Station Am-4 to the south (see Fig. 150) showed three peaks of approximately equal amplitude with an interval of about 150 msec between each pair. Peaks at Stations AM-5 and AM-6 were similar, whereas at Station AM-7 the peaks were indistinct.

Charges for Detonation II-EF were to be fired with a delay of 0.1 sec between charges, beginning with Charge II-E. Only Charges II-E and II-F detonated. Because spacing between charges was 120 ft, shock transit time (assuming spacing between charges equaled spacing between points at which ground-shock-induced pulses from each charge became air transmitted) was about 0.1 sec, and it was expected that to the north the peaks would be superimposed. Actually, two peaks were observed (Fig. 174) and were separated by about 100 to 120 msec.

At Station AM-3 (Fig. 175) the waveform was quite confusing—a dominant peak flanked earlier and later by secondary peaks of lower amplitude. Two approximately equal peaks separated by 0.1 sec would have been expected at a station perpendicular to the row.

At Stations AM-4, AM-5, AM-6, and AM-7 waveforms were similar to that at Station AM-3, whereas two approximately equal peaks separated by about 0.2 sec were anticipated.

Detonation II-IJKL was a simultaneously detonated square array. Had pressure been measured directly opposite a side of the square, a peak from the near two charges followed by one from the far two charges would have been expected. Measured off the corner of the array, a peak from the near charge would have been seen, followed by a dominant peak from the two equidistant charges, followed by a final peak from the charge at the opposite corner.

Station AM-8 was almost precisely opposite a side of the square. The waveform showed two pronounced peaks, the second larger than the first, followed by two peaks smaller than either of the first two. The waveform at Station AM-9

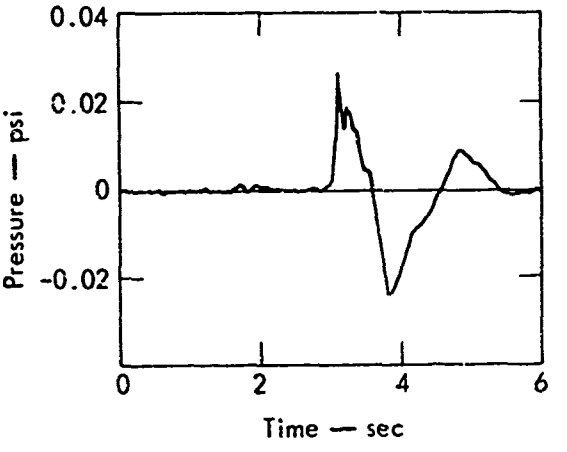

Fig. 174. Station AM-2 record for Detonation II-EF showing two primary peaks in first positive pulse.

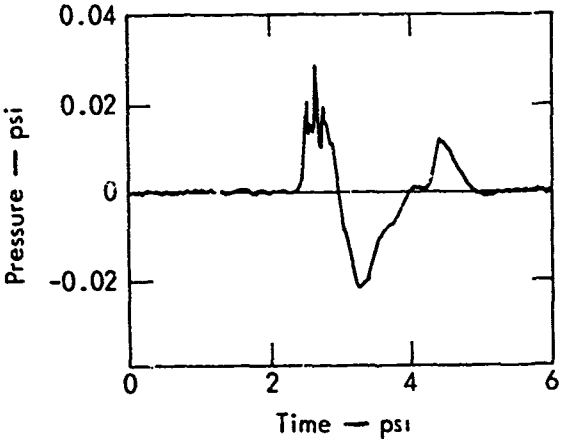

Fig. 175. Station AM-3 record for Detonation II-EF showing very complex first positive pulse.

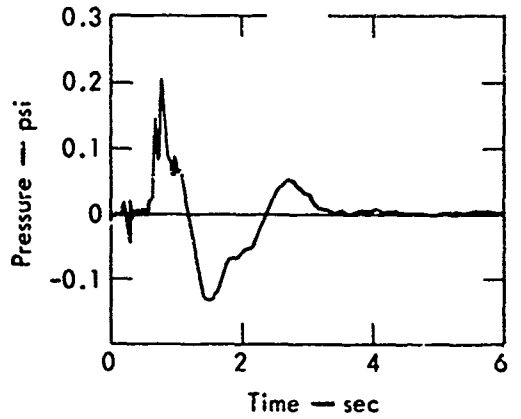

Fig. 176. Station AM-9 record for Detonation II-IJKL showing two prominent peaks in first positive pulse as would be expected in direction perpendicular to one side of array (30 July 1970).

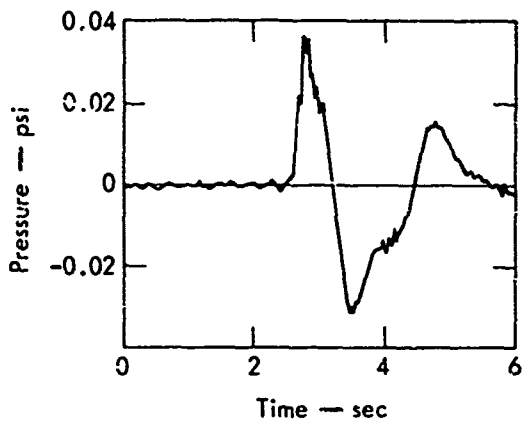

Fig. 177. Station AM-2 record for Detonation II-IJKL (30 July 1970).

(Fig. 176) was similar, even though its location was displaced from the axis of the square. Stations AM-2 (Fig. 177) and AM-4 were approximately opposite a corner of the square and waveforms were about as expected. Waveforms at Stations AM-1 and AM-10 (Fig. 178), displaced slightly from the diagonal axis of the square, were similar. It was anticipated that Stations AM-3, AM-5, AM-6, and AM-7 would have waveforms like

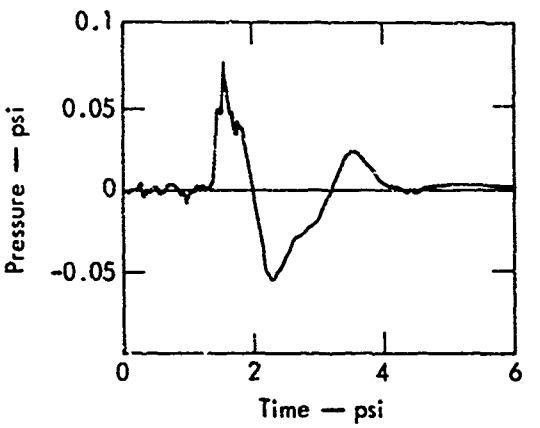

Fig. 178. Station AM-10 record for Detonation II-IJKL (30 July 1970).

those of Stations AM-1 and AM-10. Waveforms of Stations AM-3 and AM-7 were close to those of Stations AM-1 and AM-10, but the waveforms for Stations AM-5 and AM-6 were more nearly similar to those of Station AM-4. The abrupt change between Stations AM-6 and AM-7 cannot be explained, inasmuch as the difference in azimuth was no more that 2 deg.

Attenuation of Peak Pressure and Impulse

Table 38 gives results of log-log least-square fits to data of the Phase II detonations and a comparison with Detonation Echo. Separate fits are provided for north and south lines and for all stations combined. Primarily because of low positive peaks at Station AM-8, attenuation rates along the south line were greater than along the entire line. On Detonation II-IJKL high positive and negative peaks at Station AM-4 contributed to the greater attenuation rate along the south line. Along the north line, attenuation rates were quite similar to those along the entire line.

Table 38. Summary of attenuation equations for airblast data.

	II-ABCD	II-EF	II-IJKL	Echo
Peak positive overpressure				
All stations	$\Delta p+ = 189r^{-1.146}$	$\Delta p+ = 284r^{-1.153}$	$\Delta p+ = 151r^{-1.002}$	$\Delta p+ = 97r^{-1.058}$
South only	$\Delta p+ = 1856r^{-1.406}$	$\Delta p+ = 1483r^{-1.608}$	$\Delta p+ = 6835r^{-1.418}$	$\Delta p+ = 10r^{-0.794}$
North only	$\Delta p+ = 187r^{-1.150}$	$\Delta p+ = 125r^{-1.037}$	$\Delta p+ = 50r^{-1.167}$	$\Delta p+ = 127r^{-1.097}$
Peak negative pressure				
All stations	$\Delta p- = 208r^{-1.134}$	$\Delta p- = 154r^{-1.102}$	$\Delta p- = 84r^{-0.972}$	$\Delta p- = 56r^{-1.030}$
South only	$\Delta p- = 126r^{-1.083}$	$\Delta p- = 223r^{-1.153}$	$\Delta p- = 3793r^{-1.399}$	$\Delta p- = 851r^{-1.341}$
North only	$\Delta p- = 114r^{-1.051}$	$\Delta p- = 54r^{-0.952}$	$\Delta p- = 99r^{-0.997}$	$\Delta p- = 72r^{-1.076}$
Positive impulse				
All stations	$I+ = 12r^{-0.953}$	$I+ = 28r^{-1.038}$	$I+ = 38r^{-1.000}$	$I+ = 6.7r^{-0.960}$
South only	$I+ = 36r^{-1.073}$	$I+ = 919r^{-1.441}$	$I+ = 54r^{-1.039}$	$I+ = 4.7r^{-0.920}$
North only	$I+ = 22r^{-1.034}$	$I+ = 11r^{-0.91}$	$I+ = 38r^{-1.000}$	$I+ = 7.7r^{-0.981}$
Negative impulse				
All stations	$I- = 27r^{-0.983}$	$I- = 51r^{-1.050}$	$I- = 88r^{-1.039}$	$I- = 21r^{-1.016}$
South only	$I- = 44r^{-1.039}$	$I- = 156r^{-1.181}$	$I- = 329r^{-1.185}$	$I- = 293r^{-1.313}$
North only	$I- = 37r^{-1.031}$	$I- = 32r^{-0.982}$	$I- = 105r^{-1.063}$	$I- = 26r^{-1.052}$

Table 39. Comparison of airblast data from single- and multiple-charge detonations.

	Ratio of multiple-charge airblast overpressure to single-charge airblast overpressure		
	II-ABCD	II-EF	II-IJKL
Peak positive overpressure	0.95	1.39	2.46
Peak negative pressure	1.73	1.68	2.59
Positive impulse	1.86	2.15	3.94
Negative impulse	1.59	1.84	3.33

Comparison of Single-Charge and Multiple-Charge Peak Pressure and Impulse

Table 39 summarizes the comparison of airblast parameters for Phase II detonations with the single-charge Echo detonation. The comparison was made from fits to the entire line at an approximately midrange distance of 3000 ft. Variations of peak pressures with azimuth about each of the three shots were relatively small because (1) on II-ABCD only Station AM-3 was close to perpendicular to the row, (2) on II-EF no stations were precisely perpendicular to a line between the two charges detonated, and (3) on II-IJKL no consistent azimuthal differences in waveform were evident. Fits to all the data may give pressures higher by a few percent than would have been obtained solely off the ends of the rows.

Average ratios of overpressure from the Phase II multiple-charge detonations to overpressure from the Echo detonation are given in Table 39. The spacings for Phase II charges were greater than any for which previous information was available. Detonation II-ABCD showed a multiple- to single-charge ratio of peak ground-shock-induced overpressure of 0.95. Corresponding values for rows of 64-lb charges at closer spacing approximated 1.

For the square array detonation, II-IJKL, a ratio of 2.46 (Table 39) was observed for positive peaks. Data from five 64-lb charges gave 2.85 for the spacing of 2.5 ft/lb$^{1/3}$ and 1.75 for 4 ft/lb$^{1/3}$. It was anticipated that the Detonation II-IJKL ratio would be less than 1.75 both because of the larger spacing (4.4 ft/lb$^{1/3}$) and because there were only four, rather than five, charges in the array.

SUMMARY

Positive peak overpressures and positive phase impulse from the Tugboat Phase I explosions were about five times those predicted on the basis of measurements made from cratering explosions in soil. Peak overpressures estimated by applying multiple-charge overpressure amplification factors to the Detonation Echo results were small enough that the possibility of blast damage on the Phase II detonations was expected to be acceptable.

Peak overpressures for the II-ABCD, II-EF, and II-IJKL multiple-charge Phase II detonations were approximately 1, 1.4, and 2.5 times that for a single-charge detonation having a yield equal to one of the charges in the multiple-charge array. Positive impulses were about 2, 2, and 4 times that for a comparable single charge. These data indicate that in Detonation II-ABCD, Charges II-C and II-D contributed very little to the positive phase impulse observed. The data pertaining to the reduction of overpressure from the delay of successive charge detonations in a row were not adequate to draw more definite conclusions.

No glass was broken, and estimates of the probability of breakage based on maximum measured peak overpressures were never greater than five panes per thousand.

CONCLUSIONS

Project Tugboat has provided data for airblast from detonations in submerged coral which were not previously available. Ground-shock-induced peak overpressures were about five times those produced by TNT and NM in dry soil but close to those produced by detonations in water and in a saturated clay shale. Gas venting peaks were very small (as they were for NM detonations in saturated clay shale) and could be identified only by time of arrival. The conclusion is that the magnitude of the gas-venting pulse is more dependent on medium than on explosive type. The relation of peak overpressures to cavity pressure at the time of mound rupture should be investigated in future experiments in water-saturated media. Possibly because of the two low-order detonations, the waveforms of Detonation II-ABCD were not as expected. Detonation II-EF should have had nearly single-peak waveforms to the north and double peaks separated by about 0.2 sec to the

south. Instead, double peaks were separated by about 0.1 sec to the north, and at most other stations the peaks consisted of a dominant peak flanked by peaks of lesser amplitude. The conclusion is that the origin of all of the individual peaks in the first positive phase is not fully understood.

Section 8
Pressure, Acceleration, and Velocity Measurements in Water Surface Layer

PROGRAM OBJECTIVES

The K-Division of the Lawrence Livermore Laboratory, fielded an instrumentation program designed to measure shock pressure, velocity, and acceleration in the surface water layer over five of the twelve 10-ton charges detonated during Phase II. The objective of the program was to develop instrumentation and fielding techniques that would furnish the experimental data needed to determine the amount of energy imparted to the water by the explosions. This information can be used to compare with computer calculations in an effort to understand the cratering phenomenology in water-covered and saturated media.[42]

EXPERIMENTAL PROCEDURES

The twelve charges were planned for detonation in three salvos of four charges each. Two of the planned detonations were instrumented. On the first salvo (II-ABCD), one canister was located on the surface (WS-1) and one submerged to about 2 ft off the coral surface (UW-1). Both canisters were over Charge II-D. On the last salvo (II-IJKL), a submersible canister was located over each of the four charges about 2 ft off the coral surface.

The instrumentation canisters housing the transducers and associated electronics were attached to the explosive fill pipes. This was done with 10-ft aluminum beams in such a way as to allow only vertical motion of the instruments. This technique was used to insure proper gage orientation to the shock wave regardless of the wave action at detonation time. The canisters were designed to be about 10% buoyant in sea water and were set free from the aluminum arms and fill pipe by means of explosive bolts a few milliseconds before detonation. Signal transmission was via a special water-blocked, neoprene-jacketed RG-58 electronic signal cable to the recording trailer located about 1500 ft from shore on the coral fill area. A styrofoam float near each canister was used to store coiled signal cable. This coiled cable was designed to supply additional recording time by uncoiling with the expanding water surface. In addition, an anchored rope float line was used to deploy the cables to shore. This prevented cable damage from the sharp coral formations. Figure 179 is a plan view of the charge array and the K-Division instrumentation.

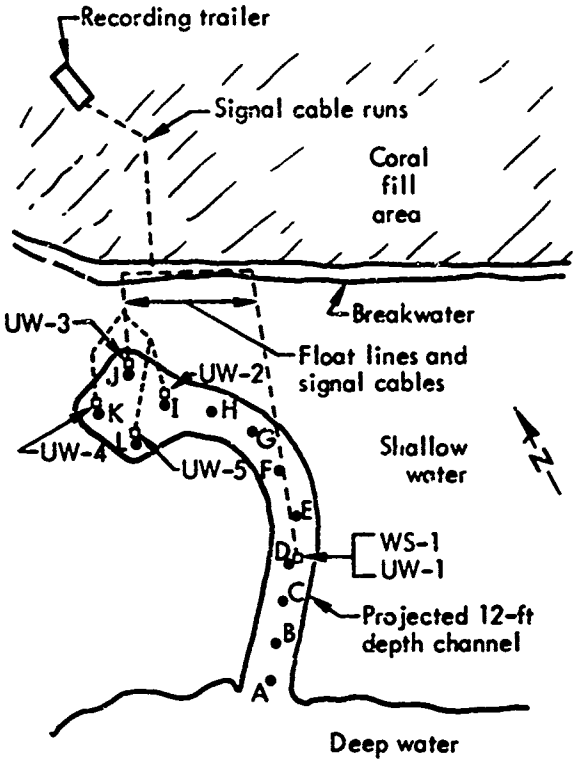

Fig. 179. Plan view of instrumentation layout.

Figure 180 shows a typical instrument canister installation and the canister locations with respect to the explosive charge. Figure 181 shows the instrumentation hardware both before and after installation.

The K-Division instrumentation participation on Project Tugboat was conceived at a late date. A period of just over 2 mo lapsed between conception and field execution of the surface instrumentation program. Consequently, in such a short time the gage canisters could be designed and fabricated only for a maximum acceleration of 1500 g.

The following were the useful ranges of the

Pressure gages—3000 psi

Velocity gage—400 ft/sec

First type of accelerometer—1000 g

Second type of accelerometer—3000 g

Frequency-modulated systems were employed for signal transmission and were combined at the instrumentation canister to conserve on cable runs to shore. The transducers were used with 1-MHz center frequency (±200 kHz deviation) voltage-controlled oscillators. The variable reluctance transducers were used to frequency-modulate a dual-oscillator, balanced modulator circuit. Center carrier frequencies for this system ranged from 25 to 100 kHz with center carrier deviations of ±4 kHz.[43] These frequencies and the 1-MHz VCO frequencies were then combined on a single cable. In addition system power requirements were supplied on this cable. The UW2 and UW4 systems were an exception and each required two coaxial cables.

RESULTS

The initial salvo (Detonation II-ABCD), which was instrumented with canisters WS-1 and UW-1 on Charge II-D, was detonated on 23 April 1970. It was ascertained after the detonation that Charge II-D was considerably less in explosive yield than anticipated. However, good data were obtained from both canisters. The signal cables remained intact for over 3 sec. This long coverage made it possible to record the entire velocity time-history of the water mound. Peak velocities of 66 and 61 ft/sec were recorded by the subsurface and surface gages, respectively. In addition, the surface velocity gage indicated a velocity increase due to the gas acceleration phase

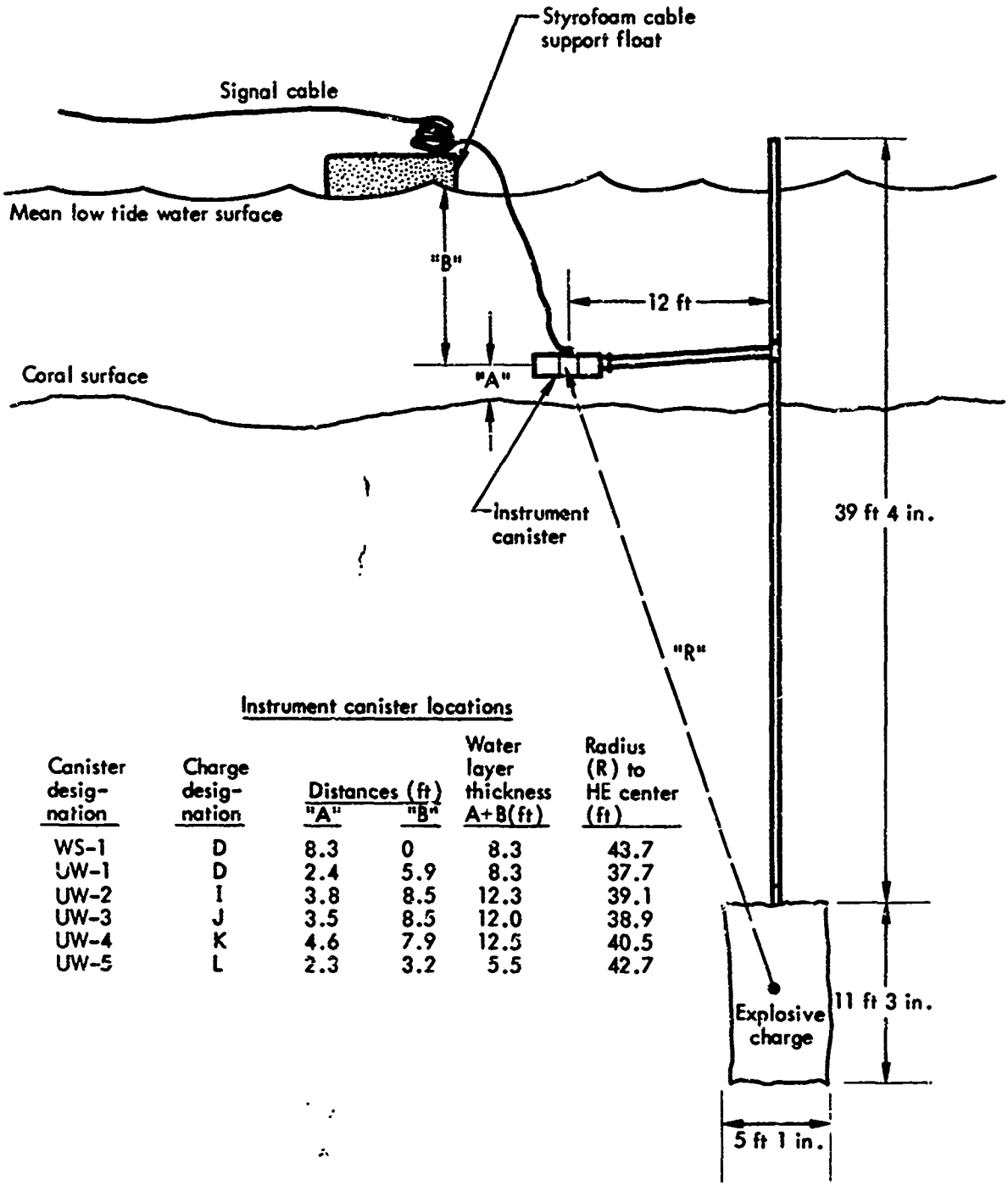

Instrument canister locations

Canister designation	Charge designation	Distances (ft) "A"	Distances (ft) "B"	Water layer thickness A+B(ft)	Radius (R) to HE center (ft)
WS-1	D	8.3	0	8.3	43.7
UW-1	D	2.4	5.9	8.3	37.7
UW-2	I	3.8	8.5	12.3	39.1
UW-3	J	3.5	8.5	12.0	38.9
UW-4	K	4.6	7.9	12.5	40.5
UW-5	L	2.3	3.2	5.5	42.7

Fig. 180. Diagram of typical instrument canister installation.

of the explosion. Peak accelerations of 356 and 311 g were recorded from the subsurface and surface gages, respectively. The pressure gage mounted in the bottom of the submersible canister recorded 414 psi. Table 40 summarizes these data, and Figs. 182 and 183 are photographs of each signal.

Table 40. Instrumentation results from Charge II-D Detonation.

Canister No.	Type of instrument	Radius to center of charge (ft)	Signal time of arrival (msec)	Peak signal value	Time of signal cable breakage (sec)
UW-1 (subsurface canister)	Pressure gage	37.6	8.1	414 psi	3
	Velocity gage	37.7	24.5[a]	65.9 ft/sec	3
	Accelerometer	37.7	8.2	356.6 g	3
WS-1 (surface canister)	Accelerometer	43.7	8.2	311 g	3.5
	Velocity gage	43.7	29.5[a]	61.1 ft/sec	3.5

[a]Surface water begins to move.

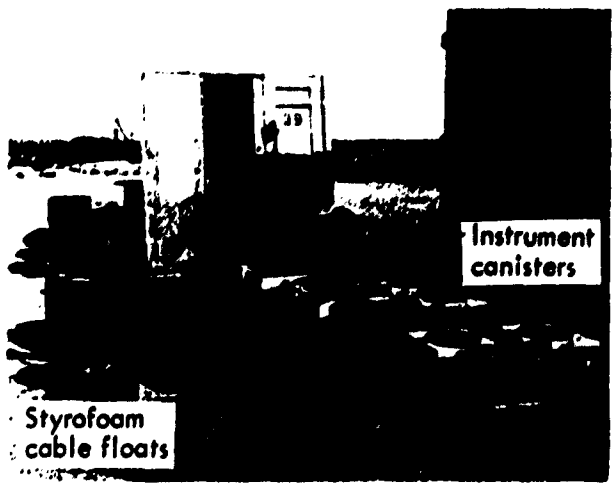

(a) Instrument canisters being prepared for installation.

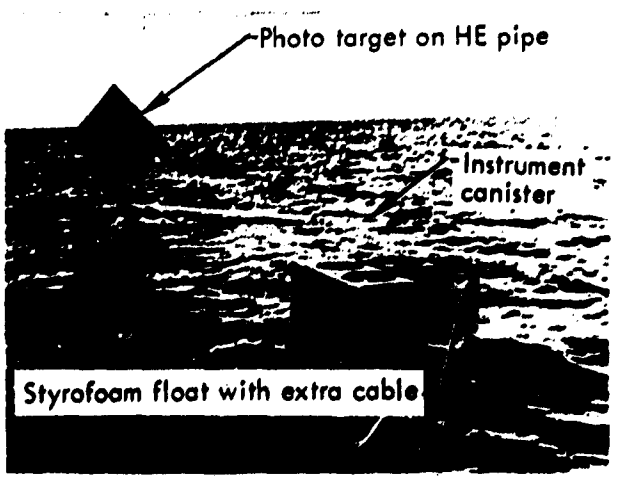

(b) WS-1 canister as installed on Charge II-D.

Fig. 181. Instrumentation systems.

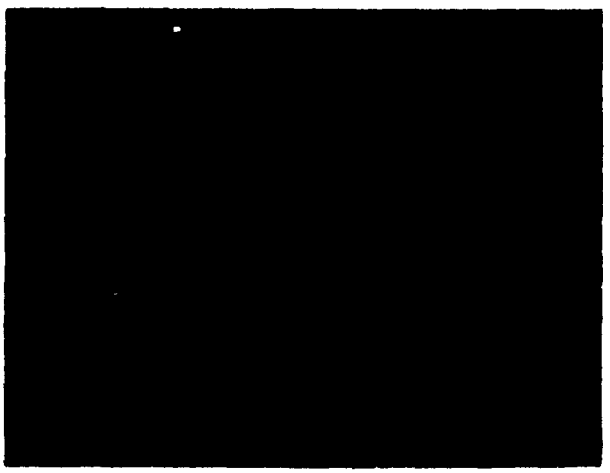

(a) Velocity gage signal (100 msec/cm; ~30 ft/sec/cm; peak signal: 61.1 ft/sec).

(b) Accelerometer signal (2 msec/cm; ~300 g/cm; peak signal: 311 g).

Fig. 182. Surface canister (WS-1) data from Charge II-D.

Table 41. Results of instrumentation on Charges II-I, II-J, II-K, and II-L.

Canister No.	Type of instrument	Radius to center of charge (ft)	Signal time of arrival (msec)	Peak amplitude	Time of signal cable breakage (msec)
UW-4 Charge II-I	Pressure gage	39.1	None	None	3.3
	Velocity gage	39.1	None	None	3.7
	Accelerometer	39.1	4.2	2780 g	11.0
UW-5 Charge II-J	Pressure gage	38.9	5.8	2513 psi	6.3
	Velocity gage	38.9	6.0	None	6.3
	Accelerometer	38.9	6.0	983 g (saturated)	6.3
UW-2 Charge II-K	Pressure gage	40.5	5.5	2235 psi	6.0
	Velocity gage	40.5	None	None	6.0
	Accelerometer	40.5	5.5	2689 g	9.6
UW-3 Charge II-L	Pressure gage	42.7	4.5	2258 psi	6.2
	Velocity gage	42.7	None	None	4.9
	Accelerometer	42.7	4.8	993 g (saturated)	4.9

(a) Velocity gage signal (100 msec/cm; ~30 ft/sec/cm; peak signal: 65.9 ft/sec).

(b) Accelerometer signal (2 msec/cm; ~150 g/cm; peak signal: 356.6 g).

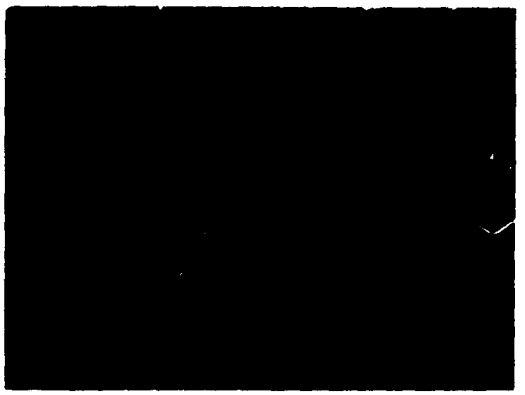

(c) Pressure gage signal [0.5 msec/cm (7.5-msec delay); ~ 400 psi/cm; negative signal indicates positive pressure].

Fig. 183. Subsurface canister (UW-1) data from Charge II-D.

(a) Charge II-I (accelerometer signal: 0.2 msec/cm (3.5-msec delay); ~700 g/cm).

(b) Charge II-J (pressure gage signal: 0.2 msec/cm (5-msec delay); ~1650 psi/cm).

Fig. 184. Pressure and acceleration signals from Charges II-I and II-J.

(a) Charge II-K (accel ter signal: 0.2 msec/cm (5-se ; ~770 g/cm).

(b) Charge II-K (pressure gage signal: 0.2 msec/cm (5-msec delay); ~430 psi/cm).

(c) Charge II-I (pressure gage signal: 0.1-msec/cm (4.2-msec delay); ~2200 psi/cm (negative signal is positive pressure); note cable breakage at 4.8 msec).

Fig. 185. Pressure and acceleration signals from Charges II-K and II-I.

The last salvo (Detonation II-IJKL) was detonated on 1 May 1970, with significant but less desirable instrumentation results. Each charge performed properly and resulted in accelerations which were nearly double the design limit of the gage canisters. Exceeding the design limit resulted in the early destruction of the canisters and the loss of considerable data. Peak accelerations of 2780 g and pressures of 2513 psi were recorded. The signal cables were severed as early as 3.3 msec and as late as 11.0 msec. Velocity data were not obtained for any the charges. Table 41 summarizes the data obtained. Figures 184 and 185 show the pressure and acceleration signals.

CONCLUSION

Project Tugboat was very useful in developing LLL's capability to instrument surface water environments. Indeed, it was fortuitous for the program that the instrumented Charge II-D went at a much lower yield than anticipated as much more information was obtained about the overall capability of the instrumentation.

Data were obtained which can be used to develop calculational codes for harbor cratering detonations. Calculations were not made for Tugboat due to the lack of funds for the extensive programs needed to obtain equation-of-states for both the coral formation and the HE energy source.

References

1. Department of the Army, Office of the Chief of Engineers, "Laboratory Soils Testing," Engineer Manual EM 1110-2-1906, Washington, D.C., 10 May 1965.
2. D.R. Stephens and H.C. Heard, Lawrence Livermore Laboratory, private communication (6 May 1971).
3. D.R. Stephens and E.M. Lilly, "Loading-Unloading Pressure-Volume Curves for Rocks," Proc. ANS Topical Meeting, Engineering with Nuclear Explosives, Las Vegas, Nevada (1970), Vol. 1 (CONF-700101).
4. J. Handin and R.V. Hager, Jr., "Experimental Deformation of Sedimentary Rocks under Confining Pressure: Tests at Room Temperature on Dry Samples," Bull. Amer. Ass. Petrol. Geol. 41, 1 (1957).
5. D.F. Cluff, W.K. Kikuchi, R.A. Apple, and Y.H. Sinoto, "The Archeological Surface Survey of Puukohola Heiau and Mailekini Heiau, South Kohala, Kawaihae, Hawaii Island" Hawaii State Archeological Journal 69-3, Department of Land and Natural Resources, Division of State Parks, State of Hawaii, Honolulu, Hawaii, December 1969.
6. U.S. Army Materiel Command, "AMC Safety Manual," AMC Regulation No. 385-224, Washington, D.C., 21 July 1967, p. 152.
7. K.T. Sakai and R.F. Bourque, Summary of Underwater Cratering Tests Conducted at Site 300 During 1970, U.S. Army Engineer Waterways Experiment Station Explosive Excavation Research Laboratory, Livermore, Calif., Rept. EERO-TM-70-11 (1971).
8. C.M. Snell, Shock Wave Interaction and Near Surface Cavitation, Project Tugboat, U.S. Army Engineer Waterways Experiment Station Explosive Excavation Research Laboratory, Livermore, Calif., Rept. EERL/TM-71-17 (1972).
9. K. Terzaghi and R.B. Peck, Soil Mechanics in Engineering Practice (John Wiley & Sons, Inc., New York, 1967), pp. 311, 312, 217.
10. J.W. Strange, Effects of Explosions in Shallow Water, U.S. Army Engineer Waterways Experiment Station, Vicksburg, Miss., Rept. TM-2-406 (1955).
11. H.C. Kranzer and J.B. Keller, "Water Waves Produced by Explosions," J. Appl Phys. 30 (3), 398 (1959).
12. E. Buckingham, "Model Experiments and the Forms of Empirical Equations," Trans., Amer. Soc. Mech. Eng. vol. 37, p. 263 (1915).
13. V.E. Brock, "A Preliminary Report on a Method of Estimating Reef Fish Populations," J. Wildlife Mgt., 18 (3) 297 (1954).
14. W.A. Gosline, University of Hawaii, private communication (1959).
15. W.A. Gosline and V.E. Brock, Handbook of Hawaiian Fishes (University of Hawaii Press, Honolulu, Hawaii, 1965).
16. L.M. Lowrie and W.V. Mickey, Project Dugout Strong-Motion Seismic Measurements, U.S. Coast and Geodetic Survey, Rockville, Md., Rept. PNE-605F (1965).

17. M.K. Kurtz, Jr. and B.B. Redpath, Project Pre-Gondola Seismic Site Calibration, U.S. Army Engineer Waterways Experiment Station Explosive Excavation Research Laboratory, Livermore, Calif., Rept. PNE-1100 (1968).
18. M.V. Mickey, L.M. Lowrie, and T.R. Shugart, Earth Vibrations From a Nuclear Explosion in a Salt Dome, Project Dribble, Salmon Event, U.S. Coast and Geodetic Survey, Rockville, Md., Rept. VUF-3014 (1967).
19. G.W. Housner, "The Behavior of Inverted Pendulum Structures During Earthquakes," Bull. Seis. Soc. Am. 53 (2), 403 (1963).
20. D.E. Hudson, "Response Spectrum Techniques in Engineering Seismology," in Proc. World Conf. on Earthquake Engineering (Earthquake Engineering Research Institute, University of California, Berkeley, 1956), pp. 4-1 to 4-12.
21. L.J. Vortman, Airblast From Project Tugboat Detonations, Sandia Laboratories, Albuquerque, N. Mex., Rept. SC-RR-70-541 (1970).
22. R.B. Vaile, Jr., Surface Structure Program, Underground Explosion Tests at Dugway, Stanford Research Institute, Menlo Park, Calif., Rept. AFSWP-298 (1952).
23. E.B. Doll, High Explosive Tests, Operation Jangle, Armed Forces Special Weapons Project, Rept. WT-365 (1951).
24. D.C. Sachs and L.M. Swift, Small Explosion Tests, Project Mole, Stanford Research Institute, Menlo Park, Calif., Rept. AFSWP-291, Vols. I and II (1955).
25. B.F. Murphey and E.S. Ames, Air Pressure Versus Depth of Burst, Sandia Laboratories, Albuquerque, N. Mex., Rept. SC-TM-42-59 (51) (1959).
26. B.F. Murphey, High Explosive Crater Studies: Tuff, Sandia Laboratories, Albuquerque, N. Mex., Rept. SC-4574(RR) (1961).
27. L.J. Vortman et al., 20-Ton HE Cratering Experiment in Desert Alluvium, Project Stagecoach, Sandia Laboratories, Albuquerque, N. Mex., Rept. SC-4596 (RR) (1962).
28. L.J. Vortman et al., 20-Ton and 1/2-Ton High Explosive Cratering Experiments in Basalt Rock, Project Buckboard, Sandia Laboratories, Albuquerque, N. Mex., Rept. SC-4675(RR) (1960).
29. W.R. Perret et al., Project Scooter Final Report, Sandia Laboratories, Albuquerque, N. Mex., Rept. SC-4602(RR) (1963).
30. L.J. Vortman, Airblast and Craters from Rows of Two to Twenty-five Charges, Sandia Laboratories, Albuquerque, N. Mex., Rept. SC-RR-68-655 (1969).
31. The CAPSA Series, Sandia Laboratories, Albuquerque, N. Mex., unpublished data.
32. J.W. Reed and L.J. Vortman, Airblast Measurements, Project Pre-Schooner II, Sandia Laboratories, Albuquerque, N. Mex., Rept. PNE-512F (1968).
33. L.J. Vortman, Close-in Airblast from a Row Charge in Basalt, Sandia Laboratories, Albuquerque, N. Mex., Rept. PNE-608F (1965).
34. L.J. Vortman, Comparison of Airblast from Two Sizes of Row Charges, Sandia Laboratories, Albuquerque, N. Mex., Rept. SC-RR-66-415 (1966).

35. J. M. Keefer, W. F. Jackson, and D. P. Lefevre, "Ballistic Research Laboratories, Aberdeen Proving Ground, "Close-in Airblast," chapter in Project Pre-Gondola II, Summary Report, U. S. Army Engineer Waterways Experiment Station Explosive Excavation Research Laboratory, Livermore, Calif., Rept. PNE-1112 (1971).

36. C. A. Rappleyea, Crater, Ejecta, and Air-Blast Studies from Five High-Explosive Charges in a Horizontal Square Array, Sandia Laboratories, Albuquerque, N. Mex., Rept. SC-RR-66-480 (1967).

37. L. J. Vortman, Sandia Laboratories, Albuquerque, N. Mex., "Close-in Airblast Measurements," chapter in Project Pre-Gondola III, Phase I, Summary Report, U. S. Army Engineer Waterways Experiment Station Explosive Excavation Research Laboratory, Livermore, Calif., Rept. PNE-1114 (1970).

38. L. Rudlin, Measurements of the Airblast from the Underwater Explosion of TNT Spheres, U. S. Naval Ordnance Laboratory, White Oak, Md., Rept. NAVORD-3913 (1955).

39. J. F. Pittman, Characteristics of the Air Blast Field Above Shallow Underwater Explosions, U. S. Naval Ordnance Laboratory, White Oak, Md., Rept. NAVORD-6106 (1955).

40. J. F. Pittman, Airblast from Shallow Underwater HBX-1 Explosions, U. S. Naval Ordnance Laboratory, White Oak, Md., Rept. NOLTR 68-45 (1968).

41. J. W. Reed, B. J. Pape, J. E. Minor, and R. C. DeHart, Evaluation of Window Pane Damage Intensity in San Antonio Resulting from Medina Facility Explosion on November 13, 1963, Sandia Laboratories, Albuquerque, N. Mex., Rept. SC-4-68-1746 (1963).

42. J. T. Cherry, "Computer Calculations of Explosion-Produced Craters," Int. J. Rock Mech. Min. Sci. 4, 1 (1966).

43. S. Spataro, An FM Acceleration/Velocity Measurement System, Lawrence Livermore Laboratory, Rept. UCRL-72193 (1970).